COMMUNAUTE FRANCAISE DE BELGIQUE
ACADEMIE UNIVERSITAIRE WALLONIE-EUROPE
UNIVERSITE DE LIEGE – GEMBLOUX AGRO-BIO TECH

PARTICULATE SOILS ADHERENCE AND SURFACE CLEANABILITY: INFLUENCE OF BIOMACROMOLECULES AT INTERFACES AND OF SUBSTRATE HYDROPHOBICITY

Yetioman TOURE

Essai présenté en vue de l'obtention du grade de
Docteur en sciences agronomiques et ingénierie biologique

Promoteur: Prof. Marianne SINDIC

2014

TOURE Yetioman (2014). Particulate soils adherence and surface cleanability: influence of biomacromolecules at interfaces and of substrate hydrophobicity (PhD Thesis). Gembloux, Belgium, University of Liege – Gembloux Agro-Bio Tech – 225p., - 26 tabl., - 36 fig.

Abstract

Cleaning of particulate soils is an important issue in food and pharmaceutical production. Understanding the adherence of these soils is a fundamental requirement for improving surfaces cleanability. The combination of particles and macromolecules substances appears in many processes. Adsorbed compounds from these mixtures may influence interactions at interfaces and thus fouling and cleaning.

This thesis deals with a deeper understanding of the physico-chemical mechanisms affecting soiling and cleanability of open substrates in the presence of biomacromolecules (dextran, bovine serum albumin – BSA, beta-lactoglobulin – β-LGB). Model substrates were chosen according to their hydrophobicity. The influence of macromolecules was examined by introducing them in the quartz suspension taken as a model of hard hydrophilic soil used for soiling, or by conditioning the substrate prior to soiling. The substrates were pretreated with ethanol (-Eth.), piranha or UV-Ozone (-UVO); soiled by spraying the quartz suspensions, then dried, before cleaning assessment. The removal of the soiling particles was evaluated after exposure to water in a radial flow chamber (RFC). Auxiliary characterizations were surface tension and contact angle measurements, surface analysis of the substrate by X-ray photoelectron spectroscopy (XPS) and Scanning electron microscopy (SEM).

The interpretation of XPS data allowed the complexity due to the ubiquitous presence of organic contaminants to be coped with, and the surface composition to be expressed in terms of both the amount of adlayer and the mass concentration of adlayer constituents. The contact of substrates with proteins led to their adsorption, which dominated the composition of the organic layer with respect to contaminants initially present, and was not markedly desorbed upon rinsing. Dextran was easily removed in presence of water, independently on the substrate nature.

Surface hydrophobicity was shown to influence the morphology of the aggregates resulting from drying. The rounder aggregates formed on polystyrene when soiling was performed with suspension in pure water are more sensitive to wall shear stress than flatter ones formed on more hydrophilic substrate. This is the result of the competing processes of droplet rolling and coalescing, on the one hand, and droplet spreading, on the other hand. It affects the shape and compactness of the adhering aggregates, the efficiency of shear forces upon cleaning and finally, the adherence of soiling particles.

The presence of proteins (either native or denatured) at the interface improved strongly the cleanability of more hydrophilic substrate (glass, StSteel-UVO). This is attributed to the lower surface tension. The dependence of cleanability on capillary forces, and in particular on the liquid surface tension, is predominant as compared with its dependence on the size and shape of the soiling aggregates, which influence the efficiency of shear forces exerted by the flowing water upon cleaning. The cleanability of less hydrophilic substrate (stainless steel only pre-cleaned with ethanol) did not change markedly in the presence of proteins; this may be due to a more complex interaction between surface tension and contact angle, on one hand, and a more complex interaction between proteins and contaminants, on the other hand. The presence of dextran did not affect the cleanability, as neither the liquid surface tension nor the contact angle was appreciably affected.

TOURE Yetioman (2014). Adhérence des souillures particulaires et nettoyabilité de surfaces: influence des biomacromolécules aux interfaces et de l'hydrophobicité des substrats (Thèse de doctorat en anglais). Université de Liège – Gembloux Agro-Bio Tech, – 226p., - 26 tabl., - 36 fig.

Résumé

Le nettoyage des souillures particulaires est une préoccupation majeure dans les industries alimentaires et pharmaceutiques. La compréhension des facteurs influant l'adhérence de ces salissures est une exigence fondamentale pour l'amélioration de la nettoyabilité des surfaces. Des mélanges de biomacromolécules et de particules sont fréquents dans les procédés de production. L'adsorption de composés issus de ces combinaisons pourrait influencer les interactions aux interfaces et par conséquent l'encrassement et le nettoyage des surfaces.

Cette recherche doctorale vise une compréhension approfondie des mécanismes physico-chimiques affectant l'encrassement des surfaces ouvertes en présence de biomacromolécules (dextrane, albumine de sérum bovin – BSA, beta-lactoglobuline – β-LGB) aux interfaces. Des substrats modèles ont été choisis selon leur hydrophobicité. L'effet des biomacromolécules a été examiné en les impliquant suivant deux procédés: introduction dans la suspension de particules de quartz utilisées comme modèle de souillure particulaire hydrophile rigide pour l'encrassement; adsorption préalable sur les supports avant l'encrassement. Les surfaces ont été prétraitées à l'éthanol (-Eth.), au piranha ou à l'UV-Ozone (-UVO), encrassées par aspersion de la suspension de quartz et séchées avant les tests de nettoyage. L'aptitude au nettoyage des surfaces encrassées a été évaluée après leur exposition à un flux d'eau dans une chambre à flux radial (RFC). Les analyses annexes étaient basées sur la détermination de la tension superficielle et de la mouillabilité, l'analyse de surface des substrats par spectroscopie photoélectronique aux rayons X (XPS) et par microscope électronique à balayage (SEM).

L'interprétation des données XPS a permis de maîtriser la complexité de la composition chimique de surface due à l'omniprésence des contaminants organiques. Cette composition a été exprimée à la fois en termes de proportion de couche organique adsorbée et de concentration massique des constituants de celle-ci. Il ressort que les protéines s'adsorbent au contact des supports, et dominent la composition organique de la couche adsorbée par rapport aux contaminants initialement présents. La désorption des protéines n'est pas significative avec le rinçage. En revanche, la quasi-totalité du dextrane se désorbe en présence de l'eau, quelle que soit la nature du substrat.

L'hydrophobicité de la surface influence la morphologie des agrégats résultant du séchage. Lorsque l'encrassement s'effectue à l'aide d'une suspension aqueuse pure de particules, les agrégats arrondis formés sur le polystyrène sont plus sensibles aux contraintes de cisaillements par rapport aux agrégats aplatis formés sur des substrats plus hydrophiles. Ceci est le résultat de processus de compétitions, d'une part, entre le roulement et la coalescence des gouttelettes, et d'autre part, l'étalement des gouttelettes. Ce mécanisme affecte la forme et la compacité des agrégats adhérés, l'efficacité des forces de cisaillements pendant le nettoyage et finalement l'adhérence des particules de salissures.

La présence de protéines (native ou dénaturée) à l'interface particule-substrat améliore considérablement l'aptitude au nettoyage des substrats les plus hydrophiles (verre, acier inoxydable prétraité UVO). Cela est attribué à la diminution de la tension superficielle. La dépendance de la nettoyabilité aux forces capillaires et en particulier à la tension superficielle du liquide, est prédominante par rapport à sa dépendance à la taille et à la forme des salissures qui influent sur l'efficacité des forces de cisaillement exercées par le flux d'eau au cours du nettoyage. La nettoyabilité des substrats moins hydrophiles (acier inoxydable prétraité seulement à l'éthanol) est peu affectée par la présence de protéines. Ceci pourrait être dû, d'une part, aux interactions plus complexes entre la tension superficielle et l'angle de contact, et d'autre part, aux interactions complexes entre les protéines et les contaminants. La présence de dextrane aux interfaces n'affecte pas significativement la nettoyabilité.

Aux quatre personnes qui ont inconditionnellement été des catalyseurs aux étapes cruciales de ma vie. À mon défunt père, qui a semé sans avoir vu croître. À mon oncle, Manghan Ouattara, qui a su arrosé le jeune plant et lui a accordé une confiance sans limite. À ma mère, qui m'a appris la persévérance, le goût d'apprendre et le sens de l'engagement. Et à ma merveilleuse épouse, Tiborine, qui m'encourage dans mes initiatives avec tant d'amour et m'apporte tout le soutien affectif et psychologique dont j'ai besoin.

This PhD thesis is the result of several years of scientific collaboration between two laboratories: Institute of Condensed Matter and Nanosciences (IMCN) - Bio & Soft Matter (BSMA), Université catholique de Louvain; and the laboratory of Agro-food Quality and Safety - Analysis Quality and Risk Unit, Université de Liège-Gembloux Agro-Bio Tech. Other scientific teams to a lesser extent were also involved: Walloon Agricultural Research Centre (CRA-W) - Department of Valorisation of Agricultural Products; and the Centre for Protein Engineering (CIP) - Institute of Chemistry, Université de Liège. I would like to express my gratitude to all these partners for their interest in this work. This PhD also represents more than four years of my life during which many things happened and for which I am grateful.

«*Nani gigantum humeris insidentes*», cette métaphore latine qui signifie en français «des nains sur des épaules de géants», est connue de Bernard de Chartres. Ces mots illustrent parfaitement l'importance pour tout homme ayant une ambition scientifique de s'appuyer sur des Anciens. Je paraphraserai Newton dans sa lettre à Robert Hooke en 1676, en disant que si j'ai été aussi loin dans cette thèse, c'est parce que j'ai pu m'appuyer sur la haute stature du Professeur émérite Paul G. Rouxhet, qui a trouvé ce sujet digne d'intérêt dès notre première rencontre et qui m'a fait confiance en acceptant cette collaboration. Monsieur Rouxhet, merci d'avoir eu beaucoup de respect à mon égard, d'avoir été compréhensif face à mes erreurs de jeunesse et pour les innombrables corrections effectuées et répétées. Merci également pour votre patience, pour votre approche constructive, pour les longues séances de travail et de discussion même pendant des weekends et chez vous à la maison, pour votre contribution scientifique remarquable à ce travail, pour m'avoir appris beaucoup de choses sur la science et le comportement humain. Je voudrais dire merci à votre merveilleuse épouse pour sa sympathie et son accueil chaleureux pour les fois où nous travaillions chez vous à la maison pour tenir certains délais.

Je voudrais réitérer les mêmes remerciements à la Prof. Christine C. Dupont-Gillain pour sa simplicité, son soutien scientifique et matériel. Madame Dupont, vous n'avez ménagé aucun effort pour me permettre de faire des analyses au SEM, à l'XPS et au DCA tout au long de cette thèse. Et ceci dans un laboratoire où scientifiquement parlant, le dynamisme et les interactions entre personnes sont sans reproches. J'ai envie de crier waouh! qu'il est merveilleux votre laboratoire! Je voudrais exprimer ma reconnaissance à tous vos collaborateurs qui m'ont aidé d'une manière ou d'une autre à réaliser des analyses et aussi pour leurs disponibilités. Je pense particulièrement à Michel Genet et Pierre Eloy pour l'XPS, Sylvie Derclaye pour le SEM et Yasmine Adriaensen pour le DCA.

Un dicton de notre riche culture africaine dit en substance : « *Lorsque tu adores une montagne, souviens-toi d'abord de la termitière qui t'a permis d'apercevoir le sommet de cette montagne la première fois* ». Je trouve difficilement les mots qui vont contribuer à remercier ma promotrice la Prof. Marianne Sindic. Madame, merci pour votre totale confiance en moi et la liberté que vous m'avez donnée pour effectuer ces recherches, pour votre supervision. Merci à vous de m'avoir non seulement permis mais encouragé à profiter des

nombreuses opportunités qu'offre la réalisation d'un doctorat. Vous avez toujours favorisé mon implication dans la valorisation et la diffusion de mes travaux. Vous avez su me laisser mener ce travail avec beaucoup d'autonomie tout en étant toujours présente dès la moindre interrogation. Vous avez su m'encourager pendant des moments difficiles. Je ne voudrais pas manquer l'occasion ici de remercier Charlemagne Nindjin qui a cru en moi depuis la Côte d'Ivoire, sans oublier le Professeur Amani N. George pour ses conseils précieux. C'est grâce à eux que le premier contact a été établi.

Au fur et à mesure que j'avançais dans cette thèse, j'ai pu bénéficier du soutien scientifique et technique de nombreuses personnes: André matagne, Erik Goormaghtigh, Ouissam Abbas, Nicolas Mabon, Quentin Arnould, Marjorie Servais, Guy Delimme, Lynn Doran, Dominique Cortese et Alain Someville. Leur contribution à ce travail, leur expertise et leurs conseils avisés m'ont été très utiles. Je les en remercie sincèrement. Je remercie également Jean Detry pour ses conseils très utiles au début de ce travail.

J'adresse mes sincères remerciements aux membres de mon comité de thèse: Messieurs Michel Paquot, Georges Lognay, François Béra et Frank Delvigne, pour leur disponibilité, pour l'intérêt porté à mon travail, pour les remarques pertinentes et constructives faites tout au long de cette thèse.

Je voudrais respectueusement remercier encore la Prof. Christine Dupont et le Prof. Frank Delvigne qui m'ont fait l'honneur de donner leur appréciation sur cet essai en tant que rapporteurs. J'adresse un énorme merci à Mesdames et Messieurs les membres du jury pour l'évaluation de ce travail. Je voudrais particulièrement remercier le Prof. Frederic Francis d'avoir accepté d'être le président de jury cette thèse.

Je voudrais remercier du fond du cœur mes anciennes collègues de bureau Christine Anceau et Nadège Zdanov pour leur soutien, leur bonne humeur et leur amitié. Merci aussi à Thibaut Troch, aux secrétaires et à tous les autres membres du laboratoire que j'ai côtoyés durant ces années.

I would like to acknowledge CURAGx, FRS-FNRS, PACODEL, l'AUF, la DGTRE and the Ivory Coast government for the various financial supports.

Oh oui, il y a une chose et non des moindres que je voudrais mentionner: la contribution invisible de mon épouse Tiborine. Sur une note personnelle, je voudrais la remercier pour son soutien durant ces dernières années. Je t'aime, «*la Merveille de Mon Cœur*», et je suis impatient de passer beaucoup plus de temps avec toi pendant les soirées et les weekends. Merci de t'être montrée compréhensive sur mes rentrées tardives, mes absences souvent répétées et mon silence lorsque j'avais besoin de travailler à la maison en soirée. Merci pour tous les sacrifices consentis à mon égard. Sache que tu es la meilleure!

Enfin, j'adresse mes sincères remerciements à mes parents et à ma famille spirituelle, en particulier le couple Iwolo et Armand Gallimoni, pour leur soutien et à tous ceux qui de près ou de loin m'ont soutenu pendant ces dernières années.

INDEX

FOREWORD

This dissertation is composed of two parts:

- an overview, including a general introduction, a synthetic presentation of the thesis and a general conclusion (**Part I**),
- a detailed presentation (**Part II**), consisting in 6 sections in the form of publications or of manuscripts to be published.

Fouling is a common challenge for many industries. A goal for researchers, industrialists and surfaces designers is to find innovative strategies to reduce fouling and its related cost, and to achieve better cleaning efficiency and environmentally friendly processes. Hence, numerous methods and techniques are used with representative model foulants to mitigate the fundamental mechanisms of soils adherence and removal. The main model soil systems used for fouling and cleaning investigation in the relevant literature are summarized in ***Section I***. Furthermore, this section gives a general insight; it situates the context of the present thesis in relation with the influence of biomacromolecules on particles fouling and removal, which suffers from a lack of knowledge.

Section II reports an exploratory study of the effect of polysaccharide (dextran) on the cleanability of two model substrates (glass and polystyrene) differing according to hydrophobicity. ***Section III*** develops this approach with a comparison between polysaccharide (dextran) and protein (BSA) and presents complementary data to decipher the physico-chemical mechanisms controlling particles adherence and removal.

Section IV extends these observations to stainless steel and to an additional protein, β-lactoglobulin (β-LGB), considering the possible influence of initial surface state of the substrates. ***Section V*** examines the possible β-LGB denaturation. These results lead to a more comprehensive study presented in ***Section VI***, which considers the influence of several factors: surface nature, including the type of substrate and its initial surface state (mode of pre-cleaning); nature of the suspending liquid, including the presence of β-LGB, native or denatured.

The sections are titled as follows:

Section I: Soil model systems used to assess fouling, soil adherence and surface cleanability in the laboratory. Y. Toure, N. Mabon, M. Sindic, 2013. *Biotechnol. Agron. Soc. Environ.*, 17(3), 527-539.

Section II: Influence of soluble polysaccharide on the adherence of particulate soils. Y. Touré, P.G. Rouxhet, C.C. Dupont-Gillain and M. Sindic., 2011. *Proc. Int. Conf. on Heat Exchanger Fouling and Cleaning*, (Malayeri, M.R., Müller-Steinhagen, H. & Watkinson, A.P., eds.), June 05-10, 2011, Crete Island, Greece, http://www.heatexchanger-fouling.com, 219-226.

Section III: Conditioning materials with biomacromolecules: composition of the adlayer and influence on cleanability. Y. Touré, M. J. Genet, C.C. Dupont-Gillain, M. Sindic and P.G. Rouxhet., 2014. *J. Colloid Interface Sci.*, 432, 158-169.

Section IV: Influence of soluble proteins on the adherence of particulate soils. Y. Touré, P.G. Rouxhet, and M. Sindic., 2013. *Proc. Int. Conf. on Heat Exchanger Fouling and Cleaning*, (Malayeri, M.R., Müller-Steinhagen, H. & Watkinson, A.P., eds.), June 09-14, 2013, Budapest, Hungary, http://www.heatexchanger-fouling.com, 285-290.

Section V: Influence of whey protein denaturation on adherence of soiling particles to stainless steel. Y. Touré, P.G. Rouxhet, C.C. Dupont-Gillain and M. Sindic., 2014. *Fouling and Cleaning in Food Processing* (Wilson, D.I & Chew, Y.M.J, eds.), Publishing Depart. Chem. Eng. & Biotech., Cambridge, UK, 30-37.

Section VI: Influence of β-lactoglobulin (β-LGB) denaturation and surface hydrophobicity on hard particulate soils removal with water. Y. Touré, C.C. Dupont-Gillain, A. Matagne, E. Goormaghtigh, M. Sindic and P.G. Rouxhet. Submitted in *Chem. Eng. Sci.*.

The author **also contributed to the following paper**:

Development of frozen-fried yam slices: optimization of the processing conditions. Y. Touré, C. Nindjin, Y. Brostaux, G.N. Amani and M. Sindic, 2012. *African J. Food, Agric. Nutr. Dev.*, 12(7), 7055-7071.

The author attended the following **international scientific events**:

Oral presentation at the 9th international conference on Heat Exchanger Fouling and Cleaning organized from the 5th to the 10th of June 2011 in Crete Island, Greece.

Presentation of a poster at the Lorraine Doctoriales School organized from the 3rd to the 8th of June 2012 in Vosges, France.

Oral presentation at the 10th international conference on Heat Exchanger Fouling and Cleaning organized from the 9th to the 14th of June 2013 in Budapest, Hungary.

Oral presentation at the 6th international conference on Fouling and Cleaning in Food Processing 2014: 'Green Cleaning' organized from the 31st March to the 2nd April 2014 in Cambridge, UK.

LIST OF ABBREVIATIONS

ATR-FTIR	Attenuated total reflectance-Fourier transform infrared spectroscopy
BSA	Bovine serum albumin
β-LGB	β-lactoglobulin
CD	Circular dichroïsm
Glass-Eth	Glass pre-cleaned with ethanol
Glass-UVO	Glass pre-cleaned with ethanol and submitted to an additional UVO treatment
RFC	Radial flow cell
SEM	Scanning electron microscopy
StSteel-Eth	Stainless steel pre-cleaned with ethanol
StSteel-UVO	Stainless steel cleaned with ethanol and submitted to an additional UVO treatment
TLC	Thin layer chromatography
XPS	X-ray photoelectron spectroscopy
UVO	Ultra-violet / ozone

Part I: OVERVIEW

1. INTRODUCTION

1.1. Context of the research

Fouling - the deposition of unwanted material on equipment surfaces occurring in many processing industries - is an enormous challenge for researchers. The surface under consideration is referred to as substrate; and the removal of soils is referred to as cleaning (Jennings, 1965).

Over three decades, series of international meetings brought together researchers and industrialists interested in fouling and cleaning (see recent conference proceedings Wilson and Chew, 2014; Reza et al., 2013), but one is far to find sustainable and universal solution due to the complexity of the phenomena. Soils (or foulants) can be classified according to different criteria for making possible the grouping and comparison of data from different industries or for understanding the formation of deposit and the principles of cleaning: chemical, biological, particulate, crystallization, corrosion, mineral, composite soils (HRS Group, 2011; Fryer and Asteriadou, 2009; Rosmaninho and Melo, 2008; Quittet and Nelis, 1999). More details about soils classification are given in *Section I*.

Fouling problems are encountered in many areas such power plants, automotive industry, oil and metal refineries, detergent industry, semiconductor industry, cars and building façades, pharmaceutical and food industries. However, fouling in food sector differs from that in other domains, owing to the crucial relationship between fouling and cleaning, on the one hand, and food safety and purity, on the other hand. Fouling in food industry may compromise hygienic operation and food qualities, and affects the number of recalled products due to contamination. The severity of fouling in food industries has several drawbacks: frequent interruption for cleaning operations and reduction of process efficiency (Gillham et al, 1999), extra energy consumption (Eide et al., 2003), loss of productivity, maintenance, additional investment required to oversize units (Gillham et al., 2000), large volumes of water and cleaning chemicals required to remove deposits, and environment impact (Pascual et al., 2007). This incurs many different expenses (Bansal et al., 2008; Müller-Steinhagen, 1993) and costs about 0.25% of the gross national product (GNP) for the industrialized countries. Plant downtime due to fouling may reach 40% of the available production time and the required energy may account for 30% of the total use. The need to improve the sustainability of food manufacturing will grow with the population as the finite resources of our planet are stretched. Finding affordable answers to these challenges is an imperative. Because of the lack of understanding of the interaction between deposits entities and surfaces, and how cleaning is

affected by the environment in which the surfaces are used, cleaning processes are difficult to optimize, regarding saving energy and time and decreasing pollution.

The hydrodynamic effects are crucial for the cleaning effectiveness owing to the shear stress forces (Blel et al., 2007; Jensen et al., 2005; Lelièvre et al., 2002). However, the flow rate and the equipment design which determine the wall shear stresses, cannot alone account for cleaning efficiency (Jensen et al., 2007; Detry et al., 2009a; Blel et al., 2010). When dealing with particle adhesion, it is not sufficient to consider only the detachment force out of the context. The material, particle size and density have to be taken into account to evaluate the response to the action of hydrodynamic forces, together with surface reactions (Ziskind et al., 1995).

Fouling involving particulate soils is a daily problem for surfaces exposed to natural environments or surfaces of industrial equipment. Open surfaces are exposed to splashing of particles suspended in aqueous media and dust from air or other aerial contaminations. Particulate soils may also originate from deposition in storage tanks, in the ducts or on the plates of heaters and coolers. The presence of adhering particles and microorganisms is undesirable after cleaning and disinfection of open surfaces, where the ambient general level of hygiene is critical. In food and pharmaceutical industries, the cleaning efficiency influences the final quality of the products, the absence of cross-contaminations and the batch integrity (Jackson et al., 2008; Stephan et al., 2004). The interactions between the substrate and particulate contaminants have to be well understood in order to reduce equipment fouling, to improve the efficiency of cleaning and disinfection, or to develop easy-to-clean surfaces (Podczeck 1999).

The main constituents of food and pharmaceutical mixtures are polysaccharides, proteins, lipids and other biopolymers. These compounds may influence interactions with surfaces and adhesion (Speranza et al., 2004). It was reported that proteins at the outer surface of bacteria play a role in the initial attachment to solid surfaces in water due to specific interactions (Dufrêne et al., 1996; Flint et al., 1997; Caccavo, 1999; Boonaert and Rouxhet, 2000; Lower et al., 2005; Mercier-Bonin et al., 2009), but no data are available for particulate soils adhesion. In a study of starch granules adherence, Detry et al. (2011) reported that the presence of macromolecules, mainly polysaccharides, which were adsorbed from the liquid phase or carried by the retracting water film and deposited at the granule-substrate interface, acted as an adhesive joint, the properties of which seemed to be influenced by the detailed history of drying and subsequent exposure to humidity. Macromolecules dissolved in the starch suspension may act in various ways: modification of liquid surface tension and drop

spreading upon soiling, adsorption at the solid-liquid interface and accumulation at substrate-particulate interface upon drying.

The works performed to understand the parameters governing the cleaning processes are often focused on the influence of surface properties, and are carried out on new surfaces. In food industry, regular and effective cleaning of food contact surfaces is essential to ensure product quality and safety. However, the repeated fouling and cleaning can change the chemical composition of the surfaces which directly influences cleanability (Mauermann et al., 2011; Jullien et al., 2008; Verran and Whitehead, 2006; Leclercq-Perlat and Lalande, 1994). It was also reported that surface conditioning affects the hygienic status of the surfaces (Herrera et al., 2007; Flint et al., 2001; Parkar et al., 2001). The accumulation of organic compounds on surfaces, due to contact with aqueous media and food products, may alter the real surface state and affect interfacial interactions between soil and equipment surfaces (Storgards et al., 1999a; 1999b). The impact of the conditioning layers on microorganism attachment and resistance of microorganisms to cleaning procedures is not fully understood, and there is a lack of interest for particulate soils. Therefore, cleaning investigations should take into account particle adhesion and the presence of conditioning layers.

Studying the influence of biomacromolecules on fouling with a suspension of particles and on surface cleaning is thus important. It may give a practical information on the influence of substrate surface and particle surface properties (Jones et al., 2002) and an insight into the physico-chemical mechanisms involved (Tadros, 1980), in particular clarifying the role of the soluble macromolecules involved in particles adherence. It may also open the way to designing and evaluating easy-to-clean surfaces.

1.2. Aim and research strategy

This doctoral research is in tune with the issues of soils adherence and removal which draw the ever growing attention of engineers and scientists from many industrial sectors. Its aim was to investigate the effect of biomolecules on particulate soils adhesion to open surfaces and to improve the understanding of mechanisms affecting soiling and cleanability. Moreover, the possible consequences of repeated soiling and cleaning on hygienic properties and surface composition were studied by conditioning procedures chosen to mimic industrial application conditions.

The main lines of the work were to better understand:

- the physico-chemical mechanisms involved in particulate soils adherence and removal after splashing and drying,

- the mechanisms related to particle fouling, drying and cleaning of a surface previously conditioned by biochemical compounds,
- the relation between particles adherence and cleanability, depending on the nature of the substrate and the state of its surface, in presence of dissolved biomolecules.

More specifically, the work focuses on better understanding the cleaning mechanisms associated to different surfaces in contact with particulate soils, and the interactions between particles and substrates differing by hydrophobicity, in presence of:

- polysaccharides
- proteins
- denatured proteins.

Quartz particles were taken as a simplified model for hard and hydrophilic particulate soils, such as starch granules or particles from milk powder, cereal flours or other carbohydrate powders. Dextran represented polysaccharides and BSA and β-LGB were used as models of proteins. Substrates which differed by hydrophobicity were glass and stainless steel with different pretreatments and polystyrene. The influence of substrate nature, biomacromolecules adsorption and protein denaturation on the particulate soils adherence and detachment, was examined by spraying aqueous suspensions of quartz particles to imitate soiling by splashing. The soiled substrates were dried before performing cleaning tests with a radial flow cell (RFC). The biomacromolecules were brought into the soiling process, either into the quartz suspension or previously adsorbed on the substrate. The effect of proteins denaturation was investigated by a high temperature treatment of the suspension or of the substrate after soiling.

2. EXPERIMENTAL ASPECTS

2.1. Material choice

Three model surfaces were selected according to their hydrophobicity which was expected to influence the adherence of soil. Glass was chosen for its high hydrophilic character, and polystyrene is a hydrophobic polymer. Stainless steel was used owing to its ubiquity in food industries, and its intermediate properties between glass and polystyrene. Quartz particles with a size 10 to 30 µm were taken as a simplified particulate soil model. The particle size was chosen to be in the same range as the starch granules used by Detry et al. (2011). Dextran was chosen as a model of soluble polysaccharide because of its high solubility. It was possible to select a defined molecular size from dextrans having a variety of molecular weights. In contrast with more highly branched polysaccharides such as dextrin, dextran contains more than 95% of only one type of glucose linkage. Albumin from bovine serum (BSA) and β-

Lactoglobulin (β-LGB) from bovine milk were chosen as models of proteins. BSA is the common soluble protein used for laboratory studies, and has surfactant properties. It is a globular and structurally labile (soft) protein, which may change its conformation upon adsorption (Norde and Giacomelli 2000; Kopac et al., 2008). β-LGB is the most abundant and the most heat-labile whey protein, and plays a key role in milk fouling (Robbins et al., 1999).

2.2. Surface pretreatment

The substrates were cut to the desired dimensions: 50 mm × 50 mm for cleanability assessment; 75 mm × 25 mm × 1 mm, 16 mm x 37 mm x 1 mm or 16 mm × 10 mm for the soiling entities observation and surface characterization.

The substrates were prepared using different protocols (Figure 1) before soiling and characterization. They were first cleaned with a Kimtech Science paper wetted with ethanol, followed by an immersion either in ethanol, or in an alkaline detergent solution (RBS 50, 2%; pH 11.9) at 50°C, and sonicated (except polystyrene) in the same medium to remove dust particles. The samples were then, rinsed thoroughly with ethanol or MilliQ water; immersed (only for substrates treated with RBS) in a piranha mixture (sulfuric acid/hydrogen peroxide 2:1 (v/v)) at room temperature and rinsed thoroughly with MilliQ water, before drying with a gentle nitrogen flow nitrogen and wrapping in an aluminum foil until use. Certain coupons of glass and stainless steel were submitted to an additional UV-Ozone treatment to improve the removal of organic contamination, and used immediately.

The samples so pretreated were used as such or conditioned at room temperature or at 75°C (only for stainless steel) by immersion for 1 h, according to the sample size, in 10 or 150 ml of a dextran, BSA, or β-LGB solution or in the supernatant collected after heating the β-LGB solution at 75°C. The conditioned samples intended for XPS analysis were rinsed using a procedure which avoided repeated formation of water-air meniscus in contact with the adsorbed phase. Therefore, the coupon was not removed from the liquid but the solution was diluted, removing of 8 ml from the 10 ml of the solution and adding 8 ml of MilliQ water, with time intervals of 5 min between rinsing steps. When finally removed from the liquid, the substrates were flushed with nitrogen for removing the liquid film and wrapped in aluminum foil until use for soiling, or placed in a Petri dish for XPS analysis. In the latter case, the conditioned substrates were examined as such, or rinsed once, twice, three or four times before flushing with nitrogen.

The initial choice of dextran concentration of 0.08 g/L was based on published studies (Laskowski et al., 2007; Ma and Pawlik, 2005) but the adsorption density of polysaccharides

onto both hydrophilic and hydrophobic quartz surfaces was very low. The concentration of 8 g/L chosen for BSA is lower than the protein concentration in egg white and blood plasma (about 100 g/L from which about 50% albumin, http://en.wikepedia.org); it is higher compared to the whey protein concentration in cow milk (6 g/L, Walstra and Jenness, 1984) and to the BSA concentration at which adsorption by silica and polystyrene latex reaches a plateau (Norde and Giacomelli, 2000). The dextran concentration was then chosen to be the same as that of BSA, with the idea that this possibly enhances adsorption compared to the initial choice of (0.08 g/L). The choice of β-LGB concentration was based on β-LGB concentration in bovine milk (3 g/L) (Walstra and Jenness, 1984). Furthermore, the β-LGB concentration of 0.75 g/L was used in order to get about the same concentration as the supernatant collected after heating.

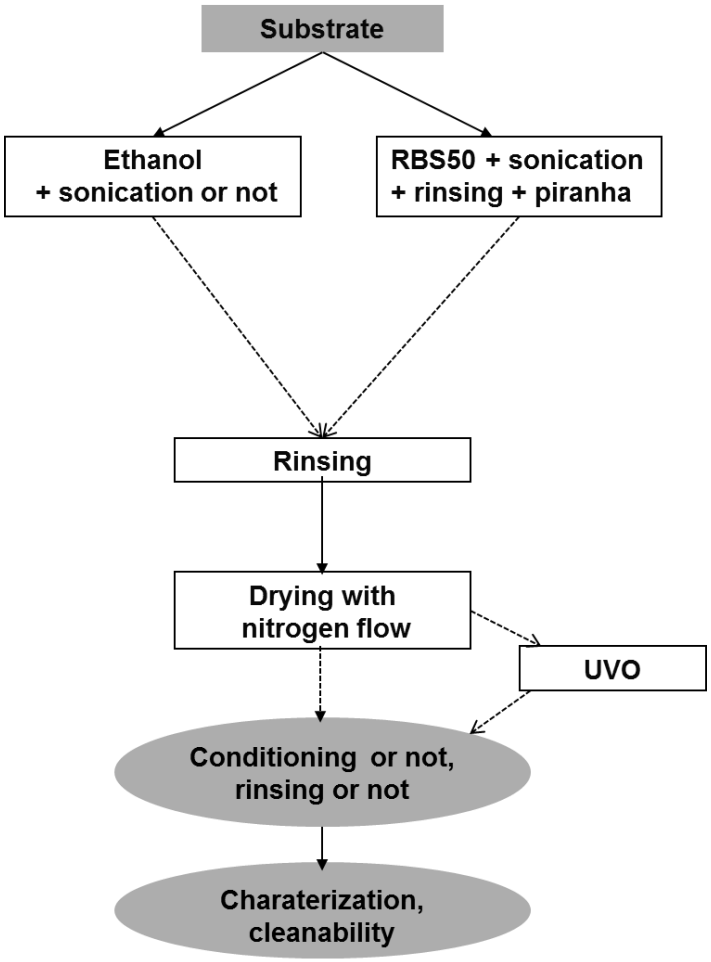

Figure 1. Sketch of the substrate pretreatment protocols.

2.3. Soil Model

Ground quartz, characterized by a particle size distribution of 1 to 60 µm, was provided by Sibelco Benelux (Belgium). A narrower size distribution (target 10 to 30 µm) was isolated

from the initial batch by repeated sedimentation, using conditions based on the following equation (Maciborski et al., 2003; Andre et al., 2011):

$$V_p = gd^2 \frac{(\rho_p - \rho_m)}{18\mu} \qquad (1)$$

where V_p is the rate of sedimentation of an isolated particle, d is the particle diameter, $(\rho_p - \rho_m)$ is the density difference between the particle and the fluid of known viscosity μ and g is the gravitational constant. Knowing the settling velocity V_p, the time t needed to traverse a height D can be determined as $t = D/V_p$. The particle size distribution (Mastersizer 2000, Malvern Instruments, United Kingdom) of the isolated fraction was unimodal, ranging from 7.6 to 32.7 μm diameter ($D_{10\%}$ = 10.6 μm; $D_{50\%}$ =17.1 μm; $D_{90\%}$ = 27.1 μm). This fraction was used as particulate soil model throughout the thesis.

As illustrated in Figure 2, four kinds of quartz particle suspensions were prepared at a concentration of 150 g/L: (a) in water, (b) in a macromolecule solution, (c) same as (b) with subsequent rinsing, (d) same as (b) with subsequent heating at 75°C (only for β-LGB) and cooling down.

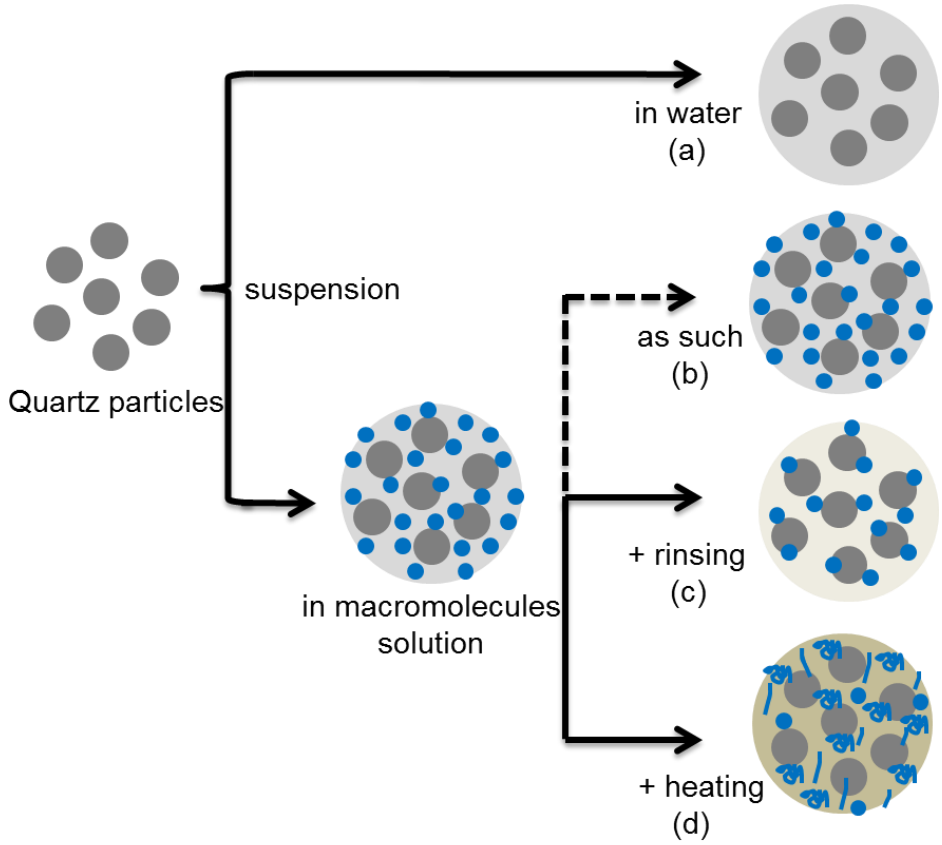

Figure 2. Schematic representation of the prepared particulate soils.

2.4. Soiling procedure and cleaning experiments

The surfaces were soiled with the above mentioned quartz particle suspensions brought at room temperature. Suspension droplets were deposited by 4 successive manual aspersions using a thin layer chromatography (TLC) sprayer located at a distance of 40 cm from the substrate (Detry et al., 2011). This did not lead to formation of a continuous liquid film and no drainage occurred. The surfaces were dried for 30 min in a dark cupboard at room temperature to have always the uniform environment conditions, or in an oven at 75°C. The coupons were then submitted within 2 min to the cleaning test. The relative moisture content and temperature of the dark cupboard, recorded with a Testo 175-H2 logger (Testo, Germany) every hour during periods of three weeks, were 39±3% and 20.6±1.9°C, respectively, and were in agreement with previous records (Detry et al., 2007; 2011).

Cleanability assessment was performed using a radial flow cell (RFC) which consists of two parallel discs with a narrow spacing in-between. The cleaning fluid is pumped at a constant volumetric flow rate through the center of the upper disc and flows radially outward between the discs (Figure 3). The wall shear stress near the surface decreases radially across the disk, submitting any adhered soil to a continuous range of shear forces in one experiment. A complete description of the device and of its hydrodynamics can be found elsewhere (Detry et al., 2007; 2009a; 2009b). Here, distilled water (20°C) was flown between the sample plate and the upper disc set 1 mm above the sample during 5 min with a flow rate of 40, 90, 190 or 390 ml/min. The duration of 5 min for each flow-rate step was chosen for practical convenience. The flow rate was selected with the aim of comparing samples, according to previous studies (Detry et al. 2007; 2011). The soiled sample was immersed in the flow cell container. Then, the upper disc of the RFC was placed and the sample was immediately exposed to a flow at the desired flow rate.

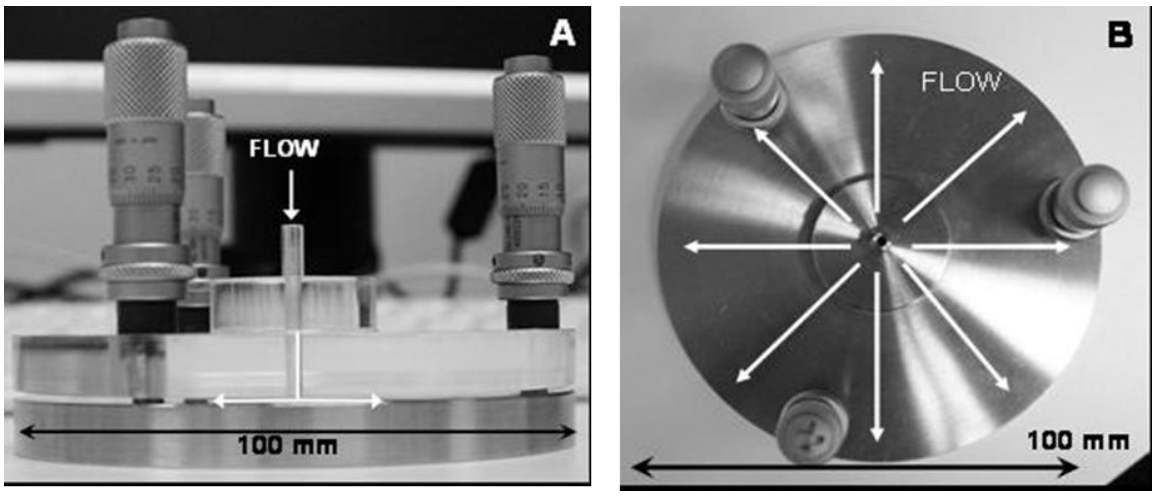

Figure 3. The radial-flow cell, side view (A) and top view (B) from (Detry et al., 2009a).

Pictures of the substrate were taken before and after cleaning, using an epifluorescence stereomicroscope (ZX9 Olympus, Belgium) equipped with a CCD camera, a mercury vapour UV lamp (100W, emission range 100-800 nm) and UV filters (passing bands: excitation 460-490 nm, emission > 520 nm). After cleaning, a circular zone with a lower density of soiling entities was observed at the center of the sample (Figure 4). This zone is where particle removal occurs. The pictures of the sample before and after cleaning were processed with a specific application of the Matlab software (The Mathworks Inc.), which gave the ratio of the number of entities initially present on the surface to the number of that remaining after cleaning, as a function of the radial position. The radial position at which the residual density of soiling entities was half the initial density was considered as the critical detachment radius (Goldstein and Dimilla 1997; 1998). The value of the critical radius was checked for consistency in the LUCIA software (LIM, Prague, Czech Republic) to insure the absence of artifacts such as the nucleation of air bubbles on the surface. At least 10 repetitions of each experiment (soiling-cleaning) were made, being distributed in at least three independent series. The error bars were given by the standard deviations.

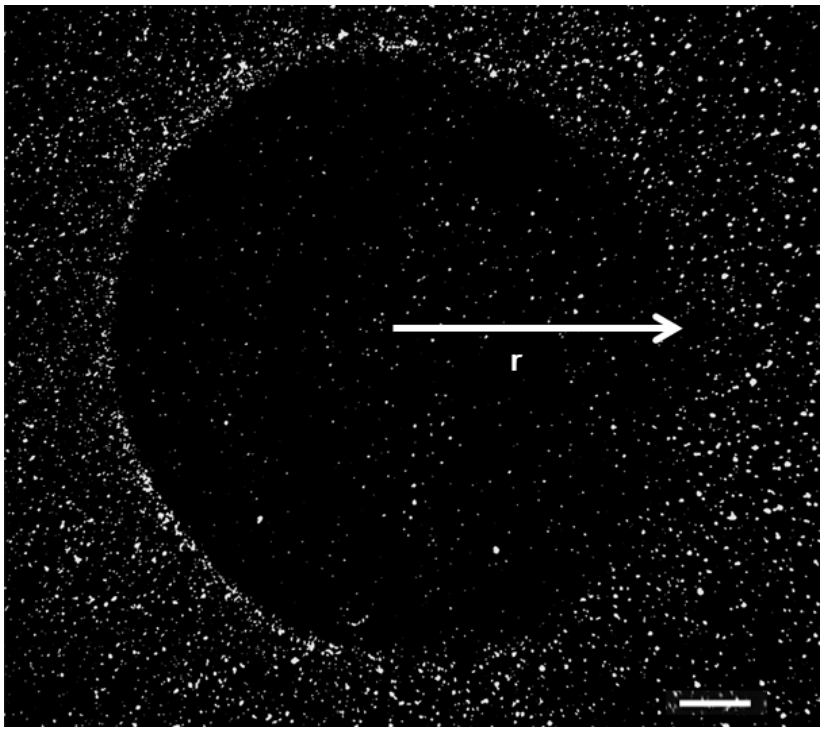

Figure 4. Representative picture obtained on a quartz-soiled stainless steel surface dried 30 min in air and submitted for 5 min to a flow rate of 40 ml/min in the radial-flow cell. Scale bar: 1 mm.

2.5. Methods of characterization

2.5.1. Characterization of the soiling entities

This concerns the soils entities left after drying the soiled substrates.

2.5.1.1. Size and height measurements

The individual size and height of the soiling entities were determined with a Nikon Eclipse E400 microscope (magnification 20X) equipped with a CCD camera, a mercury vapour UV lamp, a dichroic mirror (reflection band 446-500 nm, transmission band 513-725 nm) and UV filters (passing bands: excitation 447-517 nm, emission 496-576 nm). The equivalent diameter of entity contours was determined using the LUCIA G image analysis software (LIM, Prague, Czech Republic) and the equation below:

$$\text{diameter} = 2(\text{area} / \pi)^{1/2} \qquad (2)$$

The height of the entities was determined by focusing on the substrate and on the top particle after calibration of the microscope screw graduations with a polystyrene sheet (250 µm thickness corresponding to 147 ± 3 graduations).

Optical micrographs obtained on polystyrene were studied in more detail by image analysis in order to test the significance of differences between samples. The entities contours were defined using three different threshold gray levels: 40, 90 and 180. For each threshold, data were exported into a txt-file and processed using an Excel tool, providing the size distribution, i.e. the number of objects per class size defined as ≤ 30 µm, 30 to 90 µm and > 90 µm.

2.5.1.2. Scanning electron microscopy (SEM)

The morphology of the soiling entities was examined by scanning electron microscopy (DSM 982 Gemini from Leo, field-effect gun). The images were obtained using an accelerating voltage of 1 kV. Samples were examined after deposition of a 10 nm-thick chromium coating.

2.5.2. Substrate characterization

2.5.2.1. Contact angle

Static contact angles of water and different solutions were measured at room temperature, using the sessile drop method with a goniometer (Krüss, Germany), or using image analysis (instrument made by Electronisch Ontwerpbureau de Boer, The Netherlands; measurement 5 s after drop deposition), on the other hand. The measurements involved at least 10 drops.

Dynamic measurements of contact angles were also performed with certain systems using the Wilhelmy plate method (Krüss, Germany), recording 3 successive immersion - emersion (advancing - receding) cycles at a rate of 50 µm/s, as a function of the contact line position (Tomasetti et al., 2013).

2.5.2.2. X-ray photoelectron spectroscopy (XPS)

The surface composition was determined by XPS on substrates, either as such without particular treatment, or treated as described in subsection 2.2. The samples were fixed on a standard stainless steel holder by using a piece of double-sided insulating tape. The XPS analyses were performed with a SSX 100/206 photoelectron spectrometer from Surface Science Instruments (USA) equipped with a monochromatized micro-focused Al X-ray source (powered at 20 mA and 10 kV). A flood gun set at 6 eV and a Ni grid placed 3 mm above the sample surface were used for charge stabilization. The pressure in the analysis chamber was about 10^{-6} Pa. The angle between the perpendicular to the surface and the axis of the analyzer lens was 55°. The analyzed area was approximately 1.4 mm^2 and the pass energy was set at 150 eV for the survey spectrum and 50 eV for high energy resolution spectra. In the latter conditions, the full width at half maximum (FWHM) of the Au $4f_{7/2}$ peak of a clean gold standard sample was about 1.1 eV. The sequence of records is presented in the detailed sections (IV, V, and VI). The binding energy scale was set by fixing the C 1s component due to carbon bound only to carbon and hydrogen at 284.8 eV. The data treatment was performed with the CasaXPS program (Casa Software, Teignmouth, UK). Molar concentration ratios were calculated from peak areas (linear background subtraction) normalized on the basis of the acquisition parameters and of sensitivity factors and transmission function provided by the manufacturer. The C 1s peak was decomposed (Genet et al., 2008) by using a least square fitting procedure with a 85:15 Gaussian-Lorentzian product function. The linear regression equations between spectral data were computed using Excel software.

2.5.3. Suspending medium characterization

Surface tensions of the liquids were measured at increasing dilution (or not) with a Prolabo Tensiometer (Tensimat n°3) using Wilhelmy plate method. A deeper characterization was made on β-LGB solution and supernatants collected after heating. β-LGB powder was dissolved in MilliQ water at concentration of 3 g/L providing clear solution. Some solutions were heated for 4 h at 75°C and rapidly cooled down to room temperature. This resulted in a white turbid liquid, indicating protein aggregation. After centrifugation (Beckman centrifuge; Coulter Inc., USA; 25700 x g for 30 min), the supernatants were collected for different uses described as followed.

The UV-visible absorption spectra of β-LGB solution and supernatants were recorded with a Shimadzu UV 2401PC spectrophotometer, using a quartz cell with a light path length of 10 mm and pure water (MilliQ) as reference. The soluble protein contents in the β-LGB solution and the supernatants were determined in two ways. One way was the Kjeldahl method,

multiplying the nitrogen concentration by 6.34, specific of β-LGB. The other way was based on the absorbance at 278 nm, using the absorption coefficient of 1750 L/mol.cm determined for β-LGB (Stanley and Peter, 1989).

The intrinsic tryptophan fluorescence intensity of β-LGB solution and supernatants was measured at ambient temperature (spectrometer Jasco V-630, Japan). Fluorescence spectra were acquired with an excitation wavelength of 280 nm and recorded from 290 to 600 nm, using solutions diluted with MilliQ water to reach an absorbance of about 0.12.

Circular dichroism measurements (CD) and attenuated total reflectance-Fourier transform infrared spectroscopy (ATR-FTIR) were used to assess the secondary structure of β-LGB (α-helix, β-sheet, turn, unordered). Far-UV CD spectra (185-260 nm) were recorded with a Jasco J-810 spectropolarimeter at 20°C in Milli-Q water, using a 1 mm pathlength quartz Suprasil cell (Hellma), with protein concentrations of *ca*. 0.1 mg/ml. Four scans (20 nm/min, 1 nm bandwidth, 0.2 nm data pitch and 2 s DIT) were averaged, base lines were subtracted and no smoothing was applied. Secondary structure analyses using the CDSSTR (Manavalan et al., 1987; Sreerama and Woody, 2000), CONTINLL (Provencher and Glockner, 1981; Van Stokkum et al., 1990) and SELCON3 (Sreerema et al., 1993, 1999) algorithms were performed on the CD data with the Dichroweb analysis server (Whitmore and Wallace, 2004, 2008), using both reference datasets 3 and 6. The accuracy of the analysis was checked through the goodness-of-fit parameter (NRMSD) values.

Attenuated total reflectance Fourier transform infrared (ATR-FTIR) spectra were recorded (4 cm^{-1} resolution, 64 co-added scans) with a Vertex 70 - RAM II Bruker spectrometer (Bruker Analytical, Madison, WI, USA) operating with a Golden Gate diamond ATR accessory (Specac Ltd., Slough, UK). 10 µL of the solution were deposited on the diamond and dried with gentle air flow. More details about the instruments, the mode of measurement, the background used and the acquisition parameters may be found elsewhere (Stefanov et al., 2013; Pierna et al., 2012). After an area normalization with a linear method, mathematical models were applied to evaluate the secondary structure, as described before (Goormaghtigh et al., 2006). Data processing was performed with a homemade software running under the MatLab 7.1 environment (The MathWorks, Natick, MA).

3. MAIN RESULTS

3.1. Solutions characteristics

3.1.1. Dextran and BSA containing solutions *(Details in Sections II & III)*

The surface tensions of water, of dextran and BSA solutions and of supernatants of quartz particles suspensions in water and in dextran and BSA solutions were determined. There was no significant difference between the surface tension of water (72 mN/m), dextran solution (72.5 mN/m) and supernatant of quartz suspension in water (72.9 mN/m). The surface tension of the supernatant of the quartz suspension in dextran solution was slightly lower (68.6 mN/m). The presence of BSA in the liquid phase markedly decreased the surface tension, giving 30 and 49 mN/m for the BSA solution and for the supernatant of the quartz suspension in BSA solution, respectively.

3.1.2. β-LGB solution and supernatant *(Details in Sections V & VI)*

Heating the β-LGB solution for 4 h at 75°C resulted in a white turbid liquid, indicating protein coagulation. Figure 5 shows that the absorbance of the maximum near 278 nm decreased from 2.3 for the native solution, to 0.7 for the supernatant collected after heating. No significant absorption was observed above 310 nm, in contrast with the non-centrifuged heated solution, which showed an absorbance above 3 between 310 and 700 nm. This indicated that centrifugation insured an efficient separation between aggregates, responsible for strong light scattering, and dissolved molecules. Note that preliminary tests showed no significant variation of the supernatant absorbance at 278 nm when heating was performed at 60°C; they showed a progressive variation at 75°C, and a very quick protein coagulation near 95°C. Supernatants collected after heating for 4 h showed protein concentrations of 0.6 g/L, compared to 2.5 g/L for the native solution. Heating the β-LGB solution at 75°C thus provoked aggregation of about 75% of proteins after 4 h. In agreement with Ikeda and Li-Chan (2004), infrared spectra of the pellet obtained after heating and centrifugation showed that coagulation involved a loss of α-helices and a rise of disordered structures.

The secondary structure of β-LGB in solution investigated using CD, revealed no significant difference between the supernatant collected after heating and the native β-LGB solution. However, fluorescence spectra showed a small increase of the spectrum intensity and a red shift of the supernatant, suggesting a conformation change of molecules remaining in the aqueous phase after heating. A more convincing result is provided by Figure 6 which shows a lower surface tension for the supernatant compared to the native protein solution at the same concentration. The β-LGB remaining in the supernatant thus demonstrates a higher activity at the water/air interface (Schmitt et al., 2007; McClellan and Franses, 2003), which reveals a conformational modification of the molecules.

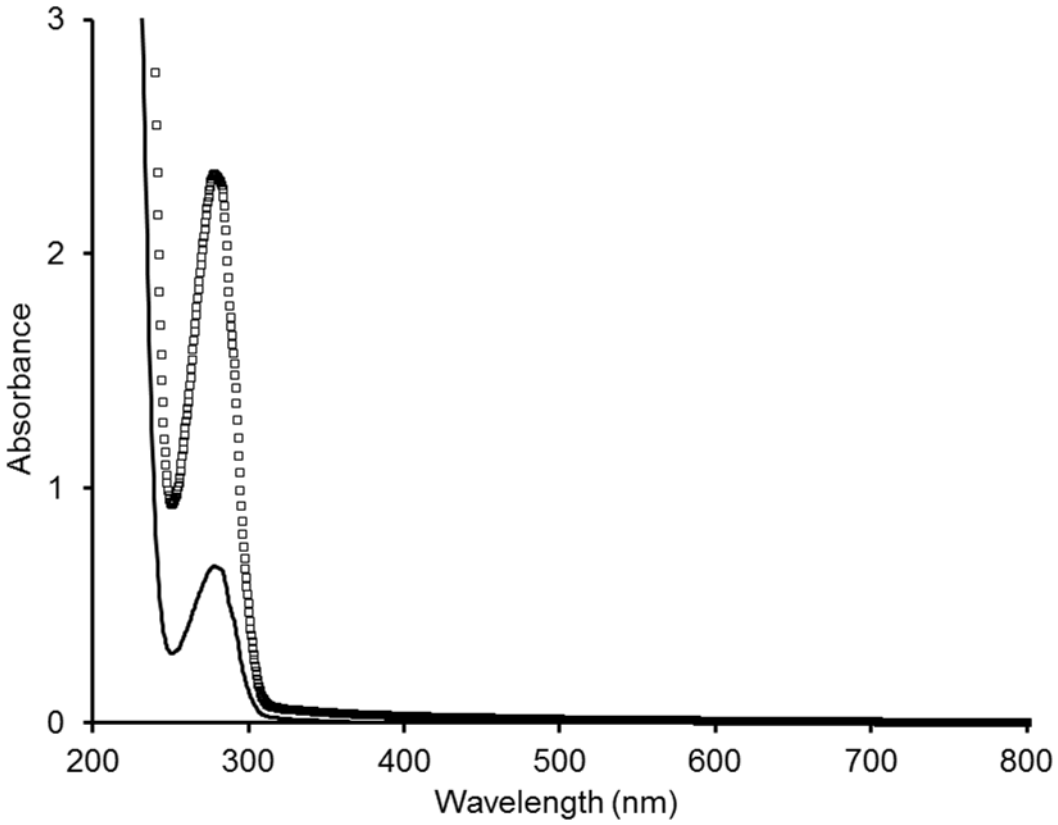

Figure 5. UV-visible absorption spectra of native β-LGB solution (▫▫▫) and supernatant collected after heating a β-LGB solution for 4 h at 75°C (—).

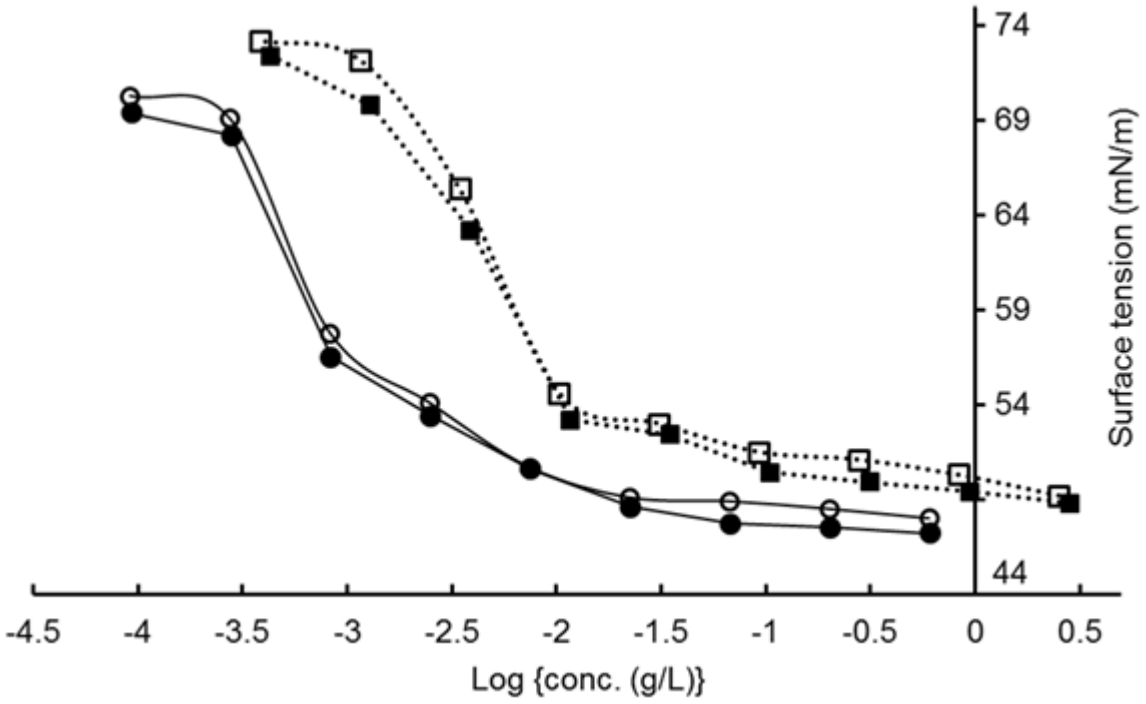

Figure 6. Variation of the surface tension as a function of the protein concentration resulting from increasing dilution of native β-LGB solution (□,■) and supernatant collected after heating a β-LGB solution for 4 h at 75°C (●,○). Open and closed symbols represent two sets of data acquired independently.

3.2. Substrate characterization

3.2.1. Chemical composition *(Details in Sections III & VI)*

The XPS spectra provide the surface composition in terms of concentrations of elements and of specific forms of certain elements, given in mole fractions with respect to the sum of all elements except hydrogen. The surface analysis of inorganic solids by X-ray photoelectron spectroscopy always shows the presence of carbon (Gerin et al., 1995; Caillou et al., 2008; Rouxhet, 2013). This is due to organic compounds which may originate from material processing, from artifacts due to sample preparation, or from contamination by adsorption from the surrounding, either the ambient atmosphere or the spectrometer vacuum chamber. Drawing meaningful information from XPS spectra is complicated by the presence of such organic contaminants in addition to expected adsorbate and by overlap of solid and adsorbate contributions.

Ideally, the adsorbed organic layer should be characterized by the adsorbed amount of each constituent, expressed in mass per unit area or in thickness. This was not possible here owing to uncertainties in modeling the organization of the layer probed by XPS. Nevertheless, data treatments allowed comparisons to be made between adlayers of samples involving the same substrate. This was based on the concentration of elements and on the decomposition of the C 1s peak, which provides the distribution of carbon among different chemical functions. The O 1s peak could not be decomposed in components specific of different forms of oxygen, due to the overlap of contributions of the substrate, of biomacromolecules (BSA, β-LGB or dextran) and of organic contaminants. However a distinct evaluation of inorganic forms of oxygen, due to the substrate (for glass and stainless steel), and of organic forms, due to the adlayer, was made by deducing the organic oxygen concentration from the concentration of carbon in oxidized form $C_{ox} = C_{tot} - C_{284.8} - C_{sh}$, where $C_{284.8}$ is the concentration of carbon bound only to carbon and hydrogen [C-(C, H)] and C_{sh} is the concentration associated to the shake up peak observed for polystyrene.

Based on the amounts of different amino acids in BSA (Hirayama et al., 1990) and β-LGB (Walstra and Jenness, 1984; http://www.uniprot.org/uniprot/P02754), the elemental composition as well as the chemical functions associated with the components of the C 1s and O 1s peaks and their concentrations were computed for these proteins. This computation provides stoichiometry formula and molar concentration ratios presented in table 1. These molar ratios were used to exploit correlations between independent spectral data (elements, C 1s peak components) which validated the C 1s peak decomposition and component assignment.

Table 1. Molar concentration ratios and stoichiometry formula computed for β-LGB and BSA based on the amounts of the different amino acids.

Molar ratio	BSA	β-LGB
C_{tot}/N	3.76	3.97
O_{tot}/N	1.15	1.20
$C_{284.8}/N$	1.75	1.92
C_{ox}/N	2.01	2.05
Molar mass	66464	18281
Formula	$C_{3.76}O_{1.15}N_1S_{0.05}H_{5.92}$	$C_{3.97}O_{1.20}N_1S_{0.04}H_{6.38}$
Molar mass of formula	85.21	88.74

Comparisons between adlayers of samples involving the same substrates were based on different quantities, which provide complementary pieces of information. The sum of concentrations of elements due to the adsorbed layer, ΣAdlayer, and due to the solid, ΣSubstrate allows a comparison to be made in terms of amount of organic compounds present at the surface. Table 2 (left part) gives the proportion of elements belonging to the organic adlayer (ΣAdlayer) computed for glass, stainless and for polystyrene samples. Data regarding additional samples, rinsed more or less than three times, are given in *Section III*. Conditioning glass and polystyrene with protein increased significantly the proportion of the organic adlayer, which was decreased slightly for glass and much more for polystyrene by subsequent rinsing. After conditioning with dextran, rinsing provoked a strong reduction (60% for polystyrene and 76% for glass) of the contribution of the amount of adlayer. For stainless steel, the amount of adlayer did not change much compared to the raw samples; in all cases the XPS spectrum was dominated by the contribution of the organic adlayer which was strongly screening the substrate.

The composition of the organic adlayer was determined by the molar ratios O_{org}/C_{tot}, N/C_{tot} and O_{org}/N, which are presented in Table 2 (central columns). With protein conditioned substrates (glass and stainless steel), the molar ratios O_{org}/C_{tot}, N/C_{tot} and O_{org}/N measured, indicate that the organic adlayer was dominated by the protein for most conditioned samples of stainless steel and glass, either rinsed or not. It was not the case for BSA-conditioned polystyrene where it is clear that after rinsing, BSA did not dominate the organic layer. Dextran-conditioned solids showed a small concentration of nitrogen, which was not observed for non-conditioned solids. This was attributed to contamination of the glass vessels by proteins, presumably BSA because experiments were conducted at the same time. For dextran-conditioned polystyrene, the molar ratio O_{org}/C_{tot} was far from the value expected for dextan, possibly due to its low adsorption and to the polystyrene substrate contribution to C_{tot}.

With glass, comparisons between the molar ratios O_{org}/C_{tot} of dextran-conditioned samples, the values expected for pure dextran and the values measured on bare samples, show that rinsing induced a complete desorption of dextran. This means that dextran was easily desorbed during the cleaning test.

Table 2. Surface composition deduced by XPS for representative bare substrates and conditioned substrates, rinsed thrice or not: contributions of the organic adlayer to the XPS spectrum; composition (mass %) of the organic adlayer present on the solids, and molar ratios in organic adlayer. Values expected for pure dextran, BSA and β-LGB.

			Proportion (%) of elements due to the adlayer	Molar ratios in organic adlayer			Organic composition (mass %)		
Substrate pre-cleaning	**conditioning liquid**	**rinse**	**ΣAdlayer**	**O_{org}/C_{tot}**	**N/C_{tot}**	**O_{org}/N**	**Protein**	**Dextran**	**Hydrocarbon**
Polystyrene									
Eth	none		5.1		n.a.			n.a.	
	Dextran (8 g/L)	none	16.3	0.06	n.a.		7.5	10.2	82.3*
		thrice	7.2	0.03	n.a.		4.4	4.1	91.5*
	BSA (8 g/L)	none	85.3	0.26	0.22	1.2	87.3	n.a.	12.7*
		thrice	37.4	0.11	0.06	1.77	34.1	n.a.	65.9*
Glass									
none	none		56.5	0.22	0.02	n.r.	11.4	n.a.	88.6
Eth			39.3	0.30	0.03	n.r.	12.8	n.a.	87.2
UVO			30.2	0.20	0.00	n.r.	1.7	n.a.	98.3
Piranha			22.2	0.30	0.00	n.r.	0.0	n.a.	100.0
Piranha	Dextran (8 g/L)	none	102.7	0.75	n.r.	n.r.	0.6	94.2	5.2
		thrice	25.2	0.31	n.r.	n.r.	6.3	49.9	43.8
	BSA (8 g/L)	none	81.6	0.30	0.23	1.34	87.3	n.a.	12.7
		thrice	64.6	0.29	0.22	1.31	86.1	n.a.	13.9
Eth	β-LGB (3 g/L)	thrice	56.9	0.30	0.21	1.46	84.4	n.a.	15.6
UVO			65.6	0.28	0.21	1.34	86.7	n.a.	13.3
Eth	β-LGB (0.75 g/L)		59.9	0.30	0.20	1.48	83.1	n.a.	16.9
UVO			53.1	0.25	0.22	1.14	92.6	n.a.	7.4
Eth	Supernatant of		53.2	0.29	0.19	1.54	78.8	n.a.	21.2
UVO	β-LGB		40.7	0.24	0.19	1.29	81.4	n.a.	18.6
Stainless Steel									
none	none		94.2	0.21	0.03	n.r.	15.7	n.a.	84.3
Eth			71.3	0.29	0.02	n.r.	10.7	n.a.	89.3
UVO			62.1	0.12	0.00	n.r.	0.0	n.a.	100.0
Eth	β-LGB (3 g/L)	none	95.6	0.29	0.20	n.r.	82.2	n.a.	17.8
		thrice	70.4	0.25	0.14	1.76	63.0	n.a.	37.0
UVO			85.6	0.32	0.15	2.17	61.2	n.a.	38.8
Eth	β-LGB (0.75 g/L)		72.3	0.24	0.14	1.72	62.9	n.a.	37.1
UVO			74.2	0.32	0.21	1.54	83.3	n.a.	16.7
Eth	Supernatant of		72.9	0.25	0.18	1.39	76.8	n.a.	23.2
UVO	β-LGB		71.2	0.30	0.19	1.60	78.6	n.a.	21.4
Expected for dextran				0.83	n.r.	n.r.			
Expected for β-LBG				0.30	0.25	1.20			
Expected for BSA				0.31	0.27	1.15			

n.r. not relevant; n.a not applied; * this includes the contribution of the polystyrene substrate

In order to get a better quantitative representation of the organic composition of the organic layer, the relative mass concentrations of the constituents were computed from the mole fraction of markers and the related molar mass. From the exploitation of the correlation data, it appeared that N could be taken as a marker for protein, ($C_{284.8}$ − 1.75*N) or ($C_{284.8}$ − 1.92*N) as a marker for hydrocarbon moieties due to contaminants and, or to polystyrene

after conditioning with BSA and β-LGB, respectively, and (C_{ox} – 2.01*N) for dextran. Multiplying the molar concentration of markers (mole/100 moles) by the molar mass of the relevant constituent and dividing by the number of marker moieties in the compound formula provides the concentration of each constituent (W, in g/100 moles of elements detected by XPS). Dividing W of each constituent by the sum of W for all constituent and multiplying by 100 finally gave the mass concentration in % of the constituent in the volume probed by XPS. The results are given in Table 2 (right part).

Consideration of both ΣAdlayer and organic composition indicated that an appreciable amount of dextran was present at the surface of glass after conditioning but most of this was lost upon rinsing. The amount of dextran present on dextran-conditioned polystyrene, even not rinsed, was not higher than the amount of protein. The organic adlayer on polystyrene conditioned with BSA represented more than 85% of protein and decreased down to about 30% after rinsing. The different quantities presented in Table 2 showed that proteins were the dominating constituent (above 80 mass %) in the adlayer present in protein-conditioned glass and were not markedly removed by rinsing, indicating that proteins were still present during the particles detachment with water flow. In the case of stainless steel, the proportion of organic adlayer was not considerably affected by the presence of β-LGB, owing to a thick layer of contaminants. However, the composition of the organic adlayer indicates a protein contribution above 60% on conditioned samples. For both glass and stainless steel, it seems that organic contaminants present before conditioning were displaced by protein adsorption or that the presence of proteins prevented contamination from the surroundings. It is noteworthy that the amounts of β-LGB in adlayer on glass and stainless steel was not affected by the protein state, either native or denatured.

3.2.2. Wetting properties *(Details in Sections III, IV & VI)*

Figure 7 presents the contact angles measured for different substrates (glass, stainless steel, polystyrene) and different pretreatments (Ethanol, UVO, piranha, conditioning), using water, aqueous solution of macromolecules (dextran, BSA, β-LGB) and the supernatant collected after heating β-LGB solution for 4 h at 75°C. The results show that the nature of the liquid had a much weaker influence on the contact angle compared to the substrate nature and pretreatment.

Glass and polystyrene gave a low and a high contact angle, respectively, as expected. However, the water contact angle of polystyrene was lower than expected, owing to the presence of oxygen, oxidized carbon and silicon at its surface, as demonstrated *in Section III*.

For both glass and stainless steel, the UVO treatment decreased contact angles from about 20° for glass and 30-40° for stainless steel to about 10°; this occurred also after piranha treatment of glass. Pre-cleaning with ethanol does not bring the water contact angle to low values expected for oxides or oxihydroxides present at the surface of glass and stainless steel, indicating that it did not remove the totality of organic surface contaminants, as revealed by XPS (Table 3.2). An additional UVO or piranha treatment insured a more effective removal of organic contaminants by oxidation, as revealed by the low contact angle achieved. It must be noted that high energy surfaces cleaned by UVO treatment and left in ambient air show a quick increase of the water contact angle due to adsorption of organic compounds. For gold and stainless steel, the increase is quite steep, the contact angle reaching values above 20 ° in a few hours, and above 60 ° in less than 1 day for gold and a few days for stainless steel. For silica slab, the increase is significant only after several days, providing a contact angle of the order of 20 ° (Rouxhet, 2013).

Conditioning glass with BSA after piranha treatment led to a slight increase of the contact angle, which remained however in the range of 10 to 20°; on the other hand, conditioning polystyrene with BSA provoked a strong decrease of the contact angle, from the range of 80 to 85° to the range of 25 to 30°. The contact angle measured with an aqueous solution containing BSA was not markedly different from that measured with water. This is in relation with the fact that the contact angle was measured in advancing conditions, and that BSA was not present on the surface to be wetted. According to the literature (Kosaka et al., 2005; Almeida et al., 2002; Yang et al., 1991), protein conditioning of hydrophilic substrates leads to an increase of the water contact angle while conditioning of hydrophobic substrates leads to a decrease of the contact angle. In the case of hydrophobic substrates, protein adsorption may be driven by hydrophobic bonding, so that hydrophilic amino acids tend to be oriented toward water and remain so upon drying. In the case of hydrophilic substrates, the hydrophilic moieties should tend to get buried during drying in order to decrease surface energy. The fact that conditioned substrates fall in the same range of contact angles may be the consequence of the two mechanisms.

In the presence of dextran, the great difference between glass and polystyrene was maintained in all conditions (substrate conditioned or not, presence of dextran or not in the solution). Moreover, conditioning the substrates with dextran led to a slight increase of the contact angle, irrespective of the liquid used. This may be due to contamination with BSA as revealed by XPS, and is thus not significant.

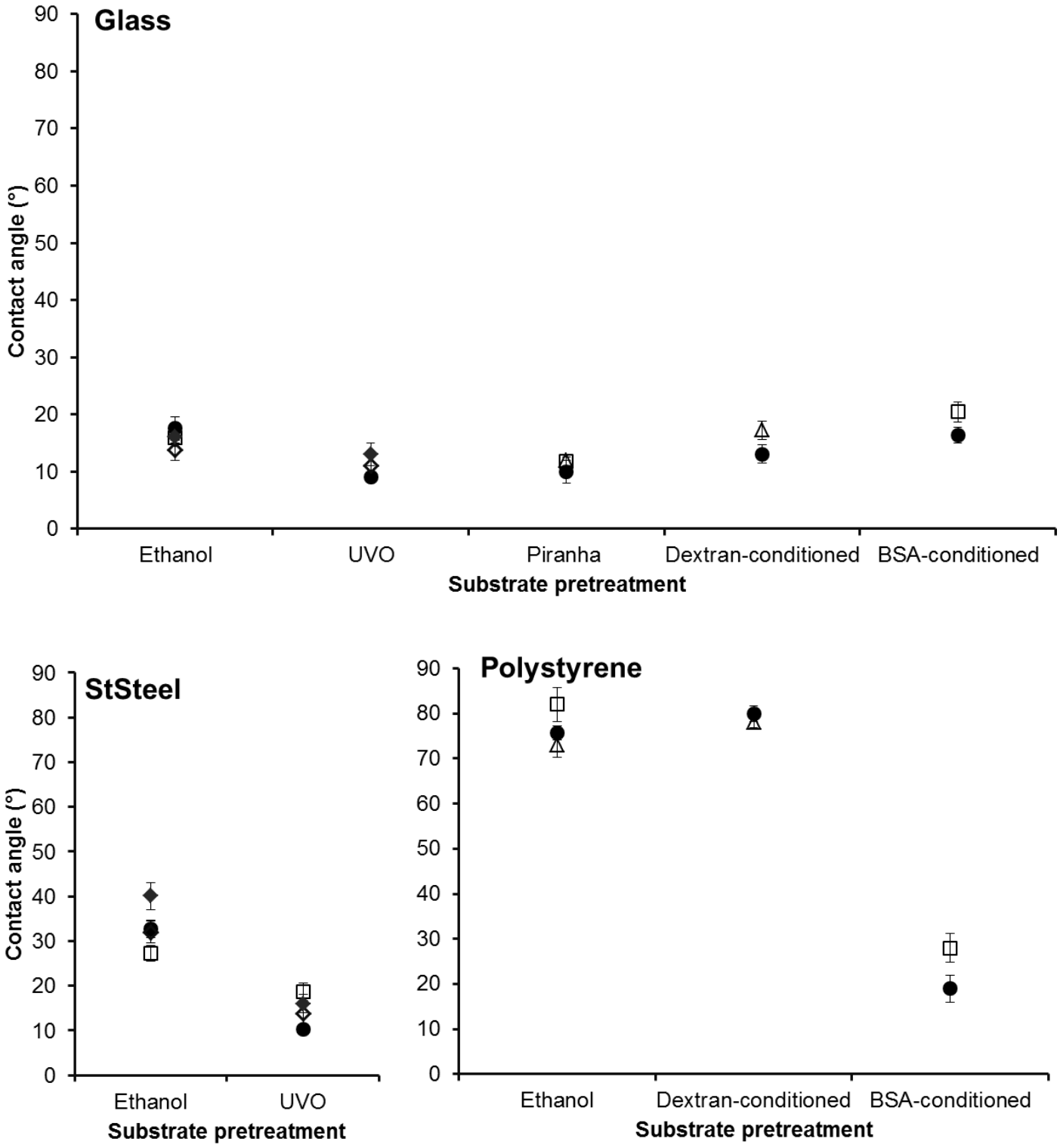

Figure 7. Contact angle measured on glass, stainless steel and polystyrene pretreated as indicated, using water (●), aqueous solution of dextran (△), BSA (□), or β-LGB (◇), and supernatant (◆) collected after heating β-LGB for 4 h at 75°C.

3.3. Soil entity distribution and morphology *(Details in Sections II & III)*

Representative optical and SEM micrographs of the quartz entities left after soiling and drying are presented in Figure 8 for the different systems involving glass and polystyrene as substrates and dextran and BSA as biomacromolecules. In absence of protein, a difference is noted between glass and polystyrene regarding both the number of soiling objects and their morphology. Measurements made on a large population showed that the density of soiling entities on polystyrene (33±4 entities/mm^2) was lower compared to glass (51±4 entities/mm^2), which was due to suspension drops rolling and coalescing (*details in Section II*). For glass, some droplets could have coalesced due to the extended wetting, resulting in the formation of elongated motifs or more dispersed particles. For polystyrene, drop coalescence did not occur owing to the lower substrate wetting, leading to the formation of more rounded aggregates.

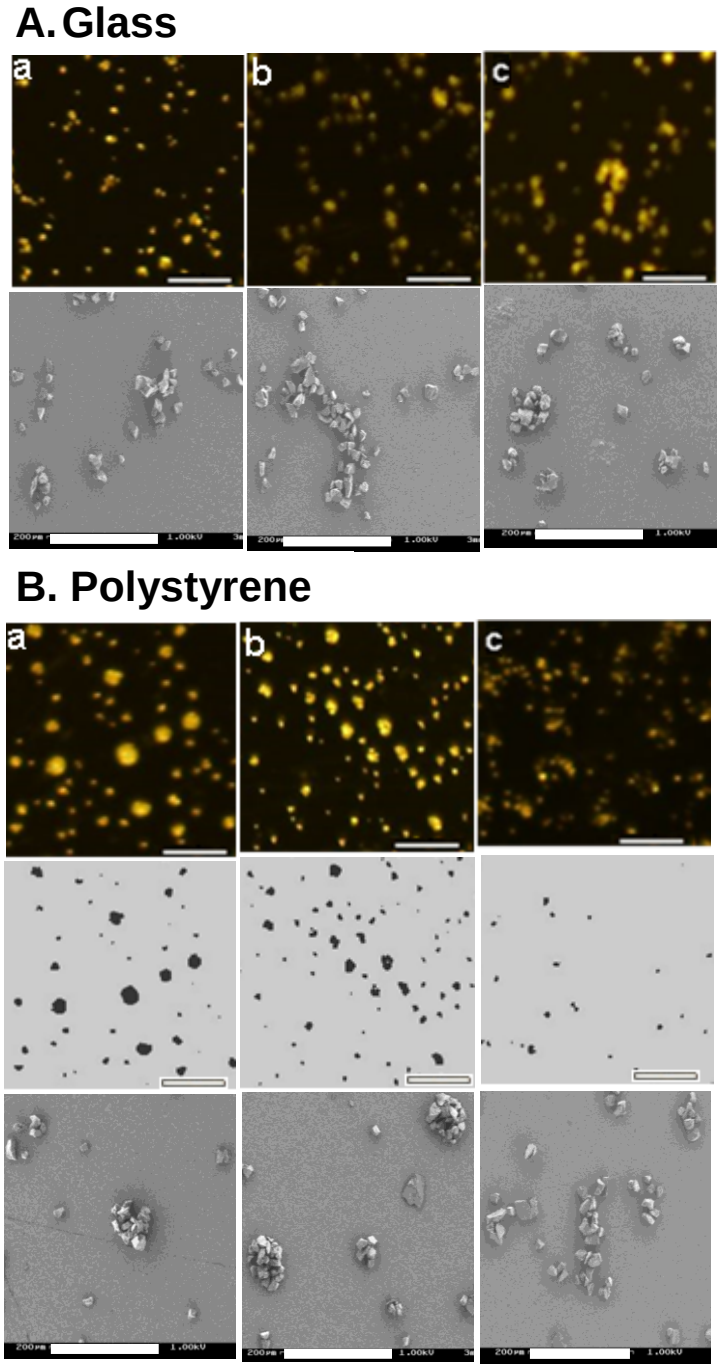

Figure 8. Representative micrographs of substrates soiled with quartz particles suspensions in water and dried. Glass (A) and polystyrene (B), bare (a) or conditioned with dextran (b) or BSA (c). Top line, stereomicroscope image, scale bar 300 µm; middle line (B), image obtained from top line after application of threshold 180; bottom line, SEM micrograph, scale bar 200 µm.

The relationship between the height of the soiling entities and the equivalent diameter of their contour was not influenced by the presence of dextran (*Section II*). However, both the height and the lateral size were larger on polystyrene compared to glass. On glass it could be observed by microscopy that the height of the aggregates never exceeded 2 layers of particles, independently of the lateral size. On polystyrene, the lateral size and the height of the entities increased to values much larger than the quartz particle size.

The optical micrographs obtained on polystyrene were studied in more detail to test the significance of differences between samples. The results were shown in the form of the surface density of objects and of their distribution in three size fractions: ≤ 30 µm, 30 to 90 µm, > 90 µm (*details in Section IV*). Increasing the threshold led to an increase of the small size fraction and a decrease of the large size fraction. Using a threshold of 180 decreased the number of counted objects and the decrease was much stronger for the systems involving BSA. In Figure 8B, the images obtained with a threshold of 180 can be compared with the direct micrographs and provide a clear evidence of lower aggregation of particles on polystyrene soiled in the presence of BSA. The dependence of the morphology of adhering soiling entities on the substrate is explained by the contact angle, which affects spreading of drops of soiling suspension.

3.4. Cleanability

The critical detachment radius, which is the output of the cleaning experiments, is related to a critical wall shear stress and the minimal hydrodynamic drag force required to remove particles in the given experimental conditions (Jensen and Friis, 2004). With the radial flow chamber used, the conversion of critical radius into critical wall shear stress may be biased when the adhering aggregate height is not negligible with respect to the channel height and when the adherence is such that flow rates above 20 ml/min are required (Detry et al., 2009a; 2009b; 2011). Owing to these limitations, this conversion was not made here, but it may be kept in mind that, for a defined flow rate, the higher the critical radius, the lower the adherence.

The influence of dextran on cleanability was examined first, using glass (hydrophilic) pre-cleaned with piranha and polystyrene (hydrophobic) (*Section II*). Both substrates were conditioned or not with dextran and soiled with quartz particle suspensions in aqueous solution containing or not a low concentration of dextran (0.08 mg/mL). Glass was found to be much less cleanable than polystyrene. Conditioning polystyrene with dextran increased slightly particles adherence, while the opposite was observed when conditioning glass with

dextran. The presence of dextran in the aqueous suspension, at the concentration used, did not affect the particles adherence, neither on polystyrene nor on glass, and whether the substrates were conditioned or not with dextran.

Using a dextran concentration hundred times higher (8 g/L) led to similar observations (*Section III*), as shown in Figure 9A, providing an independent observation that the major factor affecting cleanability was the substrate hydrophobicity. For glass, no detachment radius could be measured after cleaning at a flow rate of 40 ml/min, indicating that the shear stress generated at this flow rate was not high enough to provoke particle detachment. A flow rate of 390 ml/min had to be used in order to observe particle removal. For polystyrene, the detachment radius was larger than the microscope view field when the flow rate was 390 ml/min, indicating a much higher cleanability compared to glass. In order to examine the influence of conditioning, the detachment radii were measured by setting the flow rate at 40 ml/min.

Figure 9B presents the results of analogous experiments performed with BSA in lieu of dextran (*Section III*). The presence of BSA at the interface improved strongly the cleanability of glass, leading to values beyond those observed for polystyrene. For polystyrene substrate, the particles detachment was not significantly influenced by the presence of BSA, whether due to substrate conditioning or to the quartz suspension medium.

The comparison between soiling quartz suspensions in water, in BSA solution and in β-LGB solution was extended to stainless steel, in addition to glass and polystyrene. The presence of β-LGB in the soiling quartz suspension gave results analogous to those obtained with BSA (*Section IV*). The results revealed that stainless steel does not behave as a hydrophilic substrate. Moreover, the influence of stainless pre-cleaning procedure (ethanol treatment alone or followed by UV-Ozone treatment) emphasized the need to consider the initial surface state, owing to the surface contamination with organic compounds, as revealed by XPS results.

The presence of β-LGB at the quartz particle/stainless steel interface slightly increased the particle adherence which was further increased when β-LGB was denatured (*Section V*). However, these variations were small when compared with the difference between glass and polystyrene in the absence of protein or with the difference of glass cleanability in the presence and in the absence of protein.

The last experiments (*Section VI*) were designed to examine systematically the influence of surface nature including its initial surface state set by pre-cleaning, and of the suspending medium, including β-LGB denaturation. Glass and stainless steel treated only with ethanol (-

Eth.) or further treated with UV-Ozone (-UVO) were soiled with a quartz suspension in water and in β-LGB solution, either native or previously heated for 4 h at 75°C. As shown in Figure 10, the presence of β-LGB in the suspension used for soiling decreased strongly the particle adherence on glass, whatever the pre-cleaning. It brought the adherence on StSteel-UVO to the same range, starting from a lower level than glass. β-LGB denaturation further decreased slightly the adherence. The influence of β-LGB and of its denaturation is weak but occurs in the opposite direction for StSteel-Eth.

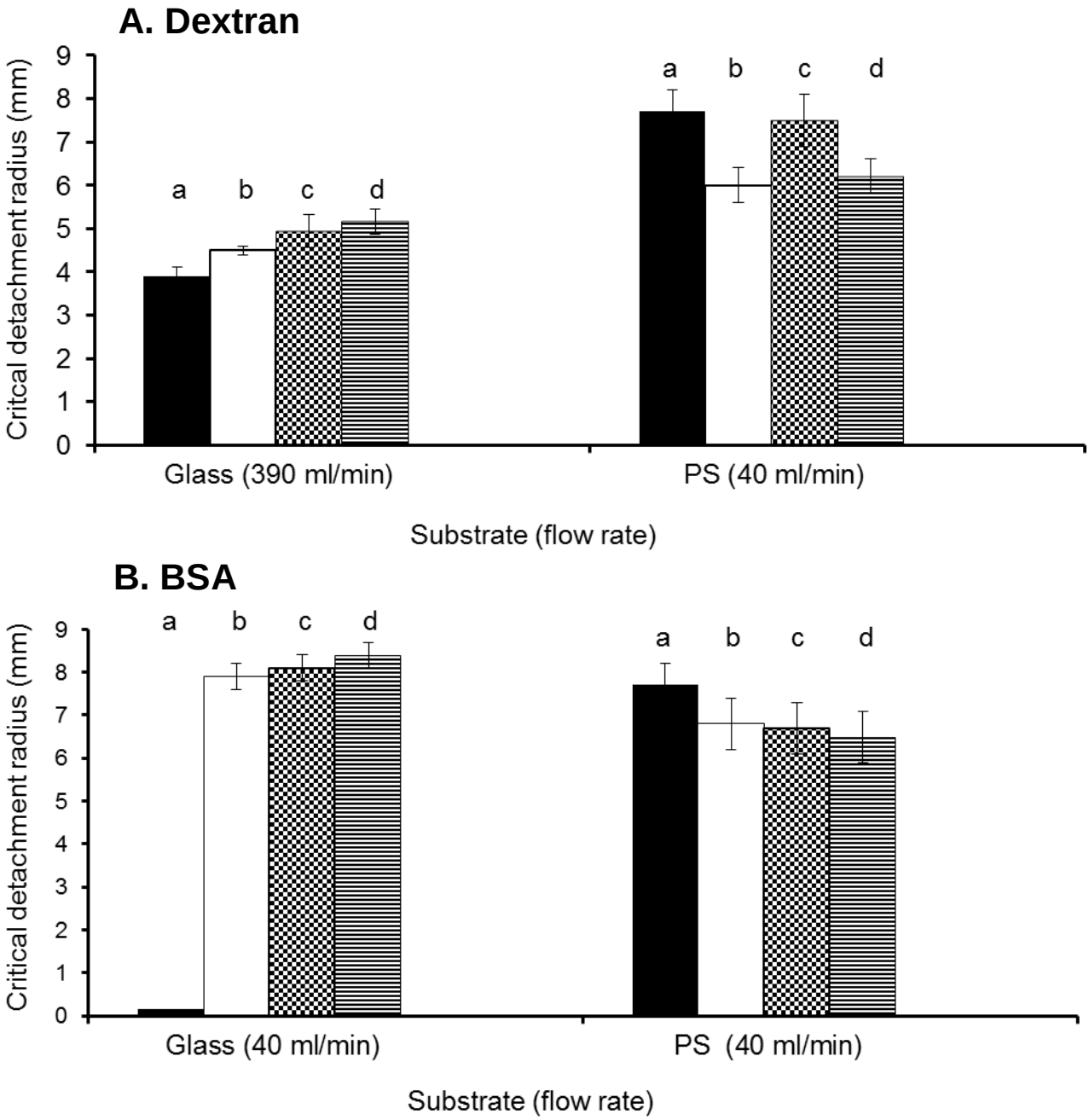

Figure 9. Critical detachment radius measured on bare substrates (a, c) and on substrates conditioned with macromolecules (b, d), soiled with quartz particles suspensions in water (a, b), or in a solution of macromolecules (c, d). The macromolecules were dextran (A) or BSA (B).

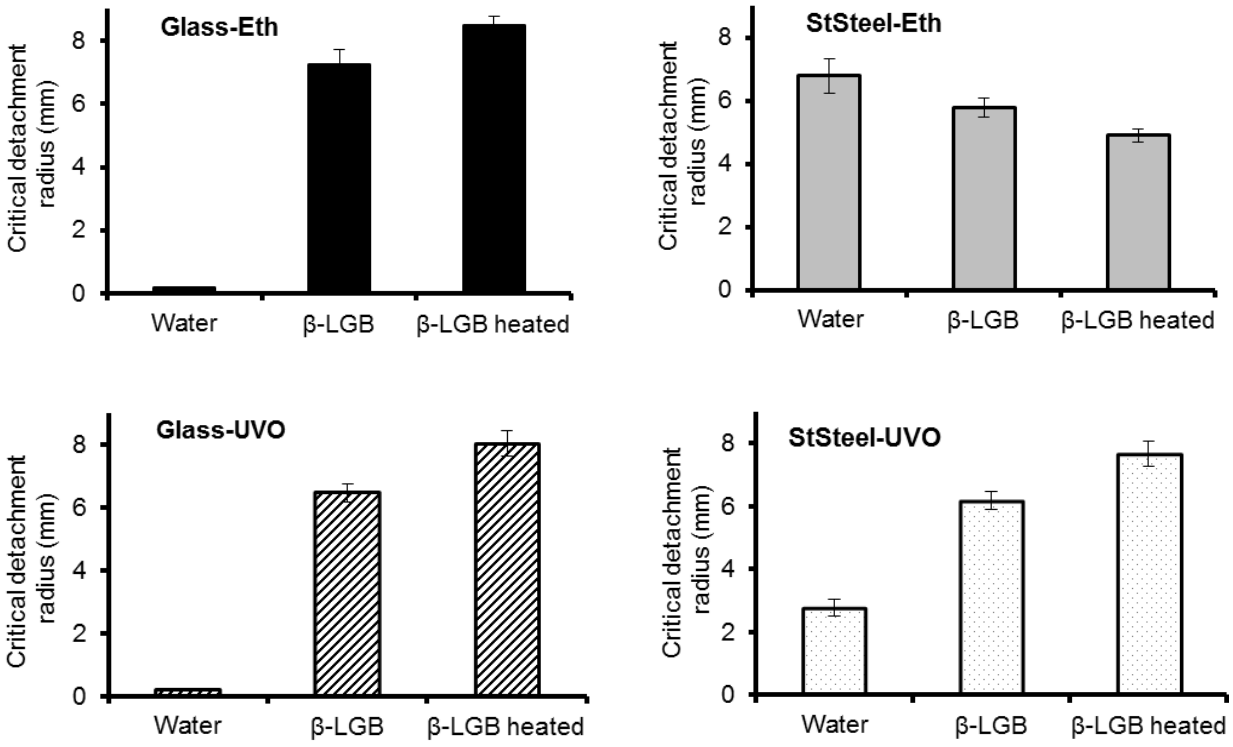

Figure 10. Critical detachment radii measured on glass and stainless steel, just pre-cleaned with ethanol (Eth) or further treated with UV-Ozone (UVO), soiled with quartz particles suspensions in water, with a suspension in β-LGB solution, and with a suspension in β-LGB solution previously heated for 4 h at 75°C.

4. PHYSICO-CHEMICAL MECHANISMS AFFECTING SOILING ENTITIES ADHERENCE

4.1. Substrate wetting and soiling entities morphology

The much higher cleanability of polystyrene, compared to glass, after soiling with a suspension of quartz particles in water was established by three independent sets of experiments presented in *Sections II, III* and *IV*. This reveals the major influence of substrate wetting as supported by the shape of soiling entities left after drying. Higher substrate wettability increases droplet spreading which leads to thinner aggregates formation. The rounder aggregates formed on hydrophobic polystyrene after soiling with suspension in pure water are more sensitive to wall shear stress than flatter ones formed on hydrophilic glass in the same conditions. This is in agreement with a study (Detry et al., 2011) of the adherence of starch granules on different substrates, including glass and polystyrene, using the same experimental approach as here. The explanation is that thinner aggregates are less sensitive to shear forces exerted by the flowing water. Moreover, capillary forces are enhanced at the interface between the particles and the substrate and insure a closer contact between the

surfaces. As a result, the adherence of soiling particles is increased as the substrate is better wetted.

4.2. Capillary forces and liquid surface tension

The examination of the influence of proteins (BSA, β-LGB) on the cleanability of glass and StSteel-UVO (Figure 10), whether proteins were brought by substrate conditioning or by the quartz suspension, is not in accordance with the only influence of the contact angle. The domination of proteins at interfaces, which was demonstrated by XPS, was found to improve markedly the glass and the StSteel-UVO cleanability although the contact angle did not change appreciably. On the other hand, conditioning polystyrene with BSA markedly decreased the water contact angle, which led to more flat aggregates, but this was not correlated with a significant change of cleanability. The explanation of the difference in the cleanability of the substrates is attributed to the strength of capillary forces developed in the course of drying, which depend on both the contact angle and the liquid surface tension.

Assuming spherical particles at a small distance of the substrate surface and considering a bridge of liquid forming a ring around the contact point, the particle-substrate capillary forces were computed using equation below (Rabinovich et al., 2002; Pitois et al., 2000):

$$F_{CAP} = 4\pi\gamma_L R\cos\left(\frac{\theta_p+\theta_s}{2}\right)\cos\left(\frac{\theta_s-\theta_p}{2}\right) \qquad (3)$$

where F_{CAP} is the capillary force (N), γ_L is the liquid surface tension (N/m), R is the soil particle radius (m), θ_S and θ_P are the contact angles of the liquid on the substrate and on the particles, respectively (*details in Sections III and VI*).

According to this computation, the higher cleanability of glass substrates (*Section III*) in presence of BSA compared to the cleanability in absence of BSA, for similar contact angles, may be attributed to the capillary forces. These were governed by a lower liquid surface tension, no matter whether BSA was brought, either by soiling suspension, or by desorption from conditioned-glass substrate into the soiling droplets.

Table 3 presents contact angles measured for systems studied in *Section VI*: substrates consisting in glass and stainless steel, pre-cleaned with ethanol (-Eth) and with additional UV-Ozone (-UVO); liquids consisting in water, β-LGB solution and supernatant collected after heating of β-LGB solution for 4 h at 75°C and computed capillary forces. Capillary forces were computed considering quartz particles of 9 µm radius, a particle contact angle θ_p of 10°, and surface tensions of 72.2, 48.8 and 47.2 mN/m for water, β-LGB solution and supernatant of the heated β-LGB solution, respectively.

For glass, whether pre-cleaned with ethanol or with an additional UVO treatment, and StSteel-UVO, F_{CAP} were around 8 µN when soiling was produced by a quartz suspension in water and slightly above 5 µN when soiling was produced by a quartz suspension in β-LGB or denatured β-LGB solution. This was not strongly affected by the value of the contact angle selected for the computation. The influence of β-LGB on the cleanability of glass and StSteel-UVO, is thus attributed to lower capillary forces due to lower liquid surface tension, in agreement with the observations with BSA.

Table 3. Selected contact angles measured on glass and stainless steel, pre-cleaned with ethanol (-Eth) and with additional UV-Ozone (UVO), using water, β-LGB solution and supernatant collected after heating of β-LGB solution for 4 h at 75°C; deduced capillary forces, considering a contact angle of 10°C of the liquids on quartz particles. Standard deviations, when relevant, are given between brackets.

Substrate	Static contact angle (°)			Deduced capillary forces (µN)		
	Water	*Native β-LGB*	*Supernatant of heated β-LGB*	*Water*	*Native β-LGB*	*Supernatant of heated β-LGB*
Glass-Eth	18 (3)	14 (2)	16 (2)	7.9	5.4	5.2
Glass-UVO	~9	11 (2)	13 (2)	≥8.0	5.4	5.2
StSteel-Eth	35 (2)	35 (3)	43 (3)	7.4	5	4.6
StSteel-UVO	10 (1)	14 (3)	15 (2)	≥8.0	5.4	5.2

4.3. Interplay of contact angle and surface tension

The similarity between the cleanability of glass soiled with a BSA-containing suspension and the cleanability of polystyrene soiled in absence of BSA (Figure 9) is due to the combination of contact angle and liquid surface tension in Eq. (3).

Considering the case of non-conditioned polystyrene soiled with a BSA-containing suspension, if the contact angle governing the capillary forces was in the range of 75 to 85° as measured (Figure 7, polystyrene) F_{CAP} would be much lower. The cleanability would thus be expected to be significantly higher than that of BSA-conditioned polystyrene, which is not the case (Figure 9B, c compared to d). As a matter of fact, the contact angle governing the capillary forces should be the receding contact angle, while the values reported in Figure 7 and Table 3 are static contact angles measured using the sessile drop method, i.e. close to advancing conditions. Attempts to measure receding contact angles with a BSA solution using the Wilhelmy plate method failed to give accurate results, because of perturbations due the weight of a layer of liquid carried along by the substrate as it was withdrawn from the solution. However, this revealed a low contact angle.

In practice, the role of capillary forces, which depend directly on both liquid surface tension and contact angle, is more important than the size and shape of the aggregates, which depend

on droplet spreading and are thus governed directly by contact angle and only indirectly by liquid surface tension. Eq. (3) is a useful tool to roughly foresee the influence of liquid surface tension, contact angle and their combination. Indeed, the capillary forces created between hydrophilic particles and different substrates decrease by only 20% as the substrate contact angle considered increases from 0 to 52°.

The cleanability of StSteel-Eth observed after soiling with suspensions in water is appreciably higher than the cleanability of other substrates (Figure 10). This is not explained by differences of computed FCAP, but it may be associated with higher contact angles and inferences of contaminants. For glass and StSteel-UVO, the slightly higher cleanability observed when soiling with quartz suspensions in denatured β-LGB solution, compared to native β-LGB solutions may not be explained by an effect of the liquid surface tension and contact angle. More numerous and detailed observations would be required to investigate these points.

4.4. Influence of surface contamination

The higher cleanability of StSteel-Eth compared to other substrates (Figure 10) after soiling with suspensions in water was not explained by differences of F_{CAP} computed using receding contact angles (*Section VI*), but it was associated with higher static contact angles. It may possibly be related to the particularity of the dynamic contact angle measurements (*Section VI*), which decreased significantly from the beginning to the end of the first immersion and suggested that the surface evolved when brought in contact with water. This might be due to a heterogeneity of the layer of contaminants or to its reorganization in contact with water. The complexity was still increased in presence of β-LGB, owing to possible interactions between β-LGB and the contaminants at particle-substrate interface. A clarification of these phenomena and of their influence on cleanability is difficult. Methods of surface chemical analysis (XPS, Time of Flight - Secondary Ion Mass Spectroscopy) are of little help, as the exposure to vacuum chambers may itself lead to adsorption of contaminants (Rouxhet, 2013).

5. CONCLUSIONS

5.1. Main achievements

The interpretation of XPS data by using peak decomposition was validated by correlations between spectral data of independent nature related to peak intensity and peak shape, respectively. The complexity due to the ubiquitous presence of organic contaminants could be

coped with, and the surface compositions could be expressed both in terms of the amount of adlayer and mass composition of the adlayer constituents.

The contact of the substrates with proteins (BSA and β-LGB, either native or denatured) present in the soiling particles suspension led to adsorption of the protein, which dominated the composition of the organic layer with respect to contaminants initially present, and was not markedly desorbed upon rinsing. In addition, the adsorption of proteins on more hydrophilic substrates seems to displace organic contaminants present or to prevent contamination from surroundings. When considering substrate surface as a model solid surface, it must be kept in mind that the presence of contaminants, which is often neglected, may have a significant influence on cleanability owing to the added complexity of the interactions between protein and contaminants at the interfaces.

Surface hydrophobicity was shown to influence the morphology of the aggregates resulting from drying. The rounder aggregates formed on polystyrene when soiling was performed with suspension in pure water are more sensitive to wall shear stress than flatter ones formed on more hydrophilic substrate. This is the result of the competing processes of droplet rolling and coalescing, on the one hand, and droplet spreading, on the other hand. It affects the shape and compactness of the adhering aggregates, the efficiency of shear forces upon cleaning and finally, the adherence of soiling particles.

The presence of proteins (either native or denatured) at the interface improved strongly the cleanability of more hydrophilic substrates (glass, StSteel-UVO). This is attributed to the lower liquid surface tension. The dependence of cleanability on capillary forces, and in particular on the liquid surface tension, is predominant as compared with its dependence on the size and shape of the soiling aggregates, which influence the efficiency of shear forces exerted by the flowing water upon cleaning. The cleanability of less hydrophilic substrate (stainless steel only pre-cleaned with ethanol) did not change markedly in the presence of proteins; this may be due to a more complex interaction between surface tension and contact angle, on one hand, and a more complex interaction between proteins and contaminants, on the other hand. The presence of dextran did not affect the cleanability, as neither the liquid surface tension nor the contact angle was appreciably affected.

5.2. Perspectives

5.2.1. Soiling systems and cleanability evalation

Rigid hydrophilic quartz particles were used as simplified particulate soils to investigate the mechanisms influencing particle adherence. The particle suspensions were prepared in pure water or in aqueous solution containing biomacromolecules (dextran, BSA, β-LGB). This led to conclusive observations. However, performing experiments with hydrophobic particle such as carbon black would have been particularly interesting to see how the biomacromolecules present in the system would affect particles adherence.

Whether heated suspension containing dextran or other water soluble additives-saccharose or xanthan would influence the particle adherence is not investigated. Nevertheless, it was shown (Linderer and Wildbrett, 1996) that saccharose and xanthan enhanced the removal of starch homogenous layer soils (100 µm) from glass under different conditions: suspension cooked for 30 min and cooled down to 50°C for 30 min under continuous stirring; soiled sample dried for 2 h at 60°C and then stored for 0.5 to7 days (20°C, 10-20% humidity) before cleaning with dishwashing and a model alkaline solution. Hence, a particular attention to polysaccharides heating and environmental conditions, especially drying or humidity conditions (or combination of both) of soiled substrates will be also of great interest for soiling involving particulate soils and biomacromolecules.

The soiling process used in this work is convenient for applications targeting open-surfaces. It is relevant to mimic and to study particulate soils adherence resulting from splashing as it occurs in real conditions and may be used for various suspension soils. But particle deposition by sedimentation instead of splashing is another issue to be considered.

While the method of soiling has been shown to be reproducible in the laboratory (Detry et al., 2007), new researchers may require a degree of familiarization with the techniques. It is thus time consuming for new operators to achieve repetitive uniform coverage and results from one trial to another. It may also be a source of results variation from different operators. An automation of this soiling method will be a considerable advanced for the soiling process.

5.2.2. Substrate model and organic contamination

The understanding of mechanisms responsible for the adherence of soils and the recognition of the environment where surfaces are used are important when developing easy-to-clean surfaces. For open-surface applications, several parameters (substrate wettability, impurities from diverse origins that may concentrate at the soil-substrate interface, soil nature, presence of biomacromolecules, temperature…) may affect soils adherence and substrate cleanability.

In the case of hard hydrophilic particle suspension in pure water or in polysaccharide solution, the best surface to reduce soil adherence would be a hydrophobic substrate (minimized droplet spreading and low capillary forces) where the affinity of the biological molecules present in the suspension for the substrate would be minimal.

When the soiling suspension contains proteins, the substrate hydrophobicity has less importance. But one thing to be clarified is the interference between protein and contaminant at the particle-substrate interface, as regard the difference between stainless steel pretreated with ethanol only and stainless steel with additional UVO treatment. In fact, the presence of organic contaminants tends to increase the particle adherence. Probing surfaces (precleaned, conditioned in different ways, soiled and cleaned) by Atomic Force Microscopy and maping interaction forces in air and in water with carefully designed probes seems to be the most promising approach (Alsteens et al., 2007). Performing such analysis may help in understanding the respective role of protein molecules and organic contaminants, regarding particularly the heterogeneity of the interfaces and the accumulation of compounds making bridges at the contact between the adhering particles and the substrate (Detry et al., 2011).

5.2.3. Complex soils

The mechanisms identified here for particulate soils adherence and removal are valid for a few layers of particles forming delimited aggregates or isolated particles, and for a simple biomacromolecule models. If a paste mainly composed of particles, or a suspension involving a mixture of polysaccharides, proteins and/or lipids, was spread on the substrates, the influence of the capillary forces and mechanical stresses appearing in the bulk of the soil upon drying could not be further ignored and may possibly influence the adherence of the deposit. Therefore, studying the adherence of quartz or other model particles in aqueous suspension containing a model mixture of simple biomacromolecules (protein, polysaccharide, lipid, …) and sprayed on the surface may also be of interest to acquire deeper knowledge on the processes described in this work, in a complex environment.

It should be stressed that the processes responsible for particle adherence described here may be considered for the fixation of a single microorganism on a substrate upon the drying of spatters but they cannot be applied to biofilms since the latter are constituted of a gel matrix of macromolecules containing dispersed microorganisms instead of particles adhering through the adhesive action of macromolecules present in low quantities.

REFERENCES

Almeida, A.T., Salvadori, M.C., Petri, D.F.S., Box, P.O. (2002). Enolase adsorption onto hydrophobic and hydrophilic solid substrates. *Langmuir*, 18, 6914-6920.

Alsteens, D., Dague, E., Rouxhet, P.G., Baulard, A.R., Dufrêne, Y.F. (2007). Direct measurement of hydrophobic forces on cell surfaces using AFM. *Langmuir Acs J. Surfaces Colloids*, 23(24), 11977-9.

Andre, C., Laux, D., Ferrandis, J.Y., Blasco, H. (2011). Real-time analysis of the growth of granular media by an ultrasonic method: Application to the sedimentation of glass balls in water. *Powder Technol.*, 208(2), 301-307.

Bansal, B., Chen, X.D., Muller-Steinhagen, H. (2008). Analysis of `classical' deposition rate law for crystallisation fouling. *Chem. Eng. Process.*, 47(8), 1201-1210.

Blel, W., Legentilhomme, P. , Le Gentil-Lelièvre, C. , Faille, C., Legrand, J.B.T. (2010). Cleanability study of complex geometries: Interaction between B. cereus spores and the different flow eddies scales. *Biochem. Eng. J.*, 49(1), 40-51.

Blel, W., Bénézech, T., Legentilhomme, P., Legrand, J., Le Gentil-Lelièvre, C. (2007). Effect of flow arrangement on the removal of Bacillus spores from stainless steel equipment surfaces during a Cleaning In Place procedure. *Chem. Eng. Sci.*, 62(14), 3798-3808.

Boonaert, C.J.P., Rouxhet, P.G. (2000). Surface of lactic acid bacteria : relationships between chemical composition and physicochemical properties. *Appl. Environ. Microbiol.*, 66(6), 2548-254.

Caccavo Jr.F. (1999). Protein-mediated adhesion of the dissimilatory Fe (III) - Reducing bacterium *Shewanella* alga BrY to hydrous ferric oxide. *Appl. Environ. Microbiol.*, 65(11), 5017-5022.

Caillou, S., Gerin, P.A., Nonckreman, C.J., Fleith, S., Dupont-Gillain, C.C., Landoulsi, J., Pancera S. M. Genet M.J., Rouxhet, P. G. (2008). Enzymes at solid surfaces: Nature of the interfaces and physico-chemical processes. *Electrochim. Acta*, 54(1), 116-122.

Detry, J.G, Sindic, M., Servais, M.J., Adriaensen, Y., Derclaye, S., Deroanne, C., Rouxhet, P.G. (2011). Physico-chemical mechanisms governing the adherence of starch granules on materials with different hydrophobicities. *J. Colloid Interface Sci., 355*(1), 210-21.

Detry, J.G., Jensen, B.B.B., Sindic, M., Deroanne, C. (2009a). Flow rate dependency of critical wall shear stress in a radial-flow cell. *J. Food Eng.*, 92(1), 86-99.

Detry, J.G., Deroanne, C., Sindic, M., Jensen, B.B.B. (2009b). Laminar flow in radial flow cell with small aspect ratios: Numerical and experimental study. *Chem. Eng. Sci.*, 64(1), 31-42.

Detry, J.G., Rouxhet, P.G., Boulangé-Petermann, L., Deroanne, C., Sindic, M. (2007). Cleanability assessment of model solid surfaces with a radial-flow cell. *Colloids Surfaces A. Physicochem. Eng. Asp.*, 302(1-3), 540-548.

Dufrêne, Y.F., Boonaert, C.J.P, Rouxhet G. P. (1996). Adhesion of *Azospirillum brasilense* : role of proteins at the cell-support interface. *Colloids Surfaces B. Biointerfaces*, *7*, 113-128.

Eide, M., Homleid, J.P., Mattsson, B. (2003). Life cycle assessment (LCA) of cleaning-in-place processes in dairies. *LWT Food Sci. Technol.* 36(3), 303-314.

Flint, S.H., Brooks, J.D., Bremer, P.J. (1997). The influence of cell surface properties of thermophilic streptococci on attachment to stainless steel. *J. Appl. Microbiol.*, 83(4), 508-517.

Flint, S., Palmer, J., Bloemen, K., Brooks, J., Crawford, R. (2001). The growth of Bacillus stearothermophilus on stainless steel. *J. Appl. Microbiol.*, 90(2), 151-157.

Fryer, P.J., Asteriadou, K. (2009). A prototype cleaning map: A classification of industrial cleaning processes. *Trends Food Sci. Technol.*, 20(6-7), 255-262.

Gerin, P.A., Dengis, P.B., Rouxhet, P.G (1995). Performance of XPS analysis of model biochemical compounds. *J. Chim. Phys.*, 92(5), 1034-1065.

Genet, M.J., Dupont-gillain, C.C., Rouxhet, P.G. (2008). XPS Analysis of Biosystems and Biomaterials. In *Medical applications of colloids* (E. Matijević, ed.) Springer, New York. 177-307.

Gillham, C.R., Fryer, P.J., Hasting, A.P.M ., Wilson, D.I . (2000). Enhanced cleaning of whey protein soils using pulsed flows. *J. Food Eng.*, 46(3), 199-209.

Gillham, C.R., Fryer, P.J., Hasting, A.P.M., Wilson, D.I. (1999). Cleaning-in-Place of whey protein fouling deposits. *Food Bioprod. Process.*, 77(2), 127-136.

Goldstein, A.S., DiMilla, P.A. (1998). Comparison of converging and diverging radial flow for measuring cell adhesion. *AIChE J.*, 44(2), 465-473.

Goldstein, A.S., Dimilla, P.A. (1997). Application of fluid mechanic and kinetic models to characterize mammalian cell detachment in a radial-flow chamber. *Biotechnol. Bioeng.*, 55(4), 616-29.

Goormaghtigh, E., Ruysschaert, J.-M., Raussens, V. (2006). Evaluation of the information content in infrared spectra for protein secondary structure determination. *Biophys. J.* 90(8), 2946-57.

Ikeda, S., Li-Chan, E.C.Y. (2004). Raman spectroscopy of heat-induced fine-stranded and particulate β-lactoglobulin gels. *Food Hydrocoll.*, 18(3), 489-498.

Herrera, J.J.R., Cabo, M.L., González, A., Pazos, I., Pastoriza, L. (2007). Adhesion and detachment kinetics of several strains of Staphylococcus aureus subsp. aureus under three different experimental conditions. *Food Microbiol.*, 24(6), 585-91.

Hirayama, K., Akashi S, Furuya, M., Furuya, K. (1990). Rapid confirmation and revision of the primary structure of bovine serum albumin by ESIMS and Frit-FAB LC/MS. *Biochem. Biophys. Res. Commun.*, 173(2), 639-646.

HRS Group. (2011). Fouling factors in heat exchangers, http://www.hrs-heatexchangers.com/en/resources/ fouling-factors-in-heat-exchangers.aspx, (07/01/12).

Jackson, L.S., Al-Taher, F.M., Moorman, M., DeVries, J.W., Tippett, R., Swanson, K.M.J., Fu, T-J., Salter, R., Dunaif, G., Estes, S., Albillos, S., Gendel, S.M. (2008). Cleaning and other control and validation strategies to prevent allergen cross-contact in food-processing operations. *J. Food Prot.*, 71(2), 445-58.

Jennings, W.G. (1965). Theory and practice of hard surface cleaning. *Adv. Food Res.*, 14, 325-458.

Jensen, B.B.B., Stenby, M., Nielsen, D.F. (2007). Improving the cleaning effect by changing average velocity. *Trends Food Sci. Technol.*, 18, S58-S63.

Jensen, B.B.B., Friis, A., Bénézech, T., Legentilhomme, P., Lelièvre, C. (2005). Local wall shear stress variations predicted by computational fluid dynamics for hygienic design. *Food Bioprod. Process.*, 83(1), 53-60.

Jensen, B.B.B., Friis, A. (2004). Critical wall shear stress for the EHEDG test method. *Chem. Eng. Process. Process Intensif.*, 43(7), 831-840.

Jones, R., Pollock, H.M., Cleaver, J.A.S., Hodges, C.S. (2002). Adhesion forces between glass and silicon surfaces in air studied by AFM: Effects of relative humidity, particle size, roughness, and surface treatment. *Langmuir*, 18(21), 8045-8055.

Jullien, C., Benezech, T., Gentil, C. Le, Boulange-Petermann, L., Dubois, P.E., Tissier, J.P., Traisnel, M, Faille, C. (2008). Physico-chemical and hygienic property modifications of stainless steel surfaces induced by conditioning with food and detergent. *Biofouling J. Bioadhesion Biofilm Res.*, 24(3), 163-72.

Kopac, T., Bozgeyik, K., Yener, J. (2008). Effect of pH and temperature on the adsorption of bovine serum albumin onto titanium dioxide. *Colloids Surfaces A. Physicochemical Eng. Asp.*, 322(1-3), 19-28.

Kosaka, P.M., Kawano, Y., Salvadori, M.C., Petri, D.F.S. (2005). Characterization of ultrathin films of cellulose esters. *Cellulose*, 12(4), 351-359.

Kralchevsky, P.A, Denkov, N.D. (2001). Capillary forces and structuring in layers of colloid particles. *Curr. Opin. Colloid Interface Sci.*, 6(4), 383-401.

Kralchevsky, P.A., Nagayama, K. (2001). Lateral capillary forces between partially immersed bodies. *Elsevier, Amsterdam*, 287-350.

Kralchevsky, P.A., Nagayama, K. (1994). Capillary forces between colloidal particles. *Langmuir*, 10(1), 23-36.

Laskowski, J.S., Liu, Q., O'Connor, C. T. (2007). Current understanding of the mechanism of polysaccharide adsorption at the mineral/aqueous solution interface. *Int. J. Miner. Process.*, 84(1-4), 59-68.

Leclercq-Perlat, M.-N., Lalande, M. (1994). Cleanability in relation to surface chemical composition and surface finishing of some materials commonly used in food industries. *J. Food Eng.*, 23(4), 501-517.

Lelièvre C., Legentilhomme, P. Gaucher, C., Legrand, J., Faille, C., Bénézech, T. (2002). Cleaning in place : effect of local wall shear stress variation on bacterial removal from stainless steel equipment. *Chem. Eng. Sci.*, 57, 1287-1297.

Linderer, M., Wildbrett, G. (1996). Starch residues in the cleaning process. *EUR, 16894 EN*, 146-155.

Lower, B.H., Yongsunthon, R., Iii, F.P.V., Lower, S.K. (2005). Simultaneous force and fluorescence measurements of a protein that forms a bond between a living bacterium and a solid surface. *J. Bacteriol.*, 187(6), 2127-2137.

Ma, X., Pawlik, M. (2005). Effect of alkali metal cations on adsorption of guar gum onto quartz. *J. Colloid Interface Sci.*, 289(1), 48-55.

Maciborski, J.D., Dolez, P.I., Love, B.J. (2003). Construction of iso-concentration sedimentation velocities using Z-axis translating laser light scattering. *Mater. Sci. Eng.*, A361, 392-396.

Manavalan, P., Johnson, W.C.Jr. (1987). Variable selection method improves the prediction of protein secondary structure from circular dichroism spectra. *Anal. Biochem.* 167, 76-85.

Mauermann, M., Calvimontes, A., Bellmann, C., Simon, F., Schöler M., Majschak, J.P. (2011). Modifications in hygienic properties of stainless steel surfaces due to repeated soiling and cleaning. *Proc. Int. Conf. Heat Exch. Fouling Clean.*, IX, 227–234.

McClellan, S.J., Franses, E.I. (2003). Effect of concentration and denaturation on adsorption and surface tension of bovine serum albumin. *Colloids Surfaces B Biointerfaces*, 28(1), 63-75.

Mercier-Bonin, M., Adoue, M., Zanna, S., Marcus, P., Combes, D., Schmitz, P. (2009). Evaluation of adhesion force between functionalized microbeads and protein-coated stainless steel using shear-flow-induced detachment. *J. Colloid Interface Sci.*, 338(1), 73-81.

Müller-Steinhagen H. (1993). Fouling: the ultimate challenge for heat exchanger design, in: *Proc. of the Sixth Inter. Symp. on Transport Phenom. in Therm. Eng.*, Seoul, Korea, 1993, 811-823.

Norde, W., Giacomelli, C.E. (2000). BSA structural changes during homomolecular exchange between the adsorbed and the dissolved states. *J. Colloid Interface Sci.*, 79(3), 259-68.

Parkar, S.G., Flint, S.H., Palmer, J.S., Brooks, J.D. (2001). Factors influencing attachment of thermophilic bacilli to stainless steel. *J. Appl. Microbiol.*, 90(6), 901-908.

Pascual, A., Llorca, I., Canut, A. (2007). Use of ozone in food industries for reducing the environmental impact of cleaning and disinfection activities. *Trends Food Sci. Technol.*, 18, S29-S35.

Pierna F.J.A., Duponchel, L., Ruckebusch, C., Bertrand, D., Baeten, V., Dardenne, P. (2012). Trappist beer identification by vibrational spectroscopy: A chemometric challenge posed at the "Chimiométrie 2010" congress. *Chemom. Intell. Lab. Syst.*, 113, 2-9.

Pitois, O., Moucheront, P., Château, X. (2000). Liquid bridge between two moving spheres: an experimental study of viscosity effects. *J. Colloid Interface Sci.* 231(1), 26–31.

Podczeck, F. (1999). Investigations into the reduction of powder adhesion to stainless steel surfaces by surface modification to aid capsule filling. *Int. J. Pharm.*, 178(1), 93-100.

Provencher, S.W., Glockner, J. (1981). Estimation of globular protein secondary structure from circular dichroism. *Biochemistry* 20, 33-37.

Quittet C., Nelis H. (1999). HACCP pour PME et artisans : secteur produits laitiers. Gembloux, Belgique : *Les Presses agronomiques de Gembloux*, pp 495.

Reza, M.R., Müller-Steinhagen, H., Watkinson, A. P. (2013). Heat Exchanger Fouling and Cleaning X - 2013 09-14 June 2013, Budapest, Hungary. *Refereed Proceedings.*

Robbins, P.T., Elliott, B.L., Fryer, P.J., Belmar, M.T., Hasting, A.P.M. (1999). A comparison of milk and whey fouling in a pilot scale plate heat exchanger: implications for modelling and mechanistic studies. *Food Bioprod. Process.*, 77(C2)(2), 97-106.

Rabinovich, Y.I, Adler, J.J., Esayanur M.S., Ata, A., Singh, R., Moudgil, B.M. (2002). Capillary forces between surfaces with nanoscale roughness. *Adv. Colloid Interface Sci.* 96(1-3), 213–30.

Rosmaninho, R., Melo, L.F. (2008). Protein–calcium phosphate interactions in fouling of modified stainless-steel surfaces by simulated milk. *Int. Dairy J.*, 18(1), 72-80.

Rouxhet, G.P. (2013). Contact angles and surface energy of solids: Relevance and limitations, in *Advances in contact angle, wettability and adhesion.*(K. L. Mittal, ed.) Vol. 1, Schrivener Publishing LLC, 347-375

Schmitt, C., Bovay, C., Rouvet, M., Shojaei-Rami, S., Kolodziejczyk, E. (2007). Whey protein soluble aggregates from heating with NaCl: physicochemical, interfacial, and foaming properties. *Langmuir Acs J. Surfaces Colloids*, 23(8), 4155-66.

Speranza, G., Gottardi, G., Pederzolli, C., Lunelli, L., Canteri, R., Pasquardini, L., Carli, E., Lui, A., Maniglio, D., Brugnara, M., Anderle, M. (2004). Role of chemical interactions in bacterial adhesion to polymer surfaces. *Biomaterials*, 25(11), 2029-2037.

Sreerama, N., Woody, R.W. (2000) Estimation of protein secondary structure from CD spectra: Comparison of CONTIN, SELCON and CDSSTR methods with an expanded reference set. *Anal. Biochem.*, 287(2), 252-260.

Sreerema, N., Venyaminov, S.Y., Woody, R.W. (1999). Estimation of the number of helical and strand segments in proteins using CD spectroscopy. *Protein Sci.*, 8, 370-380.

Sreerema, N., Woody, R.W. (1993). A self-consistent method for the analysis of protein secondary structure from circular dichroism. *Anal. Biochem.*, 209, 32-44.

Stanley, C.G., Peter, H.V.H. (1989). Calculation of protein extinction coefficients from amino acid sequence data. *Anal. Biochem.,* 182, 319-326.

Stefanov, I., Baeten, V., Abbas, O., Vlaeminck, B., De Baets, B., Fievez, V. (2013). Evaluation of FT-NIR and ATR-FTIR spectroscopy techniques for determination of minor odd- and branched-chain saturated and trans unsaturated milk fatty acids. *J. Agric. Food Chem.*, 61(14), 3403-13.

Stephan, O., Weisz, N., Vieths, S., Weiser, T., Rabe, B., Vatterott, W. (2004). Protein quantification, sandwich ELISA, and real-time PCR used to monitor industrial cleaning procedures for contamination with peanut and celery allergens. *J. AOAC Int.*, 87(6), 1448-1457.

Storgards, E., Simola, H., Sjöberg, A.-M., Wirtanen, G. (1999a). Hygiene of gasket materials used in food processing equipment Part 1: new materials. *Food Bioprod. Process.*, 77(2), 137-145.

Storgards, E., Simola, H., Sjöberg, A.-M., Wirtanen, G. (1999b). Hygiene of gasket materials used in food processing equipment Part 2: aged materials. *Food Bioprod. Process.*, 77(2), 146-155.

Tadros, T.F. (1980). Particle-surface adhesion, In: L. J. M. Berkeley R.C.W., Melling J., Rutter P.R., Vincent B., eds. *Microbial Adhesion to Surfaces*, Chichester: Ellis Horwood Ltd, Chichester pp. 93-116.

Thill, A., Spalla., O. (2003). Aggregation due to capillary forces during drying of particle submonolayers. *Colloids Surfaces A. Physicochem. Eng. Asp.*, 217(1-3), 143-151.

Tomasetti, E., Derclaye, S., Delvaux, M.H. and Rouxhet, P.G. (2013) Study of material-water interactions using the Wilhelmy plate method, in *Advances in contact angle, wettability and adhesion.*(K.L. Mittal, ed.) Vol. 1, Schrivener Publishing LLC, 131-154.

Van Stokkum, I.H.M., Spoelder, H.J.W., Bloemendal, M., Van Grondelle, R., Groen, F.C.A. (1990). Estimation of protein secondary structure and error analysis from CD spectra. *Anal. Biochem.,* 191, 110-118.

Verran, J., Airey, P., Whitehead, K.A. (2006). Assessment of organic materials and microbial components on hygienic surfaces. *Food Bioprod. Process.*, 84(4), 260-264.

Walstra, P., Jenness, R. (1984). *Dairy chemistry and physics*. John Wiley and Sons, New York.

Whitmore, L., Wallace, B.A. (2008). Protein secondary structure analyses from circular dichroism spectroscopy: methods and reference databases. *Biopolymers*, 89(5), 392-400.

Whitmore, L., Wallace, B.A. (2004). DICHROWEB: an online server for protein secondary structure analyses from circular dichroism spectroscopic data. *Nucleic Acids Res.*, 32, W668-W673

Wilson, D.I., Chew, J.Y.M. (2014). Fouling and Cleaning in Food Processing 2014 : " Green Cleaning " (pp. 348). *Dept. of Chemical Engineering, University of Cambridge.*

Yang, J., Mcguire J., Kolbe E.R. (1991). Use of the equilibrium contact angle as an index of contact surface cleanliness. *J. Food Prot.*, 54(11), 879-884.

Ziskind, G., Fichman, M., Gutfinger, C. (1995). Resuspension of particulates from surfaces to turbulent flows—Review and analysis. *J. Aerosol Sci.*, 26(4), 613-644.

Part II: DETAILED PRESENTATION

LITERATURE REVIEW - SECTION I

SOIL MODEL SYSTEMS USED TO ASSESS FOULING, SOIL ADHERENCE AND SURFACE CLEANABILITY IN THE LABORATORY

From:

Yetioman Toure, Nicolas Mabon, Marianne Sindic, 2013.

Biotechnol. Agron. Soc. Environ., 17(3), 527-539

ABSTRACT

Surface fouling is a chronic problem in processing industries. The hygienic state of surfaces is thus a critical parameter with respect to the performance of the production process and to the final quality of the product. For this reason, cleaning and disinfection are essential. The most important first step in implementing a fouling mitigation strategy through cleaning and disinfection is to understand the mechanisms of fouling. This allows ways to be found to reduce, even to eliminate fouling, or to improve the effectiveness of cleaning and disinfection. This paper reviews the relevant literature and summarizes a selection of soil model systems used to aid such improvements. Organic, mineral, microbial, particulate, and composite soil model systems are presented. These soil model systems are of particular relevance in the study of fouling, cleaning or soil adhesion onto solid surfaces in the laboratory environment. The key features of the models, as well as their practical advantages and disadvantages, are described and discussed.

Keywords: Models, fouling, adherence, cleaning, disinfection, solid surface.

1. INTRODUCTION

In processing industries, surface hygiene is undertaken primary to remove all undesirable material from surfaces. Such undesirable materials, which may include food residues, microorganisms, foreign bodies, and cleaning chemicals, are generally referred to as “soil”, and may derive from normal production processes, spillages, line-jams, equipment maintenance, packaging or general environmental contamination such as dust and dirt (Holah, 2000). In order to achieve successful surfaces hygiene, it is essential to understand the nature of the soil to be removed. Soils have been characterized by their chemical composition e.g. carbohydrate, fat, protein or mineral. Microorganisms may either be incorporated into the soil or be attached to surfaces, ultimately forming layers known as biofilms. In order to control better the fouling process, studies have paid particular attention to the parameters affecting both the formation of a particular type of soil and how its formation might be retarded or prohibited. These parameters include the role of soluble macromolecules, calcium sequestrants, pH, preheating, moisture level, temperature and flow rate.

No one cleaning agent is able to perform all the necessary functions to achieve the successful removal of all existing soil types. Several studies have been undertaken to determine fouling-related costs in industrialized countries. For the United States and New Zealand, the corresponding total annual costs are approximately 0.25% and 0.15% of the country's Gross National Product (GNP), respectively. The severe problem of fouling in heat exchanger equipment is known to have blocked normal levels of industrial production; the corresponding cost of fouling in China's total industry is more than 10 billion RMB per year (Bansal et al., 2008; Zhao et al., 2011). In France, the total cost of fouling in the dairy industry in 1991 was estimated at more than 152 million Euros (Cliaudagne, 1991). In membrane filtration applications, fouling reduces membrane flux with a consequent increase in energy costs and the need for early membrane replacement (Al-Amoudi, 2010).

Lalande et al. (1989) are among many researchers to have undertaken a large number of successful investigations providing a better understanding of the fouling process. However, a real breakthrough, i.e. complete control over fouling, has not yet been achieved. This is mainly due to the types of soil systems investigated to date and to the lack of a full understanding of fouling mechanisms. The objective of this paper is to review the existing knowledge on soil models in the area of fouling, to establish the fundamental factors involved and to present an up-to- date view on the processes taking place.

2. SOILING

2.1. Definition

Soil has been defined as any matter that is out of place on a defined solid surface. This surface is referred to as the substrate (Jennings, 1965). In the food industry, a soil can be a product residue or raw material, often in combination with a mineral deposit. This residue may have been altered to a greater or lesser extent by the processing conditions, by interaction with a cleaning solution, by subsequent contamination or by microbial contamination (Kulkarni et al., 1975). For this reason, the nature of the soil and the process that generates it must be understood before determining the treatment to be applied (cleaning-in-place, impinging jets, etc.) (Rowan, 2005). In membrane filtration applications, fouling is the process resulting in a deterioration in membrane performance (reduced membrane flux) due to the deposit of suspended or dissolved substances on its surface and pores (Al-Amoudi, 2010).

2.2. Types of soil

Soils can be classified according to different criteria. They have been divided into organic, biological, mineral and composite soils, with cleaning processes being matched accordingly. Soils have also been categorized as being free, adherent or embedded. However, although this classification facilitates the identification of appropriate cleaning techniques in general, it is far from being exhaustive.

The HRS group (2011) classified soils into four common and readily identifiable types, thus making possible the grouping and comparison of data from different industries. Fryer et al. (2009) classified soils into five types according to the mechanism of deposit formation:

– chemical soils or reaction fouling occur when chemical changes within the fluid cause a fouling layer to be deposited onto the substrate. This occurs in areas as diverse as milk (protein denaturation) and crude oil fouling;
– biological soils or soiling is caused by the growth of organisms within the fluid that is deposited onto the substrate, across several length scales, from the adhesion of single organisms to the development of biofilms and seaweed;
– deposit soils or particulate fouling occur when particles contained within the fluid settle onto the substrate. Examples of this can be seen in the deposition of suspended magnetite particles from cooling water, dust from the air or protein aggregates onto surfaces. In membrane fouling (reverse osmosis, nanofiltration, ultrafiltration and microfiltration membranes), particulate matter in water or mixed liquids can be classified as settleable solids (> 100 µm), supra-colloidal solids (1 µm to 100 µm), colloidal solids (10 µm to 1 µm) and dissolved solids (< 10 µm). A full characterization of feed waters and mixed liquids may be used as a tool to predict membrane performance and to characterize the main mechanisms to which the soils are subjected (Potts et al., 1981; Gao et al., 2013);
– crystallization or precipitation fouling occur when a component of the fluid is deposited when its solubility limit is reached, such as calcium carbonate from boiling water or calcium phosphate (whose solubility decreases with temperature). A subset of this type of fouling is “solidification fouling”, which occurs when the fluid or its components become solidified on the surface. Examples of this can be seen in the solidification of ice from water, starch from a food fluid or, as in the processing of personal care products, the deposition of toothpaste or waxes from cosmetics (Fryer et al., 2009);
– corrosion soils occur when a layer of corrosion products builds up on the substrate, forming an extra layer of usually high thermal resistance material. Often corrosion

products are conveyed by fluid to form fouling deposits elsewhere via a particulate fouling mechanism.

In order to aid development of the understanding of cleaning mechanisms and to improve industrial practice, Fryer et al. (2009) presented soil types and cleaning methods in a two-dimensional representation with soil material properties and cleaning fluid, as the axes (Figure 1). Fouling severity varies according to the deposit material properties: low viscosity fluids (e.g. tanks containing beer or milk between process runs), high viscosity fluids (e.g. toothpaste or shampoo layers left on equipment walls, or starch from food sauces), cohesive solids (e.g. deposits from milk at UHT temperatures). Deposit properties determine the fluid to be used for cleaning: cold water, hot water, hot cleaning fluid. The shaded area shows the three types of soil that are the most difficult to clean: Type 1 (shampoos, toothpastes, starch and other gels,), Type 2 (biofilms), Type 3 (milk: proteinaceous at low temperature, mineral at high temperature; brewery and confectionary scales).

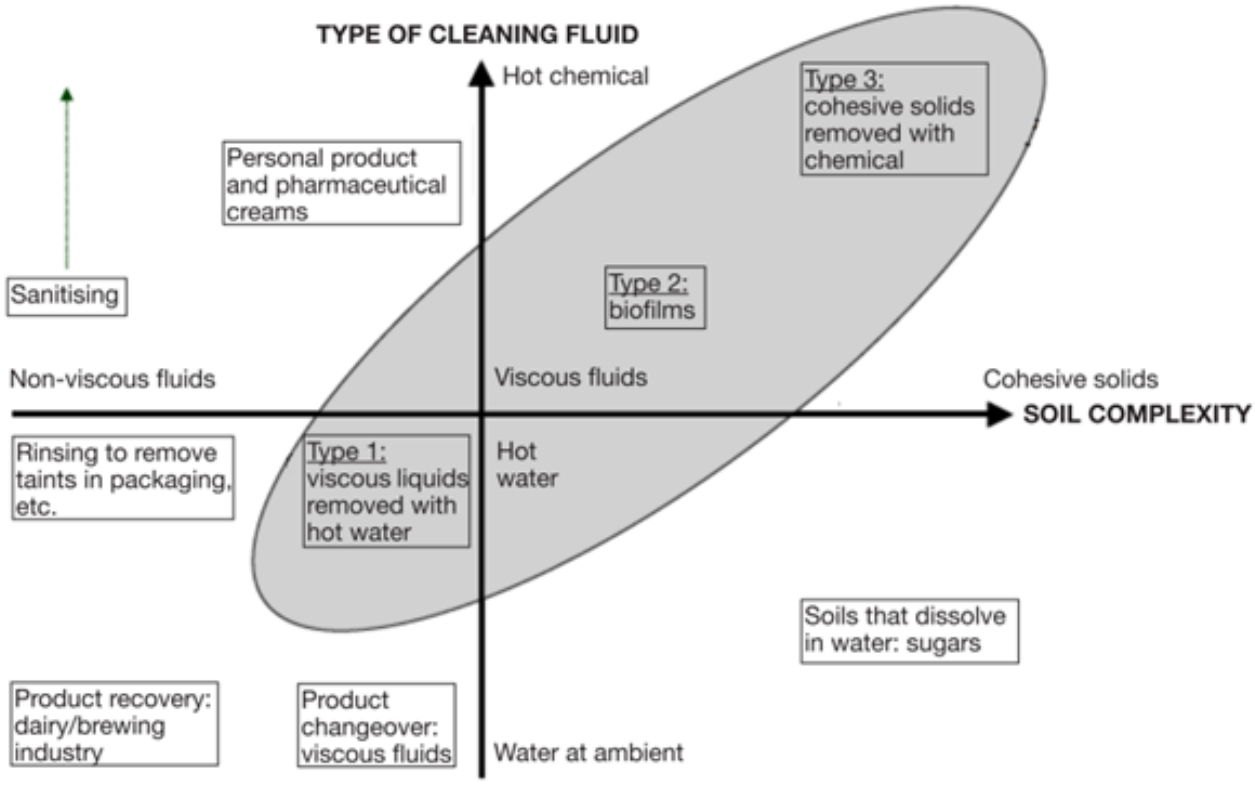

Figure 1. Cleaning map: a classification of cleaning problems based on soil type and cleaning chemical use. Three key groups: Type 1, includes most personal product fluids (shampoos, toothpastes, etc.) and some food films (starch and other gels); Type 2, biofilms; Type 3, includes many food soils such as milk (proteinaceous at low temperature, mineral at high temperature), brewery and confectionary scales (Fryer et al., 2009).

Rowan (2005) classified various types of soil encountered in the food industry according to their solubility in water (sugars, certain starches and salts), in acid solution (limestone, most mineral deposits) and in alkaline solution (with proteins, fats and emulsions). The classification of Quittet et al. (1999) is based on the nature of the soil: mineral (tartar, etc.), organic (lipid, protein, carbohydrate), microbiological (spores, viruses, molds, yeasts, bacteria, etc.), composite (consisting of a mixture of at least two of the previously listed soil classes) and other soils deriving from the environment (dust, heavy metals, etc.). Jennings (1965) suggested a simplified classification of different types of soil into two groups: homogeneous and composite soils. Paria (2003), meanwhile, proposed the most appropriate classification for textile research: lipid, particulate and composite soils.

None of the classifications proposed above is fully exhaustive or totally wrong. Indeed, the different types of soil can be defined by all these different classifications. The nature of soils and their respective solubility have been shown to be very important but the form of the soil itself must also be taken into account when cleaning treatment is planned: solid particulates (more or less hydrated powder), hydrated matrix (gel), biofilms, etc. In the following part of the review, we present different models of soiling systems used in the literature to assess substrate fouling, soil adherence or removal techniques in the laboratory.

3. SOIL MODEL SYSTEMS

3.1. Organic soils

Organic soils can be defined as any undesirable matter of a large class of gaseous, liquid or solid chemical compounds whose molecules contain carbon (combined with hydrogen, oxygen or nitrogen) such as carbohydrates, lipids and proteins, which is associated with living things (of biological origin: flora, fauna, food, human), and is out of place on a defined solid surface.

Many studies have been undertaken looking at the retention and cleanability of soil material using a basic soil consisting of starch as it is a source of carbohydrate (Boyd et al., 2001; Detry et al., 2011), using milk soil as it contains a mixture of carbohydrates, fatty acid esters, and proteins (Kon et al., 1961; Boyd et al., 2001) and using edible oil (Detry et al., 2007). In studying some surface-related aspects of stainless steel cleaning or heat transfer surfaces fouled by proteins, the proteinaceous soil models generally used have been whey protein, β-lactoglobulin (β-LG), egg albumin and heat induced whey gels used as a simple system model of a fouling agent (Fickak et al., 2011). Initial studies have been carried out on a pilot scale plate heat exchanger (PHE), described in detail by Christian et al. (2002), and

using whey protein concentrate solution as a processing fluid to simulate milk fouling. Gordon et al. (2012) used a gelatin and egg yolk solution as the model material to investigate enzyme-based cleaning of protein soils. Organic soils are often studied in paste form. Thus, baked tomato pastes with a known composition (protein, carbohydrate, sugar, fat, fiber and water) and bread dough (60.6% plain flour, 1.8% wet yeast, 1.2% salt and 36.4% water) have been used in a model to investigate the effect of surface treatment on the removal of a food soil (Saikhwan et al., 2006). Liu et al. (2002; 2006) used the same soil models to study the development and use of a micromanipulation technique for measuring the force required to disrupt deposits and to remove, for example, a fouling deposit of whey protein concentrate.

Oily soil models used to evaluate the cleanability of solid surfaces have involved the use of food grade sunflower oil sprayed or applied as a film deposition (Boulangé-Petermann et al., 2006; Detry et al., 2007), food grade mineral oil (Dillan et al., 1979) or hexadecane. Motor oil has also been used to study its removal in laundry detergent at low salinity. The relationship between micro-emulsion phase behavior and detergency has been studied for oily soils (Tongcumpou et al., 2005; Tanthakit et al., 2009), and for concentrated food emulsion (oil-in-water) (mayonnaise composition) including virgin olive oil, sunflower oil or soybean oil (Michalski et al., 1999). Basu et al. (1996) used bitumen to investigate oil displacement on solid surfaces in an aqueous environment. Both Liu et al. (2006) and Jurado-Alameda et al. (2012) used a fatty food (pork lard) as a fatty soil model to assess the capacity of ozone to facilitate the removal of fatty soils from hard surfaces and to develop effective cleaning procedures involving ozone.

Organic fouling remains a significant challenge in the membrane filtration application to desalination, drinking water, wastewater, food and other industrial applications. Developing strategies for fouling control has always been a major challenge in membrane research. Alginate and humic acid substances have been identified as major organic components in natural water, seawater and wastewater effluents. And these substances have been extensively used as model organic foulants to study membrane fouling in forward osmosis, reverse osmosis, pressure-driven membrane, ultrafiltration, nanofiltration and filtration processes (Ang et al., 2006; Resosudarmo et al., 2013; She et al., 2013). Alginate is used in membrane fouling research to represent polysaccharides and hydrophilic mater, while humic acid represents hydrophobic and natural organic matter. The influence of other types of organic matter on membrane fouling such as proteins and fatty acids has been studied in

order to further develop understanding of overall fouling mechanisms and cleaning procedures, and the role of various physical and chemical interactions, such as intermolecular adhesion forces, initial permeate flux, and membrane orientation. In these studies, bovine serum albumin and octanoic acid, representing, respectively, proteins and fatty acids, were used as the organic foulant model (Mi et al., 2008; Ang et al., 2011).

All the soil models mentioned above can be used to generate very useful data for the study of fouling and cleaning in controlled conditions. Such data may:

– explain the mechanisms of action of a chemical agent in the breaking down of a soil;
– provide identification of the surface parameters influencing the cleaning process (roughness, hydrophobicity);
– explain the adhesive strength of a soil to various substrates;
– explain the effect of soil aging on its adherence
– help determining the appropriate surface modification that will mitigate fouling;
– suggest strategies to reduce soil adhesion or facilitate soil removal.

However, the adhesion between deposit and substrate varies with the surface characteristics, inducing lack of reproducibility from one surface to another. The surfaces investigated in the studies described exhibited varying degrees of robustness towards repeated fouling and cleaning in manufacturing, indicating that some of the results of fouling and cleaning cycles in the laboratory obtained in limited numbers may be extended to real-life situations. The use of oils, proteins and carbohydrates separately or as a mixture for soiling makes the method even more realistic: the attachment of microorganisms to equipment surfaces depends on environmental conditions, amongst other criteria. Fouling may also result from more than one mechanism. For example, proteins and calcium phosphate interact with surfaces during milk processing (Rosmaninho et al., 2008) and the deposition of protein aggregates involves both reaction and particulate fouling. Membrane fouling in the presence of organic matter can be influenced by:

– membrane characteristics, including surface structure as well as surface chemical properties;
– the chemistry of the feed solution, including ionic strength, pH and the concentration of monovalent ions and divalent ions;
– the properties of organic matter, including molecular weight and polarity;
– hydrodynamic and operating conditions including permeate flux, pressure, concentration polarization;

– the mass transfer properties of the fluid boundary layer (Al-Amoudi, 2010).

3.2. Mineral fouling

Mineral scale formation or fouling is a process in which unwanted mineral materials, originally dissolved in processed fluids, are deposited onto heat transfer surfaces (Helalizadeh et al., 2000). The term "mineral scale" is used to differentiate fouling due to inorganic salt deposits from organic fouling and biofouling. Mineral scale is a recurring problem in processing plants, water heat exchangers, membrane filtration applications, household equipment and steam generation units (Kazi et al., 2010; Zhao et al., 2011). Inorganic fouling on heat exchanger surfaces and on filtration membranes is one of the most frequent problems in processing industries due to the inverse solubility of salts. Crystallization fouling is usually caused by the precipitation of salts, when their solubility limit is reached. The mechanism of crystallization fouling lies at the heart of many natural and technological processes, from the production of pharmaceuticals, food and nano-materials to oil refinery or crude oil treatment, and gas, petrochemical and scale deposition (Fiona et al., 2009), etc. Although crystallization is the underlying mechanism for scale formation, the process of deposition in exchangers is different from that occurring in industrial crystallizers (Sheikholeslami, 2003). Many researchers and industrialists have been challenged by scaling problems and have witnessed their complexity (Zhao et al., 2011). Mineral fouling has been studied for many years. On reviewing the large body of information available in this area, it appears that calcium salts (calcium carbonate, calcium sulfate, etc.) are the main types of mineral scale in heat exchangers and in filtration membrane applications. Investigations have indicated that the solubility of calcium sulfate is strongly affected by the presence and concentration of other ions in the system; water quality greatly affects induction times and the precipitation of calcium sulfate. In an attempt to optimize the thermal treatment processes of milk, several studies have been undertaken to improve the understanding and reduction of the mineral fouling process and to improve cleaning processes (Christian et al., 2002; Kazi et al., 2009). The main mineral soil models used for all the studies cited above were solutions of differing mineral content: whey protein concentrated solution with calcium and phosphorus; oxalate monohydrate (COM) and amorphous silica (SiO_2) in aqueous solution; calcium chloride solution for calcium carbonate deposition and sodium dihydrogen phosphate solution for calcium phosphate deposits in addition to calcium chloride, iron oxides and other calcium and mineral salts, oils or light greases.

Mineral fouling on surfaces in processing industries is still a complicated phenomenon and the mechanism is not yet fully understood. Most of the soil models used are generally too basic to reflect the reality of the industrial environment, even though they provide a partial understanding of mineral fouling and cleaning mechanisms.

3.3. Microbial foulants

Microbial adhesion to surfaces and the consequent formation of biofilms has been documented in many different environments. Biofilms remain a concern in a broad range of areas and specifically in the food, environmental and biomedical fields (Verran, 2002; Maukonen et al., 2003). There is a natural tendency of microorganisms to attach to wet surfaces, to multiply and to embed themselves in a slimy matrix composed of self-produced extracellular polymeric substances (EPS), forming a biofilm. Studies investigating microbial adhesion and cleaning or disinfection are generally carried out using microbial soil models such as microbial cell and spore suspension, biofilm or other material inoculated with spores.

3.3.1. Microbial cell suspension

Adhesion of cells to each other and to foreign surfaces is the key to multicellular development, colonization and pathogenesis. Specific cell surface proteins, called adhesins, predominantly confer adhesive properties (Brückner et al., 2012). In the hygienic assessment of polymeric coating, cleanability assessments of surfaces in industries using a microbiological approach involving different bacteria cell suspensions have included: *Saccharomyces cerevisiae* (Callewaert et al., 2005; Guillemot et al., 2006; Brückner et al., 2012), *Enterococcus faecalis* (Boulangé-Petermann et al., 2004), *Escherichia coli* (Foschino et al., 2003), *Campylobacter* and *Salmonella* species (De Cesare et al., 2003), *Pseudomonas aeruginosa* and *Staphylococcus aureus* (Verran et al., 2001), *Streptrococcus bovis*, *Streptrococcus waus* and *Streptrococcus thermophilus* (Flint et al., 2000), *Bacillus stearothermophilus* (Flint et al., 2001). Some of the findings of these studies were as follows:

– *S. cerevisiae* is a model system suitable for studying not only the mechanisms and regulation of cell adhesion, but also the role of this process in microbial development, ecology and evolution (Brückner et al., 2012);

– bacterial survival is governed by environmental factors such as relative humidity and the presence of nutrients in coatings, with the surface properties of the coatings playing a secondary role (Boulangé-Petermann et al., 2004);
– the type of surface finish on AISI 304 stainless steel (shot treated or not) had no significant effect on the cleanability of stainless steel. In the tested conditions, AISI 304 stainless steel was confirmed as a suitable material for the food industry, since it showed a remarkable ease of removal of bacteria before they could develop into a biofilm (Foschino et al., 2003);
– both the contact surface and the level of organic matter can influence the survival and persistence of *C. jejuni* and *Salmonella* species on food contact surfaces (De Cesare et al., 2003);
– unavoidable "sticky" compounds present on the *S. cerevisiae* cell wall could not be completely removed during successive washings of a rehydrated cell suspension before use. This led to a dramatic alteration of the surface properties of the bacterium and to a modification of its adhesive strength on 316L stainless steel, thus clearly demonstrating the necessity to work with yeast from fresh cultures (Guillemot et al., 2006).

3.3.2. Bacterial spore suspension

Bacterial spores are among the most resistant forms of living organisms. Their resistance favors their long-term persistence and prolonged survival during food processing. This contamination of equipment with bacterial spores resistant to cleaning operations is favored by the strong adhesive properties of many species of endospore-forming bacteria, such as *Bacillus cereus*, and by their ability to form biofilms (Auger et al., 2009). Packaging material may also harbor bacterial spores and contaminate the processed product (Pirttijärvi et al., 1996). The hygienic risk associated with microbial soil on surfaces is often evaluated by spore suspension, for example: *Aspergillus niger* (Foschino et al., 2003), and *Bacillus* (Faille et al., 2007; Blanpain-Avet et al., 2011). *Pseudomonas fragi*, *Photobacterium leiognathi*, *Bacillus thuringiensis* and *Bacillus stearothermophilus* suspended in phosphate buffer or in saline have also been chosen for trial work, as part of a program focusing on developing test conditions for materials, soil application methods and cleaning protocols that could be standardized. These spores are known to attach well to surfaces. They have been detected after cleaning trials and have been found to be relatively safe for controlled aerosol dispersal during spray cleaning (Holah, 2000). Mercier-Bonin et al. (2011) used *B. cereus* spores as a simplified spore model to determine their adhesive force on AISI 316L stainless

steel. The authors reported that the ability of the spores to attach to AISI 316L stainless steel was mainly affected by the presence (and number) of appendages as well as the existence of discrete bonds or of local clusters of anchoring sites and heterogeneity within the spores.
Attention should also be paid to surface nanomechanical properties, which could also influence spore removal. Such a focus would help facilitate further identification of morphological, nanomechanical and physico-chemical factors involved in spore adhesion, leading to better cleaning strategies for processing equipment in the future.

3.3.3. Biofilms as microbial soil models

Biofilms constitute a protected mode of growth that allows microorganisms to survive in hostile environments, their physiology and behavior being significantly different from their planktonic counterparts. In industry, biofilms may be a source of recalcitrant contamination, causing food spoilage. They also represent a possible source of public health problems such as outbreaks of food borne pathogens. Biofilms are difficult to eradicate due to their resistant phenotype. Moreover, conventional cleaning and disinfection regimens may also contribute to ineffective biofilm control and to the dissemination of resistance. Consequently, new control strategies are constantly emerging, focusing mainly on the use of biosolutions (enzymes, phages, interspecies interactions and antimicrobial molecules of microbial origin) (Simoes et al., 2010). Biofilms are problematic in particular food industry sectors such as brewing, dairy processing, fresh products, poultry and red meat processing (Somers et al., 2004; Chen et al., 2007). Different soil models have been used as part of a biofilm approach to evaluate the cleanability of certain substrates. Beresford et al. (2001) used a *Listeria monocytogenes* cell suspension to investigate the adhesion of *Listeria* cells in biofilm to 17 different food-use approved materials representing metals, rubbers and polymers. It has been shown that adhesion to a wide range of materials is time-dependent and characterized by reversible and irreversible stages. A mixed biofilm of *L. monocytogenes* and *Flavobacterium spp.* was used by Bremer et al. (2001) to study the survival of *L. monocytogenes* attached to stainless steel surfaces in the presence or absence of *Flavobacterium spp.* That study showed that *Flavobacterium spp.* increased significantly the number of *L. monocytogenes* cells attached to stainless steel. Adoue et al. (2007) investigated the role of surface protein in bacterial adhesion to stainless steel. The authors used protein-coated amine latex microbeads as a simplified bacterial model within the context of a long-term study of biofilm formation in a marine environment. Results showed that the BSA-coated latex beads promoted an increased adhesion to stainless steel in comparison with bare beads. Knight et al. (2010)

developed and trialed a soil model system for evaluating the efficacy of disinfectants to inactivate bacteria present in biofilm on surfaces within a dairy factory environment. The soil model system used was generated using a single or mixed isolates (pseudomonas, coliforms and staphylococci) added to 10% (v/v) UHT whole milk. Flint et al. (2001) reported an investigation into the use of conductance methods to monitor the development of biofilms of *thermophilic streptococci* on a stainless steel surface. They observed biofilm formation on the internal surfaces of plate heat exchangers used in milk processing and examined some of the factors involved in the formation of a biofilm of *B. stearothermophilus*. Gibson et al. (1999) and Frank et al. (2001) studied the effectiveness of cleaning techniques used in the food industry through the removal of bacterial biofilms using a soil model biofilm of *P. aeruginosa* or *S. aureus*. Parkar et al. (2004) used a biofilm of *B. thermophilus* spp. to investigate the mechanism of removal and inactivation of biofilms that optimally grow on surfaces (stainless steel). Results indicated that the biofilm was more difficult to remove than milk-based soil.

Microorganisms in biofilms are more resilient to biocides, and these biofilms can therefore be a persistent source of contamination in biomedical and food application. Preventing biofilm formation by minimizing the adhesion of microorganisms to surfaces represents a key strategy in reducing the risk of contamination. The development of anti-adhesive and/or anti-microbial materials is highly valuable and therefore of major interest, constitutes an important field of investigation. Numerous strategies have been used to minimize the adhesion of microorganisms, such as minimizing surface roughness, and coating surfaces with anti-microbial agents and anti-adhesive compounds. The use of natural biological macromolecules as antifouling coatings has recently been demonstrated. Meyer et al. (2013) showed that conditioning stainless steel surfaces with an aqueous extract of fish proteins could prevent adsorption and reduce bacterial adhesion to stainless steel. Increasing attention is being paid to silver-based products, due to the broad-spectrum biocidal activity of silver toward many bacteria, fungi, and viruses. In studies by Mercier-Bonin et al. (2012) and by Saulou et al. (2012), plasma-mediated coatings, containing silver nanoparticles embedded in an organosilicon or silica-like matrix, were deposited onto stainless steel in order to evaluate their anti-adhesive potentialities towards *E. coli* and *S. cerevisiae*. These studies revealed the promising capacity of deposited nanosilver-containing films in curbing the formation of biofilms on stainless steel. This technology may find its place as anti-adhesive or anti-microbial coatings for a wide variety of food industry, biomedical and

general use applications involving spoilage or pathogenic microorganisms (Saulou et al., 2012).

3.4. Particulate soil models

Particulate fouling is defined as the deposition of unwanted material (particles) on a surface. In the literature, the term "solid particle" is used to designate organic or heavy precipitated minerals in dry state. In fabric detergency, for example, the soils present may be classified as particulates (solids, usually inorganic), oils (usually organic and liquid, sometimes also waxy solids) or stains (unwanted dyestuffs) (Carrol, 1996). Particulate adhesion and removal have been widely studied. Price et al. (2002) and Saint-Lorant et al. (2007) investigated the adhesion of powder to substrate surfaces using mannitol, maltitol, lactose monohydrate, pregelatinised starch, polyethyleneglycol and heavy precipitated calcium carbonate powder. Rennie et al. (1998) used an agglomerated whole milk powder to study the adhesion of dairy powders to equipment surfaces during the drying process. In a study of the use of surfactants for particulate soil removal in dry-cleaning with carbon dioxide, Van Roosmalen et al. (2004) used clay particles as the particulate soil model. In filtration, automotive and heavy equipment testing, Arizona road dust (ARD) has been widely used as a standard test dust (aerosol). This is also an excellent choice for studying sand ingestion in jet engines as it has very similar properties to sands found throughout the world and is readily available (Reagle et al., 2012). Polystyrene latex particles have been used as a model suspension in many studies including deposition, adsorption and/or kinetics of particle deposition (Adamczyk et al., 2007; Szyk-Warszynska et al., 2007). Xue et al. (2012) used gum arabic (GA) powder to investigate the fouling of a copper surface. Elzo et al. (1996) studied mineral particle deposition on a membrane surface using glass particles as mineral particles. Polystyrene latex, melamine, glass beads and polymethylmethacrylate (Pasquino et al., 2013) are commonly used in the laboratory as particulate models. These particles are also utilized for their physico-chemical properties in a variety of further applications, including electrostatic forces generated by a net charge, an electric potential, Lifshitz–van der Waals forces, acid/basic properties, density, refractive indices, elastic properties, topography and hydrophobicity, all of which directly influence the adhesion process. Parameters such as particle shape, size, roughness, amorphous content and crystalline form may also affect adhesion and the subsequent cleaning process.

The physics of transport, deposition, detachment and re-entrainment of particles suspended in a fluid are of great interest in many areas of fluid engineering: fouling of heat exchangers,

contamination of nuclear reactors, plugging of filtration membranes, occlusion of human veins, and deposits in the micro-electronics and the paper industries. Although many models have been developed to predict the occurrence of these particular phenomena in industrial applications, we are still far from having a comprehensive description of the interplay between all the physico-chemical mechanisms involved in particulate fouling. In order to gain a better understanding of the adhesion and cleaning mechanisms of particulate soils, it seems appropriate to look at all the elements of the environment in which or from which the soils are derived, or to examine the nature of the particulate soils. The studies conducted to date have often focused on the particle itself, disregarding the involvement of other elements such as minerals or organic elements from the external environment.

3.5. Composite soils

Composite soils can be considered as artificial complex soils reflecting the industrial or domestic reality. However, according to the literature, it is uncommon or even impossible to find an exact reproduction of industrial or domestic soils when studying soil adhesion or removal. Thus, in their aim of achieving a better understanding of adhesion and cleaning mechanisms, researchers are forced to approximate real-life situations by developing artificial soil models. Studies to assess the fouling, cleanability and disinfection of dairy processing equipment have used the following: stirred yoghurt inoculated with spores (Leclercq- Perlat et al., 1994), buttermilk inoculated with spores of *B. stearothermophilus* (Holah, 2000; Frank et al., 2001), milk inoculated with spores (Wong, 1998), pudding inoculated with spores of *B. cereus* (Bénezéck et al., 2002), suspensions of whole milk powder (Boyd et al., 2001; Verran et al., 2001), reconstituted milk (Wong, 1998; Chen et al., 2004), milk (Yang et al., 1991; Flint et al., 2001), yellow film encountered in a dairy industry (Maxcy, 1972), and whole milk mixed with isolates of pseudomonas, coliforms and staphylococci (Knight et al., 2010).

Composite soils are generally used to provide a more complicated soil, and they are cleaned from selected samples using different methods. In order to assess the cleanability of stainless steel, Boyd et al. (2001) and Liu et al. (2006) used a concentrate starch soil suspension combined with the *S. aureus* bacterium, and baked tomato paste with a known composition (proteins, carbohydrates, sugars, fat, fiber and minerals). The authors found that cleanability was affected by temperature, the concentration of the cleaning agent and the type of the cleaning process, exposure time, surface roughness, and the size of the starch molecules and of the cells of the bacterium. Gram et al. (2007) used *L. monocytogenes* in cold-smoked

salmon juice or in an emulsion of a meat sausage to evaluate the effectiveness of cleaning and disinfecting products against *L. monocytogenes* attached to food-soiled inert surfaces in a laboratory model. Results showed that the efficacy of cleaning and disinfection products against *L. monocytogenes* was strongly influenced by the food matrix. Dourou et al. (2011) used beef fat, lean tissue and ground beef inoculated with *E. coli* to examine the attachment and biofilms formation on food-contact surfaces encountered in beef processing environments. The results of that study indicated that *E. coli* attachment to beef-contact surfaces was influenced by the type of soiled substrate and by temperature. In a study of the use of surfactants for particulate soil removal in dry-cleaning with carbon dioxide, Van Roosmalen et al. (2004) used as their soil models sebum (skin fat) colored with carbon black (oily and greasy soils combined with particulate soils), egg yolk (proteins and starchy soils, oily and greasy soils), butterfat with colorant (oily and greasy soils) and vegetable oil colored with chlorophyll (oily and greasy soils combined with oxidizable or bleachable soils). The authors concluded that the charged surfactant particles that formed were responsible for the removal of soil particles from the textiles. In 2000, initial work within the study concentrated on developing test conditions for materials. Three organic soils were chosen for comparative studies, as these were shown to be easily created, stable, easy to apply and relatively detectable after cleaning. These were: "Campden" soil, a mixture of milk, starch and oil; a margarine based soil for use in the assessment of moderately sized closed equipment and a soured milk based soil for use in the EHEDG Cleanability Test Method for small sized closed equipment (Holah, 2000).

When dealing with problems relating to fouling or its removal, it is beneficial to use a complex approach, because fouling may result from more than one mechanism. For example, proteins and calcium phosphate interact in milk fouling (Rosmaninho et al., 2008), and the deposition of protein aggregates involves both reaction and particulate fouling. Fouling also depends on various parameters such as solution or environmental composition (source, presence of suspended particles, effect of supersaturation, pH, etc.) (Kazi et al., 2010), operating parameters (flow velocity, thermal flux, surface and bulk temperature, etc.) and surface characteristics (energy, roughness, etc.) (Albert et al., 2011). Although often approximating the industrial reality, the use of composite soils and methods of cleaning and disinfection that give excellent results in the laboratory rarely provide the expected results in real-life application in industry. Transferring deposition or removal results from laboratory scale facilities to large-scale processing units raises different challenges from those normally

addressed when dealing with heat exchanger surfaces. In the laboratory, using a simple tube or surface unit test rig, we can readily approach the Reynolds numbers with known wall shear stress for a sample or tube heat exchanger. However, it is much more difficult to match the high Reynolds numbers or wall shear stress in other processing units, particularly with vapor phase flow. Although elements of the fouling mechanisms may be the same (e.g. transport, adhesion, aging), scale-up issues can be very different from the case of projecting single-tube laboratory results. Challenges in translating laboratory adhesion or removal data to plant units include not only the usual scale-up difficulties, but also problems in understanding the behavior of soils consisting of many components. The process by which deposits are formed in the systems represents a further challenge.

4. REAL-LIFE CONDITIONS OF APPLICATION

All the aforementioned laboratory soil model systems can be used to generate very useful information in the study of cleaning and fouling in controlled conditions, as mentioned in subsection 3.1. However, the experimental data are generally obtained for selected soil models. Furthermore, except perhaps in the case of soil panels; these experimental data cannot be easily applied to soils with a complex composition in order to predict how the equipment will become fouled or to identify the appropriate cleaning method. This was well illustrated by Watkinson et al. (2011), who attempted to extend concepts of fouling from heat exchangers to processing equipment. The study revealed that for heavy hydrocarbon fouling from the vapor-phase, for example, laboratory results taken in the laminar or low turbulent flow (compared to those in industry) indicated that physical condensation on the wall was the root cause of deposition. For the plant, bulk condensation appeared to be the primary cause of fouling. Although velocities in the laboratory were close to those in the plant, the high Reynolds numbers and wall shear stress of the plant could not be matched. This was due more to the geometry of the actual channels in the plant, leading to a complex flow, than it was due to the mode of flow. However, the level of shear stress in real time can be effectively reproduced in the laboratory, and even amplified. For example, a turbulent flow has a level of average shear stress somewhat lower than the shear stress of a laminar flow in a low height channel (Lorthois et al., 2001). Simple transport models have shown the importance of droplet size for plant conditions, but have not accounted for the adhesion process.

Pilot and full-scale studies are expensive but valuable; smaller scale experiments are often problematic for a range of reasons, as outlined below:

– Deposits on which experiments are conducted are often not truly representative of industrial systems. It is difficult to create reproducible fouling deposits. Furthermore, soil aging is not well understood, so the condition of real-life deposits can often not be reproduced. Model deposits, such as whey proteins used to simulate pasteurizer behavior, can give different results to real-life soils (Christian et al., 2002);
– results from experiments carried out are in a form that is difficult to scale-up, and the scale-up rules themselves are not known. The relationship between the cleaning rate and extent at a different scale (enabling the prediction of industrial cleaning times from pilot or lab scale data) is unclear. However, quantitative indications, for example, of the shear stress threshold necessary for the detachment of the soils are provided. The shear stress threshold value depends on the environmental conditions. The usual techniques developed in the laboratory to obtain quantitative information on soil adhesion and detachment are represented by hydrodynamic systems (flow cell, impinging jets, rotating disks, fluid dynamic gauging), optical methods (atomic force microscopy, confocal laser scanning microscopy, optical tweezers), and ultrasonic methods;
– the difficulty of comparing the cleaning of different soils in a way that generates an understanding of the mechanisms involved, for example, allowing the cleaning time of one soil to be reliably predicted from the cleaning time of another;
– the lack of effective online measurement methods available for process validation and for identifying the cleaning endpoint. It is, of course, possible to dismantle the equipment and find residues of deposit or any organisms present by swabbing and assaying. This is often the only way of measuring cleaning efficacy in the pharmaceutical industry. It is not feasible to undertake this process online, as generally, standards are set at plant start-up and some swabbing done as part of QA (quality assurance) procedures. To date, industry has evaluated the state of fouling with reference to general measurements such as pressure drop or the thermal performance drift of heat exchangers. For the first time, the National Institute of Agronomic Research (INRA, 2013) has developed a fouling sensor based on the principle of the hot wire. It is simple to install and use. This sensor is used to assess levels of contamination at critical points during the use of equipment and makes it possible to follow online the fouling of any installation treating a body of fluid: a fluidic communication pipe or any type of engine (heat exchanger, recessing engine, etc.). Further research is being conducted in order to develop new solutions;

– scaling up lab or pilot plant data is difficult (if the mechanism of cleaning is not understood) and so scaling up is going to be an empirical process (Fryer et al., 2009). The practical consequences of this are that the best way of cleaning each type of soil has been developed largely independently, so information on how to clean one particular material is not applied so easily to the cleaning of others.

5. CONCLUSIONS

The existing different soil model systems used for testing cleaning methods, and for assessing adhesion and cleanability have been reviewed. This may be useful in developing a basic understanding of the principles of cleaning soils. The soil models described in this review provide recommended test soils that can be used as a basis for comparing or verifying the cleanability of new and existing food-processing equipment. Furthermore, the use of such soil models should facilitate the assessment of the comparative cleanability of different items of equipment assessed at different times or in different laboratories. While the method has been shown to be reproducible in the laboratory, new researchers may require a degree of familiarization with the specific techniques. These soil model systems can also be readily adapted to investigate the influence of cleaning parameters, such as application time, concentration of cleaning products, temperature, product type and interactions between cleaning products and disinfectants. The soil models generally used are sometimes versatile, and there are many avenues of investigation still to be explored, such as the effect of soluble macromolecules on soil adherence. Besides, the studies performed to understand the parameters governing soils adherence and cleaning processes are frequently centered on the effect of surface properties, and are performed on new surfaces. Nevertheless, in food and pharmaceutical industries, several fouling-cleaning cycles or several cycles of equipment’s use without cleaning can change the chemical composition of the real surface state, owing to the accumulation of organic compounds, which may affect soil-equipment surface interactions, and subsequent cleaning. The impact of organic compounds layers on microorganism attachment and resistance to cleaning is not fully understood, and there is a lack of interest for particulate soils. The following sections examine how biomacromolecules may affect particulate soils adherence and cleaning mechanisms.

ACKNOWLEDGEMENTS

The authors are grateful to Professor Paul G. Rouxhet for his time and for the rich and useful discussions throughout this study. They are also grateful to Mrs Lynn Doran for her English-language assistance.

REFERENCES

Adamczyk Z., Michna A., Szaraniec M., Bratek A. & Barbasz J., 2007. Characterization of poly(ethylene imine) layers on mica by the streaming potential and particle deposition methods. *J. Colloid Interface Sci.*, **313**, 86-96.

Adoue M., Bacchin P., Lorthois S., Combes D., Schmitz P. & Mercier-Bonin M., 2007. Experimental methodology for analysing macromolecular interactions in the context of marine bacterial adhesion to stainless steel. *Chem. Eng. Res. and Des.*, **85**(A6), 792-799.

Albert F., Augustin W. & Scholl S., 2011. Roughness and constriction effects on heat transfer in crystallization fouling. *Chem. Eng. Sci*., **66**, 499-509.

Al-Amoudi A.S., 2010. Factors affecting natural organic matter (NOM) and scaling fouling in NF membranes: A review. *Desalination,* **259**, 1-10.

Ang W.S., Tiraferri A., Chen K.L. & Elimelech M., 2011. Fouling and cleaning of RO membranes fouled by mixtures of organic foulants simulating wastewater effluent.. *J. Membr. Sci.,* **376**, 196-206.

Ang W.S., Lee S. & Elimelech M., 2006. Chemical and physical aspects of cleaning of organic-fouled reverse osmosis membranes. *J. Membr. Sci.,* **272**, 198-210.

Auger S., Ramarao N., Faille C., Fouet A., Aymerich S. & Gohar M., 2009. Biofilm formation and cell surface properties among pathogenic and nonpathogenic strains of the *Bacillus cereus* group. *Appl. And Environ. Microbiol.*, **75**, 6616-6618.

Bansal B., Chen X.D. & Müller-Steinhagen H., 2008. Analysis of 'classical' deposition rate law for crystallisation fouling. *Chem. Eng. and Process.*, **47**, 1201-1210.

Basu S., Nandakumar K. & Masliyah J.H., 1996. A study of oil displacement on model surfaces. *J. of colloid and Interface Sci.,* **182**, 82-94.

Bénézech T., Lelièvre C., Membré J.M., Viet A.F. & Faille C., 2002. A new test method for In-Place Cleanability of food processing equipment. *J. of Food Eng.*, **54**, 7-15.

Beresford M.R., Andrew, P.W. & Shama G., 2001. *Listeria monocytogenes* adheres to many materials found in food-processing environments. *J. of Appl. Microbiol.*, **90**, 1000-1005.

Blanpain-Avet P., Faille C., Delaplace G. & Bénézech T., 2011. Cell adhesion and related fouling mechanism on a tubular ceramic microfiltration membrane using *Bacillus cereus* spores. *J. of Memb. Sci.,* **385-386**, 200-216.

Boulangé-Petermann L., Gabet C. & Baroux B., 2006. On the respective effect of the surface energy and micro-geometry in the cleaning ability of bare and coated steels. *Colloids and Surf. A: Physicochem. Eng. Aspects*, **272**, 56-62.

Boulangé-Petermann L., Robine E., Ritoux S. & Cromières B., 2004. Hygienic assessment of polymeric coatings by physico-chemical and microbiological approaches. *J. Adhesion Sci. Technol.*, **18**(2), 213-225.

Boyd R. D., Verran J., Hall K. E., Underhill C., Hibbert, S. & West R., 2001. The cleanability of stainless steel as determined by X-ray photo-electron spectroscopy. *Appl. Surf. Sci.*, **172**, 135-143.

Bremer J.P., Ian M. & Osborne M.C., 2001. Survival of *Listeria monocytogenes* attached to stainless steel surfaces in the presence or absence of *Flavobacterium* spp. *J. of Food Prot.*, **64**(9), 1369-1376.

Brückner S. & Mösch H.U., 2012. Choosing the right lifestyle: adhesion and development in *Saccharomyces cerevisiae*. *FEMS Microbiol. Rev.*, **36**, 25-58.

Callewaert M., Rouxhet P.G. & Boulangé-Petermann L., 2005. Modifying stainless steel surfaces with responsive polymers: effect of PS-PAA and PNIPAAM on cell adhesion and oil removal. *J. Adhesion Sci. Technol.*, **19**(9), 765-781.

Carrol B., 1996. The direct study of oily soil removal from solid substrates in detergency. *Colloid and Surf. A: Physicochem. and Eng. Aspects*, **114**, 161-164.

Chen J., Rossman M.L. & Pawar D.M., 2007. Attachment of enterohemorragic *Escherichia coli* to the surface of beef and a culture medium. *LWT – Food Sci. and Technol.*, **40**, 249-254.

Chen X.D., Li D.X.Y., Lin S.X.Q. & Necati Ö., 2004. On-line fouling/cleaning detection by measuring electric resistance - equipment development and application to milk fouling detection and chemical cleaning monitoring. *J. of Food Eng.*, **61**, 181-189.

Christian G.K., Changani S.D. & Fryer P.J., 2002. The effect of adding minerals on fouling from whey protein concentrate development of a model fouling fluid for a plate heat exchanger. *Trans Icheme*, **80**, part c, 231-239.

Cliaudagne D., 1991. Fouling costs in the field of heat exchange equipment in the French market. *In : Fouling* Mechanisms: Theoretical and Practical Aspects, Bohnet M., Bott T.R., Karabelas A.J., Pilavachi P.A., Srmrria R. & Vidil R., Eds., pp. 21-25, Editions Européennes Thermique et Industrie, Paris, France.

De Cesare A., Sheldon B.W., Smith K.S. & Jaykus L.A., 2003. Survival and persistence of Campylobacter and Salmonella species under various organic loads on food contact surfaces. *J. of Food Prot.*, **66**(9), 1587-1594.

Detry J.G., Sindic M., Servais M.J., Adriaensen Y., Derclaye S., Deroanne C. & Rouxhet P.G., 2011. Physico-chemical mechanisms governing the adherence of starch granules on materials with different hydrophobicities. *J. of Colloid and Interface Sci.*, **355**, 210-221.

Detry J.G., Rouxhet P.G., Boulangé-Petermann L., Deroanne C. & Sindic M., 2007. Cleanability assessment of model solid surfaces with a radial-flow cell, *Colloids and Surf. A: Physicochem. Eng. Aspects*, **302**, 540-548.

Dillan K.W., Goddard E.D. & McKenzie D.A., 1979. Oily soil removal from a polyester substrate by aqueous nonionic surfactant systems. *J. of the Am. oil chem. Soc.*, **56**, 59-70.

Dourou D., Beauchamp C.S., Yoon Y., Geornaras I., Belk K.E., Smith G.C., Nychas G-J.E. & Sofos J.N., 2011. Attachment and biofilm formation by *Escherichia coli* O157:H7 at different temperatures, on various food-contact surfaces encountered in beef processing. *Int. J. of Food Microbiol.*, **149**, 262-268.

Elzo D., Schmitz P., Houi D. & Joscelyne S., 1996. Measurement of particle/membrane interactions by a hydrodynamic method. *J. Membr. Sci.*, **109**, 43-53.

Faille C., Tauveron G., Le Gentil-Lelièvre C. & Slomianny C., 2007. Occurrence of *Bacillus cereus* spores with a damaged exosporium: consequences on the spore adhesion on surfaces of food processing lines. *J. of Food Prot.*, **70**(10), 2346-2353.

Fickak A., Al-Raisi A. & Chen D.X., 2011. Effect of whey protein concentration on the fouling and cleaning of a heat transfer surface. *J. of Food Eng.*, **104**, 323-331.

Fiona C. & Richard P.S., 2009. Now you see them. *Science*, **322**, 1802-1803.

Flint S., Palmer J., Bloemen K., Brooks J. & Crawford R., 2001. The growth of *Bacillus stearothermophilus* on stainless steel. *J. of Appl. Microbiol.*, **90**, 151-157.

Flint S.H., Brooks J.D. & Bremer P. J., 2000. Properties of the stainless steel substrate, influencing the adhesion of thermo-resistant streptococci. *J. of Food Eng.*, **43**, 235-242.

Foschino R., Picozzi C., Civardi A., Bandini M. & Faroldi P., 2003. Comparison of surface sampling methods and cleanability assessment of stainless steel surfaces subjected or not to shot peening. *J. of Food Eng.*, **60**, 375-381.

Frank J.F. & Chmielewski R., 20001. Influence of surface finish on the cleanability of stainless steel. *J. of Food Prot.*, **64**(8), 1178-1182.

Fryer P.J. & Asteriadou K., 2009. A prototype cleaning map: a classification of industrial cleaning processes. *Trends in Food Sci. & Technol.*, **20**, 255-262.

Gao W.J., Han M.N., Qu X., Xu C., Liao B.Q., 2013. Characteristics of wastewater and mixed liquor and their role in membrane fouling. *Bioresource Technol.*, **128**, 207-214

Gibson H., Taylor J.H., Hall K.E. & Holah J.T., 1999. Effectiveness of cleaning techniques used in the food industry in terms of the removal of bacterial biofilms. *J. of Appl. Microbiol*., **87**, 41-48.

Gordon P.W., Brooker A.D.M., Chew J.Y.M., Letzelter N., York D.W. & Wilson I.D., 2012. Elucidating enzyme-based cleaning of protein soils (gelatin and egg yolk) using a scanning fluid dynamic gauge. *Chem. Eng. Res. and Des.*, **90**, 162-171.

Gram L., Bagge-Ravn D., Yin Ng Y., Gymoese P. & Vogel F.B., 2007. Influence of food soiling matrix on cleaning and disinfection efficiency on surface attached *Listeria monocytogenes. Food Control*, **18**, 1165-1171.

Guillemot G., Vaca-Medina G., Yken M.H., Vernhet A. Schmitz P. & Mercier-Bonin M., 2006. Shear-flow induced detachment of Saccharomyces cerevisiae from stainless steel: Influence of yeast and solid surface properties. *Colloids Surf., B,* **49**, 126-135.

INRA, 2013. http://www.inra-transfert.fr/offres-technologiques.php?optim=capteur-pour-_xe9-tude-suivi-encrassement-5yc1t (2013.01.21)

Helalizadeh A., Müller-Steinhagen H. & Jamialahmadi M., 2000. Mixed salt cristallization fouling. *Chem. Eng. Process*., **39**, 20-43.

Holah J., 2000. *Food Processing Equipment Design and Cleanability*. The national Food Center, Dublin, 37p.

HSR Groups, 2011. Fouling factors in heat exchangers. http://www.hrs-heatexchangers.com/en/resources/fouling-factors-in-heat-exchangers.aspx (07/01/12)

Jennings W.G., 1965. Theory and practice of hard-surface cleaning. *Adv. Food Res.*, **14**, 325-458.

Jurado-Alameda E., García-Román M., Altmajer-Vaz D. & Jiménez-Pérez J.L., 2012. Assessment of the use of ozone for cleaning fatty soils in the food industry. *J. of Food Eng.*, doi:10.1016/j.jfoodeng.2011.12.010.

Kazi S.N., Duffy G.G. & Chen X.D., 2010. Mineral scale formation and mitigation on metals and a polymeric heat exchanger surface, *Appl. Therm. Eng.*, **30**, 2236-2242.

Kazi S.N., Duffy G.G. & Chen X.D., 2009. Fouling and fouling mitigation on different heat exchanging surfaces, *Proc. Int. Conference Heat Exchanger Fouling and Cleaning*, Schladming, Austria, 367-377.

Knight G.C. & Craven H.M., 2010. A model system for evaluating surface disinfection in dairy factory environments. *Int. J. of Food Microbiol.*, **137**, 161-167.

Kon S.K. & Cowie A.T., 1961. Milk: the mammary gland and its secretion. *Ed. Academic Press*, New York.

Kulkarni S.M., Maxcy R.B. & Arnold R.G., 1975. Evaluation of soil deposition and removal processes: an interpretive review. *J. of Dairy Sci.*, **58**(12), 1922-1936.

Lalande M., Rene F. & Tissier J.P., 1989. Fouling and its control in heat exchangers in the dairy industry. *Biofouling*, **1**, 233-250.

Leclercq-Perlat M. N. & Lalande M., 1994. Cleanability in relation to surface chemical composition and surface finishing of some materials commonly used in food industries. *J. of Food Eng.*, **23**, 501-517.

Liu W., Christian G.K., Zhang Z. & Fryer P.J., 2006. Direct measurement of the force required to disrupt and remove fouling deposits of whey protein concentrate. *Int. Dairy J.*, **16**, 164-172.

Liu W., Christian G.K., Zhang Z. & Fryer P.J., 2002. Development and use of a micromanipulation technique for measuring the force required to disrupt and remove fouling deposits. *Food Bioprod. Process*. **80**(C4), 286.

Lorthois S., Schmitz P., & Anglés-Canoy E., 2001. Experimental Study of Fibrin/Fibrin-Specific Molecular Interactions Using a Sphere/Plane Adhesion Model. *J. of Colloid and Interface Sci.*, **241**, 52-62.

Maukonen J., Mättö J., Wirtanen G., Raaska L., Mattila-Sandholm T. & Saarela M., 2003. Methodologies for the characterization of microbes in industrial environments: a review. *J. of Ind. Microbiol. and Biot.*, **30**, 327-356.

Maxcy R.B., 1972. Nature and cause of yellow film occuring on dairy equipment. *J. of Dairy Sci.*, **56**, 164- 167.

Mercier-Bonin M., Duviau M., Ellero C., Lebleu N., Raynaud P., Despax B. & Schmitz P., 2012. Dynamics of detachment of escherichia coli from plasma-mediated coatings under shear flow. *Biofouling*, **28**, 881-894.

Mercier-Bonin M., Dehouche A., Morchain J. & Schmitz P., 2011. Orientation and detachment dynamics of bacillus spores from stainless steel under controlled shear flow: modelling of the adhesion force. *Int. J. Food Microbiol.,* **146**, 182-191.

Meyer R.L., Arpanaei A., Pillai S., Bernbom N., Enghild J.J., Ng Y.Y., Gram L., Besenbacher F. & Kingshott P., 2013. Physicochemical characterization of fish protein adlayers with bacteria repelling properties. *Colloids Surf., B,* **102**, 504-510.

Mi B. & Elimelech M., 2008. Chemical and physical aspects of organic fouling of forward osmosis membranes. *J. Membr. Sci.,* **320**, 292-302.

Michalski M.C., Desobry S., Babak V. & Hard J., 1999. Adhesion of food emulsions to packaging and equipment surfaces. *Colloids and Surf. A: Physicochem. and Eng. Aspects*, **149**, 107-121.

Paria S., 2003. *Studies on surfactant adsorption at the cellulose - water interface*. PhD. Indian Institute of Technology, Bombay.

Parkar S.G., Flint S.H. & Brooks J.D., 2004. Evaluation of the effect of cleaning regimes on biofilms of thermophilic Bacilli on stainless steel. *J. of Appl. Microbiol.,* **96**, 110-116.

Pasquino R., Panariello D. & Grizzuti N., 2012. Migration and alignment of spherical particles in sheared viscoelastic suspensions. A quantitative determination of the flow-induced self-assembly kinetics. *J. of Colloid and Interface Sci.,* xxx xxx xxx, article in Press.

Pirttijärvi T.S.M., Graeffe T.H. & Salkinoja-Salonen M.S., 1996. Bacterial contaminants in liquid packaging boards: assessment of potential for food spoilage. *J. Appl. Bacteriol., 81,* 445-458.

Potts D.E., Ahlert R.C. & Wang S.S. 1981, A critical review of fouling of reverse osmosis membranes. *Desalination*, **36**, 235-264.

Price R., Young P.M., Edge S. & Staniforth J.N., 2002. The influence of relative humidity on particulate interactions in carrier-based dry powder inhaler formulations. *Int. J. of Pharm.*, **246**, 47-59.

Quittet C. & Nelis H., 1999. Guide HACCP: Secteur des produits laitiers. Ed. Les Presses Agronomiques de Gembloux a.s.b.l., Gembloux.

Reagle C., Delimont J., Ng W., Ekkad S.V. & Rajendran V., 2012. A Novel Optical Technique for Measuring the Coefficient of Restitution of Microparticle Impacts in a Forced Flowfield, ASME Turbo Expo 2012, GT2012-68252.

Rennie P.R., Chen X.D. & Mackereth A.R., 1998. Adhesion characteristics of whole milk powder to a stainless steel surface. Powder Technol., 97(31), 191-199.

Resosudarmo A., Ye Y., Le-Clech P. & Chen V., 2013. Analysis of UF membrane fouling mechanisms caused by organic interactions in seawater. *Water res.*, **47**, 911-921.

Rosmaninho, R. & Melo, L. F., (2008). Protein calcium phosphate interactions in fouling of modified stainless-steel surfaces by simulated milk. *Int. Dairy J.*, **18**, 72-80.

Rowan C., 2005. Cleaning and Sanitizing. *Food and Beverage Int.*, 46-49.

Saikhwan P., Geddert T., Augustin W., Scholl S., Paterson W.R. & Wilson D.I., 2006. Effect of surface treatment on cleaning of a model food soil. *Surf. and Coat. Technol.*, **201**(3-4), 943-951.

Saint-Lorant G., Leterme P., Gayot A. & Flament M.P., 2007. Influence of carrier on the performance of dry powder inhalers. *Int. J. of Pharm.*, **334**, 85-91.

Saulou C., Despax B., Raynaud P., Zanna S., Seyeux A., Marcus P., Audinot J-N. & Mercier-Bonin M., 2012. Plasma-Mediated Nanosilver-Organosilicon Composite Films Deposited on Stainless Steel: Synthesis, Surface Characterization, and Evaluation of Anti-Adhesive and Anti-Microbial Properties on the Model Yeast Saccharomyces cerevisiae. *Plasma Process. Polym.*, **9**, 324-338.

She Q., Wong Y.K.W., Z.S. & Tang C.Y. , 2013. Organic fouling in pressure retarded osmosis: Experiments, mechanisms and implications. *J. Membr. Sci.*, **428**, 181-189.

Simoes M., Simoes L. C. & Vieira M. J., 2010. A review of current and emergent biofilm control strategies. *LWT - Food Sci. and Technol.*, **43**, 573-583.

Sheikholeslami R., 2003. Nucleation and kinetics of mixed salts in scaling. *AIChE J.*, **49**(1), 194-202.

Somers E.B. & Wong A.C., 2004. Efficacy of two cleaning and sanitizing combinations on *Listeria monocytogenes* biofilms formed at low temperature on a variety of materials in the presence of ready-toeat-meat residue. *J. of Food Prot.*, **67**, 2218-2229.

Szyk-Warszynska L. & Trybala A., 2007. Deposition of core latex particles encapsulated in polyelectrolyte shells at modified mica surfaces. *J. of Colloid and Interface Sci.*, **314**, 398-404.

Tanthakit P., Nakrachata-Amorn A., Scamehorn J.F., Sabatini D.A., Tongcumpou C. & Chavadej S., 2009. Micro-emulsion formation and detergency with oily soil: V. Effects of water hardness and builder. *J Surfact Deterg.*, **12**, 173-183.

Tongcumpou C., Acosta E.J., Quencer L.B., Joseph A.F., Scamehorn J.F., Sabatini D.A., Yanumet N. & Chavadej S., 2005. Micro-emulsion formation and detergency with oily soils: III. Performance and mechanisms. *J. of Surfact. and Deterg.*, **8**(2), 147-156.

Van Roosmalen M.J.E., Woerlee G.F. & Witkamp G.J., 2004. Surfactants for particulate soil removal in dry-cleaning with high-pressure carbon dioxide. *J. of Supercrit. Fluids*, **30**, 97-109.

Verran J., 2002. Biofouling in food processing: biofilm or biotransfer potential? *Food and Bioprod. Process.*, **80**, 292-298.

Verran J., Rowe D.L. & Boyd R.D., 2001. The effect of nanometer dimension topographical features on the hygienic status of stainless steel. *J. of Food Prot.*, **64**(8), 1183-1187.

Watkison A.P., Fan Z. & Petkovic B., 2011. Extending fouling concepts from heat exchangers to process equipment. *Proc. Int. Conf.: Heat Exch. Fouling and Clean.*, Crete Island, Greece.

Wong A.C.L., 1998. Biofilms in food processing environments. *J. of Dairy Sci.*, **81**, 2765-2770.

Xue H.S., Fan J.R. & Hu Y.C., 2011. Particulate fouling during the pool boiling heat transfer of MWCNT nanofluid. *Heat Mass Transf.*, DOI 10.1007/s00231-011-0922-5, In press.

Yang J., McGuire J. & Kolbe E., 1991. Use of the equilibrium contact angle as an index of contact surface cleanliness. *J. of Food Prot.*, **54**, 879-884.

Zhao X. & Chen X.D., 2011. A critical review of basic crystallography to salt crystallization fouling in heat exchangers. *Proc. Int. Conf.*: *Heat exch. Fouling and Clean.*, Crete Island, Greece.

SECTION II

INFLUENCE OF SOLUBLE POLYSACCHARIDE ON THE ADHERENCE OF PARTICULATE SOILS

From:

Yetioman Toure, Paul G. Rouxhet, Christine C. Dupont-Gillain and Marianne Sindic, 2011. *Proc. Int. Conf. on Heat Exchanger Fouling and Cleaning*, (Malayeri, M.R., Müller-Steinhagen, H. & Watkinson, A.P., eds.), June 05-10, 2011, Crete Island, Greece, http://www.heatexchanger-fouling.com, 219-226.

ABSTRACT

The removal of particulate soils from solid surfaces is the key process of cleaning many industrial devices, such as heat exchangers and spray dryers (food and pharmaceutical sector), and may be influenced by the presence of solutes, in particular of macromolecules. The present study deals with the influence of soluble polysaccharide on the adherence of particulate fouling of open surfaces and on subsequent cleaning. Model substrates differing by hydrophobicity (glass and polystyrene) were soiled with a suspension of quartz particles, taken as a model of hard hydrophilic soil. Dextran was chosen as a model of soluble polysaccharide. The substrates were soiled with or without previous conditioning with the polysaccharide solution (80 mg/l). The quartz particles suspension was prepared in three ways: (i) suspension in a polysaccharide solution (80 mg/l), (ii) same as (i) and subsequent washing three times, (iii) suspension in water. The substrates were soiled by spraying the suspension and dried for 30 min before cleaning treatment with a water flow in a radial flow chamber. The aggregates observed after soiling differed considerably between glass and polystyrene, whether the substrate and/or the quartz particles were or were not conditioned with dextran. Conditioning polystyrene with dextran increased slightly the adherence of quartz particles, while the opposite was observed when conditioning glass with dextran, whatever the mode of quartz particles conditioning. The effect of conditioning quartz particles with dextran at the concentration used was not significant.

1. INTRODUCTION

Particulate soils are a concern in many cleaning processes of different industries: heat exchangers; spray dryers (food and pharmaceutical industry); laundry and dish washing (detergent industry); de-inking (recycling of papers) and microchips cleaning (semiconductor industry). The removal of those soils from solid surfaces is a daily problem in food industry, in catering industry or in medical applications where high hygienic levels must be maintained. In food and pharmaceutical industries, the cleaning efficiency influences the final quality of the products, absence of cross-contaminations and batch integrity (Stephan et al., 2004; List and Müller, 2005). The presence of adhering particles and microorganisms is also undesirable after cleaning and disinfection of open surfaces, where the ambient general level of hygiene is critical. Open surfaces are exposed to

splashing and aerial contamination. The interactions between the substrate and particulate contaminants have to be well understood in order to reduce equipment fouling, to improve the efficiency of cleaning and disinfection or to develop easy-to-clean surfaces (Podczeck, 1999). The hydrodynamic effects are important for the cleaning efficiency due to the shear stress forces acting at the wall (Lelièvre et al., 2002; Jensen et al., 2005; Blel et al., 2007). However, the wall shear stress, mainly governed by the flow rate and the equipment design, alone cannot explain cleaning performance (Jensen et al., 2007; Detry et al., 2009a; Blel et al., 2010). The size and the density of particles are major parameters which control the interaction with substrates. According to Ziskind et al. (1995), large particles with size reaching the external region of the boundary layer ($1.8 < d^+_p < 70$ where d^+_p is the dimensionless diameter of the particle = $d^+_p.V^*/v$, V^* is the friction velocity (($V^* = (\tau w/\rho m)^{1/2}$, τw, mean wall shear stress, ρm, fluid density) and v, the kinematic viscosity) are subjected to the effect of the large scale motions in the external region. On the other hand, small particles for which the dimensionless diameter d^+_p is less than 1 are located deeper in the viscous sublayer, where the instantaneous velocity distribution is linear. But, whatever the size of the particles, eddies generated near the wall induce mean and fluctuating shear forces. When these hydrodynamic forces are greater than the adhesion ones, resuspension occurs.

In the food and pharmaceutical industries, fouling leads to frequent interruptions of production process for cleaning. Polysaccharides, proteins, lipids and other biopolymers are the main components of food mixtures. These compounds contain a variety of different functional groups (carboxylic, phosphoric, amino, hydroxyl) that can individually interact with surfaces and mediate adhesion processes (Speranza et al., 2004). Proteins on the outer surface of the bacteria are known to play an important role in the initial attachment to solid surfaces (Flint et al., 1997; Caccavo, 1999; Lower et al., 2005). But the role of proteins and other biopolymers in the particulate soils adhesion remains unknown. According to Detry et al. (2011), the presence of soluble macromolecules (mainly polysaccharides with a small proportion of proteins) in the aqueous phase of starch suspensions plays a role in particle-substrate interactions. However, the role of each of these macromolecules in the adhesion mechanism according to the surface nature is not clearly defined.

Studying the influence of soluble macromolecules on fouling with a suspension of particles and on surface cleaning is important because: (i) it may give practical information on the influence of surface nature and particle surfaces properties (Jones et al., 2002); (ii) it may

give an insight into the physico-chemical mechanisms involved (Tadros, 1980); (iii) in particular it may clarify the role of the soluble macromolecules involved in particles adherence; (iv) it opens the way to designing and evaluating easy-to-clean surfaces.

The aim of the present study was to assess the influence of soluble polysaccharide on particulate soils adhesion on open surface and to improve the understanding of mechanisms affecting soiling and cleanability. Model substrates differing by hydrophobicity (glass and polystyrene) were soiled with a suspension of quartz particles and cleaned using a radial-flow cell. These particles were taken as a simplified particulate soil model. Dextran was chosen as a model of soluble polysaccharide because of its high solubility and because it was possible to select a defined molecular size from dextrans having a variety of molecular weights. In contrast with more highly branched polysaccharides such as dextrin, dextran contains more than 95% of only one type of glucose linkage. The substrates and the quartz particles were involved with or without previous conditioning with the polysaccharide solution. Untreated substrates and quartz are the blanks. Conditioned substrates simulate surfaces on which polysaccharides may be adsorbed for any reason (poor previous cleaning, several cycles of use without cleaning…). Conditioned particles represent a model complex mixture containing polysaccharides. Furthermore using washed and non-washed quartz particles offers a comparison between the effects of polysaccharides adsorbed on particles solely or adsorbed on particles and deposited on substrate.

2. EXPERIMENTAL

2.1. Material

Glass slides (75 mm × 25 mm × 1 mm, 50 mm × 50 mm × 1 mm and 16 mm x 37 mm x 1 mm) were purchased from Menzel-Gläser (Germany). Polystyrene sheets (300 mm × 300 mm × 0.25 mm) were purchased from Goodfellow (United Kingdom) and cut to the desired dimensions (75 mm ×25 mm×0.25 mm and 16 mm × 37 mm ×0.25). MilliQ water was produced by a MilliQ-50 system from Millipore (France). The chemical products used were ethanol 96%, Sulfuric acid (98%), Hydrogen peroxide solution (30%) purchased from Sigma-Aldrich (Wisconsin, USA) and RBS 50 cleaning agent (Chemical Products R. Borghgraef, Belgium). A solution of dextran from *Leuconostoc mesenteroides*, (20% (w/w), mol wt 500 000) was purchased from Sigma-Aldrich (Wisconsin, USA). Ground quartz particles (M400) were provided by Sibelco Benelux (Belgium).

2.2. Substrate pretreatment

Before soiling, the glass samples were immersed for 10 min at 50°C in an alkaline detergent medium, 2% (v/v) RBS 50 aqueous solution (pH = 11.9) and sonicated for 10 min in ultrasonic cleaner (Branson 3200, USA) to remove dust particles from test surface. The samples were then rinsed with MilliQ water and cleaned by immersion in a piranha mixture (sulfuric acid/hydrogen peroxide 2:1 (v/v)) at room temperature for 10 min and rinsed thoroughly with MilliQ water. Polystyrene samples were first cleaned with ethanol, dried with Kimtech Science paper (Kimberly–Clark, United Kingdom) and immersed for 30 min in ethanol. These samples were then rinsed thoroughly with MilliQ water. Both glass and polystyrene samples were dried with a gentle flow of nitrogen and wrapped in aluminum foil. The glass and polystyrene samples so pretreated were divided in two groups. The first group was conditioned for 1 h in an 80 mg/l dextran solution at room temperature, flushed with nitrogen for removing the liquid film and wrapped in aluminum foil until examination. The second group was not conditioned (called bare surface).

2.3. Soil preparation and treatment

Quartz particles with a size about 10 to 30 µm were isolated from initial batch (particle size distribution 1.1 to 60.3 µm) by repeated sedimentation. According to Stokes law, the rate of sedimentation of an isolated particle (V_p), considered as a sphere, is defined by Eq. (1) (Maciborski et al., 2003; Andre et al., 2011):

$$V_p = gd^2 \frac{(\rho_p - \rho_m)}{18\mu} \qquad (1)$$

where d is the particle diameter, $(\rho_p - \rho_m)$ is the density difference between the particle and the fluid of known viscosity µ and g is the gravitational constant. Knowing the settling velocity V_p, the time t needed to traverse a height D can be determined as $t=D/V_p$. The particle size distribution of the isolated fraction used here, determined using a particle size analyzer (Mastersizer 2000, Malvern Instruments, United Kingdom), was unimodal, ranging from 7.6 to 32.7 µm diameter (D10%=10.6 µm; D50%=17.1 µm; D90%=27.1 µm).

The quartz particles suspension (15% w/v) was pretreated in three ways: (i) suspension in a polysaccharide solution (80 mg/l), (ii) same as (i) and subsequent washing three times after keeping at 4°C for 72 h by sedimentation and replacement of the supernatant by water, (iii) suspension in water (15% w/v). For preparing suspension (i), 7.5 g samples of quartz were first mixed with 25 ml of distilled water and stirred for 30 min at room temperature. Then, 25 ml of a dextran solution in distilled water (160 mg/l) were added and the entire mixture was stirred for 1 h. Afterward, the suspensions were kept at 4°C (dextran storage

temperature) for 72 h (to leave time for possible dextran adsorption). The choice of dextran concentration in the suspension was based on the studies of Ma and Pawlik (2005).

2.4. Soiling procedure

The surfaces were soiled with the above mentioned quartz particles suspensions. The suspension was brought 30 min at room temperature and soiling was performed by manual aspersion using a thin layer chromatography (TLC) sprayer located 40 cm from the substrate. The surfaces were dried for 30 min in a dark cupboard at room temperature to have always the uniform environment conditions. The relative moisture content and temperature of the drying place, recorded with a Testo 175-H2 logger (Testo, Germany) every hour during periods of three weeks, were 39±3% and 20.6±1.9°C, respectively.

2.5. Cleanability assessment

2.5.1. Radial flow cell

The radial-flow cell (Fig. 1) was adapted from the design of Décavé (Décavé, 2002) and made of stainless steel (Detry et al., 2007). It consisted of an upper disk with a 2 mm diameter central inlet and a lower disk in which the soiled square sample (A) was fitted. A trench was made along the perimeter of the square recess in the lower disk to avoid any perturbation generated by deformations of the sample near the cut edges. The distance (h) between the upper disk and both the sample and the lower disk was set by three adjustable micrometric screws and controlled to be 1.00±0.02 mm with calibrated steel spacers. The fluid entering the cell was pumped from a 10 liter tank (C) by a peristaltic pump (D) (Watson Marlow 323SciQ, pumphead 314, 4 rollers). Before entering the cell (B), the fluid passed through a 1 liter glass container (E) (filled to a volume of 750 ml) to suppress the pulses from the pump. A complete description of the device and of its hydrodynamics can be found elsewhere (Detry et al., 2007; 2009a; 2009b).

2.5.2. Procedure

The cleaning fluid used was distilled water and cleaning was performed at 20°C at three flow rates (90, 190 and 390 ml/min) for 5 min. The soiled sample was immersed in the flow cell container. Then, the upper disk of the RFC was placed and the sample was immediately exposed to a flow at the desired flow rate. After 5 min, the upper disk of the RFC was gently removed from the flow cell. The sample was removed and dried at room temperature.

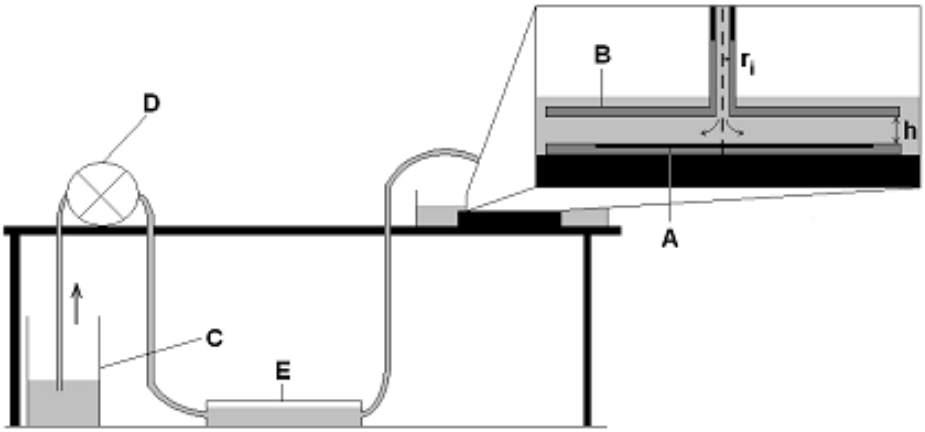

Figure 1. Scheme of the radial-flow cell installation, (A)Sample; (B) radial-flow cell; (C) cleaning fluid tank; (D) pump; (E) glass container; (r_i) inlet radius; (h) disk spacing (Detry et al., 2007).

2.5.3. Quantification

Pictures of the substrate were taken before and after cleaning, using an epifluorescence stereomicroscope (ZX9 Olympus, Belgium) equipped with a CCD camera, a mercury vapour UV lamp (100W, emission range 100–800 nm) and UV filters (passing bands: excitation 460–490 nm, emission > 520 nm). As showed in Figure 2, a circular zone with a lower density of aggregates was observed at the centre of the sample. This zone is where removal occurs. The radial position at which the residual density of aggregates becomes ≥ 50% is known as the critical detachment radius (Goldstein and DiMilla, 1997, 1998). The pictures of the sample before and after cleaning were processed with a specific application of the Matlab software (The Mathworks Inc.), which gives the ratio of the number of aggregates initially presents on the surface to the number of aggregates remaining after removal according to the radial position. A graph could then be plotted and the radial position corresponding to a residual density of aggregates of 50% was determined. The value of the critical radius was checked for consistency in the LUCIA software to insure the absence of artifacts such as the nucleation of air bubbles on the surface. At least 10 repetitions of each experiment (soiling-cleaning) were made, being distributed in at least three independent series and one soiled-surface sample was used per-flow rate.

The critical radius of detachment which was the output parameter of the cleaning experiments can be associated to a critical wall shear stress which corresponds to the minimal hydrodynamic drag force required to detach a soil from its surface under the given experimental conditions (Jensen and Friis, 2004). However, recent studies showed that the

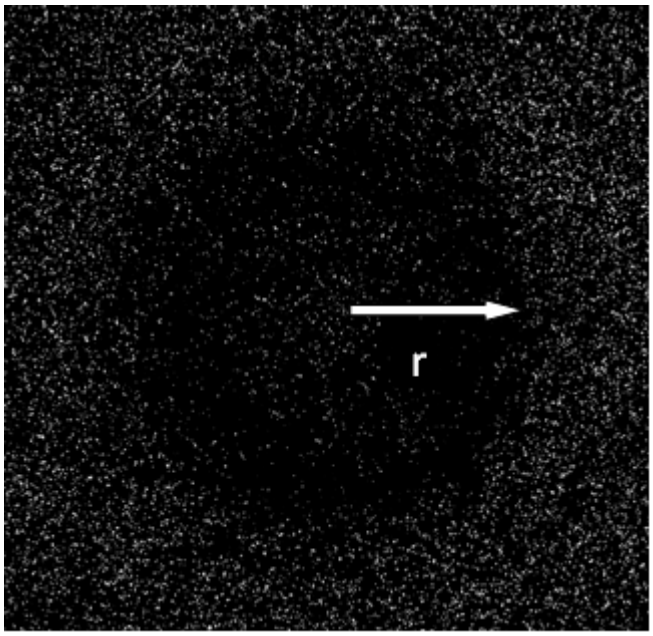

Figure 2. Representative picture obtained on a glass substrate soiled with quartz particles, dried 30 min and submitted for 5 min to a flow rate of 390 ml/min in the radial-flow cell. Scale bar: 1 mm.

conversion of critical radius into critical wall shear stress may be biased when the adhering aggregate height is not negligible with respect to the channel height and when the adherence is such that flow rates above 20 ml/min are required (Detry et al., 2007; Detry et al., 2009a). Owing to the limitations imposed by both the hydrodynamic regime and soil thickness, the results of the present study are expressed in terms of critical radius, keeping in mind that for a defined flow rate, the higher the critical radius, the lower the adherence.

2.6. Methods of characterization

2.6.1. Characterization of the soiling entities

This concerns the entities, typically aggregates, left after drying subsequent to soiling with the quartz suspension.

2.6.1.1. Individual size measurements

For each type of sample, at least 50 entities were observed with a Nikon Eclipse E400 microscope (magnification 20X) equipped with a CCD camera, a mercury vapour UV lamp, a dichroic mirror (reflection band 446–500 nm, transmission band 513–725 nm) and UV filters (passing bands: excitation 447–517 nm, emission 496–576 nm). The entities were first selected randomly; a targeted selection was also made to measure the extreme sizes.

The equivalent diameter of entity contours was determined using the LUCIA G image analysis software (LIM, Prague, Czech Republic) and the Eq. (2):

$$\text{diameter} = 2(\text{area} / \pi)^{1/2} \qquad (2)$$

The height of the entities was determined by focusing on the substrate and on the top particles after calibration of the microscope screw graduations with a polystyrene sheet (250 µm thickness corresponding to 147 ± 3 graduations).

2.6.1.2. Size measurements on a large population

The equivalent diameter of entity contours was also determined on a broader set, using the image analysis of micrographs obtained with an optical microscope (10X objective). The soiled glass and polystyrene surfaces were compared by measuring the size of the zone of contact between the suspension droplet after drying and the surfaces. Size measurements were made in the same logic as described above in the case of the individual size measurement. For each type of sample, two slides (75 x 25 mm^2) were examined. For each slide, five fields (1 field = 0.25 cm^2) were chosen randomly and a picture was taken at a random place in each field (one picture corresponding to 0.52 mm^2). An image analyzer software (LUCIA G) was used to measure the equivalent diameter of the entity contours as described above. The data were exported in a txt-file and processed using an excel tool, providing the size distribution (classes with a 10 µm increment).

2.6.2. Scanning electron microscopy (SEM)

The morphology of the soiling entities was examined by scanning electron microscopy (secondary electrons mode, external detector, DSM 982 Gemini from Leo, field-effect gun). The images presented here were obtained using an accelerating voltage of 1 kV. Samples were examined after deposition of a 10 nm-thick chromium coating.

2.6.3. Contact angle and liquid surface tension

Static contact angles were measured using the sessile drop method with a goniometer (Krùss, Germany). Surface tensions of water and dextran solution were measured with a Prolabo Tensiometer (Tensimat n3) using Wilhelmy plate method.

3. RESULTS

3.1. Wetting properties

Table 1 presents the surface tensions of water and of dextran solution and their contact angles measured on the substrates, bare and conditioned with the dextran solution. There is no significant difference between the surface tension of water and dextran solution (80 mg/l) which are 71.8 and 72.3 mN/m, respectively. There is also no significant difference of contact angle between water and dextran solution, neither between bare and conditioned substrates. However, the difference between contact angles measured on glass and

polystyrene is great, whatever the substrate pretreatment. It must be noted that contact angles measured on glass may be appreciably higher if the surface is left for a long time (about 1 day) in contact with the surrounding atmosphere, owing to adsorption of organic contaminants by the high energy solid. The water contact angle of polystyrene was lower than expected; this will be discussed *in Section III*.

Table 1. Surface tension of the liquids and contact angles on the substrates in the indicated state.

Liquids	Surface tension (mN/m)	Contact angles (°)			
		Bare glass	Conditioned glass	Bare polystyrene	Conditioned polystyrene
Water	71.6 *± 0.8	11 ± 2	12 ± 2	72 ± 2	73 ± 3
Dextran solution (80 mg/l)	72.3 ± 0.0	12 ± 1		74 ± 2	

*Mean ± Standard deviations

3.2. Size and shape of adhering aggregates

Representative micrographs of the quartz aggregates left after soiling and drying are presented in Fig. 3 and 4 for the different systems investigated. Optical micrographs are presented on the left hand side and SEM micrographs on the right hand side. A difference is noted between glass (Fig. 3) and polystyrene (Fig. 4), regarding both the number of soiling objects (optical microscope) and their morphology (SEM). On glass many quartz particles are isolated, while they are aggregated on polystyrene. With glass, there is no clear influence of conditioning the substrate or the quartz particles with dextran. With polystyrene, there may be a difference depending on whether the substrate was conditioned or not with dextran.

The relationship between the height of the soiling entities and the equivalent diameter of their contour is presented in Fig. 5. No distinction is made between different samples involving the same substrate. There was indeed no significant difference in the plots according the pretreatment of the substrate and of quartz particles. Both the height (in a lower extent) and the lateral size are larger on polystyrene compared to glass. On glass it could be observed by microscopy that the height of the aggregates never exceeded 2 layers of particles, independently of the lateral size. This can also be observed in Fig. 5 from the height of aggregates which is comprised between 15 and 38 µm, knowing that the diameter of the quartz particles ranges from 7.5 to 32.7 µm, with an average size of 17.1 µm (see subsection 2.3).

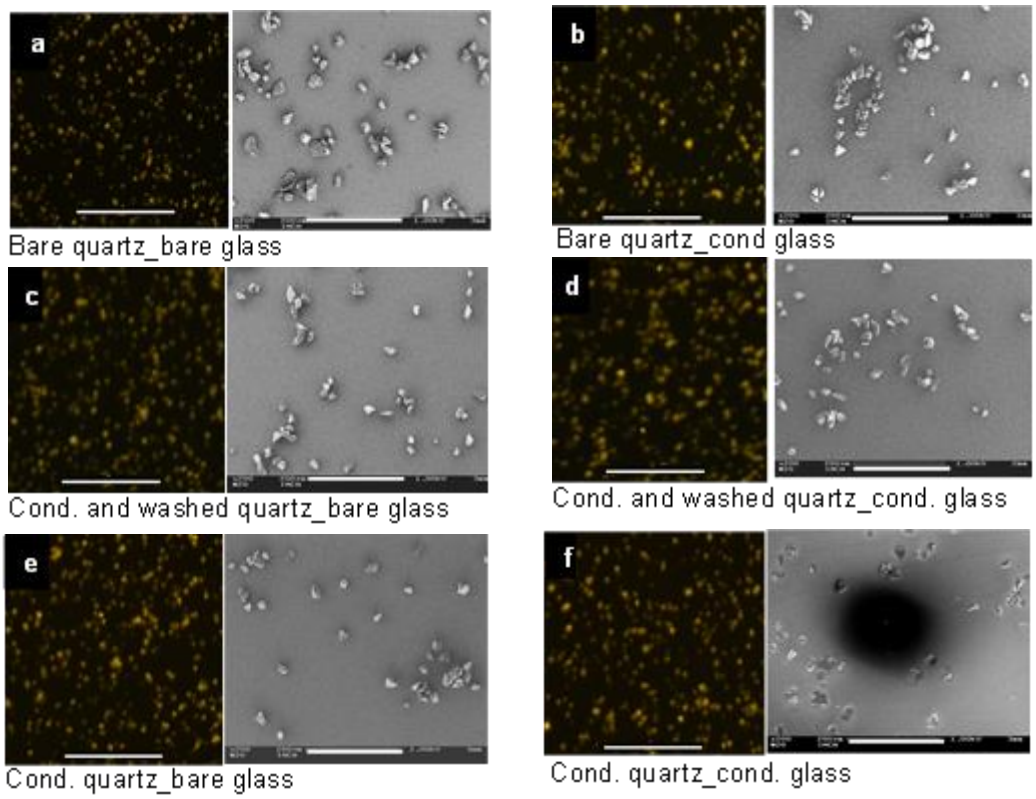

Figure 3. Illustration of the types of deposits formed on glass with the different treatments. For each image pair: left = stereomicroscope picture, scale bar 1 mm; right = SEM picture, scale bar 200 µm

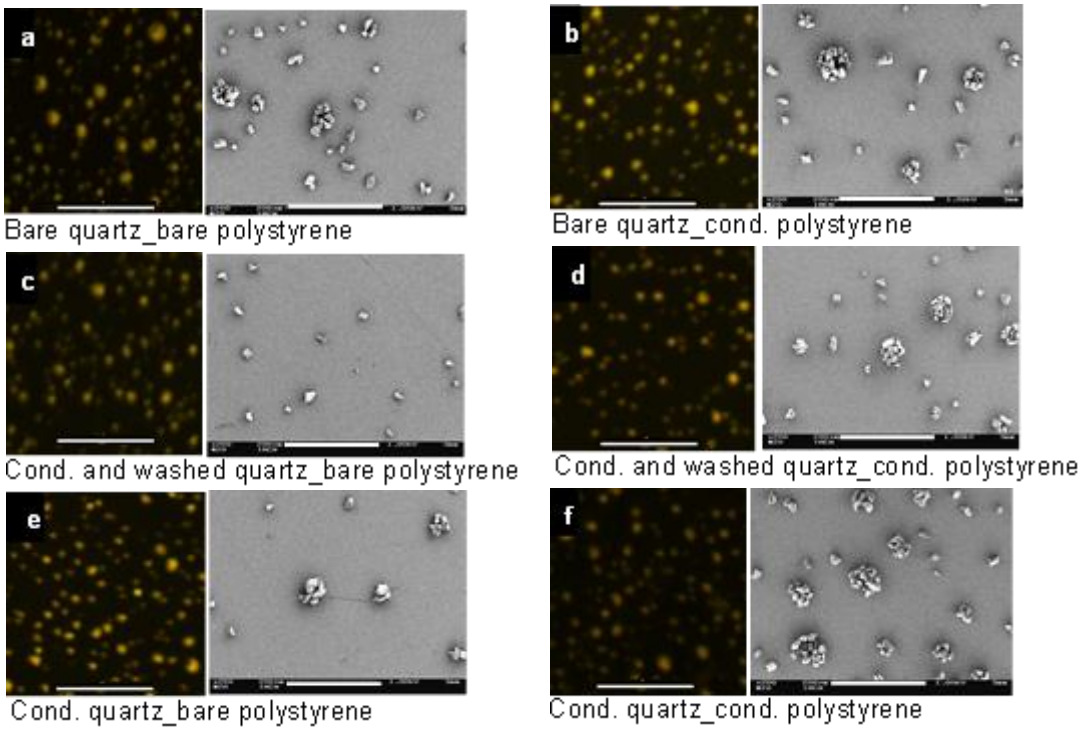

Figure 4. Illustration of the types of deposits formed on polystyrene with the different treatments. For each image pair: left = stereomicroscope picture, scale bar 1 mm; right = SEM picture, scale bar 200 µm

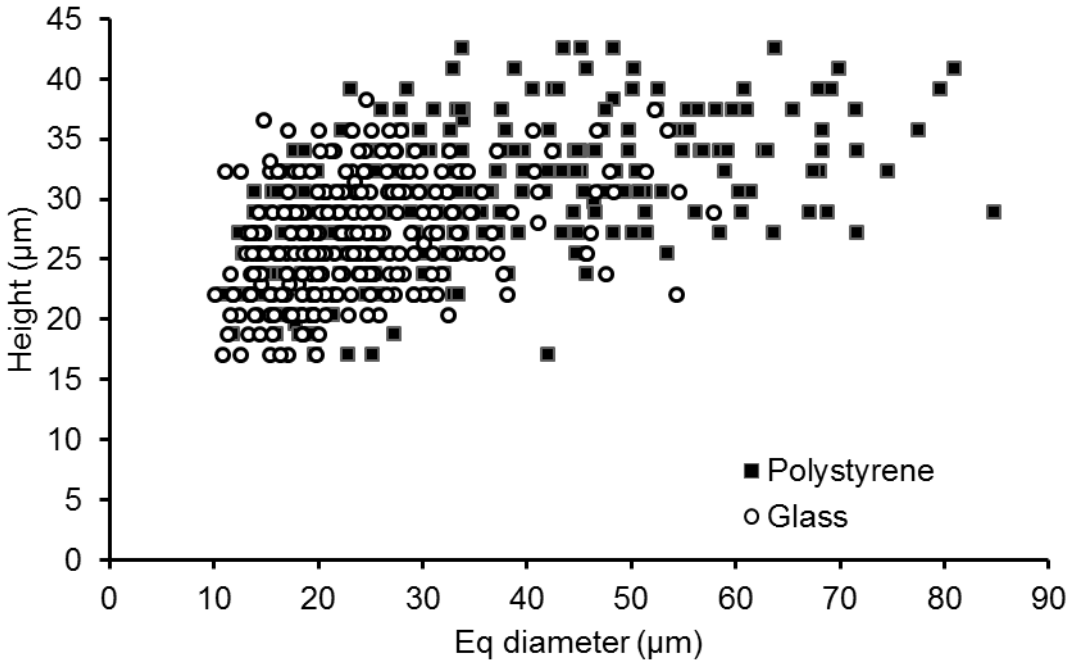

Figure 5. Height of the soiling entities formed on glass and polystyrene plotted as a function of their lateral dimension (equivalent diameter of the contour)

On polystyrene, the lateral size and the height of the entities increased to values much larger than the quartz particle size. Compared to glass, polystyrene is less wetted by the soiling suspension. As a consequence, the suspension drops tend to minimize their contact area with the surface, possibly rolling and coalescing, and gather the quartz particles to leave larger aggregates after drying.

Measurements made on a larger population showed that the density of soiling entities on glass (51±4 entities/mm^2) was higher compared to polystyrene (33±4 entities/mm^2). The lateral size distributions of the soiling entities are presented in Fig. 6, without making a distinction between different samples involving the same substrate. Again larger soiling entities were found on polystyrene compared to glass. The D50% were 55 µm and 30 µm on polystyrene and glass, respectively. The glass substrate gave a high proportion of entities with a lateral size smaller than 40 µm.

3.3. Quartz aggregates removal

The critical detachment radii are presented in Fig. 7 for the substrates treated in different ways, using quartz suspension treated in different ways. Remember that a larger critical detachment radius at a given flow rate reveals a lower hydrodynamic drag force required to detach soiling particles from the substrate. Increasing the flow rate allows increasing drag forces to be applied. For glass no detachment radius could be measured after cleaning at

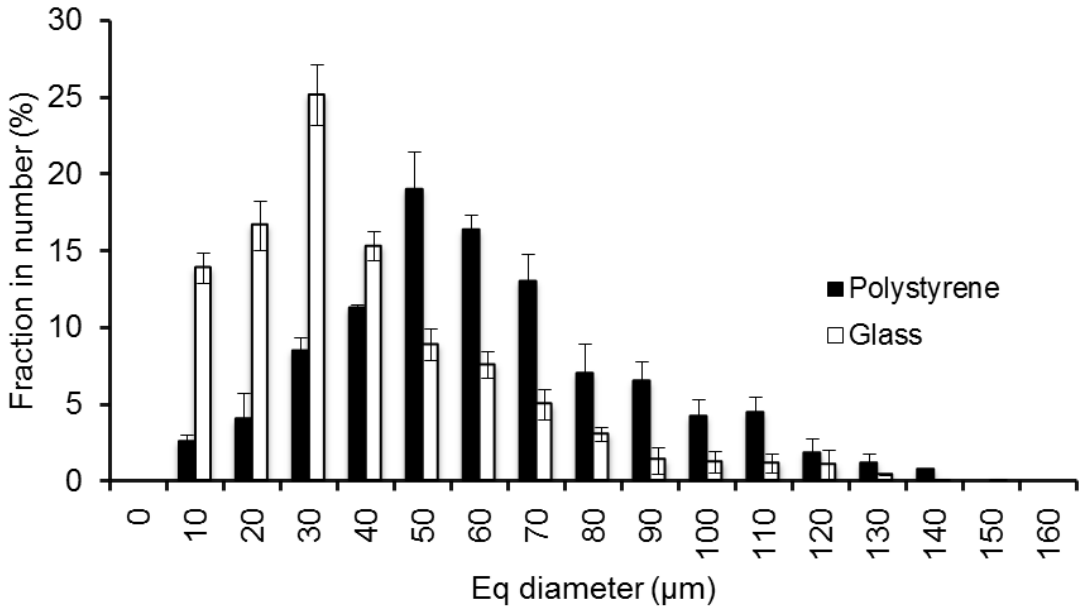

Figure 6. Histograms (% in number) of the lateral size of the soiling entities formed on glass and polystyrene (equivalent diameter of the contour).

flow rates of 90 to 190 ml/min, but a detachment of small clusters of particles from the aggregates situated near the inlet occurred at both flow rates (results not showed). Detachment radii could be measured after cleaning at 390 ml/min. For polystyrene, the detachment radius was larger than the microscope view field. Detachment radii could be measured when the flow rate was set at 90 and 190 ml/min.

These results show that the soiling moieties were adhering much more firmly on glass compared to polystyrene. They indicate that conditioning the substrate with dextran increased slightly but always the adherence of quartz particles to polystyrene (Fig. 7B), while the opposite was observed when conditioning glass with dextran (Fig.7A). In contrast the presence of dextran in the quartz suspension did not seem to have an effect on adherence, whatever the substrate and whether the latter was conditioned or not with dextran.

4. DISCUSSION

4.1. Influence of the substrate

The difference of wetting between the substrates were reflected in the size and shape of the soiling entities formed after spraying the quartz particles suspensions on glass and polystyrene, as shown in Fig. 3, 4 and 5. The morphology of soiling entities results from drop spreading, which decreases as the surface contact angle increases and, capillarity effects which develop upon drying (de Lazzer et al., 1999; Kralchevsky and Nagayama,

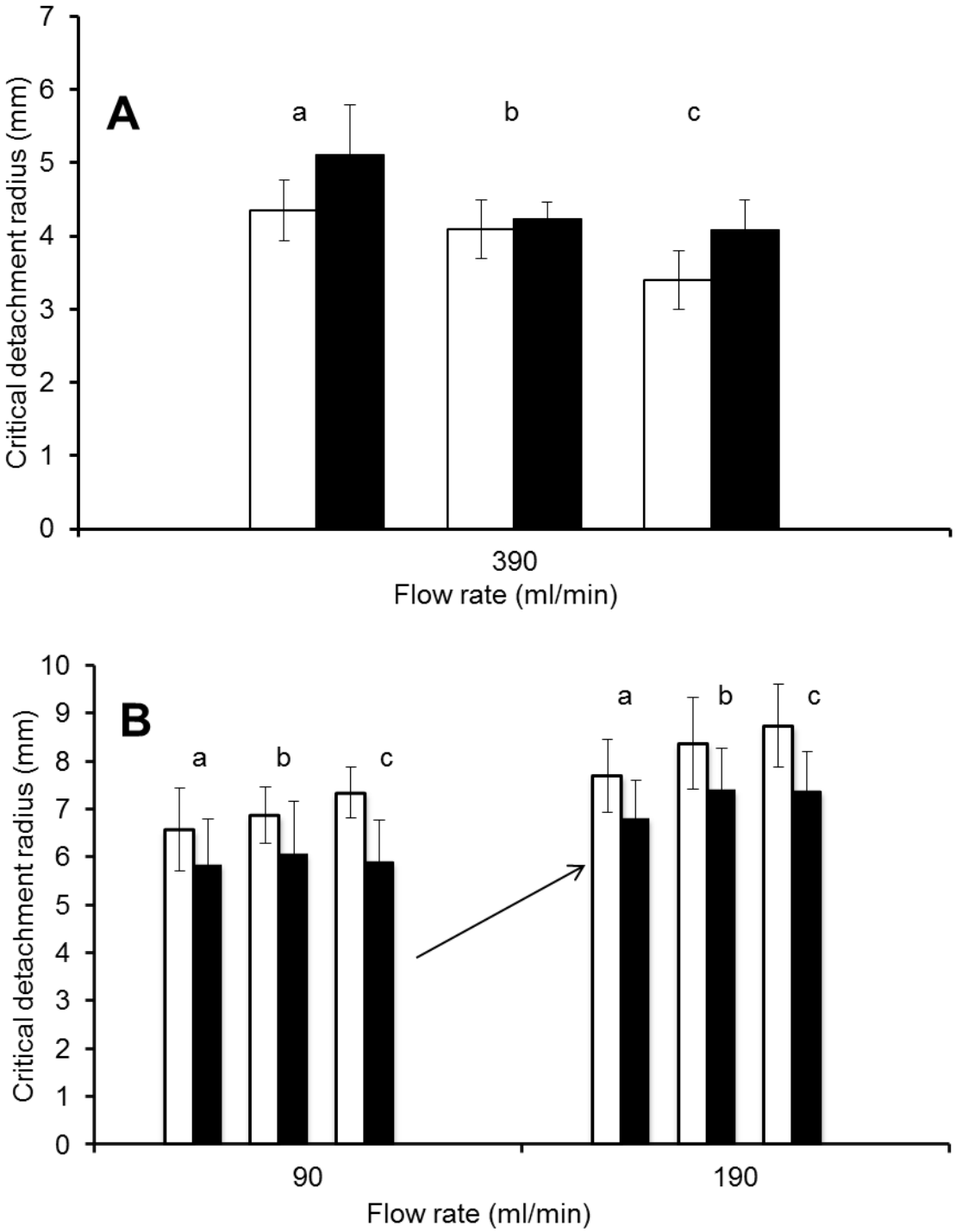

Figure 7. Critical detachment radius measured on substrates soiled with the quartz particles suspensions: (A): glass, cleaning at 390 ml/min; (B) polystyrene, cleaning at 90 and 190 ml/min. White, bare substrate; black, substrate conditioned with dextran; a, quartz suspended in water; b, quartz suspended in dextran solution; c, quartz pretreated with dextran solution and washed.

2001; Rabinovich et al., 2002). When the sprayed suspension drops impact onto the surface, they spread or not and start to evaporate, which leads to the formation of meniscuses and to the appearance of capillary forces at particle-particle and particle-substrate interfaces.

Hydrophilic glass is well wetted by water and dextran solution. Liquid drops spread thus over the surface and presumably dry more quickly. Moreover the particle-substrate capillary forces are similar to particle-particle capillary forces. After drying they leave a larger number of soiling entities, which have a smaller size: aggregates constituted of maximum 2 layers of particles and even isolated particles (Fig. 3). Some droplets could have coalesced due to the extended substrate wetting, resulting in the formation of irregular aggregates.

For the hydrophobic polystyrene, drop coalescence did not occur owing to the lower substrate wetting, resulting in the formation of more circular aggregates. The particle-substrate capillary forces are appreciably lower than the particle-particle capillary forces. As a consequence, particles are free to gather into compact aggregates.

The dependence of the morphology of adhering soiling entities on the substrate is thus explained by the contact angle which affects suspension drop spreading and influences the relative capillary forces at the particle-substrate and particle-particle interfaces upon drying.

4.2. Influence of substrate wetting on cleanability

The removal of soiling entities may be facilitated by the development of lower capillary forces at the substrate-particle interface upon drying, which creates a less intimate contact between the particles and the substrate. This may explain the lower adherence on polystyrene compared to glass. Detry et al. (2009a) compared two spreading medium (ethanol vs water) and showed that when capillary forces are controlling the adhesion of particles aggregates, the adherence is higher when the spreading medium has a higher surface tension.

The lower adherence of quartz soil on polystyrene compared to glass may also be due to the round shape and larger thickness of the soiling entities. Aggregate properties are indeed known to affect the relation between flow rate and critical radius detachment. Removal of particle agglomerates presenting a higher contact area than frontal area is known to require higher hydrodynamic forces than detachment of pairs or particles (Yamamoto et al., 1994). Rounder fibroblasts are for instance more affected by a change in flow rate than flatter ones (Brooks and Tozeren, 1996; Bundy et al., 2001). Similar effects can be expected for the rounder aggregates formed on hydrophobic polystyrene after soiling compared to the flatter deposits formed on glass in the same conditions. Bacteria (more rigid and less viscoelastic than fibroblasts) are more affected than them by a change in flow rate (Bundy et al., 2001). In the case of quartz particle, other factors such as their roughness and their non spherical

shape will influence their contact area and their adhesion strength (Das et al., 1994; Ziskind et al., 1995).

4.3. Influence of soluble polysaccharides

The surface tension of dextran solution (80 mg/l) was 72.3 mN/m, close to the value of 71.6 mN/m for water. This factor could generate an effect of the nature of the quartz suspension used for soiling. There was indeed no significant difference of contact angle between water and dextran solution.

However adsorbed dextran might influence the soil adherence. Fig. 7 shows that conditioning the substrates with dextran solution decreases slightly but systematically the detachment radius on polystyrene and thus increases slightly the soil adherence (fig. 7B), while the opposite was observed on glass (fig.7B), whatever the mode of quartz particle conditioning. Detry et al. (2011) made a similar study by preconditioning polystyrene with a supernatant of starch suspension, which contains soluble macromolecules, and observed a decrease of starch granule adherence. It was concluded that macromolecules may act as an adhesive joint, the properties of which seem to be influenced by the detailed history of drying and exposure to humidity. In our study, dextran was used as soluble macromolecule at a concentration (80 mg/l) which may be too low to have a marked effect. A thorough study must be conducted to elucidate the effect of soluble polysaccharides concentration on particulate soils adhesion.

5. CONCLUSIONS

The effect of soluble polysaccharides represented by dextran on particulate soils removal from hydrophilic and hydrophobic open solids surface has been studied. Surface observation after soiling and exposure to a confined radial shear flow showed the importance of surface wettability and capillary forces. Surface hydrophobicity was shown to influence the morphology of the aggregates formed by droplet spreading. Droplet spreading and the competition between capillary forces at the particle-surface and particle-particle interfaces affect the shape and compactness of the adhering aggregates, the efficiency of shear forces upon cleaning and finally, the adherence of soiling particles. In particular, the rounder aggregates formed on hydrophobic polystyrene after soiling are more sensitive to wall shear stress than flatter ones formed on glass in the same conditions.

The aggregates observed after soiling differed considerably between glass and polystyrene, whether the surface and/or the quartz particles are conditioned with dextran. Conditioning

polystyrene with dextran increased slightly the adherence of quartz particles. The opposite was observed when conditioning glass with dextran, whatever the mode of quartz particle conditioning. The effect of conditioning quartz particles with dextran at the concentration used was not significant. A study on a wide range of concentration of dextran is underway in order to better elucidate the effect of soluble polysaccharides on the adhesion of particulate soils.

NOMENCLATURE

d	particle diameter, µm
D	separation height of particles, m
d^+_p	dimensionless diameter of the particle
d_p	diameter of the particle (m)
h	disk spacing, m
r	radial position, m
ri	inlet radius, m
t	time to traverse the separation height of particles, s
τ_w	mean wall shear stress (Pa)
V*	friction velocity ($m.s^{-1}$)
v	kinematic viscosity ($m^2\ s^{-1}$)
V_p	speed of an isolated Particle, m/s^1
µ	viscosity, Pa.s
ρ_m	density the fluid, kg/m^3
ρ_p	density of the dispersed particle, $kg/\ m^3$

SUBSCRIPT

Cond.	conditioned
RFC	radial-flow cell
SEM	scanning electron microscopy
TLC	thin layer chromatography

REFERENCES

Andre, C., Laux, D., Ferrandis, J.Y. and Blasco, H., 2011, Real-time analysis of the growth of granular media by an ultrasonic method: Application to the sedimentation of glass balls in water, *Powder Technology,* 208, pp. 301–307.

Blel, W., Legentilhomme, P., Le Gentil-Lelièvre, C., Faille C., Legrand J. and Bénézech, T., 2010, Cleanability study of complex geometries: Interaction between B. cereus spores and the different flow eddies scales, *Biochemical Engineering Journal*, 49, pp. 40-51.

Blel, W., Bénézech, T., Legentilhomme, P., Legrand, J. and LeGentil-Lelièvre, C., 2007, Effect of flow arrangement on the removal of Bacillus spores froms tainless steel equipment surfaces during a Cleaning In Place procedure, *Chemical Engineering Science*, 62, pp. 3798-3808.

Brooks, S.B. and Tozeren, A., 1996, Flow past an array of cells that are adherent to the bottom plate of a flow channel, *Computers & Fluids*, 25(8), pp. 741-757.

Bundy, K.J., Harris, L.G., Rahn, B.A. and Richards, R.G., 2001, Measurement of fibroblast and bacterial detachment from biomaterials using jet impingement, *Cell Biology International*, 25(4), pp. 289-307.

Caccavo, J.R., 1999, Protein-mediated adhesion of the dissimilatory Fe(III)-reducing bacterium Shewanella alga BrY to hydrous ferric oxide, *Applied and Environmental Microbiology*, 65(11), pp. 5017-5022.

Das, S.K., Schechter, R.S. and Sharma, M.M., 1994, The role of surface roughness and contact deformation on the hydrodynamic detachment of particles from surfaces, *Journal of Colloid and Interface Science*, 164, pp. 63-77.

Décavé, E., 2002, *Comportement cellulaire sous écoulement hydrodynamique: aspects expérimentaux et théoriques*, PhD Thesis, Université Joseph Fourier, Grenoble, France.

de Lazzer, A., Dreyer, M. and Rath, H. J., 1999, Particle-surface capillary forces, *Langmuir*, 15, pp. 4551-4559.

Detry, J. G., Rouxhet, P. G., Boulangé-Petermann, L., Deroanne, C. and Sindic, M., 2007, Cleanability assessment of model solid surfaces with a radial-flow cell, *Colloids and Surfaces A: Physicochem. Eng. Aspects*, 302, pp. 540–548.

Detry, J. G., Jensen, B. B. B. Sindic, M. and Deroanne, C., 2009a, Flow rate dependency of critical wall shear stress in a radial-flow cell, *Journal of Food Engineering*, 92, pp. 86-99.

Detry, J. G., Deroanne, C., Sindic, M. and Jensen, B. B. B, 2009b, Laminar flow in radial flow cell with small aspect ratios: Numerical and experimental study, *Chemical Engineering Science*, 64, pp. 31-42.

Detry J. G., Sindic M., Servais M. J., Adriaensen Y., Derclaye S., Deroanne C. and Rouxhet P. G., 2011, Physico-chemical mechanisms governing the adherence of starch

granules on materials with different hydrophobicities, *Journal of Colloid and Interface Science,* 355, pp. 210–221

Docoslis, A., Giese, R. F. and van Oss, C. J., 2000, Influence of the water–air interface on the apparent surface tension of aqueous solutions of hydrophilic solutes, *Colloids and Surfaces B: Biointerfaces*, Vol. 19, 2, pp. 147-162

Flint, S.H., Brooks, J.D. and Bremer, P.J., 1997, The influence of cell surface properties of thermophilic streptococci on attachment to stainless steel, *Journal of Applied Microbiology*, 83(4), pp.508-5017.

Goldstein, A. S. and DiMilla, P. A., 1997, Application of fluid mechanic and kinetic models to characterize mammalian cell detachment in a radial-flow chamber, *Biotechnology and Bioengineering*, 55(4), pp. 616-629.

Goldstein, A. S. and DiMilla, P. A., 1998, Comparison of converging and diverging radial flow for measuring *Cell, Adh. AIChE Journal*, 44(2), pp. 465-473.

Jensen, B.B.B., Stenby, M. and Nielsen, D.F., 2007, Improving the cleaning effect by changing average velocity,
Trends in Food Science & Technology. 18, pp. S52–S63.

Jensen, B.B.B., Friis, A., Bénézech, T., Legentilhomme, P. and Lelièvre, C., 2005, Local wall shear stress variations predicted by computational fluid dynamics for hygienic design, *Trans. IchemE Part C: Food and Bioproducts Processing*, 83(C1), PP. 53-60.

Jensen, B. B. B. and Friis, A., 2004, Critical wall shear stress for the EHEDG tests method, *Chemical Engineering and Processing*, 43, pp. 831-840.

Jones, R., Pollock, H. M., Cleaver, J. A. S. and Hodges, C. S., 2002, Adhesion forces between glass and silicon surfaces in air studied by AFM: Effect of relative humidity, particle size, roughness, and surface treatment, *Langmuir*, 18, pp. 8045-8055.

Kralchevsky, P. A. and Nagayama, K., 2001, Capillary Bridges and Capillary-bridge Forces. In: Kralchevsky, P.A.and Nagayama, K., eds. *Attachment of colloid particles and proteins to interfaces and formation of two-dimensional arrays,* Amsterdam: Elsevier, pp. 469-502.

Lelièvre, C., Legentilhomme, P., Gaucher, C., Legrand, J., Faille, C. and Bénézech, T., 2002, Cleaning in place: effect of local wall shear stress variation on bacterial removal from stainless steel equipment, *Chemical Engineering Science,* 57, pp. 1287-1297.

List, W. and Müller, J., 2005, Reinigungsvalidierung unter besonderer berücksichtigung von proteinrückständen, Pharm. Ind., 67, pp. 1359-1365.

Lower, B.H., Yongsunthon, R., Vellano III, F.P. and Lower, S.K., 2005, Simultaneous force and fluorescence measurements of a protein that forms a bond between a living bacterium and a solid surface, *Journal of Bacteriology*, 187(6), PP. 2127-2137.

Ma, X. and Pawlik, M., 2005, Effect of alkali metal cations on adsorption of guar gum onto quartz, *Journal of Colloid and Interface Science*, 289, pp. 48–55.

Maciborski, J. D., Dolez, P. I. and Love, B. J., 2003, Construction of iso-concentration sedimentation velocities using Z-axis translating laser light scattering, *Materials Science and Engineering*, A361, pp. 392–396.

Podczeck, F., 1999, Investigations into the reduction of powder adhesion to stainless steel surfaces by surface modification to aid capsule filling, *International Journal of Pharmaceutics*, 178, pp. 93-100.

Rabinovich, Y. I., Adler, J. J., Esayanur, M. S., Ata, A., Singh, R. and Moudgil, B. M., 2002, Capillary forces between surfaces with nanoscale roughness, *Advances in Colloids and Interface Science*, 96, pp. 213-230.

Speranza, G., Gottardi, G., Pederzolli, C., Lunelli, L., Canteri, R., Pasquardini, L., Carli, E., Lui, A., Maniglio, D., Brugnara, M. and Anderle, M., 2004, Role of chemical interactions in bacterial adhesion to polymer surfaces, *Biomaterials*, 25 (11), pp. 2029-2037.

Stephan, O., Weisz, N., Vieths, S., Weiser, T., Rabe, B. and Vatterott, W., 2004, Protein quantification, sandwitch elisa, and real-time pcr used to monitor industrial cleaning procedures for contamination with peanut and cellery allergens, *Journal of AOAC International*, 87, pp. 1448-1457.

Tadros, T. F., 1980, Particle-surface adhesion, In: L. J. M. Berkeley R.C.W., Melling J., Rutter P.R., Vincent B., eds. Microbial adhesion to surfaces, Chichester: Ellis Horwood Ltd, Chichester pp. 93-116.

Yamamoto, T., Periasamy, R., Donovan, R. and Ensor, D.,1994, Flow cell for real time observation of single particle adhesion and detachment, *Journal of Adhesion Science and Technology*, 8(5), pp. 543-552.

Ziskind, G., Fichman, M. and Gutfinger, C., 1995, Resuspension of particulates from surfaces to turbulent flows - Review and analysis, *Journal of Aerosol Science*, 26(4), pp. 613-644.

SECTION III

CONDITIONING MATERIALS WITH BIOMACROMOLECULES: COMPOSITION OF THE ADLAYER AND INFLUENCE ON CLEANABILITY

From:

Yetioman Touré, Michel J. Genet, Christine C. Dupont-Gillain, Marianne Sindic and Paul G. Rouxhet, 2014.

J. Colloid Interface Sci., 432, 158-169.

ABSTRACT

The influence of substrate hydrophobicity and biomacromolecules (dextran, bovine serum albumin - BSA) adsorption on the cleanability of surfaces soiled by spraying aqueous suspensions of quartz particles (10 to 30 µm size), then dried, was investigated using glass and polystyrene as substrates. The cleanability was evaluated using radial flow cell (RFC). The surface composition was determined by X-ray photoelectron spectroscopy (XPS). The interpretation of XPS data allowed the complexity due to the ubiquitous presence of organic contaminants to be coped with, and the surface composition to be expressed in terms of both the amount of adlayer and the mass concentration of adlayer constituents.

When soiled with a suspension of particles in water, glass was much less cleanable than polystyrene, which was attributed to its much lower water contact angle, in agreement with previous observations on starch soil. Dextran was easily desorbed and did not affect the cleanability. The presence of BSA at the interface strongly improved the cleanability of glass while the contact angle did not change appreciably. In contrast, soiling polystyrene with quartz particles suspended in a BSA solution instead of water did not change markedly the cleanability, while the contact angle was much lower and the aggregates of soiling particles were more flat. These observations are explained by the major role of capillary forces developed upon drying, which influence the closeness of the contact between the soiling particles and the substrate and, thereby, the adherence of particles. The capillary forces are proportional to the liquid surface tension and depend in a more complex way on contact angles of the particles and of the substrate. The dependence of cleanability on capillary forces, and in particular on the liquid surface tension, is predominant as compared with its dependence on the size and shape of the soiling aggregates, which influence the efficiency of shear forces exerted by the flowing water upon cleaning.

Keywords: Fouling; Cleaning; Particulate soiling; Protein adsorption; Polysaccharide adsorption; Radial-flow cell; XPS; Capillary forces

ABBREVIATIONS

BSA: bovine serum albumin

RFC: radial flow cell

XPS: X-ray photoelectron spectroscopy

1. INTRODUCTION

Fouling is the accumulation of unwanted matter on surfaces of materials. The fouling matter may consist of living organisms (biofouling). Non-living fouling has been classified according to different criteria for understanding the formation of deposit and the principles of cleaning: chemical, particulate, crystallization, corrosion, mineral, composite soils (Fryer and Asteriadou, 2009). Particulate fouling may occur when particles settle out onto the substrate by splashing of a suspension or by sedimentation, e.g. of particles (clays, oxides, protein aggregates, etc) suspended in aqueous media or dust from air. Cleaning is an important issue in food and pharmaceutical industries. Its efficiency influences the final quality of the products, and is crucial to insure the absence of cross-contaminations and batch integrity (Stephan et al., 2004). The presence of adhering particles and microorganisms is also undesirable after cleaning and disinfection of open surfaces in applications where hygiene is critical.

Hydrodynamic effects are crucial for the cleaning efficiency, through the shear stress forces acting at the equipment walls (Lelièvre et al., 2002; Jensen et al., 2005; Blel et al., 2007). However, the wall shear stress, mainly governed by the flow rate and the equipment design, is not the only factor explaining cleaning performance. Physico-chemical processes at interfaces created at different stages of fouling and cleaning may be important (Jensen et al., 2007 ; Detry et al., 2009a; Blel et al., 2010). Under this respect, typical examples are fouling with particles (Määttä et al., 2011; 2007; Detry et al., 2011; Pesonen-Leinonen et al., 2006a; 2006b; Kuisma et al., 2007) and with a continuous layer of more or less complex composition (Mauermann et al., 2009; 2011; Piispanen et al., 2011), but these two situations differ according to the influence of the substrate surface properties on drying and cleaning. The interactions between the substrate and particulate contaminants need to be better understood in order to reduce equipment fouling, to improve the efficiency of cleaning and disinfection, or to develop easy-to-clean surfaces (Podczeck, 1999). Chemical compounds present in food and pharmaceutical mixtures may influence interactions with surfaces and adhesion processes (Speranza et al., 2004). Proteins at the outer surface of bacteria are known to play an important role in the initial attachment to solid surfaces in water (Dufrêne et al., 1996; Flint et al., 1997; Caccavo, 1999; Boonaert and Rouxhet, 2000; Lower et al., 2005; Mercier-Bonin et al., 2009). In a work devoted to soiling by starch suspension, it was reported (Detry et al., 2011) that the presence of macromolecules, mainly polysaccharides, which were adsorbed from the liquid phase or carried by the retracting water film and

deposited at the granule-substrate interface, acted as an adhesive joint, the properties of which seemed to be influenced by the detailed history of drying and subsequent exposure to humidity. Macromolecules dissolved in the starch suspension may act in various ways: (i) modification of liquid surface tension and drop spreading upon soiling, (ii) adsorption at the solid-liquid interface, (iii) accumulation at substrate-particulate interface upon drying. In a previous study, (Touré et al., 2011), we showed that conditioning polystyrene substrate with dextran (80 mg/L) slightly increased the adherence of quartz particles and that the opposite occurred when conditioning glass substrate with dextran, whether quartz particles were or not conditioned with dextran themselves. However the presence of dextran preserved the large difference between polystyrene and glass regarding droplet spreading, aggregation of soiling particles and cleanability.

The aim of the present study is to improve the understanding of mechanisms affecting soiling and cleanability by comparing the influence of polysaccharides and proteins on hydrophilic and hydrophobic substrates. Therefore, a particular effort was made to analyze the surfaces by X-ray photoelectron spectroscopy (XPS), coping with the complexity due the ubiquitous presence of organic contaminants at the surface of high energy solids. Quartz particles were kept as a simplified particulate soil model. Glass and polystyrene were chosen as model substrates to examine the influence of substrate hydrophobicity. Dextran is a model of soluble polysaccharide available with a defined molecular size. Bovine serum albumin (BSA) was chosen because it is the common soluble protein used for laboratory studies, and has surfactant properties. It is a globular and structurally labile (soft) protein, which may change its conformation upon adsorption (Norde and Giacomelli 2000; Kopac et al., 2008). The influence of macromolecules was examined by involving them in two ways, introducing them into the quartz suspension used for soiling or conditioning the substrates with them prior to soiling.

2. EXPERIMENTAL

2.1. Substrates and chemicals

Glass slides were purchased from Menzel-Gläser (Germany); the bulk composition was 72.2% SiO_2, 14.3% Na_2O, 1.2% K_2O, 6.4% CaO, 4.3% MgO, and 1.2% Al_2O_3. Slides of 50 mm × 50 mm × 1 mm size were used for soiling and cleaning experiments; slides of 37 mm × 16 mm × 1 mm size were used for surface characterization, either as such for contact angle measurement or after being cut to 16 mm × 10 mm for XPS analysis. Polystyrene sheets (300 mm × 300 mm × 0.25 mm) were purchased from Goodfellow (United Kingdom) and

cut to the desired dimensions (50 mm × 50 mm, 37 mm × 16 mm or 16 mm × 10 mm) according to the need.

MilliQ water was produced by a MilliQ-50 system from Millipore (France). The chemical products used were ethanol 96%, sulfuric acid (98%), hydrogen peroxide solution (30%) purchased from Sigma-Aldrich (Wisconsin, USA) and RBS 50 cleaning agent (Chemical Products R. Borghgraef, Belgium). Dextran from *Leuconostoc mesenteroides,* (20% w/w solution, molar mass 500000 g/mol) and albumin from bovine serum (BSA) (lyophilized powder, ≥ 98%, essentially fatty acid free, essentially globulin free, molar mass 66000 g/mol) were purchased from Sigma-Aldrich (Wisconsin, USA).

2.2. Substrate conditioning

Before use, the glass substrates were cleaned by immersion for 10 min at 50°C in an alkaline detergent solution (RBS 50 diluted 50 times; pH 11.9) and sonicated for 10 min in ultrasonic cleaner (Branson 3200, USA) to remove dust particles. The samples were then rinsed with MilliQ water and cleaned by immersion in a "piranha mixture" (sulfuric acid / hydrogen peroxide 2/1 v/v) at room temperature for 10 min and rinsed thoroughly with MilliQ water.

Polystyrene substrates were first cleaned with ethanol, dried with Kimtech Science paper (Kimberly–Clark, United Kingdom) and immersed for 30 min in ethanol. They were then rinsed thoroughly with MilliQ water.

Both glass and polystyrene substrates were dried with a gentle flow of nitrogen and wrapped in an aluminum foil. The substrates were used as such or conditioned by immersion for 1 h in a 8 g/L dextran or BSA solution at room temperature (volume of 150 mL for the 50 x 50 mm slides, 10 mL for smaller slides). The conditioned slides intended for XPS analysis were rinsed using a procedure which avoided repeated formation of water-air meniscus in contact with the adsorbed phase. Therefore the slide was not repeatedly taken out of the liquid but the solution was diluted, removing of 8 ml from the 10 ml of the solution and adding 8 ml of MilliQ water, with time intervals of 5 min between rinsing steps. When finally taken out of the liquid, the substrates were flushed with nitrogen for removing the liquid film and wrapped in aluminum foil until use for soiling or placed in a Petri dish for XPS analysis. In the latter case, the conditioned substrates were examined as such, or rinsed once or three times before drying as described in section 2.6.4. The concentration of 8 g/L chosen for BSA is lower than the protein concentration in egg white and blood plasma (about 100 g/L from which about 50% albumin, http://en.wikepedia.org); it is higher compared to the whey

protein concentration in cow milk (6 g/L, Walstra and Jenness, 1984) and to the BSA concentration at which adsorption by silica and polystyrene latex reaches a plateau (Norde and Giacomelli, 2000). The dextran concentration was chosen to be the same as that of BSA; this might possibly enhance adsorption with respect to the much lower concentration used previously (Touré et al., 2011), which affected only slightly cleanability.

2.3. Soil preparation

Ground quartz was provided by Sibelco Benelux (Belgium). The material was M400, characterized by a particle size distribution of 1.1 to 60.3 µm. A narrower size distribution (target 10 to 30 µm) was isolated from the initial batch by repeated sedimentation. The particle size distribution (Mastersizer 2000, Malvern Instruments, United Kingdom) of the isolated fraction was unimodal, ranging from 7.6 to 32.7 µm diameter (D10%=10.6 µm; D50%=17.1 µm; D90%=27.1 µm).

Three kinds of quartz suspensions were prepared at a concentration of 150 g/L: (i) in MilliQ water, (ii) in a dextran solution (8 g/L), (iii) in a BSA solution (8 g/L). For preparing the suspensions in dextran and BSA solutions, 7.5 g of quartz were first mixed with 25 ml of MilliQ water and stirred for 30 min at room temperature. Then, 25 ml of a dextran or BSA solution in MilliQ water (16 g/L) were added and the entire mixture was stirred for 1h. The suspensions were kept at 4°C, which was the temperature of dextran and BSA storage, for 72h.

2.4. Soiling procedure

The glass and polystyrene substrates (size 50 mm x 50 mm) were soiled with the quartz suspensions brought at room temperature, by manual aspersion using a thin layer chromatography (TLC) sprayer located 40 cm from the substrate (Detry et al.; 2007; 2011). This did not lead to formation of a continuous liquid film and no drainage occurred. The substrates were dried for 30 min in a dark cupboard at 20.6±1.9°C, with a relative humidity 39±3%. The specifications of these conditions were determined with a Testo 175-H2 logger (Testo, Germany) during three weeks and were in agreement with previous records (Detry et al. 2007; 2011).

2.5. Cleaning experiments

Cleaning experiments were performed in a radial flow cell (RFC). This consisted of an upper disk with a 2 mm diameter central inlet and a lower disk in which the soiled square sample was fitted to be cleaned. The distance between the upper disk and both the sample and the

lower disk was set by three adjustable micrometric screws and controlled to be 1.00±0.02 mm with calibrated steel spacers. A complete description of the device and of its hydrodynamics can be found elsewhere (Detry et al., 2009b). The cleaning fluid used was distilled water and cleaning was performed at 20°C at controlled flow rates (40 or 390 ml/min) for 5 min. The flow rate was selected with the aim of comparing samples, according to previous studies (Detry et al. 2007; 2011). The sample was then removed and dried at room temperature. Pictures of the substrate were taken before and after cleaning, using an epifluorescence stereomicroscope (ZX9 Olympus, Belgium) equipped with a CCD camera, a mercury vapour UV lamp (100W, emission range 100-800 nm) and UV filters (passing bands: excitation 460-490 nm, emission > 520 nm). After cleaning, a circular zone with a lower density of aggregates was observed at the center of the sample. The pictures of the sample before and after cleaning were processed with a specific application of the Matlab software (The Mathworks Inc.), which gave the ratio of the number of aggregates initially present on the surface to the number of aggregates remaining after cleaning, as a function of the radial position. The radial position at which the residual density of aggregates was half the initial density was considered as the critical detachment radius (Goldstein and Dimilla 1997; 1998). The value of the critical radius was checked for consistency in the LUCIA G image analysis software (LIM, Prague, Czech Republic) to insure the absence of artifacts such as the nucleation of air bubbles on the surface. At least 10 repetitions of each experiment (soiling-cleaning) were made, being distributed in at least three independent series. Experiments at different flow rates were performed on different soiled samples. The error bars show the standard deviations.

2.6. Methods of characterization

2.6.1. Scanning electron microscopy (SEM)

The surface of soiled samples was examined by scanning electron microscopy (DSM 982 Gemini from Leo, field-effect gun) in secondary electrons mode (external detector) and backscattered electrons mode (in-lens detector). The images presented here were obtained using an accelerating voltage of 1 kV. Samples were examined after deposition of a 10 nm-thickness chromium coating.

2.6.2. Optical microscopy

Optical micrographs (20X objective) of soiled polystyrene were submitted to image analysis using LUCIA G image analysis software (LIM, Prague, Czech Republic). For each type of

sample, two slides (50 x 50 mm^2) were examined. For each slide, five fields (1 field = 0.25 cm^2) were chosen randomly and a picture was taken at a random place in each field (one picture corresponding to 0.52 mm^2). The equivalent diameter of entity contours was determined based on their measured area and using and Eq. (1):

$$\text{diameter} = 2(\text{area} / \pi)^{1/2} \quad (1)$$

The entity contours were defined using three different threshold gray levels: 40, 90 and 180. For each threshold, data were exported into a txt-file and processed using an Excel tool, providing the size distribution, i.e. the number of objects per class size defined as ≤ 30 μm, 30 to 90 μm and > 90 μm.

2.6.3. Contact angle and liquid surface tension

Static contact angles of water, dextran solution, BSA solution, and supernatants of quartz particles on the substrates were measured using the sessile drop method with a goniometer (Krüss, Germany). Advancing and receding contact angles of water were determined by recording wetting curves (cycles of immersion and emersion) using the Wilhelmy plate method (Tensiometer K100, Krüss, Germany); therefore the effect of buoyancy was corrected and the records were made as a function of the position of the three-phase contact line on the sample slide (Tomasetti et al., 2013). The surface tension of the liquids was measured with a Prolabo Tensiometer (Tensimat n°3) using the Wilhelmy plate method. All these measurements were performed at room temperature.

2.6.4. X-ray photoelectron spectroscopy

Slides of about 16 mm × 10 mm were used for surface analysis by X-ray photoelectron spectroscopy (XPS). The substrates were analyzed either (i) just cleaned; (ii) conditioned by immersion for 1 h in a 8 g/L dextran or BSA solution at room temperature; (iii) same as (ii) and then rinsed once or three times. The analysis was also performed on quartz samples obtained by freeze drying (i) the sediment collected from a suspension (150 g/L) in MilliQ water; (ii) the sediment from suspension (150 g/L) in dextran or BSA solution (8 g/L); (iii) the sediment as (ii), rinsed twice, three times or four times by sedimentation and replacement of the supernatant by water. The final sediments were stored at 4°C for 72 h before being frozen. Finally, dextran and BSA thick layers were also analyzed. These were prepared by successively drying 5 drops of a solution in water deposited on polystyrene.

Both glass and polystyrene samples were fixed on a standard stainless steel holder by using a piece of double-sided insulating tape. Quartz powders (from freeze-dried sediments) were

placed in a stainless steel trough with an inner diameter of 4 mm and mildly pressed with a polyacetal surface cleaned with isopropanol, to obtain a smooth surface.

The XPS analyses were performed with a SSX 100/206 X-ray photoelectron spectrometer from Surface Science Instruments (USA) equipped with a monochromatized micro-focused Al X-ray source (powered at 20 mA and 10 kV). A flood gun set at 6 eV and a Ni grid placed 3 mm above the sample surface were used for charge stabilization. The pressure in the analysis chamber was about 10^{-6} Pa. The angle between the normal to the surface and the axis of the analyzer lens was 55°. The analyzed area was approximately 1.4 mm^2 and the pass energy was set at 150 eV for the survey spectrum and 50 eV for high energy resolution spectra. In the latter conditions, the full width at half maximum (FWHM) of the Au $4f_{7/2}$ peak of a clean gold standard sample was about 1.1 eV. The following sequence of spectra was recorded: survey spectrum, C 1s and K 2p (glass samples only), O 1s, N 1s, Si 2p, S 2p (on some samples treated with BSA) and C 1s again to check for sample charging stability and absence of sample degradation.

The binding energy scale was set by fixing the C 1s component due to carbon bound only to carbon and hydrogen at 284.8 eV. The data analysis was performed with the CasaXPS program (Casa Software, Teignmouth, UK). Molar concentration ratios were calculated from peak areas (linear background subtraction) normalized on the basis of the acquisition parameters and of sensitivity factors and transmission function provided by the manufacturer. The C 1s peak was decomposed by using a least square fitting procedure with a 85:15 Gaussian-Lorentzian product function. The linear regression equations between spectral data were computed using Excel software.

3. RESULTS

3.1. Surface cleanability

The critical radius of detachment, which was the output of the cleaning experiments, is related to a critical wall shear stress and the minimal hydrodynamic drag force required to detach particles in the given experimental conditions (Jensen and Friis, 2004). However, recent studies showed that the conversion of critical radius into critical wall shear stress may be biased when the adhering aggregate height is not negligible with respect to the channel height and when the adherence is such that flow rates above 20 ml/min are required (Detry et al. 2007; 2009a). Owing to these limitations, this conversion was not made here, but it may be kept in mind that a higher adherence was revealed by a lower critical radius at a given flow rate, and by a larger flow rate for a given critical radius.

Figure 1A presents the critical detachment radii measured for the substrates, conditioned or not with dextran, soiled with a quartz suspension in water or in a dextran solution. For glass, no detachment radius could be measured after cleaning at a flow rate of 40 ml/min, indicating that the shear stress generated at this flow rate was not high enough to provoke particle detachment. Therefore a flow rate of 390 ml/min was used; this shows that the presence of dextran decreased slightly the adherence. For polystyrene, the detachment radius was larger than the microscope view field when the flow rate was 390 ml/min, indicating a much higher cleanability compared to glass. In order to examine the influence of conditioning, the detachment radii were measured by setting the flow rate at 40 ml/min. The presence of dextran in the quartz suspension did not influence the adherence, but conditioning the substrate with dextran led to a slight increase of the adherence.

Figure 1B presents the critical detachment radii measured for the substrates, conditioned or not with BSA, soiled with a quartz suspension in water or in a BSA solution. For both substrates, the detachment radii could be compared after cleaning at flow rates of 40 ml/min. For polystyrene substrate, the detachment radius was not significantly influenced by the presence of BSA, whether due to substrate conditioning or to the quartz suspension medium. In contrast, the presence of BSA increased dramatically the critical detachment radius for the glass substrate, and thus decreased the adherence, leading to values beyond those observed for polystyrene.

3.2. Soil morphology

Representative optical and SEM micrographs of the soiled substrates before cleaning are presented in Figure 2 for the different systems investigated. When polystyrene was not conditioned with BSA, the SEM images showed that many quartz particles formed dense rounded aggregates. For glass and BSA-conditioned polystyrene, particles were more dispersed or formed elongated motifs. The presence of more numerous coarse aggregates on bare or dextran-conditioned polystyrene was also revealed by optical micrographs.

The micrographs of Figure 2 are representative of observations made. In order to test the significance of differences between samples, the optical micrographs obtained on polystyrene were studied in more detail by image analysis.

The detailed results are shown in Supporting Material (Table S1) in the form of the density of objects and their distribution in 3 size fractions: $\leq$ 30 µm, 30 to 90 µm, $>$ 90 µm. Increasing the threshold led to an increase of the small size fraction and a decrease of the large size fraction. Using a threshold of 180 decreased the number of counted objects and

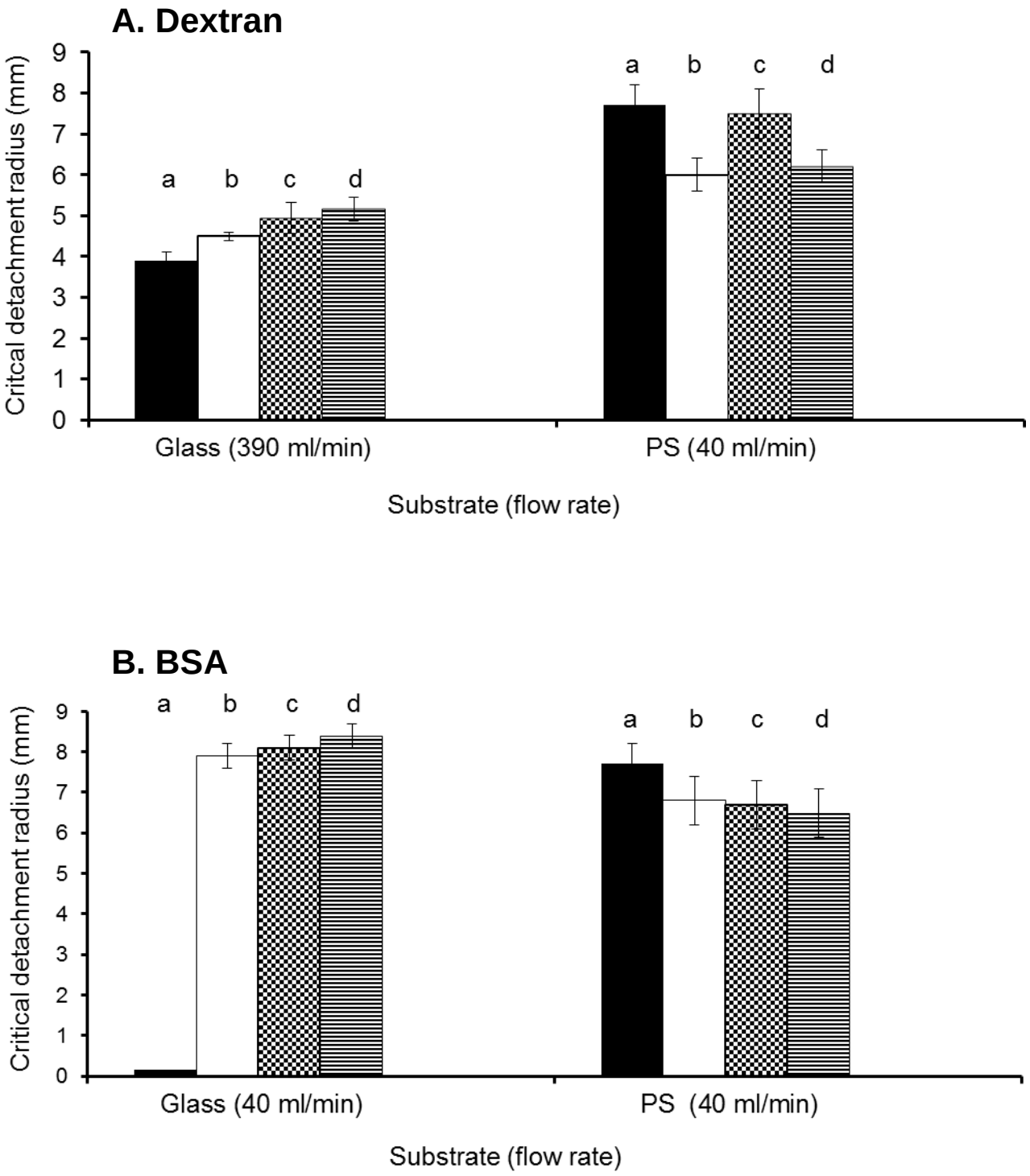

Figure 1. Critical detachment radius measured on bare substrates (a, c) and on substrates conditioned with macromolecules (b, d), soiled with quartz particles suspensions in water (a, b), or in a solution of macromolecules (c, d). The macromolecules were dextran (A) or BSA (B).

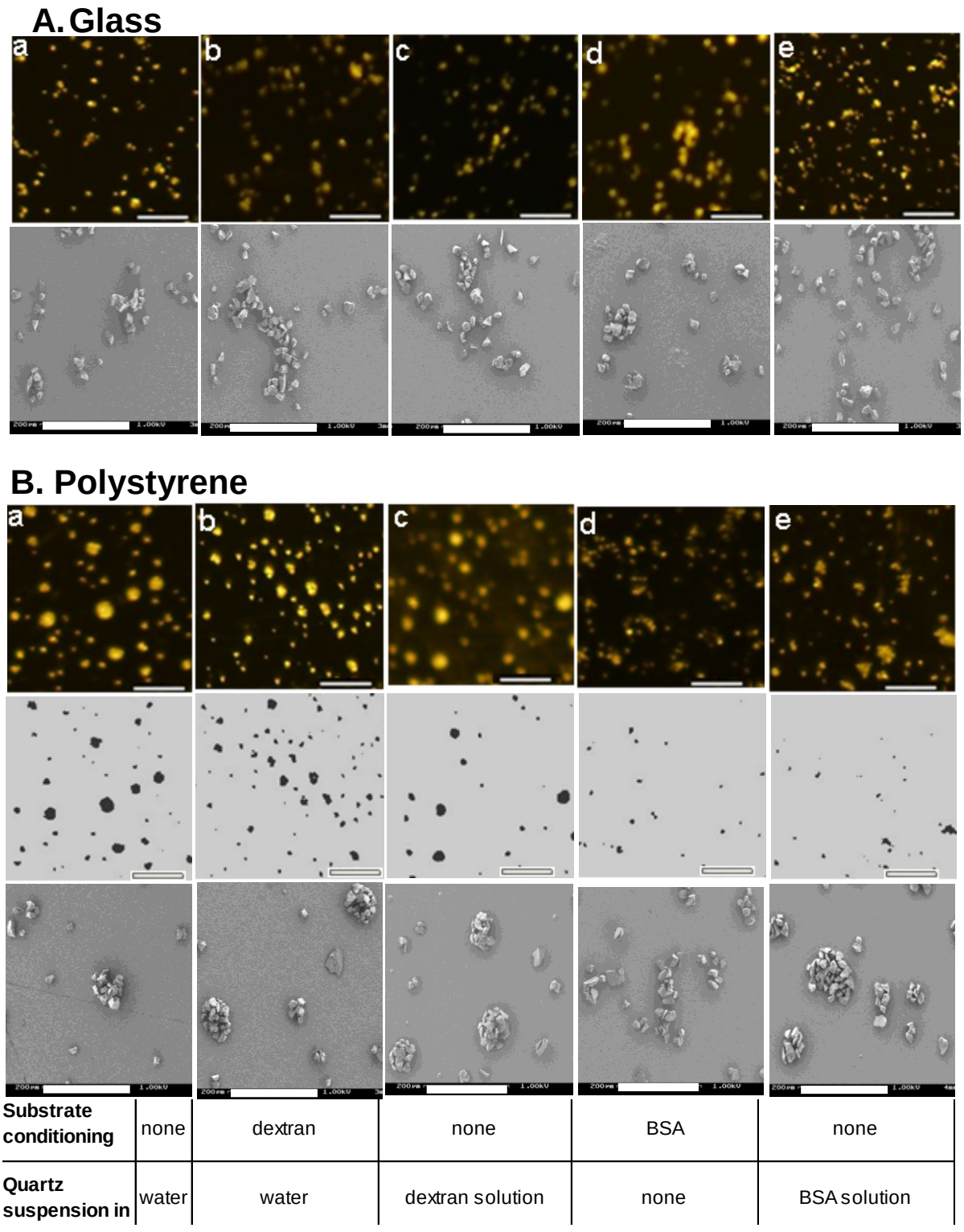

Figure 2. Micrographs of glass (A) and polystyrene (B) surfaces conditioned or not as indicated, and soiled with quartz particles suspensions in water, dextran solution or BSA solution, as indicated. Top line in A and B, optical micrographs (scale bar 300 µm); middle line in B, same obtained by image analysis with a threshold of 180; bottom line in A and B, SEM micrographs made with the external detector (scale bar 200 µm).

the decrease was much stronger for the two systems involving BSA. In Figure 2B, the images obtained with a threshold of 180 can be compared with the direct micrographs and provide a clear evidence of lower aggregation of particles on polystyrene soiled in the presence of BSA.

Combination of SEM and optical microscopy thus showed that particles were more aggregated on bare and dextran-conditioned polystyrene compared to glass samples and to BSA-conditioned polystyrene. The situation was less clear and possibly intermediate in the case of bare polystyrene soiled with a suspension of quartz in a BSA solution.

3.3. Contact angle

Figure 3A presents the contact angles measured on the substrates, conditioned or not with dextran, using the supernatant of a quartz suspension in water or in a dextran solution, or using a dextran solution. The results show that the great difference between glass and polystyrene was maintained in all conditions (substrate conditioned or not, presence of dextran or not in the solution, supernatant or pure solution). They also show that conditioning the substrates with dextran (b, d and f compared to a, c and e) led to a slight increase of the contact angle, irrespective of the liquid used.

Figure 3B show analogous results obtained with BSA instead of dextran. Conditioning glass with BSA (b, d, f) led to a very slight increase of the contact angle, which remained however in the range of 10 to 20°. On the other hand, conditioning polystyrene with BSA provoked a strong decrease of the contact angle, from the range of 80 to 85° to the range of 25 to 30°. The contact angle measured with a solution containing BSA (pure solution or supernatant) was not markedly different from that measured with pure water.

3.4. Liquid surface tension

Table 1 presents the surface tensions of water, of dextran and BSA solutions and of supernatants of quartz particles suspensions in water and in dextran and BSA solutions. There was no significant difference between the surface tension of water, dextran solution and supernatant of quartz suspension in water. The surface tension of the supernatant of the quartz suspension in dextran solution was slightly lower. The presence of BSA in the liquid phase markedly decreased the surface tension, giving 30 and 49 mN/m for the BSA solution and for the supernatant of the quartz suspension in BSA solution, respectively.

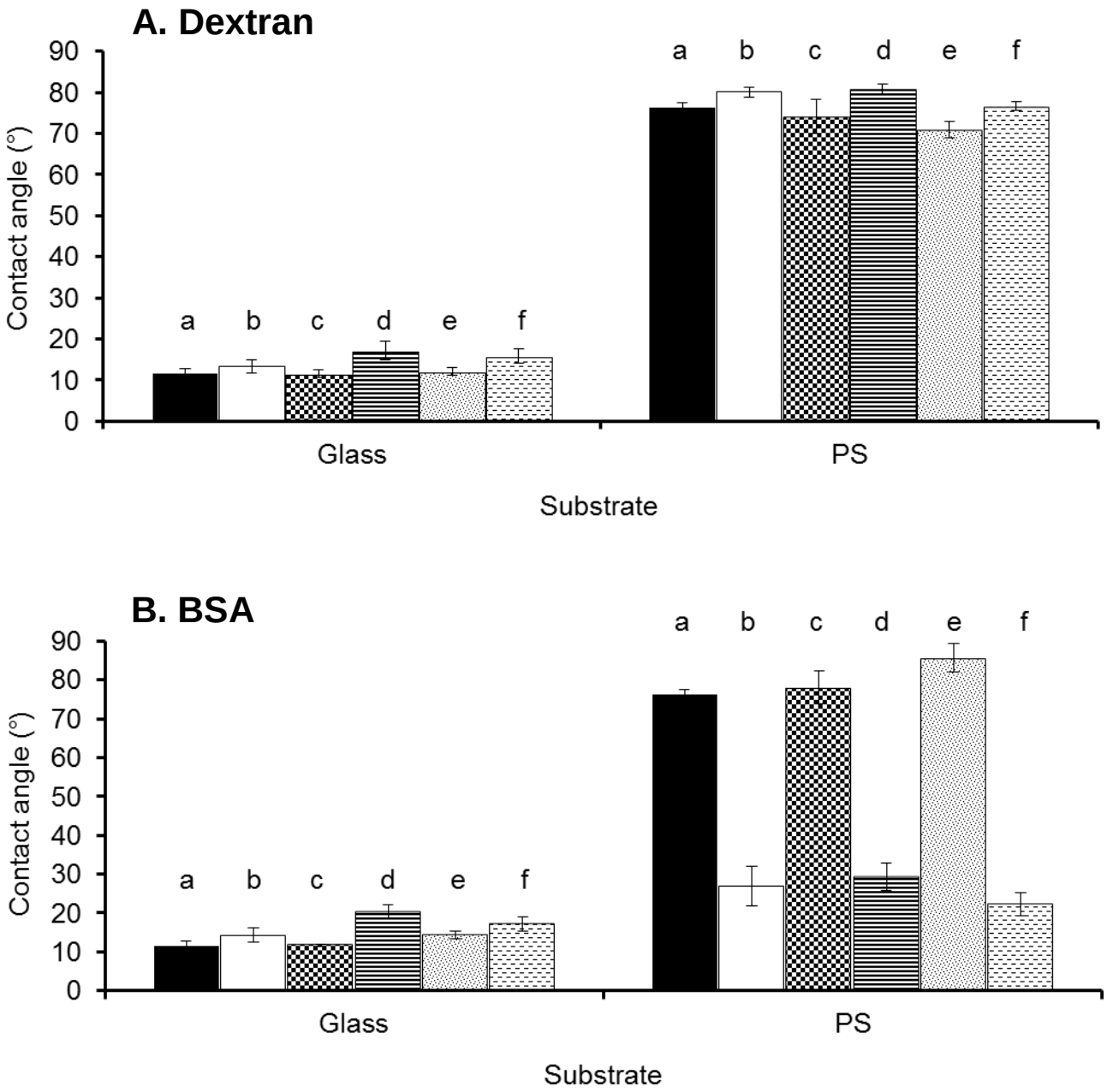

Figure 3. Contact angle measured on bare substrates (a, c, e) and on substrates conditioned with macromolecules (b, d, f), using the supernatant of quartz suspensions in water (a, b), or the supernatant of quartz suspensions in solutions of macromolecules (c, d), or using a solution of macromolecules (e, f). The macromolecules were dextran (A) or BSA (B).

Table 1. Surface tension (mN/m) of water, of solutions (8 g/L) of dextran and BSA and of supernatants of suspensions of quartz particles in water, dextran solution or BSA solution.

Water	Solution		Supernatant of quartz particles		
	Dextran	BSA	in water	in dextran solution	in BSA solution
72.2 ± 1.1*	72.8 ± 0.1	30.0 ± 1.1	72.9 ± 0.3	68.6 ± 1.1	48.7 ± 2.3

*Mean ± standard deviation

3.5 Surface composition

Table 2 gives the surface elemental composition determined by XPS on the residue obtained after evaporation of drops of dextran and BSA solution, on bare substrates, on conditioned substrates, rinsed or not, on quartz powder collected from a suspension in water, and on quartz powder conditioned by suspension in a dextran or BSA solution, and rinsed or not. The presence of oxygen, oxidized carbon and silicon at the surface of non-conditioned polystyrene may explain that the water contact angle (Figure 3) was lower than expected (Dupont-Gillain et al., 2000). Figure 4 presents representative O 1s, N 1s and C 1s peaks recorded with the siliceous solids. Non-conditioned glass and quartz showed the presence of carbon. This was attributed to organic contaminants which were not removed by the cleaning procedure or were adsorbed from the surrounding, either the ambient atmosphere or the spectrometer vacuum chambers (Rouxhet, 2013).

The C 1s peak was decomposed (Rouxhet et al., 2008; Rouxhet and Genet, 2011), allowing the possibility of 4 components, in addition to the shake up contribution at 291.4 eV (C_{sh}) observed in the case of samples with polystyrene substrate. The full width at half maximum was imposed to be the same for the 4 components. No constraint was imposed on the binding energy of the components except when their intensity was very weak, in which case the binding energy was constrained to be in range observed otherwise. The component attributed to carbon only bound to carbon and hydrogen [**C**-(C,H)] was set at 284.8 eV. Other components were found at 286.3 ± 0.2 eV, assigned to carbon making a single bond with oxygen or nitrogen [**C**-(O,N)], and 288.0 ± 0.2 eV, assigned to carbon making one double or two single bonds with oxygen, typical of amide function in proteins [N-**C**=O] and of acetal link in polysaccharides [O-**C**-O], respectively. For certain samples, a very weak component was found near 289.3 eV, which may be due to ester or carboxyl. The results of the C 1s peak decomposition are presented in Table 2.

The O 1s peak was found at 532.6 eV for dextran [C-**O**H, C-**O**-C], and had a maximum near 531.4 eV for BSA [N-C=**O**]. Glass and quartz powder showed an O 1s peak at 532.7 eV and532.3 eV, respectively. The position and shape of the O 1s peak of conditioned samples varied according to the respective contributions. Its decomposition was not performed, owing to the overlap of the contribution of siliceous solids with that of the organic adlayer, particularly dextran.

The main N 1s peak at 399.0 - 400.0 eV and a minor component, typically 20 times less intense, near 402 eV were attributed to amide or non-protonated amine and to protonated

Table 2. Surface concentration (mole fraction with respect to all elements except hydrogen, in %) measured by XPS on dextran, BSA, bare substrates and conditioned substrates, rinsed (1, 2, 3 or 4 times) or not, quartz powders collected from suspension in water, or in dextran or BSA solution: elements and carbon present in different functions associated to C 1s peak components. The results for quartz powders involving 3 rinsing steps, on the one hand, and 2 and 4 rinsing steps, on the other hand, are from independent experiments.

			Mole fraction of element (%)						Mole fraction of carbon (%)				
Element, function			**C**	**O**	**N**	**Si**	**S**	**Na**	**C-(C,H)**	**C-(O,N)**	**N-C=O O-C-O**	**O-C=O**	**Shake up**
Binding energy (eV)									284.8	286.3	288.0	289.3	291.4
Dextran			62.8	35.3	1.6	0.3	n.m.	n.m.	18.0	35.5	8.4	1.0	
BSA			67.3	17.9	13.9	b.d.l	0.5	0.4	37.4	16.1	13.8	b.d.l.	
Solid	**condit.**	**rinse**											
Glass	none		17.5	58.4	0.0	22.3	n.m.	1.9	12.2	3.1	1.2	1.0	
Powder	none		7.0	63.5	0.0	29.5	n.m.	n.m.	4.8	1.3	0.6	0.3	
Glass	dextran	none	39.0	49.2	0.2	10.1	n.m.	1.6	8.7	23.7	6.1	0.6	
Glass	dextran	none	54.0	45.2	0.1	0.5	n.m.	0.2	5.3	39.0	9.1	0.6	
Glass	dextran	1	16.5	61.1	0.1	21.8	n.m.	0.5	8.9	5.6	1.5	0.5	
Glass	dextran	3	18.2	59.5	0.3	21.5	n.m.	0.5	11.3	4.8	1.5	0.6	
Powder	dextran	none	23.7	57.5	0.0	18.9	n.m.	n.m.	3.3	16.3	3.6	0.5	
Powder	dextran	3	6.6	62.2	0.3	30.9	n.m.	n.m.	4.7	1.3	0.6	b.d.l.	
Powder	dextran	none	20.2	59.9	0.0	19.9	n.m.	n.m.	3.5	13.5	2.9	0.3	
Powder	dextran	2	7.2	67.3	0.0	25.5	n.m.	n.m.	5.7	1.1	b.d.l.	0.5	
Powder	dextran	4	7.0	67.4	0.0	25.5	n.m.	n.m.	5.5	1.2	b.d.l.	0.3	
Glass	BSA	none	63.1	20.5	15.0	0.8	n.m.	0.5	30.3	18.3	14.2	0.3	
Glass	BSA	none	53.3	27.1	12.0	6.1	0.4	1.0	26.8	14.7	11.2	0.7	
Glass	BSA	1	45.3	33.9	10.3	9.3	0.2	1.0	23.6	12.3	9.1	0.2	
Glass	BSA	3	42.9	35.5	9.4	10.8	0.2	1.2	22.5	11.0	8.8	0.5	
Powder	BSA	none	28.1	45.1	6.7	20.1	n.m.	n.m.	14.0	7.9	6.2	b.d.l.	
Powder	BSA	3	40.3	35.9	10.4	13.4	n.m.	n.m.	19.1	12.2	9.0	b.d.l.	
Powder	BSA	none	34.5	41.8	8.6	15.1	n.m.	n.m.	17.2	10.0	7.3	b.d.l.	
Powder	BSA	2	27.2	47.0	6.6	19.2	n.m.	n.m.	13.5	8.0	5.7	b.d.l.	
Powder	BSA	4	31.5	44.1	7.2	17.2	n.m.	n.m.	17.3	7.6	6.6	b.d.l.	
Polystyrene	none		94.9	3.5	0.0	1.7	n.m.	n.m.	86.3	2.5	b.d.l.	b.d.l.	6.0
Polystyr.	dextran	none	82.8	12.9	2.4	2.0	n.m.	n.m.	69.0	9.5	2.2	b.d.l.	2.0
Polystyr.	dextran	none	87.0	9.2	1.1	2.7	n.m.	n.m.	76.9	6.1	0.9	b.d.l.	3.1
Polystyr.	dextran	1	80.7	12.9	0.9	5.5	n.m.	n.m.	73.6	4.4	0.4	b.d.l.	2.3
Polystyr.	dextran	3	84.0	10.8	0.6	4.6	n.m.	n.m.	78.6	3.0	b.d.l.	b.d.l.	2.4
Polystyr.	BSA	none	65.6	19.0	14.4	0.3	0.6	0.2	35.7	17.2	12.7	b.d.l.	b.d.l.
Polystyr.	BSA	none	64.7	19.9	14.1	0.3	0.6	0.4	35.6	16.9	12.3	b.d.l.	b.d.l.
Polystyr.	BSA	1	81.8	11.3	5.6	1.2	0.1	b.d.l	63.5	9.0	2.9	3.4	3.0
Polystyr.	BSA	3	80.4	12.4	5.2	1.9	0.1	b.d.l	63.7	8.8	3.9	1.0	3.0

n.m. not measured

b.d.l. below detection limit

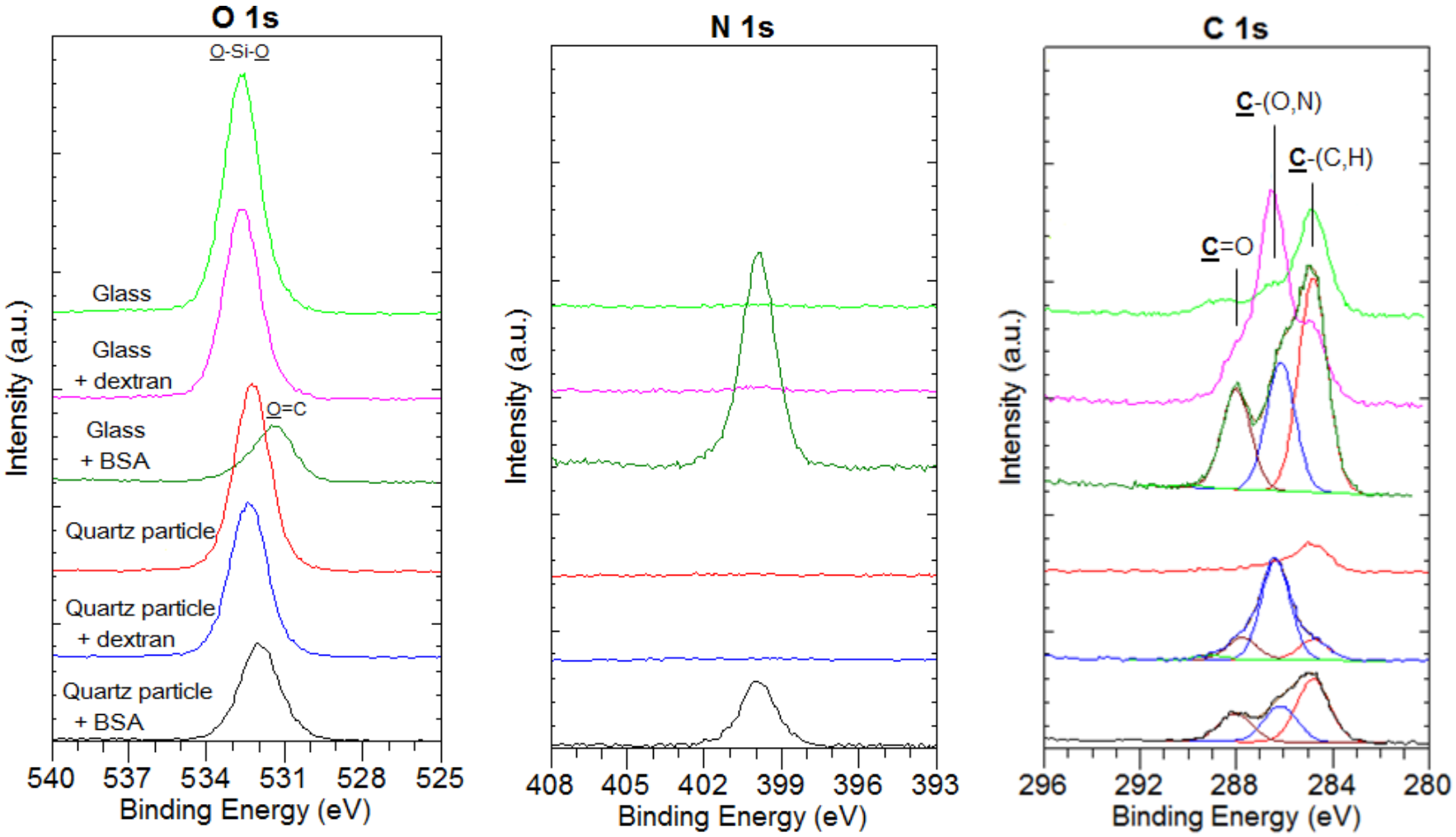

Figure 4. Representative O 1s, N 1s and C 1s peaks recorded on quartz powder and glass substrate, conditioned or not with dextran and BSA, and illustration of C 1s peak decomposition.

amine, respectively. For samples showing a high N concentration, a S 2p doublet was found with the S $2p_{3/2}$ component near 163.7 eV, which was attributed to sulfur-containing residues of BSA (Caillou et al., 2007).

The Si 2p peak of glass and quartz samples was found near 103.0 eV. Silicon was detected in low concentration on polystyrene samples and attributed to surface contamination. Glass samples showed a Na 1s peak near 1071.5 - 1072.0 eV. Non-conditioned glass also showed low concentrations of calcium (about 1%), potassium (about 0.25%) and chloride (about 0.25%) but these peaks were not recorded after conditioning.

Extraction of meaningful information from XPS spectra is complicated by several features: presence of organic contaminants in addition to expected adsorbate, overlap of solid and adsorbate contributions in the C 1s peak of polystyrene samples and in the O 1s peak of siliceous samples. On the other hand, peak decomposition is an interpreting approach which involves a trade-off between imposing constraints and generating information (Rouxhet and Genet, 2011). Correlations between independent spectral data (elements, C 1s peak components) were used to validate peak decomposition and component assignment, and to identify useful markers for the determination of surface molecular composition. Therefore reference data were deduced from the amino acid sequence of BSA (Hirayama et al., 1990) and are presented in Supporting Material. They concern the elemental composition as well as the chemical functions associated with the components of the C 1s and O 1s peaks and their concentrations.

Figure 5a presents the correlation between the concentration of carbon in an oxidized form

$$C_{ox} = C_{tot} - C_{284.8} - C_{sh} \quad (2)$$

and the concentration of nitrogen, N, for all samples except those involving dextran: non-conditioned solids, BSA and solids conditioned with BSA. The regression line was computed without considering the non-conditioned solids and provided a slope of 1.99, close to the value of 2.01 expected for BSA (details in Supporting Material). The intercept was small, in agreement with data obtained for non-conditioned solids, and attributed to organic contaminants present on glass and quartz powder and to a slight oxidation of polystyrene surface. Correlations between the concentration of C_{288} (attributed to N-**C**=O) and $C_{286.3}$ (attributed to **C**-N) and the N concentration are shown in Supporting Material. A comparison with data expected for BSA indicates that the separation between these two components is less reliable than the separation between the contributions of C_{ox} and $C_{284.8}$.

Dextran and dextran-conditioned solids showed a small concentration of nitrogen, which

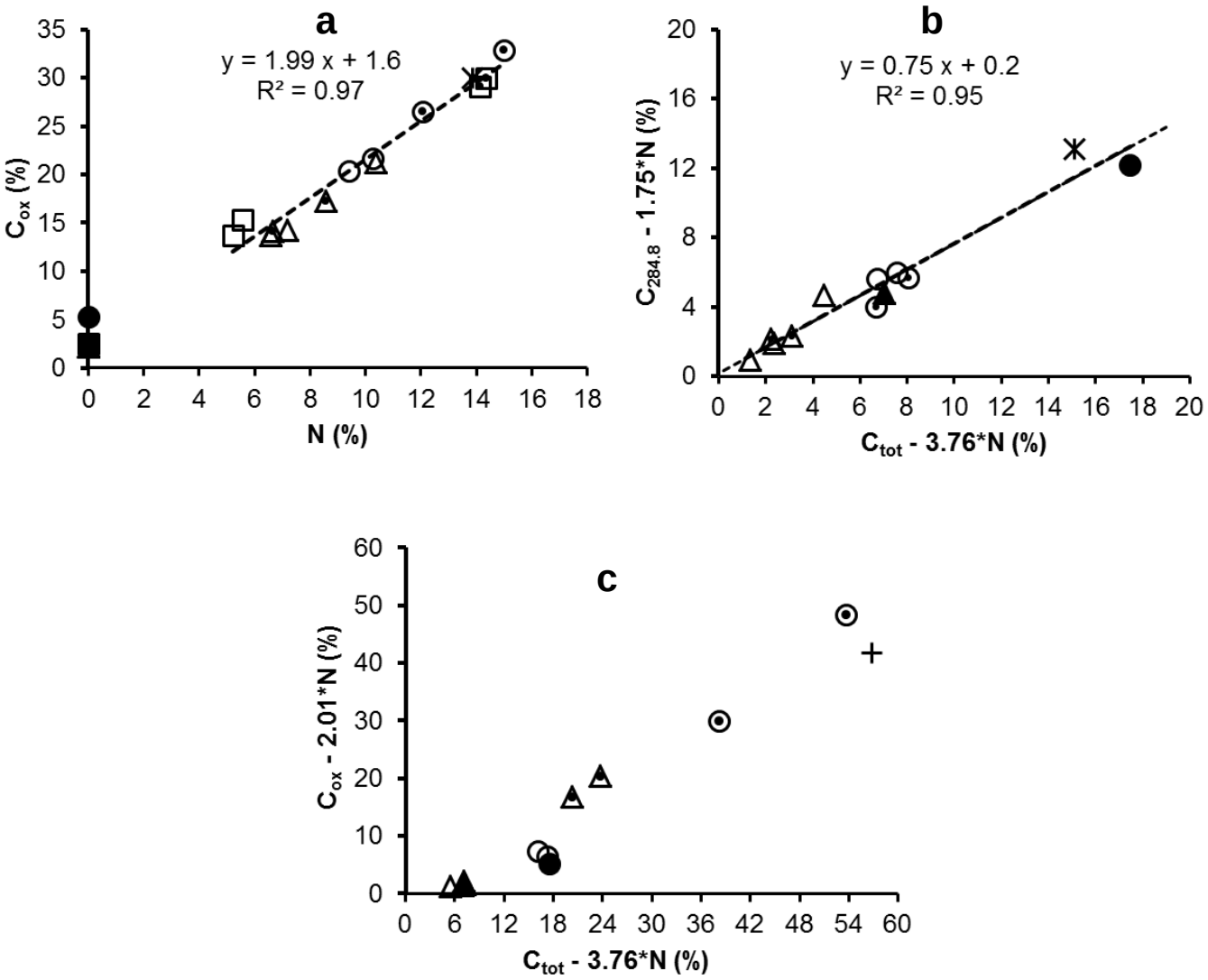

Figure 5. Correlations between the indicated sums of concentrations regarding the elemental nature of carbon (mole fraction of elements): BSA **(✱**, only in a and b**)**; dextran (✕, only in c); glass (●,○), polystyrene (■,□, only in a) and quartz powder (▲,△), bare (closed symbols) or conditioned and rinsed (open symbols) or conditioned and not rinsed (open symbols with dot). a and b, substrate conditioning with BSA; c, substrate conditioning with dextran. Dashed line: regression line with its equation; in a this was computed excluding the non-conditioned solids.

was not observed for non-conditioned solids (Table 2). This was attributed to contamination of the glass vessels by proteins, presumably BSA. The contribution of BSA to the concentrations should be $C_{ox\text{-}BSA}$ = 2.01*N and O_{BSA} = 1.15*N (details in Supporting Material). The concentration ratio (C_{ox} -2.01*N)/(O- 1.15*N) = 1.24 (from Table 2) measured for dextran sample is in excellent agreement with the expected value of 1.20. The non-BSA contributions for conditioned samples may be due to dextran, for which the contributions should be O_{dextr} = $C_{ox\text{-}dextr}$/1.2, or to organic contaminants, for which the

contributions should be $O_{cont} = C_{ox\text{-}cont}$ if oxidized carbon is present in the form of alcohol, aldehyde, ketone or ester functions. The concentration of organic oxygen can then be deduced as follows:

$$O_{org} = N*1.15 + (C_{ox} - 2.01*N)/1.2 = 0.83*C_{ox} - 0.52*N \quad (3)$$

if the non-protein adsorbate is pure dextran, or

$$O_{org} = N*1.15 + (C_{ox} - 2.01*N) = C_{ox} - 0.86*N \quad (4)$$

if the non-protein adsorbate is only contaminants.

The concentration of oxygen due to siliceous solids may then be evaluated as $O_{inorg} = O_{tot} - O_{org}$ and should be related to the concentration of the inorganic elements according to the formulas SiO_2 and Na_2O. The plot of O_{inorg}, evaluated by equation (4), vs. (2*Si + 0.5*Na) is presented in Figure 6 (regression equation y = 1.18 x - 3.7) and is close to the expected 1:1 relationship. It is not significantly different if O_{inorg} is evaluated using equation (3), which gives the regression equation y = 1.13 x - 0.07. The regression equations thus do not permit to decide whether organic oxygen other than that of protein is due to dextran or to contaminants.

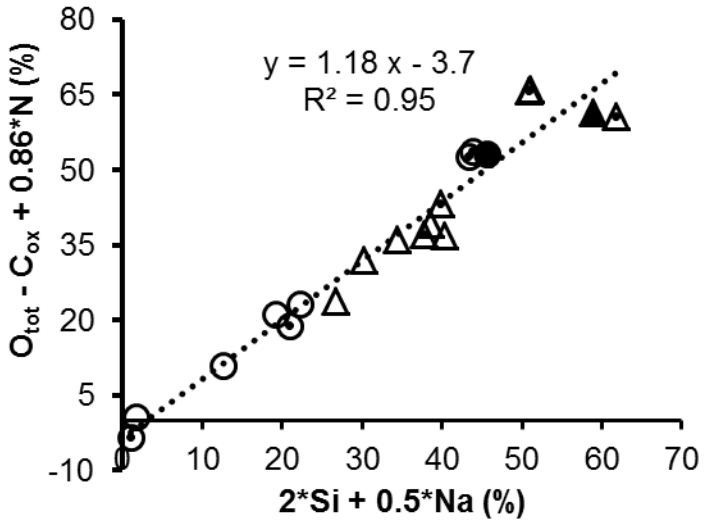

Figure 6. Correlations between the concentration of inorganic oxygen, evaluated from Equ. (4), and the weighted sum of Si and Na concentrations (mole fraction of elements) for the siliceous solids: glass (●,○), quartz powder (▲,△), bare (closed symbols) or conditioned with BSA (open symbols) or conditioned with dextran (open symbols with dot). Dashed line: regression line with its equation.

The correlations presented in Figures 5 a and 6, concerning all solids, bare or conditioned with BSA, and siliceous solids, bare or conditioned with dextran, demonstrate that the C 1s peak decomposition and components assignment are reliable. According to the amino acid

composition of BSA (Supporting Material), its contribution to carbon concentration is expected to be $C_{ox\ BSA}$ = 2.01*N, in agreement with Figure 5a, $C_{284.8\text{-}BSA}$ = 1.75*N and $C_{tot\text{-}BSA}$ = 3.76*N. Plots based on these considerations provide a direct visualization of the chemical nature of compounds other than BSA present at the surfaces, more specifically their relative content in oxidized carbon [C_{ox}] and carbon in the form of hydrocarbon moieties [**C**-(C,H)]. Polystyrene substrate must be excluded from these plots owing to the contribution of the substrate to the carbon peak.

Figure 5b presents the plot of ($C_{284.8}$ − 1.75*N) vs (C_{tot} −3.76*N) for BSA, and for glass and quartz powder, bare and conditioned with BSA. It shows that carbon which is not due to BSA is of hydrocarbon nature in a defined proportion of about 75%, in agreement with values reported for adventitious contamination (Gerin et al.., 1995). In the case of the BSA sample, the additional carbon may also be due to compounds which are present as traces in the BSA solution and accumulate at the liquid-air interface upon evaporation of the solution drop during sample preparation. It is indeed well known that the surface of solid food products is strongly enriched in lipids compared to proteins (Rouxhet and Genet, 2011). It may be noted in Figure 5b that the amount of carbon not due to BSA is much higher for bare siliceous solids than for BSA-conditioned siliceous solids. This suggests that BSA adsorption displaces organic contaminants present before conditioning or prevents contamination from the gas phase during sample handling in air and XPS analysis.

Figure 5c presents the plot of (C_{ox} − 2.01*N) vs (C_{tot} −3.76*N) for dextran and for glass and quartz powder conditioned with dextran. It shows that carbon which was not due to BSA was mainly in oxidized form for non-rinsed dextran-conditioned samples. Most of dextran was removed by rinsing, leaving an organic adlayer which contained a high proportion of hydrocarbon typical of contaminants, as revealed by Figure 5b.

It appears thus that N may be taken as a marker for BSA, ($C_{284.8}$ − 1.75*N) may be taken as a marker for hydrocarbon moieties due to contaminants and, or to polystyrene, and (C_{ox} − 2.01*N) may be taken as a marker for dextran or oxidized carbon of contaminants.

4. DISCUSSION

4.1. Surface composition

Ideally the surface composition should provide the adsorbed amount of each kind of adsorbate. The adsorbed amount should be expressed in mass per unit area or thickness of the adsorbed layer. This would require simulations based on models of the adsorbed layer

involving hypothetical degrees of coverage and layer thicknesses, and would have a weak reliability owing to the complexity of the adsorbed layer and the lack of XPS measurements at different take-off angles. However comparisons of adsorbed amounts can be made between samples of the same solid, based on the sum of concentrations of elements due to the adsorbed layer, Σads, and due to the solid (glass or polystyrene substrate, or quartz powder), Σsol, which may be evaluated as follows, neglecting hydrogen. For siliceous samples,

$$\Sigma ads = C_{284.8} + 2*C_{ox} \quad (5)$$

where the second term provides an approximation for oxidized carbon, oxygen and nitrogen;

$$\Sigma sol = 3* Si + 1.5*Na \quad (6)$$

which accounts for inorganic elements and oxygen bound to them.

For polystyrene samples,

$$\Sigma ads = 5.91*N + 2*(C_{ox} - 2*N) \quad (7)$$

where the first term accounts for carbon, oxygen and nitrogen of BSA, while the second term provides an approximation for carbon and oxygen which are not due to BSA;

$$\Sigma sol = C_{284.8} + C_{sh} - 1.75*N \quad (8)$$

where the third term accounts for the part of $C_{284.8}$ due to BSA.

Table 3 (left part) gives the values of Σads and Σsol computed for the different samples. Conditioning the solids with BSA increased appreciably the importance of the organic adlayer, which was slightly decreased by subsequent rinsing. After conditioning with dextran, rinsing provoked a strong reduction of the contribution of the amount of adlayer.

In order to express the relative concentration of organic compounds at the surface (adlayer on siliceous solids, adlayer and substrate for polystyrene samples), the mass concentration of molecular compounds is much more explicit than the molar concentration of elements. The relative mass concentration of organic compounds in the adsorbed layer may be computed from the mole fraction of markers and the related molar mass as recalled in Supporting Material (Table S5 and related text). In order to evaluate the mass % of non-BSA compounds, two models were considered, which differed according to hypotheses made regarding the relationship between oxygen and oxidized carbon. In model A, the compounds other than BSA were considered globally with the marker (C – 3.76*N), which accounts for carbon and hydrogen (in the form of CH_2 or H-C-OH), and (Cox – 2.01*N), which accounts for oxygen. In model B, the presence of dextran and hydrocarbon was considered, being accounted for by (Cox – 2.01*N) and ($C_{284.8}$ – 1.75*N), respectively. Application of model

A to BSA-conditioned siliceous solids showed that BSA was the dominating constituent (about 90 mass % or above) in the adlayer and was not markedly removed by rinsing. In case of polystyrene samples, the same conclusion appeared based on the values of Σads. For dextran-conditioned substrates, the two models A and B provided consistent results.

Table 3. Surface composition deduced by XPS for bare substrates and conditioned substrates, rinsed (1, 2, 3 or 4times) or not: contributions of the organic adlayer (sum of constituting elements Σads, in mole %) and of the solid (sum of constituting elements Σsol, in mole %) to the XPS spectrum; composition (mass %) of the organic adlayer present on the solids, computed according to two models. The results for quartz powders involving 3 rinsing steps, on the one hand, and 2 and 4 rinsing steps, on the other hand, are from independent experiments.

					Organic composition (mass %)				
			Sum of elements (mole %)		**Model A**		**Model B**		
			Adlayer	Solid	Protein	Non protein	Protein	Dextran	Hydrocarbon
Solid	**condit.**	**rinse**							
Glass	none		22.7	69.7	0.0	100.0		n.a.	
Powder	none		9.2	88.4	0.0	100.0		n.a.	
Glass	dextran	none	69.4	32.6	1.8	98.2	1.9	85.8	12.3
Glass	dextran	none	102.7	1.7	0.5	99.5	0.6	94.2	5.2
Glass	dextran	1	24.1	66.1	3.0	97.0	3.1	60.0	36.8
Glass	dextran	3	25.1	65.4	6.1	93.9	6.3	49.9	43.8
Powder	dextran	none	44.1	56.6	0.0	100.0	0.0	92.3	7.7
Powder	dextran	3	8.5	92.6	21.9	78.1	22.3	28.2	49.5
Powder	dextran	none	36.9	59.7	0.0	100.0	0.0	90.2	9.8
Powder	dextran	2	8.8	76.4	0.0	100.0	0.0	34.7	65.3
Powder	dextran	4	8.5	76.6	0.0	100.0	0.0	33.6	66.4
Glass	BSA	none	95.9	3.0	90.4	9.6		n.a.	
Glass	BSA	none	79.9	19.7	87.3	12.7		n.a.	
Glass	BSA	1	66.9	29.5	88.7	11.3		n.a.	
Glass	BSA	3	63.3	34.3	86.1	13.9		n.a.	
Powder	BSA	none	42.2	60.4	91.2	8.8		n.a.	
Powder	BSA	3	61.5	40.2	97.3	2.7		n.a.	
Powder	BSA	none	51.7	45.4	95.8	4.2		n.a.	
Powder	BSA	2	40.8	57.7	93.4	6.6		n.a.	
Powder	BSA	4	45.8	51.6	91.2	8.8		n.a.	
Polystyr.	none		5.1	92.3	n.a.			n.a.	
Polystyr.	dextran	none	28.0	66.9	14.9	85.1*	15.5	14.5	70.0*
Polystyr.	dextran	none	16.3	78.0	7.2	92.8*	7.5	10.2	82.3*
Polystyr.	dextran	1	11.3	74.3	6.6	93.4*	6.8	6.7	86.5*
Polystyr.	dextran	3	7.2	80.0	4.2	95.8*	4.4	4.1	91.5*
Polystyr.	BSA	none	87.2	11.3	87.2	12.8*		n.a.	
Polystyr.	BSA	none	85.3	11.6	87.3	12.7*		n.a.	
Polystyr.	BSA	1	41.3	57.0	34.1	65.9*		n.a.	
Polystyr.	BSA	3	37.4	57.8	33.0	67.0*		n.a.	

n.a not applied

* this includes the contribution of the polystyrene substrate

Consideration of both Σads and organic composition indicated that an appreciable amount of dextran was present at the surface of siliceous solids after conditioning but most of this was

released upon rinsing. The amount of dextran present on dextran-conditioned polystyrene, even not rinsed, was not higher than the amount of protein.

4.2. Distribution of soiling particles and wetting properties

Conditioning glass with BSA slightly increased the contact angle, while conditioning polystyrene with BSA markedly decreased the contact angle (Figure 3B). It is noteworthy that the contact angle measured on bare polystyrene was not markedly affected by the presence of BSA in the liquid phase (compare a, c and e in Figure 3B). This is in relation with the measurement of the contact angle in advancing conditions, and the fact that BSA was not present on the surface to be wetted. The influence of protein adsorption and subsequent drying on the water contact angle was reported for several systems: non-annealed and annealed films of cellulose derivatives conditioned with BSA (Kosaka et al., 2005); silicon wafer, silanized silicon wafer and polystyrene conditioned with enolase (Almeida et al., 2002); set of materials with water contact angle ranging from 11 to 100° fouled with β-lactoglobulin and rinsed (Yang et al., 1991). In these works, protein conditioning of hydrophilic substrates led to an increase of the water contact angle while conditioning of hydrophobic substrates led to a decrease of the contact angle. The contact angle measured on most of these substrates after conditioning was in the range of 50 to 70°. The same trend was observed here. The water contact angle measured after protein adsorption was however not higher than 20° for glass and 25 to 30° for polystyrene. The prefered orientation of certain amino acid residues at the surface of protein-conditioned substrates was demonstrated by Time-of-Flight Secondary Ion Mass Spectroscopy (Dupont-Gillain et al., 2010). In the case of hydrophobic substrates, protein adsorption may be driven by hydrophobic bonding, so that hydrophilic amino acids tend to be oriented toward water and remain so upon drying. In the case of hydrophilic substrates, the hydrophilic moieties should tend to get buried during drying in order to decrease surface energy. The fact that conditioned substrates fall in the same range of contact angles may be the consequence of the two mechanisms; however clarifying the relative importance of these mechanisms would require a comparison with the contact angle of thick protein layers. Under that respect, it may be noted that the results of Yang et al. (1991) covered a range of adsorbed amounts of 0.2 to 4 $\mu g/cm^2$, corresponding to a thickness about 1.4 to 28 nm, depending on the substrate. Accordingly they included adsorbed amounts which were much higher than one monolayer.

Conditioning glass with dextran slightly increased the contact angle (Figure 1B). This may be due to contamination with BSA as revealed by XPS, and is thus not significant. The influence of conditioning polystyrene with dextran was not significant.

On hydrophobic materials (polystyrene and dextran conditioned-polystyrene), particles were assembled in dense rounded aggregates (Figure 2). This was due to a lack of suspension droplet spreading: as water evaporated, particles were brought together and finally got compacted by capillary forces (Kralchevsky and Denkov, 2001; Kralchevsky and Nagayama K., 2001; 1994). On glass substrates and BSA conditioned-polystyrene, quartz particles were better dispersed, owing to spreading and coalescence of suspension droplets. As dewetting occurred, meniscuses were formed, and particles moved under the influence of lateral capillary forces, which led to the formation of aggregates in the form of elongated motifs (Thill and Spalla, 2003).

4.3. Cleanability

The lower cleanability of glass compared to polystyrene, when non-conditioned, (Figure 1a) is a robust observation, as it reproduces two previous independent observations (Touré et al., 2011; 2013). It may be explained by the lower contact angle (Figure 3a), in agreement with a study (Detry et al., 2011) of the adherence of starch granules on different substrates, including glass and polystyrene, using the same experimental approach as here (soiling with droplets of a starch suspension and drying, cleaning with the radial flow cell used in this work). A higher substrate wettability increases droplet spreading which leads to thinner aggregates and decreases the efficiency of shear forces exerted by the flowing water. Moreover it enhances capillary forces at the interface between the particles and the substrate and insures a closer contact between their surfaces. As a result, the adherence of soiling particles is increased.

Literature data show that the wettability is important upon cleaning in air with a wet cloth, and may be related to the competition between substrate wetting and the capture of soiling particles by the liquid-air interface. The surface cleanability of materials soiled in air (rotating drum in a dry atmosphere in air) with a mix of inorganic particles (mainly quartz) presumably coated with paraffin oil was evaluated by the cleaning index (essentially ratio of soil removed by cleaning to initial soil), measured after cleaning with a microfiber cloth moistened with water, a solution of surfactant or a weakly alkaline model detergent (Pesonen-Leinonen et al., 2006a). The cleaning index decreased as the water contact angle of the substrate increased. Surface cleanability was also investigated (Määttä et al., 2007;

2011) using a soil model made of a suspension of chromium oxide or chromium acetyl acetonate particles in 1-propanol containing triolein, and cleaning with a microfiber cloth moistened with a detergent solution. For all substrates, the removal of chromium oxide was more efficient compared to the organic salt. A more detailed influence of the substrate hydrophilicity was possibly masked by unsatisfactory water contact angle measurements by drop shape analysis, as indicated by the lack of consistency between two instruments.

The influence of the nature of the suspending medium of soiling particles will be considered now. In the above example, removal of chromium oxide particles from poly(vinyl chloride) was not influenced by the presence of triolein in the soiling suspension (Pesonen-Leinonen et al., 2006b). In the study of the adherence of starch granules (Detry et al., 2011), SEM micrographs obtained with the in-lens detector showed that macromolecules or sub-micrometer size starch fragments were adsorbed from the liquid phase and, or carried by the liquid film retracting during drying, and were accumulated at the granule-substrate interface. SEM micrographs with in-lens and external detectors were obtained here on soils formed on the two substrates, bare or conditioned with dextran or BSA, using quartz suspension in water or in dextran or BSA solutions, without rinsing. Figure 7 shows a representative micrograph, obtained on a quartz aggregate present on polystyrene conditioned with dextran and soiled with a quartz suspension in dextran solution. The micrographs did not demonstrate any accumulation of macromolecules in or around the aggregates, presumably owing to the low concentration in the solution.

The influence of BSA on glass cleanability, whether it was brought by glass conditioning or by the quartz suspension, is not in accordance with the only influence of the contact angle discussed above in the comparison between non-conditioned glass and polystyrene. The domination of BSA at interfaces, which was demonstrated by XPS, was found to improve markedly the glass cleanability (Figure 1B, glass) although the contact angle (Figure 3B, glass) and particles distribution (Figure 2) did not change appreciably. On the other hand, conditioning polystyrene with BSA markedly decreased the water contact angle (Figure 3B, polystyrene), which led to more flat aggregates (Figure 2), but this was not correlated with a significance change of cleanability (Figure 1B, polystyrene).

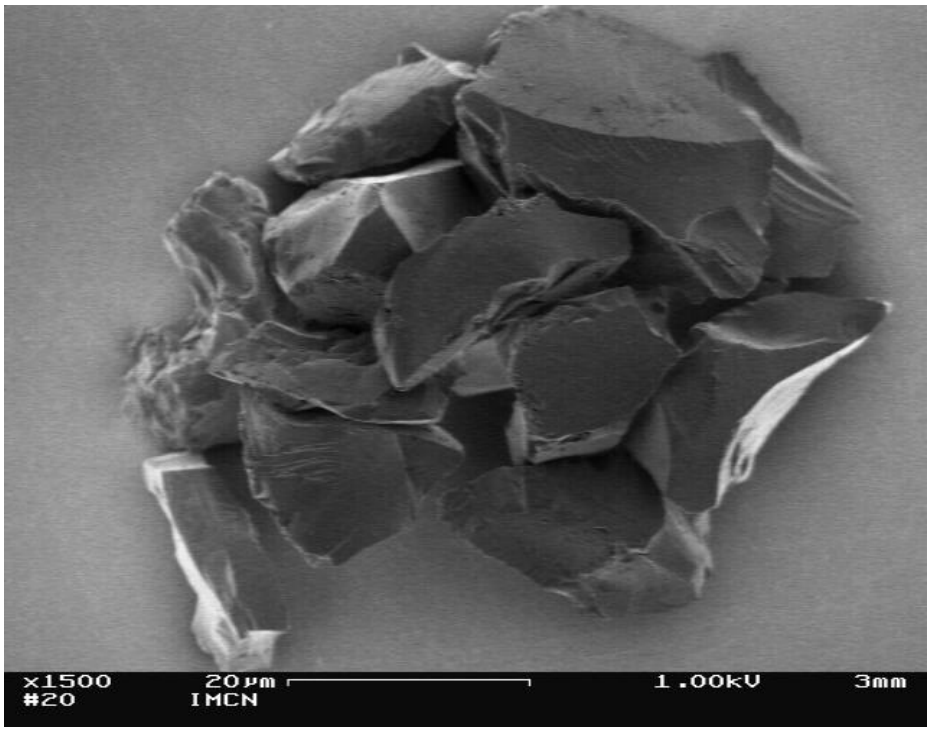

Figure 7. SEM micrograph (in-lens detector; scale bar 20µm) recorded on an aggregate present on polystyrene conditioned with dextran and soiled with a suspension of quartz particles in dextran solution.

Actually, the key to explain cleanability seems to be the strength of capillary forces developed in the course of drying, which depend on both the contact angle and the liquid surface tension. Assuming that spherical particles are at a small distance of the substrate surface and considering a bridge of liquid forming a ring around the contact point, the capillary forces created by meniscuses between a quartz particle and the substrate can be evaluated by the following equations (Rabinovich et al., 2002; Pitois et al., 2000):

$$F_{CAP} = 4\pi\gamma_L R\cos\left(\frac{\Theta_p + \Theta_s}{2}\right)\cos\left(\frac{\Theta_s - \Theta_p}{2}\right) \qquad (9)$$

where F_{CAP} is the capillary force (N), γ_L is the liquid surface tension (N/m), R is the soil particle radius (m), θ_S and θ_P are the contact angles of the liquid on the substrate and on the particles, respectively. Capillary forces were computed considering quartz particles of 9 µm radius, a particle contact angle θ_P in the range of 10 to 20° as measured for glass, and surface tensions of 72.2 and 48.7 mN/m for water and for the supernatant of quartz suspensions in BSA solution, respectively (Table 1). The results for F_{CAP} are as follows for situations differing according to the liquid and a range of contact angles:

- water suspension, θ_S 10 to 20°, relevant for glass: F_{CAP} = 8.0 to 7.7 µN;
- BSA-containing suspension, θ_S 10 to 20°, relevant for glass: F_{CAP} = 5.4 to 5.2 µN;

- water suspension, θ_S 75 to 80°, relevant for non-conditioned polystyrene: F_{CAP} = 5.1 to 4.5 µN;
- BSA-containing suspension, θ_S 25 to 30°, relevant for BSA-conditioned polystyrene: F_{CAP} = 5.2 to 5.0 µN.

Note that the hypotheses regarding particle size and shape are not critical if the results are only used for comparison with each other. It appears that the lower cleanability of glass soiled with a quartz suspension in water is due to higher capillary forces developed during drying. The similarity between the cleanability of glass soiled with a BSA-containing suspension and the cleanability of polystyrene soiled in absence of BSA is due to the combination of contact angle and liquid surface tension in Eq. (9).

Glass soiled with a suspension of quartz particles in water deserves a special comment. The higher cleanability of the conditioned glass compared to the non-conditioned glass (Figure 1B, b compared to a), for similar contact angles (Figure 3B), indicates that, for conditioned glass, the capillary forces were governed by a lower liquid surface tension, due to BSA desorption into the soiling droplets.

The influence of contact angle deserves also some comments. Consider the case of non-conditioned polystyrene soiled with a BSA-containing suspension. If the contact angle governing the capillary forces was in the range of 75 to 85° as measured (Figure 3B, c) F_{CAP} would be in the range of 3.4 to 2.8 µN. The cleanability would thus be expected to be significantly higher than that of BSA-conditioned polystyrene, which is not the case (Figure 1B, c compared to d). Actually the contact angle governing the capillary forces should be the receding contact angle, while the values reported in Figure 3 were measured using the sessile drop method, i.e. close to advancing conditions. While this calls for caution regarding the F_{CAP} values computed above, the comparison between bare glass soiled with a water suspension (receding contact angle below 10°) and bare polystyrene soiled with a water suspension (receding contact angle about 70°, leading to computed F_{CAP} = 5.3 µN) is still valid. Attempts made to measure receding water contact angles of a BSA solution using the Wilhelmy plate method failed to give accurate results, because of perturbations due the weight of a layer of liquid carried along by the substrate as it was withdrawn from the solution (to be published), but this revealed a low contact angle. For BSA-conditioned substrates soiled with a suspension in water, the use of Eq. (9) is further complicated by the uncertainty regarding the liquid surface tension, which depends on the extent of by BSA desorption.

It turns out that the role of capillary forces, which depend directly on both liquid surface tension and contact angle, is more important than the size and shape of the aggregates, which depend on droplet spreading and are thus governed directly by contact angle and only indirectly by liquid surface tension. Eq. (9) is a useful tool to roughly foresee the influence of liquid surface tension, contact angle and their combination. For a given liquid surface tension, the capillary forces will not be reduced by more than 20%, with respect to perfectly wetting surfaces (contact angle close to zero), if the contact angles of the facing surfaces do not exceed the paired values of 10 – 50, 20 – 45, 30 – 40. According to the symmetry properties of Eq. (9), it thus not matter whether the pair is taken as particle – substrate or substrate – particle.

The above discussion is consistent with the fact that the cleanability of glass or polystyrene was not markedly affected by the presence of dextran, as neither the liquid surface tension nor the contact angle was appreciably affected. Moreover dextran was readily desorbed in the presence of water.

5. CONCLUSIONS

The interpretation of XPS data by using peak decomposition was validated by correlations between spectral data of independent nature related to peak intensity and peak shape, respectively. The complexity due to the ubiquitous presence of organic contaminants could be coped with, and the surface compositions could be expressed both in terms of the amount of adlayer and mass composition of the adlayer constituents.

When soiled with a suspension of particles in water, glass was much less cleanable than polystyrene, in agreement with the previous observations on starch soil. The presence of dextran did not affect the cleanability of glass or polystyrene. The presence of BSA at the interface improved strongly the cleanability of glass while the contact angle did not change appreciably. In contrast, soiling polystyrene with quartz particles suspended in a BSA solution instead of water did not change markedly the cleanability, while the contact angle was much lower. These observations are explained by the major role of capillary forces developed upon drying, which influence the closeness of the contact between the soiling particles and the substrate and, thereby, the adherence of particles. The capillary forces are proportional to the liquid surface tension but are not expected to be reduced by more than 20%, with respect to perfectly wettable surfaces (contact angle close to zero), if the contact angles of the facing surfaces do not exceed paired values of about 10 – 50, 20 – 45 or 30 – 40. The dependence of cleanability on capillary forces is predominant compared with its

dependence on the size and shape of the soiling aggregates, which influence the efficiency of shear forces exerted by the flowing water upon cleaning.

ACKNOWLEDGEMENTS

This study was supported by the Walloon Region. The support of National Foundation for Scientific Research (FNRS, Belgium) is also gratefully acknowledged. The authors thank Adriaensen Yasmine for the XPS experiments and Sylvie Derclaye for the SEM examinations.

REFERENCES

Almeida, A. T., Salvadori, M. C., Petri, D. F. S., Box, P. O. (2002). Enolase adsorption onto hydrophobic and hydrophilic solid substrates. *Langmuir, 18*, 6914–6920.

Blel, W., Bénézech, T., Legentilhomme, P., Legrand, J., Le Gentil-Lelièvre, C. (2007). Effect of flow arrangement on the removal of Bacillus spores from stainless steel equipment surfaces during a Cleaning In Place procedure. *Chem. Eng. Sci.*, *62*(14), 3798–3808.

Blel, W., Legentilhomme, P. , Le Gentil-Lelièvre, C. , Faille, C., Legrand, J. B. T. (2010). Cleanability study of complex geometries: Interaction between B. cereus spores and the different flow eddies scales. *Biochem. Eng. J.*, *49*(1), 40–51.

Boonaert, C. J. P., Rouxhet, P. G. (2000). Surface of lactic acid bacteria : relationships between chemical composition and physicochemical properties. *Appl. Environ. Microbiol.*, *66*(6), 2548–254.

Caccavo Jr., F. (1999). Protein-mediated adhesion of the dissimilatory Fe (III) - Reducing bacterium *Shewanella* alga BrY to hydrous ferric oxide. *Appl. Environ. Microbiol.*, *65*(11), 5017–5022.

Caillou, S., Boonaert, C. J. P., Dewez, J., Rouxhet, P. G. (2007). Oxidation of proteins adsorbed on hemodialysis membranes and model materials. *J. Biomed. Mater. Res. Part B Appl. Biomater.*, *84B*(1), 240–248.

Detry, J. G, Sindic, M., Servais, M. J., Adriaensen, Y., Derclaye, S., Deroanne, C., Rouxhet, P. G. (2011). Physico-chemical mechanisms governing the adherence of starch granules on materials with different hydrophobicities. *J. Colloid Interface Sci.*, *355*(1), 210–21.

Detry, J. G., Jensen, B. B. B., Sindic, M., Deroanne, C. (2009a). Flow rate dependency of critical wall shear stress in a radial-flow cell. *J. Food Eng.*, *92*(1), 86–99.

Detry, J.G., Deroanne, C., Sindic, M., Jensen, B. B. B. (2009b). Laminar flow in radial flow cell with small aspect ratios: Numerical and experimental study. *Chem. Eng. Sci.*, *64*(1), 31–42.

Detry, J. G., Rouxhet, P. G., Boulangé-Petermann, L., Deroanne, C., Sindic, M. (2007). Cleanability assessment of model solid surfaces with a radial-flow cell. *Colloids Surfaces A. Physicochem. Eng. Asp.*, *302*(1-3), 540–548.

Dufrêne, Y. F., Boonaert, C. J. P, Rouxhet G. P. (1996). Adhesion of *Azospirillum brasilense* : role of proteins at the cell-support interface. *Colloids Surfaces B. Biointerfaces*, *7*, 113–128.

Dupont-Gillain, C. C., Mc Evoy, K. M., Henry, M., Bertrand, P. (2010). Surface spectroscopy of adsorbed proteins: input of data treatment by principal component analysis. *J. Mater. Sci. Mater. Med.*, *21*(3), 955–61.

Dupont-Gillain, C. C., Adriaensen, Y., Derclaye, S., Rouxhet, P. G. (2000). Plasma-oxidized polystyrene : wetting properties and surface reconstruction. *Langmuir*, *16*, 8194-8200

Flint, S. H., Brooks, J. D., Bremer, P. J. (1997). The influence of cell surface properties of thermophilic streptococci on attachment to stainless steel. *J. Appl. Microbiol.*, *83*(4), 508–517.

Fryer, P. J., Asteriadou, K. (2009). A prototype cleaning map: A classification of industrial cleaning processes. *Trends Food Sci. Technol.*, *20*(6-7), 255–262.

Gerin, P.A., Dengis, P.B., Rouxhet, P.G (1995). Performance of XPS analysis of model biochemical compounds. *J. Chim. Phys.*, *92*(5), 1034–1065.

Goldstein, A. S., DiMilla, P. A. (1998). Comparison of converging and diverging radial flow for measuring cell adhesion. *AIChE J.*, *44*(2), 465–473.

Goldstein, A S, DiMilla, P. A. (1997). Application of fluid mechanic and kinetic models to characterize mammalian cell detachment in a radial-flow chamber. *Biotechnol. Bioeng.*, *55*(4), 616–29.

Hirayama, K., Akashi S, Furuya, M., Furuya, K. (1990). Rapid confirmation and revision of the primary structure of bovine serum albumin by ESIMS and Frit-FAB LC/MS. *Biochem. Biophys. Res. Commun.*, *173*(2), 639-646.

Jensen, B. B. B., Friis, A. (2004). Critical wall shear stress for the EHEDG test method. *Chem. Eng. Process. Process Intensif.*, *43*(7), 831–840.

Jensen, B. B. B., Stenby, M., Nielsen, D. F. (2007). Improving the cleaning effect by changing average velocity. *Trends Food Sci. Technol.*, *18*, S58–S63.

Jensen, B. B. B., Friis, A., Bénézech, T., Legentilhomme, P., Lelièvre, C. (2005). Local wall shear stress variations predicted by computational fluid dynamics for hygienic design. *Food Bioprod. Process.*, *83*(1), 53–60.

Kopac, T., Bozgeyik, K., Yener, J. (2008). Effect of pH and temperature on the adsorption of bovine serum albumin onto titanium dioxide. *Colloids Surfaces A. Physicochemical Eng. Asp.*, *322*(1-3), 19–28.

Kosaka, P. M., Kawano, Y., Salvadori, M. C., Petri, D. F. S. (2005). Characterization of ultrathin films of cellulose esters. *Cellulose*, *12*(4), 351–359.

Kralchevsky, P. A, Denkov, N. D. (2001). Capillary forces and structuring in layers of colloid particles. *Curr. Opin. Colloid Interface Sci.*, *6*(4), 383–401.

Kralchevsky, P. A., Nagayama, K. (2001). Lateral capillary forces between partially immersed bodies. *Elsevier, Amsterdam*, 287–350.

Kralchevsky, P. A., Nagayama, K. (1994). Capillary forces between colloidal particles. *Langmuir*, *10*(1), 23–36.

Kuisma, R., Fröberg, L., Kymäläinen, H.-R., Pesonen-Leinonen, E., Piispanen, M., Melamies, P., Hautala, M., Sjöberg, A-M., & Hupa, L. (2007). Microstructure and cleanability of uncoated and fluoropolymer, zirconia and titania coated ceramic glazed surfaces. *J. Eur. Ceram. Soc.*, *27*(1), 101–108.

Lelièvre C., Legentilhomme, P. Gaucher, C., Legrand, J., Faille, C., Bénézech, T. (2002). Cleaning in place : effect of local wall shear stress variation on bacterial removal from stainless steel equipment. *Chem. Eng. Sci.*, *57*, 1287–1297.

Lower, B. H., Yongsunthon, R., Iii, F. P. V., Lower, S. K. (2005). Simultaneous force and fluorescence measurements of a protein that forms a bond between a living bacterium and a solid surface. *J. Bacteriol.*, *187*(6), 2127–2137.

Määttä, J., Piispanen, M., Kuisma, R., Kymäläinen, H.-R., Uusi-Rauva, A., Hurme, K.-R., Arevad, S., Sjöberg, A.-M, Hupa, L. (2007). Effect of coating on cleanability of glazed surfaces. *J. Eur. Ceram. Soc.*, *27*(16), 4555–4560.

Määttä, J., Kuisma, R., Kymäläinen, H.-R. (2011). Modifications of surface materials and their effects on cleanability as studied by radiochemical methods. *Constr. Build. Mater.*, *25*(6), 2860–2866.

Mauermann, M., Eschenhagen, U., Bley, T., Majschak, J. P. (2009). Surface modifications – Application potential for the reduction of cleaning costs in the food processing industry. *Trends Food Sci. Technol.*, *20*, S9–S15.

Mauermann, M., Calvimontes, A., Bellmann, C., Simon, F., Schöler M., Majschak, J. P. (2011). Modifications in hygienic properties of stainless steel surfaces due to repeated soiling and cleaning. *Proc. Int. Conf. Heat Exch. Fouling Clean., IX*, 227–234.

Mercier-Bonin, M., Adoue, M., Zanna, S., Marcus, P., Combes, D., Schmitz, P. (2009). Evaluation of adhesion force between functionalized microbeads and protein-coated stainless steel using shear-flow-induced detachment. *J. Colloid Interface Sci.*, *338*(1), 73–81.

Norde, W., Giacomelli, C. E. (2000). BSA structural changes during homomolecular exchange between the adsorbed and the dissolved states. *J. Colloid Interface Sci.*, *79*(3), 259–68.

Pesonen-Leinonen, E., Kuisma, R., Redsven, I., SJOBERG, A., Hautala, M. (2006a). Can contact angle measurements be used to predict soiling and cleaning of plastic flooring materials? In *Contact angle, wettability and adhesion (*K. L. Mittal, ed.) Vol. 4, VSP/Brill, Leiden, 203–214.

Pesonen-Leinonen, E., Redsven, I., Neuvonen, P., Hurme, K.-R., Pääkko, M., Koponen, H.-K., Pakkanen, T.T., Uusi-Rauva, A., Hautala, M., Sjöberg, A.-M. (2006b). Determination of soil adhesion to plastic surfaces using a radioactive tracer. *Appl. Radiat. Isot.*, *64*(2), 163–169.

Piispanen, M., Kronberg, T., Areva, S., Hupa, L. (2011). Effect of mechanical and chemical wear on soil attachment and cleanability of sanitary ware with additional coatings. *J. Am. Ceram. Soc.*, *94*(3), 951–958.

Pitois, O., Moucheront, P., Château, X. (2000). Liquid bridge between two moving spheres: an experimental study of viscosity effects. *J. Colloid Interface Sci. 231*(1), 26–31.

Podczeck, F. (1999). Investigations into the reduction of powder adhesion to stainless steel surfaces by surface modification to aid capsule filling. *Int. J. Pharm.*, *178*(1), 93–100.

Rabinovich, Y. I, Adler, J. J., Esayanur M. S., Ata, A., Singh, R., Moudgil, B. M. (2002). Capillary forces between surfaces with nanoscale roughness. *Adv. Colloid Interface Sci. 96*(1-3), 213–30.

Rouxhet, G. P., Misselyn-Bauduin, A. M., Ahimou, F., Genet, M. J., Adriaensen, Y., Desille, T., Bodson, P., Deroanne, C. (2008). XPS analysis of food products: toward chemical functions and molecular compounds. *Surf. Interface Anal.*, *40*(3-4), 718–724.

Rouxhet, G. P. (2013). Contact angles and surface energy of solids: Relevance and limitations, in *Advances in contact angle, wettability and adhesion.*(K. L. Mittal, ed.) Vol. 1, Schrivener Publishing LLC, 347-375

Rouxhet, G. P., Genet, M. J. (2011). XPS analysis of bio-organic systems. *Surf. Interface Anal.*, *43*(12), 1453–1470.

Speranza, G., Gottardi, G., Pederzolli, C., Lunelli, L., Canteri, R., Pasquardini, L., Carli, E., Lui, A., Maniglio, D., Brugnara, M., Anderle, M. (2004). Role of chemical interactions in bacterial adhesion to polymer surfaces. *Biomaterials*, *25*(11), 2029–2037.

Stephan, O., Weisz, N., Vieths, S., Weiser, T., Rabe, B., Vatterott, W. (2004). Protein quantification, sandwich ELISA, and real-time PCR used to monitor industrial cleaning procedures for contamination with peanut and celery allergens. *J. AOAC Int.*, *87*(6), 1448–1457.

Thill, A., Spalla., O (2003). Aggregation due to capillary forces during drying of particle submonolayers. *Colloids Surfaces A. Physicochem. Eng. Asp.*, *217*(1-3), 143–151.

Tomasetti, E., Derclaye, S., Delvaux, M.H. and Rouxhet, P.G. (2013) Study of material-water interactions using the Wilhelmy plate method, in *Advances in contact angle, wettability and adhesion.*(K. L. Mittal, ed.) Vol. 1, Schrivener Publishing LLC, 131-154.

Touré, Y., Rouxhet P. G. and Sindic, M.. (2013). Influence of soluble proteins on the adherence of particulate soils. *Ref. Proc. Int. Conf. Heat Exch. Fouling Clean.*, *X*, 285–90.

Touré ,Y., Rouxhet P. G., Dupont-Gillain, C. C., Sindic, M. (2011). Influence of soluble polysaccharide on the adherence of particulate soils. *Ref. Proc. Int. Conf. Heat Exch. Fouling Clean.*, *IX*, 219–226.

Walstra, P., Jenness, R. (1984). *Dairy chemistry and physics*. John Wiley and Sons, New York.

Yang, J., Mcguire J., Kolbe E. R. (1991). Use of the equilibrium contact angle as an index of contact surface cleanliness. *J. Food Prot.*, *54*(11), 879–884.

SUPPORTING MATERIAL

1. Results of image analysis of soiled polystyrene

The optical micrographs obtained on polystyrene were quantified by image analysis. Table S1 presents the relative importance of the different size fractions (≤ 30 µm, 30 to 90 µm, > 90 µm) and the density of the soiling entities as the threshold used for data treatment increases from 40 to 180.

Table S1. Size distribution (% in number) and total number (per field of 0.25 cm^2) of objects counted on polystyrene substrate after soiling in different conditions, as indicated.

Substrate conditioning	**none**	**dextran**	**none**	**BSA**	**none**
Quartz suspension in	**water**	**water**	**dextran solution**	**none**	**BSA solution**
Threshold 40					
Size fraction (%)					
≤ 30 µm	2	3	1	7	4
30-90 µm	63	69	20	54	64
> 90 µm	36	28	78	39	32
Total count	**2860**	**2946**	**1259**	**2698**	**3004**
Threshold 90					
Size fraction (%)					
≤ 30 µm	16	18	5	28	23
30-90 µm	80	78	81	66	71
> 90 µm	4	5	13	7	6
Total count	**3025**	**2941**	**2259**	**2335**	**2529**
Threshold 180					
Size fraction (%)					
≤ 30 µm	31	40	24	72	64
30-90 µm	69	59	74	28	36
> 90 µm	0	2	2	0	0
Total count	**1410**	**2276**	**858**	**448**	**599**

2. Concentrations of elements and chemical functions expected for BSA

Table S2 presents the respective amounts of different amino acids in BSA (Hirayama et al., 1990), the elemental composition of each amino acid, and the elemental composition and molar mass deduced for BSA. This provides concentration ratios expressed by the formula $C_{3.763}O_{1.153}N_1S_{0.050}H_{5.918}$ and the molar mass of 66464 g/mol.

Tables S3 and S4 give the listing of the chemical functions accounting for C, N and O in each amino acid and the values deduced for BSA, respectively. The concentrations of

Supporting Material

elements were pooled according to their expected contribution to components of the C 1s, N 1s and O 1s peaks (Rouxhet and Genet, 2011; Genet et al., 2008). Carbon bound only to carbon and hydrogen [**C**-(C,H)] and carbon bound to sulfur (Dietrich et al., 2011; Singh and Whitten, 2008) are expected to contribute to the component set at 284.8 eV. Carbon making a single bond with oxygen or nitrogen [**C**-(O,N) is expected near 286.3 eV. Carbon of the peptidic link [N-**C**=O] is expected near 288 eV, as well as carbon bound to 2 or 3 nitrogen atoms (arginine, histidine). The component due to carboxylic acid [O=**C**-OH] is expected near 289 eV; it may be noted that carbon of deprotonated carboxyl should contribute to the 288 eV component but this was not considered here. The enumeration of nitrogen atoms makes a distinction between amide [**N**-C=O] expected near 399.8 eV, and other functions. The latter are expected below 400 eV, but some of them may be protonated and be responsible for a component above 401 eV. As the O 1s peak is concerned, above 532 eV are expected contributions of the OH of alcohol (532.6 eV) and carboxyl (533.4 eV) ; below 532 eV are expected contributions of oxygen making a double bond with carbon in carboxylic acid (531.8 eV), amide (531.3 eV) and carboxylate (531.1 eV).

This computation provides molar concentration ratios which were used to exploit correlations between spectral data in this paper:

$C / N = 3.76$

$O / N = 1.15$

$C_{284.8} / N = 1.75$

$C_{286.3} / N = 1.04$

$C_{288} / N = 0.84$

$C_{289} / N = 0.13$

$C_{ox} / N = (C_{tot} - C_{284.8}) / N = 2.01$

3. Correlations between spectral data

Figure S1 presents graphs of correlations guided by the stoichiometry of the amide function, which are complementary to Figure 5a. They present data for non-conditioned substrates, BSA and substrates conditioned with BSA. The regression lines were computed on the basis of data for BSA and solids conditioned with BSA. The correlation between the concentration of C_{288}, attributed to [N-**C**=O] and the N concentration is close to expectation: experimental slope of 1.03 and 1.07, compared to expected ratios of 0.84 and 1.04 (Section

Supporting Material

1), for Figure S1a and S1b, respectively. However the agreement between measurements and expectations is better for the regression line relating Cox and N (Figure 5a). This indicates that the C 1s peak decomposition and component assignment are reliable but that the separation between the component attributed to **C**-(C,H) and the components due to oxidized forms of carbon is more accurate than the separation between the latter components.

Supporting Material

Table S2. Elemental composition of bovine serum albumin, computed from amino acid amounts and compositions.

Amino acid		**Number of atoms in amino acid residue**					**Number of atoms in BSA**				
Name	**Number**	**C**	**O**	**N**	**S**	**H**	**C**	**O**	**N**	**S**	**H**
Alanine (Ala)	46	3	1	1	0	5	138	46	46	0	230
Arginine (Arg)	23	6	1	4	0	12	138	23	92	0	276
Asparagine (Asn)	13	4	2	2	0	6	52	26	26	0	78
Aspartic acid (Asp)	41	4	3	1	0	5	164	123	41	0	205
Cysteine (Cys)	35	3	1	1	1	5	105	35	35	35	175
Glutamic acid (Glu)	59	5	3	1	0	7	295	177	59	0	413
Glutamine (Gln)	20	5	2	2	0	8	100	40	40	0	160
Glycine (Gly)	16	2	1	1	0	3	32	16	16	0	48
Histidine (His)	17	6	1	3	0	7	102	17	51	0	119
Isoleucine (Ile)	14	6	1	1	0	11	84	14	14	0	154
Leucine (Leu)	61	6	1	1	0	11	366	61	61	0	671
Lysine (Lys)	59	6	1	2	0	12	354	59	118	0	708
Methionine (Met)	4	5	1	1	1	9	20	4	4	4	36
Phenylalanine (Phe)	27	9	1	1	0	9	243	27	27	0	243
Proline (Pro)	28	5	1	1	0	7	140	28	28	0	196
Serine (Ser)	28	3	2	1	0	5	84	56	28	0	140
Tryptophan (Trp)	2	11	1	2	0	10	22	2	4	0	20
Threonine (Thr)	34	4	2	1	0	7	136	68	34	0	238
Tyrosine (Tyr)	20	9	2	1	0	9	180	40	20	0	180
Valine (Val)	36	5	1	1	0	9	180	36	36	0	324
Chain ends		0	1	0	0	2	0	1	0	0	2
Total	583						2935	899	780	39	4616
Mass of element per mole							35252	14383	10925	1250	4652
Molar mass of BSA							66464				

Supporting Material

Table S3. Listing of chemical functions in amino acids.

Amino acid	Carbon in amino acid residue										Nitrogen in a.a.residue			Oxygen in a.a. residue		
	CH_3	CH_2	CH	$\underline{C}$-C_3	C-S	C-O	C-N	N-C=O N-C-N	O=COH	Sum C	N-C=O	N-C N=C	Sum N	O=COH	OH	Sum O
Alanine (Ala)	1	0	0	0	0	0	1	1	0	3	1	0	1	0	0	1
Arginine (Arg)	0	2	0	0	0	0	2	2	0	6	1	3	4	0	0	1
Asparagine (Asn)	0	1	0	0	0	0	1	2	0	4	2	0	2	0	0	2
Aspartic acid (Asp)	0	1	0	0	0	0	1	1	1	4	1	0	1	2	0	3
Cysteine (Cys)	0	0	0	0	1	0	1	1	0	3	1	0	1	0	0	1
Glutamic acid (Glu)	0	2	0	0	0	0	1	1	1	5	1	0	1	2	0	3
Glutamine (Gln)	0	2	0	0	0	0	1	2	0	5	2	0	2	0	0	2
Glycine (Gly)	0	0	0	0	0	0	1	1	0	2	1	0	1	0	0	1
Histidine (His)	0	1	0	0	0	0	3	2	0	6	1	2	3	0	0	1
Isoleucine (Ile)	2	1	1	0	0	0	1	1	0	6	1	0	1	0	0	1
Leucine (Leu)	2	1	1	0	0	0	1	1	0	6	1	0	1	0	0	1
Lysine (Lys)	0	3	0	0	0	0	2	1	0	6	1	1	2	0	0	1
Methionine (Met)	0	1	0	0	2	0	1	1	0	5	1	0	1	0	0	1
Phenylalanine (Phe)	0	1	5	1	0	0	1	1	0	9	1	0	1	0	0	1
Proline (Pro)	0	2	0	0	0	0	2	1	0	5	1	0	1	0	0	1
Serine (Ser)	0	0	0	0	0	1	1	1	0	3	1	0	1	0	1	2
Tryptophan (Trp)	0	1	4	2	0	0	3	1	0	11	1	1	2	0	0	1
Threonine (Thr)	1	0	0	0	0	1	1	1	0	4	1	0	1	0	1	2
Tyrosine (Tyr)	0	1	4	1	0	1	1	1	0	9	1	0	1	0	1	2
Valine (Val)	2	0	1	0	0	0	1	1	0	5	1	0	1	0	0	1

Supporting Material

Table S4. Listing of chemical functions in bovine serum albumin, computed from amino acid amounts (Table S2) and compositions (Table S3), and pooled according to the expected contribution in the XPS spectrum.

	Carbon in BSA										**Nitrogen in BSA**			**Oxygen in BSA**				
Amino								**N-C=O**				**N-C**						
acid	**CH_3**	**CH_2**	**CH**	**$\underline{C}C_3$**	**C-S**	**C-O**	**C-N**	**N-C-N**	**O=COH**	**Sum C**	**N-C=O**	**N=C**	**Sum N**	**OH**	**O=C$\underline{O}$H**	**$\underline{O}$=COH**	**N-C=O**	**Sum O**
Ala	46	0	0	0	0	0	46	46	0	138	46	0	46	0	0	0	46	46
Arg	0	46	0	0	0	0	46	46	0	138	23	69	92	0	0	0	23	23
Asn	0	13	0	0	0	0	13	26	0	52	26	0	26	0	0	0	26	26
Asp	0	41	0	0	0	0	41	41	41	164	41	0	41	0	41	41	41	123
Cys	0	0	0	0	35	0	35	35	0	105	35	0	35	0	0	0	35	35
Glu	0	118	0	0	0	0	59	59	59	295	59	0	59	0	59	59	59	177
Gln	0	40	0	0	0	0	20	40	0	100	40	0	40	0	0	0	40	40
Gly	0	0	0	0	0	0	16	16	0	32	16	0	16	0	0	0	16	16
His	0	17	0	0	0	0	51	34	0	102	17	34	51	0	0	0	17	17
Ile	28	14	14	0	0	0	14	14	0	84	14	0	14	0	0	0	14	14
Leu	122	61	61	0	0	0	61	61	0	366	61	0	61	0	0	0	61	61
Lys	0	177	0	0	0	0	118	59	0	354	59	59	118	0	0	0	59	59
Met	0	4	0	0	8	0	4	4	0	20	4	0	4	0	0	0	4	4
Phe	0	27	135	27	0	0	27	27	0	243	27	0	27	0	0	0	27	27
Pro	0	56	0	0	0	0	56	28	0	140	28	0	28	0	0	0	28	28
Ser	0	0	0	0	0	28	28	28	0	84	28	0	28	28	0	0	28	56
Trp	0	2	8	4	0	0	6	2	0	22	2	2	4	0	0	0	2	2
Thr	34	0	0	0	0	34	34	34	0	136	34	0	34	34	0	0	34	68
Tyr	0	20	80	20	0	20	20	20	0	180	20	0	20	20	0	0	20	40
Val	72	0	36	0	0	0	36	36	0	180	36	0	36	0	0	0	36	36
Ch. ends								-1	1		-1	1			1	1	-1	1
	302	636	334	51	43	82	731							82	101	101	615	
Total	1366					813		655	101	2935	615	165	780	183		716		899

Supporting Material

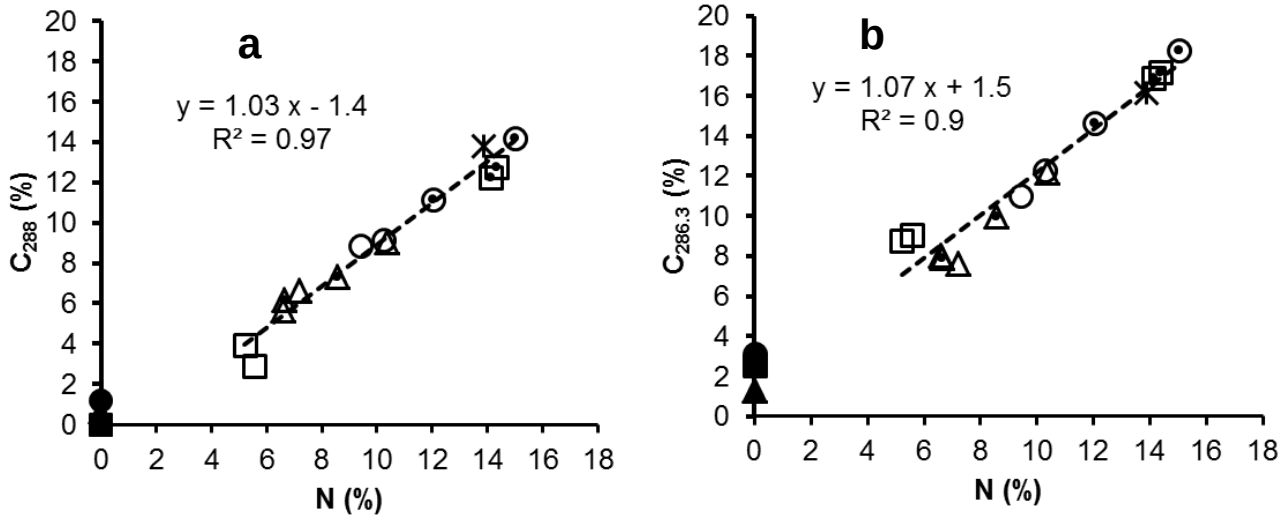

Figure S1. Correlation between the indicated concentrations (mole fraction of carbon responsible for components of the C 1s peak): BSA **(✱)**; glass (●,○), polystyrene (■,□) and quartz powder (▲,△), bare (closed symbols) or conditioned and rinsed (open symbols) or conditioned and not rinsed (open symbols with dot). Dashed line: regression line with its equation, computed excluding the non-conditioned substrates.

4. Conversion of elemental concentration ratios into weight % of compounds

The correlations between XPS data show that the composition of the organic layer present at the surface of conditioned substrates may be quantified by using appropriate markers. The concentrations of markers (mole %) may be converted into concentrations of constituents or model compounds (mass %), which provide a more practical presentation of the surface composition. Multiplying the molar concentration of markers (X, mole/100 moles) by the molar mass (MM) of the relevant constituent or model compound and dividing by the number of marker moieties (Nr) in the compound formula provides the concentration of each compound (W, in g/100 mol of elements detected by XPS). Dividing W of each compound by the sum of W for all compounds (T) and multiplying by 100 finally gives the mass concentration in % of the constituent in the volume probed by XPS. Table S5 presents the scheme of the procedure used for the conversion and recalls the markers used in the two models A and B.

Supporting Material

Table S5. Table used for converting marker concentrations (molar percentage of relevant element) into mass concentration (%) of model compounds.

Constituent or model		Marker			W=	Concentration
Nature	MM	Definition	Nr (a)	X (b) (mol %)	X∗MM / Nr (c)	W∗100 / T (mass %)
Model A: BSA + contaminants						
BSA $C_{3.76}O_{1.15}N_1S_{0.05}H_{5.92}$	85.2	N	1	●●●	●●●	●●●
Contaminants						
HC..H	14	C_{tot} – 3.76*N	1	●●●	●●●	●●●
Oxygen	16	C_{ox} – 2.01*N	1	●●●	●●●	●●●
Total					T = ●●●	100
Model B: BSA + dextran + hydrocarbon						
BSA $C_{3.76}O_{1.15}N_1S_{0.05}H_{5.92}$	85.2	N	1	●●●	●●●	●●●
Dextran $C_6H_{10}O_5$	162	C_{ox} – 2.01 * N	6	●●●	●●●	●●●
Hydrocarbon CH_2	14	$C_{284.8}$ – 1.75*N	1	●●●	●●●	●●●
Total					T = ●●●	100

(a) number of markers per considered compound.
(b) measured marker concentration X (mole/100 moles excluding hydrogen).
(c) in g of compounds / 100 moles of elements, excluding hydrogen.

REFERENCES

Genet, M. J., Dupont-gillain, C. C., Rouxhet, P. G. (2008). XPS analysis of biosystems and biomaterials. In *Medical applications of colloids* (E. Matijević, ed.) Springer, New York. 177–307.

Hirayama, K., Akashi S, Furuya, M., Furuya, K. (1990). Rapid confirmation and revision of the primary structure of bovine serum albumin by ESIMS and Frit-FAB LC/MS. *Biochem. Biophys. Res. Commun. 173*(2), 639-646.

Dietrich P. M., Horlacher, T., Girard-Lauriault, P.-L., Gross, T., Lippitz, A., Min, H., Wirth, T., Castelli R., Seeberger P. H., & Unger W. E. S. (2011). Adlayers of dimannoside thiols on gold: surface chemical analysis. *Langmuir 27*(8), 4808–15.

Rouxhet, P. G., & Genet, M. J. (2011). XPS analysis of bio-organic systems. *Surf. Interface Anal. 43*(12), 1453–1470.

Supporting Material

Singh, J., & Whitten, J. E. (2008). Adsorption of 3-Mercaptopropyltrimethoxysilane on Silicon Oxide Surfaces and Adsorbate Interaction with Thermally Deposited Gold. *J. Phys. Chem. C 112*(48), 19088–19096.

SECTION IV

INFLUENCE OF SOLUBLE PROPTEINS ON THE ADHERENCE OF PARTICULATE SOILS

From:

Yetioman Toure, Paul G. Rouxhet and Marianne Sindic, 2013.

Proc. Int. Conf. on Heat Exchanger Fouling and Cleaning, (Malayeri, M.R., Müller-Steinhagen, H. & Watkinson, A.P., eds.), June 09-14, 2013, Budapest, Hungary, http://www.heatexchanger-fouling.com, 285-290.

ABSTRACT

Adsorbed compounds from food and pharmaceutical mixtures may influence interactions at interfaces and thus fouling and cleaning. In this study, quartz particles (10 to 30 µm) were used as a model soil for examining the effect of dissolved proteins on the cleanability of substrates after soiling and drying. Glass and stainless steel pretreated by UV-Ozone (StSteel-UVO) were used as model hydrophilic substrates, while hydrophobic substrates were represented by stainless steel cleaned with ethanol (StSteel-Eth) and polystyrene. BSA and β-LGB were used as proteins. The quartz suspensions used for soiling were prepared in pure water and in a solution of each protein. After soiling and drying, the cleanability was evaluated using a radial-flow cell, with pure water as the cleaning fluid.

The presence of proteins in the suspension used for soiling hydrophilic substrates (Glass and StSteel-UVO), decreased the adherence of quartz particles. Its effect was less marked and tended to be opposite for less hydrophilic substrates (StSteel-Eth, Polystyrene). The adherence cannot be explained by a simple relation with the contact angle. Other factors may be the solution surface tension itself and the protein behavior at the interfaces created by drying and by rehydratation during cleaning.

When considering the influence of substrate on soiling, it must be kept in mind that high surface energy solids (metals, oxides) are readily contaminated in contact with air and lose their hydrophilicity. This may improve the substrate behavior regarding cleanability with respect to particulate soil.

1. INTRODUCTION

Fouling involving particle deposition and drying is of major concern for surfaces exposed to natural environments or surfaces of industrial equipment. Particulate soils may occur in storage tanks, in the ducts or on the plates of heaters and coolers. The problem is particularly severe in food and pharmaceutical processing, where fouling deposits may endanger microbial sterility and product purity (Stephan et al., 2004; List and Müller, 2005). The efficiency of a plant is lowered by the formation of fouling deposit on heat transfer and other surfaces (Bott, 1995).

Polysaccharides, proteins, lipids and other biopolymers are the main constituents of food and pharmaceutical mixtures. Proteins on the outer surface of bacteria are known to play an

important role in the initial attachment to solid surfaces (Dufrêne et al., 1996; Flint et al., 1997; Caccavo, 1999; Lower et al., 2005). Baking has a major effect on the subsequent removal of soils as illustrated by tomato paste used as food model deposit (Liu et al., 2006). In this case, a micromanipulation probe made it possible to directly observe the influence of substrate surface properties on the interfacial intercations in adhesive failure conditions, and to differentiate this process from failure within the deposit. Details in the mode of drying a starch deposit were found to influence adherence measured with a radial flow cell, which was attributed to the properties of soluble macromolecules accumulated during drying and forming an adhesive joint between the substrate and the soiling particles (Detry et al., 2011).
The aim of the present work is to improve the understanding of mechanisms affecting soiling and cleanability by assessing the role of dissolved proteins. Quartz particles were taken as a simplified particulate soil model. Glass, stainless steel and polystyrene were chosen as model substrates to examine the influence of substrate hydrophobicity. Albumin from bovine serum (BSA) and β-Lactoglobulin (β-LGB) from bovine milk were chosen as models of dissolved proteins in the soiling suspension.

2. MATERIALS AND METHODS

2.1. Material

Stainless steel (AISI304-2R, 1 mm thick) plates were provided by Arcelor (France). The face used for the study had a mirror finish and was protected with a plastic sheet which was removed before substrate preparation. Glass slides (50 mm × 50 mm × 1 mm) and polystyrene sheets (300 mm × 300 mm × 0.25 mm) were purchased from Menzel-Gläser (Germany) and Goodfellow (United Kingdom), respectively. MilliQ water was produced by a MilliQ-50 system from Millipore (France). Absolute ethanol was purchased from Sigma-Aldrich (Wisconsin, USA). Albumin from bovine serum (BSA) (lyophilized powder, ≥98%, essentially fatty acid free and globulin free; molar mass 66000) and β-Lactoglobulin (β-LGB) from bovine milk (lyophilized powder; ≥85%,) were purchased from Sigma-Aldrich (Wisconsin, USA).

2.2. Substrate preparation

The substrates were first cleaned with ethanol and dried with Kimtech Science paper. Secondly, stainless steel and glass substrates were sonicated (ultrasonic cleaner Branson 3200, USA) in ethanol for 15 min, while polystyrene substrate was immersed for 30 min in ethanol. The substrates were then rinsed thoroughly with ethanol, dried with a gentle flow of

nitrogen and wrapped in an aluminum foil until use. These substrates will referred to as Glass, Polystyrene and StSteel-Eth. Certain coupons of stainless steel (named StSteel-UVO) were submitted to an additional UV-Ozone treatment for 20 min (UVO-cleaner, Model 42, Jelight Company, USA) to improve the removal of organic contamination, and used immediately.

2.3. Contact angles and liquid surface tension measurement

Static contact angles of water and of BSA and β-LGB solutions were measured on 16 mm × 10 mm coupons of the substrates, using the sessile drop method with a goniometer (Krüss, Germany). The measurements involved at least 10 drops. The surface tensions of the liquids were measured with a Prolabo Tensiometer (Tensimat n°3) using the Wilhelmy plate method with a platinum plate.

2.4. Particulate soil model

Quartz particles with a size about 10 to 30 µm were separated as described by Touré et al. (2011) and used as particulate soil model. Three kinds of quartz suspensions were prepared at a concentration of 150 g/L: (i) suspension in a BSA solution (8 g/l), (ii) suspension in a β-LGB solution (8 g/l), (iii) suspension in water. For preparing the suspensions in BSA and β-LGB solutions, 7.5 g samples of quartz were first mixed with 25 ml of MilliQ water and stirred for 30 min at room temperature. Then, 25 ml of a BSA or β-LGB solution in distilled water (16 g/l) were added and the entire mixture was stirred for 1 h. The suspensions were kept at 4 °C (BSA and β-LGB storage temperature) for 72 h.

2.5. Soiling and cleanability assessment

The substrates (coupons of 50 mm × 50 mm) were soiled with the quartz suspensions brought at room temperature. Suspension droplets were deposited by 4 successive manual aspersions using a sprayer located at a distance of 40 cm. They did not lead to the formation of a continuous film and no drainage occurred. Water was evaporated by drying for 30 min in a dark cupboard at 20.6±1.9 °C and 39±3% relative humidity (Detry et al., 2007, 2011; Touré et al., 2011). The coupons were then submitted within 2 min to the cleaning test.

Cleanability assessment was performed at 20 °C in a radial-flow cell (RFC). This consisted of an upper disk with a 2 mm diameter central inlet and a lower disk in which the soiled square sample was fitted to be cleaned. The distance between the upper disk and both the sample and the lower disk was set by three adjustable micrometric screws and controlled to be 1.00±0.02 mm with calibrated steel spacers. A complete description of the device, its

hydrodynamics and its utilization can be found elsewhere (Detry et al., 2009, 2011). Distilled water was flown during 5 min with a flow rate of 40 ml/min. The sample was then removed and dried at room temperature. Pictures of the substrate were taken before and after cleaning, using an epifluorescence stereomicroscope (ZX9 Olympus, Belgium) equipped with a CCD camera. After cleaning, a circular zone with a lower density of aggregates was observed at the center of the sample. The pictures of the sample before and after cleaning were processed with a specific application of the Matlab software (The Mathworks Inc.), which gave the ratio of the number of aggregates initially present on the surface to the number of aggregates remaining after cleaning, as a function of the radial position. The radial position at which the residual density of aggregates became ≥ 50% was considered as the critical detachment radius (Goldstein and DiMilla, 1997, 1998). The value of the critical radius was checked for consistency in the LUCIA software to insure the absence of artifacts such as the nucleation of air bubbles on the surface. At least 10 repetitions of each experiment (soiling-cleaning) were made, being distributed in at least three independent series.

The critical radius of detachment, the output parameter of the cleaning experiments, reflects the critical wall shear stress which corresponds to the minimal hydrodynamic drag force required to detach a soil from surface under given experimental conditions (Jensen and Friis, 2004). With the radial flow chamber used, the conversion of critical radius into critical wall shear stress is not reliable above flow rates of 20 ml/min (Detry et al., 2011). Therefore, the results of the present study are expressed in terms of critical radius, keeping in mind that for a defined flow rate, the higher the critical radius, the lower the adherence.

3. RESULTS

The critical detachment radii measured on Glass, StSteel-UVO, StSteel-Eth and Polystyrene, soiled with a quartz suspension in water and in BSA and β-LGB solutions are presented in Fig.1A. For all the substrates, the critical detachment radius was measured after cleaning for 5 min at a flow rate of 40 ml/min. Remember that the higher the critical detachment radius the lower the particle adherence (Detry et al., 2011). For Glass, no detachment radius could be measured when the quartz particles were suspended in pure water, but a detachment of a few particles occurred near the inlet. As regards the substrates soiled with quartz particles suspended in pure water, the critical detachment radius increased according to the order Glass (not measurable) < StSteel-UVO (about 2.5 mm) < StSteel-Eth (about 6.7 mm) < Polystyrene (about 7.5 mm). For Glass and StSteel-UVO, the critical detachment radius

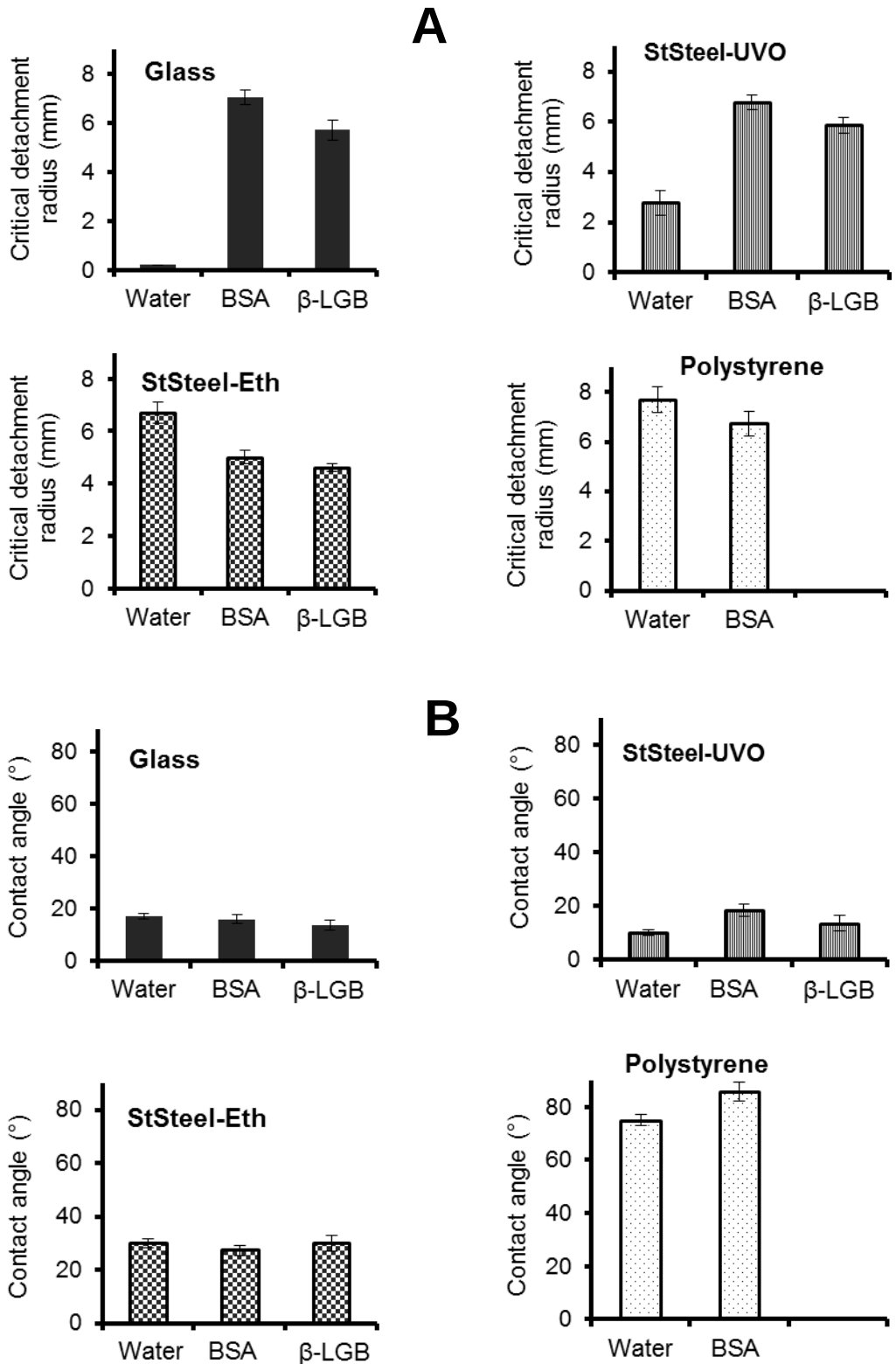

Figure 1 A. Critical detachment radii measured on Glass, StSteel-UVO, StSteel-Eth and Polystyrene substrates soiled with suspensions of quartz particles in water and in BSA and β-LGB solutions. B. Contact angles measured on the same substrates with water and with BSA and β-LGB solutions.

dramatically increased when soiling was made with quartz suspensions in BSA or β-LGB solutions. The critical detachment radii were in the same range for Glass and StSteel-UVO soiled with a suspension in BSA solution and for StSteel-Eth and Polystyrene soiled with a suspension in pure water. In contrast, the presence of proteins decreased the critical detachment radius for StSteel-Eth. No test was made for Polystyrene soiled with a suspension in a β-LGB solution owing to the low effect observed for BSA solution compared to water.

Fig. 1B presents the contact angles measured on the four substrates using pure water and BSA and β-LGB and solutions. There was not much influence of the nature of the liquid on the contact angle. Glass and Polystyrene gave a low and a high contact angle, respectively, as expected. StSteel-UVO presented a lower contact angle than StSteel-Eth, with a difference which was particularly marked with water.

In order to assess the influence of substrate preparation on surface properties, the water contact angle was measured at different stages of the preparation of the inorganic substrates. The results presented in Table 1 show that cleaning with ethanol decreased slightly the water contact angle and that UVO treatment decreased it much more, both for glass and for stainless steel.

The surface tensions (with standard deviations) of the liquids were 72.9 (0.3), 30 (1.1) 48.8 (0.2) mN/m for water, BSA solution and β-LGB solution, respectively.

Table 1. Water contact angle measured on glass and stainless steel after the indicated preparation stage.

Substrate	Contact angle (°)		
	not treated	ethanol treated	UVO treated
Glass	24.2* ± 2.2	17 ± 1.2	< 10
Stainless steel	43.2 ± 3.9	30 ± 1.5	10.3 ± 1

*Mean ± standard deviation

4. DISCUSSION

The surface analysis of inorganic solids by X-ray photoelectron spectroscopy always shows the presence of carbon (Gerin et al., 1995; Caillou et al., 2008; Rouxhet, 2013). This is due to organic compounds which may originate from material processing, from artifacts due to sample preparation, or from contamination by adsorption from the surrounding, either the ambient atmosphere or the spectrometer vacuum chamber. Table 1 shows that initial surface cleaning with ethanol does not bring the water contact angle to low values expected for

oxides or oxihydroxides present at the surface of glass and stainless steel, indicating that it did not remove the totality of organic surface contaminants. An additional UVO treatment insured a more effective removal of organic contaminants by oxidation, as revealed by the low contact angle achieved.

It must be noted that high energy surfaces cleaned by UVO treatment and left in ambient air show a quick increase of the water contact angle due to adsorption of organic compounds. For gold and stainless steel, the increase is quite steep, the contact angle reaching values above 20 ° in a few hours, and above 60 ° in less than 1 day for gold and a few days for stainless steel. For silica slab, the increase is significant only after several days, providing a contact angle of the order of 20° (Rouxhet, 2013). Such decrease of wettability may improve cleanability after soiling and drying, as observed when a tomato paste was baked on oil-coated stainless steel compared to bare stainless steel (Liu et al., 2006).

The robustness of the observations regarding adherence was demonstrated by the reproducibility of results obtained with Glass and Polystyrene, in experiments performed at a time interval of 17 months.

Fig. 1 shows that the adherence of the quartz particles brought by a suspension in water is much higher on the most hydrophilic substrates, Glass and StSteel-UVO having a water contact angle in the range of 10 to 17°, than on the two other substrates, StSteel-Eth and Polystyrene. According to previous observations (Detry et al., 2011), this may be due to better droplet spreading and increase of capillary forces which affect the shape of the adhering aggregates and the efficiency of shear forces exerted by the cleaning fluid, and the strength of the particle-substrate contact. However the relation between soil adherence and substrate contact angle is far from monotonous as indicated by StSteel-Eth and Polystyrene, which give a similar adherence, with water contact angles of 30 and 75 °, respectively.

The relationship between soil adherence and contact angle fails if the soils made from suspensions in protein solutions are considered. As shown in Fig. 1, the presence of proteins decreases strongly the adherence on the two hydrophilic substrates and increases slightly the adherence on the two other substrates while it hardly affects the contact angle of each substrate.

For the two hydrophilic substrates, the adherence decreases with the liquid surface tension, which may be attributed to lower capillary forces and consequently to looser contact between the quartz particles and the substrates after drying. However this relation fails and even seems to be reversed for the two other substrates.

In the study of starch particles adhesion on different substrates, drying was shown to provoke an accumulation of dissolved macromolecules, forming a bridge between the particles and the substrate. Accumulated protein or adsorbed proteins may affect particle removal as do surfactants in particulate soil detergency (Rojvoranum et al., 2011), e.g. by creating electrostatic or steric repulsion. A possible explanation for the difference observed between Glass or StSteel-UVO, on one hand, and StSteel-Eth, on the other hand, may be a different behavior of proteins according to the substrate. It is indeed known that protein adsorption (affinity, adsorbed amount, reversibility, mobilitity in the adsorbed phase, behavior upon drying) is strongly influenced by substrate hydrophobicity (Andrade and Hlady, 1987; Jacquemart et al., 2004; Van Tassel, 2006; Gurdak et al., 2006; Rabe et al., 2011). This may also influence the distribution and the state (native, denaturated) of proteins at the quartz-substrate interface and the possibility that they act as a linking or as a dispersing agent.

5. CONCLUSIONS

When soiling with hydrophilic particles such as quartz was made in pure water, the soil adherence increased with substrate hydrophilicity. This is in agreement with the expected influence on droplet spreading and capillary forces created upon drying, which affect the shape and compactness of the adhering aggregates. The presence of proteins in the suspension used for soiling hydrophilic substrates (Glass and StSteel-UVO), decreased the adherence of quartz particles. This effect was less marked and tended to be opposite for less hydrophilic substrates (StSteel-Eth, Polystyrene).

The comparison of different substrates and two proteins showed that the adherence cannot be explained by a simple relation with the contact angle. Other factors may be the solution surface tension itself and the protein behavior at the interfaces created by drying and by rehydratation during cleaning. A broader study, including protein denaturation, is under way to elucidate the effect of soluble proteins on the adhesion of particulate soils.

When considering the influence of substrate on soiling, it must be kept in mind that high surface energy solids (metals, oxides) are readily contaminated in contact with air and lose their hydrophilicity. Amazingly this may improve the substrate behavior regarding cleanability with respect to particulate soil.

ABBREVIATIONS

BSA	bovin serum albumin
β-LGB	beta-lactoglobulin
RFC	radial-flow cell
StSteel-Eth	stainless steel cleaned with ethanol
StSteel-UVO	stainless steel cleaned with ethanol and an additional UVO treatment
UVO	ultraviolet–ozone

REFERENCES

Andrade, J. D., and Hlady, V., 1987, Plasma protein adsorption: The big twelve, *Ann. N.Y. Acad Sci.*, 516, pp. 158-172.

Bott, T. R., 1995, *Fouling of Heat Exchangers*, Elsevier, New York.

Caccavo, J. R., 1999, Protein-mediated adhesion of the dissimilatory Fe(III)-reducing bacterium *Shewanella alga BrY* to hydrous ferric oxide, *Appl. Environ. Microbiol.*, 65(11), pp. 5017-5022.

Caillou, S., Gerin, P. A., Nonckreman, C. J., Fleith, S., Dupont-Gillain, C. C., Landoulsi, J., Pancera, S. M., Genet, M. J., and Rouxhet, P. G, 2008, Enzymes at solid surfaces: nature of the interfaces and physico-chemical processes, *Electrochim. Acta*, 54, pp. 116-122.

Detry, J. G., Sindic, M., Servais, M. J., Adriaensen, Y., Derclaye, S., Deroanne, C. and Rouxhet, P. G., 2011, Physico-chemical mechanisms governing the adherence of starch granules on materials with different hydrophobicities, *J. Colloid Interface Sci.*, 355, pp. 210-221.

Detry, J. G., Deroanne, C., Sindic, M., and Jensen, B. B. B, 2009, Laminar flow in radial flow cell with small aspect ratios: Numerical and experimental study, *Chem. Eng. Sci.*, 64, pp. 31-42.

Detry, J. G., Rouxhet, P. G., Boulangé-Petermann, L., Deroanne, C., and Sindic, M., 2007, Cleanability assessment of model solid surfaces with a radial-flow cell, *Colloids Surfaces A: Physicochem. Eng. Aspects*, 302, pp. 540-548.

Dufrêne, Y. F., Boonaert, C. J.-P., and Rouxhet P. G. 1996, Adhesion of Azospirillum brasilense: role of proteins at the cell-support interface, *Colloids Surfaces B: Biointerfaces*, 7(3-4), pp. 113-128.

Flint, S.H., Brooks, J.D. and Bremer, P.J., 1997, The influence of cell surface properties of thermophilic streptococci on attachment to stainless steel, *J. Appl. Microbiol.*, 83(4), pp. 508-5017.

Gerin, P. A., Dengis, P. B., and Rouxhet, P. G., 1995, Performance of XPS analysis of model biochemical compounds. *J. Chim. Phys.*, 92, pp. 1043-1065.

Goldstein, A. S. and DiMilla, P. A., 1998, Comparison of converging and diverging radial flow for measuring cell adhesion, *AlChE J.*, 44(2), pp. 465-473.

Goldstein, A. S. and DiMilla, P. A., 1997, Application of fluid mechanic and kinetic models to characterize mammalian cell detachment in a radial-flow chamber, *Biotechnol. Bioeng.*, 55(4), pp. 616-629.

Gurdak, E., Rouxhet, P.G. and Dupont-Gillain, C. C., 2006, Factors and mechanisms determining the formation of fibrillar collagen structures in adsorbed phases, *Colloids Surfaces B-Biointerfaces,* 52, pp. 76-88.

Jacquemart, I., Pamula, E., De Cupere, V. M., Rouxhet, P. G., and Dupont-Gillain, C. C., 2004, Nanostructured collagen layers obtained by adsorption and drying, *J. Colloid Interface Sci*., 278, pp. 63-70.

Jensen, B. B. B. and Friis, A., 2004, Critical wall shear stress for the EHEDG tests method, *Chem. Eng. Process.*, 43, pp. 831-840.

List, W., and Müller, J., 2005, Reinigungsvalidierung unter besonderer berücksichtigung von proteinrückständen, *Pharm. Ind.,* 67, pp. 1359-1365.

Liu, W., Zhang, Z., and Fryer, P. J., 2006, Identification and modeling of different removal modes in the cleaning of a model food deposit, *Chem. Eng. Sci.*, 61, pp. 7528-7534.

Lower, B.H., Yongsunthon, R., Vellano III, F.P. and Lower, S.K., 2005, Simultaneous force and fluorescence measurements of a protein that forms a bond between a living bacterium and a solid surface, *J. Bacteriol*., 187(6), pp. 2127-2137.

Rabe, M., Verdes, D., and Seege, S., 2011, Understanding protein adsorption phenomena at solid surfaces, *Adv. Colloid Interface Sci.*, 162, pp. 87-106.

Rojvoranun, S., Chadavipoo, C., Pengjun, W., Chavadej, S., Scamehorn, J. F., and Sabatini, D. A., 2011, Mechanistic studies of particulate soil detergency: I. Hydrophobic soil removal. *J. Surfact. Deterg.,* 15(3), pp. 277-289

Rouxhet, P. G., 2013, Contact angles and surface energy of solids: Relevance and limitations, in *Advances in Contact Angle, Wettability and Adhesion,* ed. Mittal K. L., Schrivener Publishing, 1, pp. 347-375.

Stephan, O., Weisz, N., Vieths, S., Weiser, T., Rabe, B. and Vatterott, W., 2004, Protein quantification, sandwitch ELISA, and real-time PCR used to monitor industrial cleaning procedures for contamination with peanut and cellery allergens, *J. AOAC International*, 87, pp. 1448-1457.

Touré, Y., Rouxhet, P. G., Dupont-Gillain C. C., and Sindic, M., 2011, Influence of soluble polysaccharide on the adherence of particulate soils, in *Proc. Int. Conf. Heat exchanger fouling and cleaning IX*, eds. M. R. Malayeri, H. Müller-Steinhagen and A. P. Watkinson, Crete Island, Greece, pp. 219-226.

Van Tassel, P.R., 2006, Protein adsorption kinetics: influence of substrate electric potential. In *Proteins at Liquid – Solid Interfaces (Principle and Practice)*, ed. P. Dejardin, pp. 1-22, Springer, ISBN-10 3-540-32657-X, Berlin, Germany

SECTION V

INFLUENCE OF WHEY PROTEIN DENATURATION ON ADHERENCE OFSOILING PARTICLES TO STAINLESS STEEL

From:

Yetioman Toure, Paul G. Rouxhet, Christine C. Dupont-Gillain and Marianne Sindic, 2014. *Fouling and Cleaning in Food Processing* (Wilson, D.I & Chew, Y.M.J, eds.), Publishing Depart. Chem. Eng. & Biotech., Cambridge, UK, 30-37.

ABSTRACT

This work reports on the influence of β-lactoglobulin (β-LGB) and of its denaturation on the adherence of quartz particles, taken as a model of particulate soil, on stainless steel AISI 304 with mirror finish. The substrate was soiled with quartz suspensions in water or in β-LGB solutions as such or previously heated at 75°C, and dried at room temperature or in an oven at 75°C. Cleanability was evaluated after exposure to water in a radial flow chamber. Auxiliary characterizations were the surface tension and protein concentration of the solution, surface analysis of the substrate by X-ray photoelectron spectroscopy (XPS) and contact angle measurements.

The contact of stainless steel with β-LGB led to adsorption of the protein, which dominated the composition of the organic layer with respect to contaminants initially present, and was not markedly desorbed upon rinsing. The presence of β-LGB at the quartz particle/substrate interface slightly increased the adherence, which was further increased when the protein was denatured. On the other hand, denaturation of β-LGB enhanced its surfactant effect at the water/air interface. Comparison with systems investigated before suggests that the influence of protein via droplet spreading and soiling particles aggregation may be of minor importance compared to direct effects on the substrate/quartz interface. Stainless steel does not behave as a hydrophilic substrate owing to its surface contamination with organic compounds. It appears suitable to examine the influence of the initial surface state of stainless steel on its behavior regarding soiling and cleaning.

1. INTRODUCTION

Proteins are often used in food industry to improve fabricated foods qualities like texture and appearance. Whey proteins have high functional properties, which are valuable in numerous applications such as gelation, foaming and whipping, water retention, emulsification, and thermal stability. Whey is the liquid remaining after removal of casein from milk and contains mainly globular proteins (6 g/L in bovine milk). The main proteins are β-lactoglobulin (β-LGB), α-lactalbumin, bovine serum albumin (BSA), and immunoglobulins. β-LGB is the most abundant, representing more than 50% of the total whey protein (Fox and Mcsweeney, 1998).

In dairy industry, two kinds of fouling are identified as a result of heating: type A, soft and spongy deposits, containing more than 50% proteins, mainly β-LGB, and about 8% mineral compounds; type B, hard deposits, granular in structure, called mineral fouling, containing about 80% minerals, mainly calcium phosphate, and 15% proteins (Fickak et al., 2011; Changani et al., 1997; Visser and Jeurnink, 1997). A controversial question concerns whey protein implication in deposit layer formation and removal. Although the connection between the thermal stability and conformational changes of β-LGB is well established, the role of the denatured state in the build-up of the fouling deposit is still unclear. Trends reported in the literature are not conclusive and are focused on protein deposits or on the effect of mineral elements concentration on deposit formation (Blanpain-Avet et al., 2012; Bansal and Chen, 2006; 2009).

Fouling involving particle deposition and drying is of major concern for surfaces exposed to natural environments or surfaces of industrial equipment. Particulate soils may originate from splashing, or deposition in storage tanks, in the ducts or on the plates of heaters, coolers and other open surfaces. The problem is particularly severe in food and pharmaceutical processing, where fouling deposits may endanger microbial sterility and product purity (Stephan et al., 2004). The influence of macromolecules (Touré et al., 2014; 2013; 2011) on the adherence of model particulate soils (quartz particles) was examined using substrates which differed according to hydrophobicity. The effect of dextran was weak, possibly owing to its low adsorption or easy desorption. The presence of BSA had little effect on the adherence to polystyrene but improved drastically the cleanability of glass. This was attributed to prevention of tight bonds between the particle soil and the substrate or to induction of a repulsion between the surfaces in contact. Since whey protein are often submitted to heating, the study of the influence of heating and protein denaturation on particle soil adherence will contribute to improve cleanability and better understand the mechanisms involved. To our knowledge, no data are available on this subject.

The present work investigates the effect of β-LGB and its denaturation on the adherence of particulate soils to stainless steel, the ubiquitous substrate in food industry, and on its cleanability. Quartz particles were taken as a simplified particulate soil model. β-LGB was chosen because it is the most abundant and the most heat-labile whey protein, and plays a key role in fouling (Robbins et al., 1999). The protein was involved in the soiling process by its introduction into the quartz suspension. A previous study with BSA showed that there is no significant difference in cleanability depending on whether the protein was brought by conditioning the substrate before soiling or by its presence in the soiling suspension, or both

ways (Touré et al., 2014). The influence of denaturation was examined by a high temperature pretreatment of the soiling suspension or by drying the soiled substrate at high temperature. The soiling suspension was characterized at different stages regarding soluble protein concentration and surface tension. The substrate/solution interfaces were characterized by X-ray photoelectron spectroscopy (XPS) analysis of substrates conditioned with solutions in representative states and by contact angle measurements.

2. EXPERIMENTAL

2.1. Materials

Stainless steel (AISI 304-2R, 1mm thick) plates were provided by Arcelor (France). The face used for the study had a mirror finish and was protected with a plastic sheet which was removed before substrate preparation. The substrate was cut to the desired dimensions: 50 mm × 50 mm for fouling and cleanability assessment; 16 mm × 10 mm for surface characterization. The coupons were cleaned with ethanol, sonicated (ultrasonic cleaner Branson 3200, USA) in ethanol for 10 min, rinsed thoroughly with MilliQ water, dried with a gentle flow of nitrogen and wrapped in aluminium until use. Ground quartz particles (M400) were provided by Sibelco Benelux (Belgium). Quartz particles with a size about 10 to 30 µm were isolated from the initial batch (particle size distribution 1.1 to 60.3 µm) as described before (Touré et al., 2011) and used as a model of hard particulate soil. MilliQ water was produced by a MilliQ-50 system from Millipore (France). Absolute ethanol and β-lactoglobulin (β-LGB) from bovine milk (lyophilized powder; ≥85 %,) were purchased from Sigma-Aldrich (Wisconsin, USA).

2.2. Soiling procedure and cleanability assessment

Four kinds of quartz suspensions were prepared at a concentration of 150 g/L: (a) in water, (b) in a native β-LGB solution (3 g/L), (c) same as (b) and subsequent heating for 0.5 h at 75°C, (d) analogous to (c) but heated for 4 h. In addition, certain samples were soiled with suspension (a) or (b) and dried for 0.5 h in an oven at 75°C before the cleaning process. Further details on soil preparation and handling can be found in Touré et al. (2013, 2011). The choice of β-LGB concentration in the suspension was based on β-LGB concentration in bovine milk (3 g/L) (Walstra and Jenness, 1984). The soiling procedure, cleanability assessment and data processing are detailed in previous studies (Detry et al., 2011; Touré et al., 2011; 2013). Briefly, suspension droplets were deposited by aspersion at room temperature. Cleanability assessment was performed at 20 °C in a radial-flow cell (RFC).

Distilled water was flown during 5 min with a flow rate of 40 ml/min. Pictures taken before and after cleaning, were processed with a specific application of the Matlab software, which gave the radial position. The radial position at which the residual density became ≥ 50% was considered as the critical detachment radius (Goldstein and DiMilla, 1998; 1997). At least 10 repetitions of each experiment (soiling-cleaning) were made.

With the radial flow chamber used, the conversion of critical radius into critical wall shear stress is not reliable above flow rates of 20 ml/min (Detry et al., 2011). Therefore, the results of the present study are expressed in terms of critical radius, keeping in mind that for a defined flow rate, the higher the critical radius, the lower the adherence.

2.3. Contact angle measurement and surface analysis

Static contact angles were measured using the sessile drop method with a goniometer (Krüss, Germany). The measurements involved at least 10 drops.

The XPS analyses were performed on a SSX 100/206 photoelectron spectrometer from Surface Science Instruments (USA) equipped with a monochromatized micro focused Al X-ray source (powered at 20 mA and 10 kV). The analysis details were described by Toure et al. (Touré et al., 2014). The following sequence of spectra was recorded: survey spectrum, C 1s, Fe 2p, Cr 2p, O 1s, N 1s, S 2p and C 1s again to check the stability of sample charging and the absence of organic compounds degradation as a function of time. The data analysis was performed with the CasaXPS program (Casa Software, Teignmouth, UK). Molar concentration ratios were calculated from peak areas (linear background subtraction) normalized on the basis of the acquisition parameters and of sensitivity factors and transmission function provided by the manufacturer. The C 1s peak was decomposed by using a least square fitting procedure with a 85:15 Gaussian/Lorentzian product function.

2.4. Solution and supernatant characterization

β-LGB powder was dissolved in MilliQ water at concentration of 3g/L providing clear solution. Solutions were heated for 0.5 h or 4 h at 75°C and rapidly cooled down to room temperature. This resulted in white turbid liquids, indicating protein aggregation. After centrifugation using Beckman instrument (Coulter Inc., USA; 25696 x g for 30 min), the supernatants were collected for different uses. The UV-visible absorption spectra of β-LGB solution and supernatants collected after heating were recorded with a Shimadzu UV 2401PC spectrophotometer, using a quartz cell with a light path length of 10 mm and pure water (MilliQ) as reference. The soluble protein contents in the β-LGB solution and the supernatants

were determined by the Kjeldahl method, multiplying the concentration by 6.34, specific of β-LGB. The surface tension of the liquids was measured at increasing dilution, with a Prolabo Tensiometer (Tensimat n°3) using the Wilhelmy plate method.

3. RESULTS AND DISCUSSION

3.1. Characterization of solutions

Figure 1 shows that the absorbance around 270-280 nm decreases from 2.34 for the native solution to 1.28 and 0.70 for the supernatant collected after heating at 75°C for 0.5 and 4 h, respectively. Note that preliminary tests of heating at different temperatures showed no important variation of absorbance at 60°C, a progressive variation at 75°C, and almost complete removal of proteins due to their aggregation after 4 h at 90 or 100°C. Table 1 presents the protein concentration. Supernatants collected after 0.5 and 4 h heating show protein concentrations of 1.1 and 0.6 g/L, respectively, to be compared with 2.5 g/L for the native solution. Heating the β-LGB solution at 75°C thus provoked aggregation of about 50 and 75% of proteins after 0.5 and 4 h, respectively (Table 1, Figure 1).

Figure 2 presents the evolution of the surface tension as a function of the concentration obtained by increasing dilution of the β-LGB solution and of supernatants collected after heating. The surface tension of the supernatant from 4 h heating is always lower compared to the supernatant from 0.5 h heating and to the native solution. The proteins remaining in the supernatant collected after 4 h are thus responsible for a lower surface tension, meaning a higher activity at the water/air interface. This in agreement with the observation (Schmitt et al., 2007) of a lowering of the surface tension of whey protein solution heated at 85°C in presence of NaCl, the decrease being higher as the NaCl concentration and protein aggregation increased. It was also found that heat aggregation of BSA provoked a decrease of the surface tension of the solution (McClellan and Franses, 2003). The lowering of protein solution surface tension as a result of heating reveals changes of conformation of the molecules still dissolved which are unfolded and expose hydrophobic residues.

Table 1. Protein concentration of native β-LGB solution and supernatants collected after heating at 75°C (standard deviation, 3 replications)

	Native	Supernatant heating 0.5 h	Supernatant heating 4 h
Concentration (g/L)	2.5 ± 0.2	1.1 ± 0.2	0.6 ± 0.1

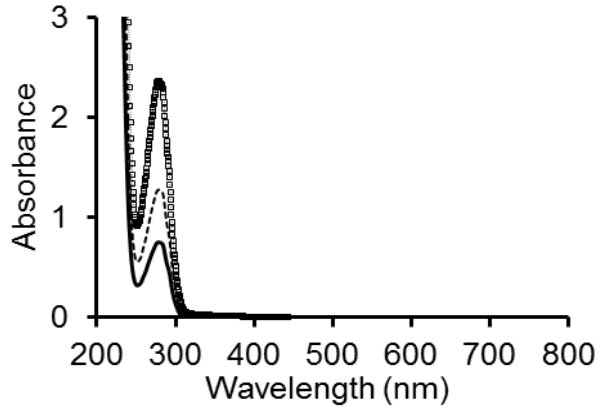

Figure 1. UV-visible absorption spectra: native β-LGB solution (▫▫▫); supernatant collected after heating 0.5 h (---) and 4 h (—) at 75°C.

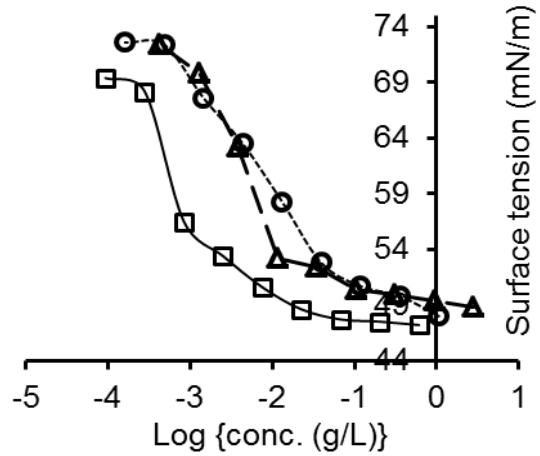

Figure 2. Variation of the surface tension as a function of the protein concentration resulting from increasing dilution of: native β-LGB solution (Δ); supernatant collected after heating 0.5 h (○) and 4 h (□) at 75°C.

3.2. Surface chemical composition

Figure 3 shows representative O 1s and C 1s XPS peaks recorded on stainless steel substrates (SS) just cleaned, or rinsed twice after immersion in the solution of β-LGB or the supernatants collected after heating. The carbon peak of cleaned stainless steel is due to contaminants remaining after cleaning or adsorbed from the surroundings, either the ambient atmosphere or the spectrometer vacuum chamber. The C 1s peak was decomposed (Rouxhet and Genet, 2011; Rouxhet et al., 2008), allowing the possibility of 4 components. The component attributed to carbon only bound to carbon and hydrogen [**C**-(C,H)] was set at 284.8 eV. Other components were found at 286.3 ± 0.2 eV, assigned to carbon making a single bond with oxygen or nitrogen [**C**-(O,N)], and 288.0 ± 0.2 eV, assigned to carbon typical of amide function in proteins [N-**C**=O].

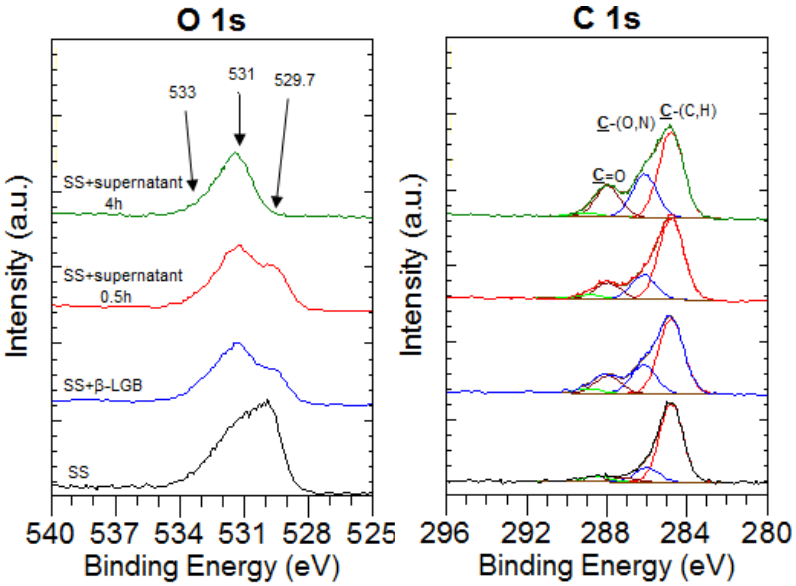

Figure 3. Representative O 1s and C 1s peaks recorded on stainless steel, as such (SS), or immersed in β-LGB solution or in supernatants collected after heating 0.5 or 4 h at 75°C and rinsed. Illustration of C 1s peak decomposition.

For certain samples, a very weak component was found near 289.3 eV, which may be due to ester or carboxyl. A signature typical of proteins appeared after treatments with β-LGB.

The O 1s peak component near 529.7 eV is attributed to metal oxides of stainless steel. The peak showed a maximum at about 531.0 eV for conditioned substrates, which may comprise oxygen of amide of β-LGB [N-C=**O**] and of metal hydroxides of the substrate. The contribution near 533.0 eV is attributed to C–OH or C–O–C. The position and shape of the O 1s peak varied according to the respective contributions. Its decomposition was not performed, owing to the overlap of contributions of the substrate, protein and organic contaminants.

The XPS spectra provide the concentrations of elements and of specific forms of carbon, given in mole fractions with respect to the sum of all elements except hydrogen. Owing to the complexity of the adsorbed layer, the adsorbed amount cannot be expressed in mass per unit area or thickness. However, comparisons of adsorbed amounts can be based on the sum of concentrations of elements due to the adsorbed layer, Σadlayer, and due to the stainless steel, Σsubstrate, which may be evaluated as follows.

$\Sigma adlayer = C_{tot} + N + O_{org}$, where the third term is an evaluation of oxygen due to β-LGB and organic contaminants;

$\Sigma substrate = Fe + Cr + O_{inorg}$, which accounts for metal elements and oxygen bound to them.

Based on the amounts of different aminoacids in β-LGB (Walstra and Jenness, 1984), the elemental composition and the expected contributions to the C 1s peak components were computed as performed before for BSA (Hirayama et al., 1990) and validated by correlations between independent experimental spectral data (Touré et al., 2014). This provides the formula $C_{3.97}O_{1.20}N_1S_{0.04}H_{6.38}$ and the molar mass of 18281 Dalton, with molar ratios O/N = 1.20 and $C_{ox}/N = (C_{tot} - C_{284.8})/N = 2.05$. There is no significant difference between variants A and B of β-LGB.

The contribution of β-LGB to the organic adlayer should be $C_{ox\beta\text{-}LGB} = 2.05*N$ and $O_{\beta\text{-}LGB} = 1.20*N$. The contributions of O due to organic contaminants should be $O_{cont} = C_{oxcont} = (C_{ox} - 2.01*N)$ if oxidized carbon is present in the form of alcohol, aldehyde, ketone or ester functions, as expected. The concentration of organic oxygen can then be deduced:

$$O_{org} = 1.20*N + (C_{ox} - 2.05*N) = C_{ox} - 0.85*N \quad (1)$$

where $1.20*N$ and $(C_{ox} - 2.0*5N)$ are oxygen contribution due to β-LGB and to organic contamination, respectively.

The concentration of oxygen due to stainless steel substrate may then be evaluated as:

$$O_{inorg} = O_{tot} - O_{org}. \quad (2)$$

The XPS analysis was performed on coupons prepared in different ways: just cleaned, or cleaned then immersed in the protein solution either at room temperature or at 75°C for 0.5 or 4 h, or in the supernatant collected after heating the β-LGB solution at 75°C for 0.5 or 4 h. The analysis was performed after rinsing or not with water (immersion twice for 5 min), and flushing with nitrogen for removing the liquid film.

Table 2 gives the proportion of elements belonging to the organic adlayer (∑adlayer) and to the substrate (∑substrate), respectively, and the molar ratios O_{org}/C_{tot}, N/C_{tot} and O_{org}/N determined on the different samples and expected for β-LGB. In XPS, the first layer at the surface with a thickness equal to the electron inelastic mean free path (order of 3 nm) and the next layer of the same thickness are responsible for 63 and 23% of the signal, respectively. It appears that the organic adlayer is thick enough to strongly screen the contribution of the substrate to the XPS spectrum. Comparisons between the molar ratios O_{org}/C_{tot}, N/C_{tot} and O_{org}/N of β-LGB conditioned samples, the values expected for pure β-LGB and the values measured on native substrate; indicate that the organic layer was dominated by the protein for most conditioned samples. In particular, it shows that rinsing provokes only a moderate desorption, as also observed for BSA and other substrates. This means that β-LGB was not quickly desorbed during the cleaning test. A detailed comparison between different samples according to their history (heating in the β-LGB solution, treating with supernatant, heating time) may not be made owing to the lack of replicates allowing the significance of differences to be ascertained.

Table 2. Surface chemical composition measured by XPS on stainless steel samples with different treatments as indicated.

Conditioning liquid			Proportion (%) of elements due to		Molar ratios in organic adlayer		
	Heating	Rinsing	adlayer	substrate	O_{org}/C_{tot}	N/C_{tot}	O_{org}/N
none	none		55.0	45.0	0.22	0.02	12.1
	4 h		57.5	42.5	0.18	0.02	7.8
β-LGB	none	none	95.6	4.4	0.29	0.20	1.5
		twice	80.6	19.4	0.29	0.15	1.9
	0.5 h	none	95.8	4.2	0.28	0.16	1.7
		twice	78.0	22.0	0.25	0.12	2.1
	4 h	none	100.6	-0.6	0.31	0.20	1.5
		twice	103.2	-3.2	0.31	0.19	1.6
supernatant 0.5 h	none	none	98.1	1.9	0.32	0.22	1.5
		twice	94.1	5.9	0.30	0.19	1.6
supernatant 4 h	none	none	82.3	17.7	0.28	0.15	1.8
		twice	76.9	23.1	0.23	0.13	1.9
computed for β-LGB			100.0	0.0	0.30	0.25	1.2

3.3. Contact angles and surface cleanability

The water contact angle of the non-conditioned stainless steel (Figure 4B) is higher than expected for chromium and iron oxides constituting the surface, which is attributed to the presence of organic contaminants, as revealed by XPS (Table 2). The slightly higher contact angle measured with the supernatant containing a low concentration of β-LGB in denatured form is difficult to interpret as it characterizes the contact between 4 phases: naked substrate, substrate with adsorbed protein, liquid, and air.

Figure 4A presents the critical detachment radius measured on stainless steel pretreated in different ways: dried at room temperature after soiling with a quartz particles suspension in water and in β-LGB solution, or with a quartz suspension in β-LGB solution heated previously at 75°C for 0.5 or 4 h; dried at 75°C after soiling with a suspension in water or β-LGB solution. Remember that the higher the critical detachment radius the lower the particle adherence. The presence of β-LGB in the quartz suspension decreased the critical detachment radius (b compared to a). This was further decreased when the soiling suspension containing β-LGB was previously preheated 4 h (d) or when the sample soiled with a suspension in β-LGB solution was dried at 75°C (f). Note that protein aggregates were not identified under the microscope. In absence of β-LGB, the enhanced adherence of the quartz particles observed after drying at high temperature compared to room temperature (e compared to a) may be due to a more complete removal of the water, as observed for soiling with starch particles (Detry et al., 2011).

The influence of BSA on contact angle and cleanability of glass (Touré et al., 2014) led to emphasize a direct action of the protein at the interface. This did not act by influencing droplet spreading and soiling particles aggregation. It might prevent the formation of tight bonds between glass and silica upon drying or prevent the formation of junctions made of hydrophobic organic contaminants, or which may act as a detergent. While the presence of BSA increased drastically the cleanability of glass, it decreased slightly the cleanability of polystyrene. The presence and the denaturation of β-LGB also tend to decrease slightly the cleanability of stainless steel. An important remark is that stainless steel does not behave as a hydrophilic substrate owing to its surface contamination with organic compounds. Therefore, it appears suitable to examine the influence of the initial surface state of stainless steel on its behavior regarding soiling and cleaning.

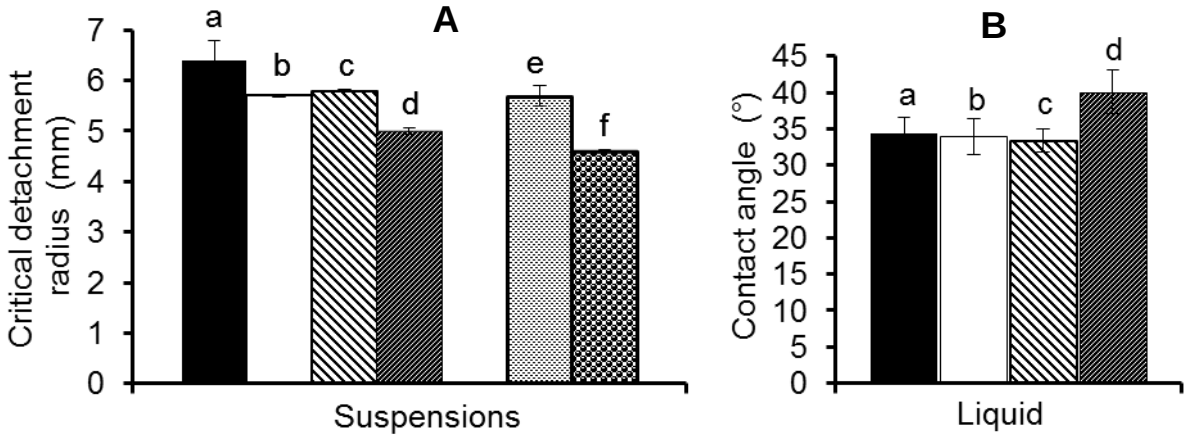

Figure 4. A. Critical detachment radius measured on stainless steel: samples dried at room temperature after soiling with a quartz particles suspension in water (a), in β-LGB solution (b), or with a quartz suspension in β-LGB solution previously heated at 75°C for 0.5 h (c) or 4 h (d); (e) and (f), same as (a) and (b), respectively, except that soiled samples were dried at 75°C. B. Contact angle measured on stainless steel with water (a), native β-LGB solution (b), supernatant collected after heating at 75°C for 0.5 h (c) and 4 h (d).

4. CONCLUSIONS

The contact of stainless steel with β-LGB present in the soiling quartz particles suspension led to adsorption of the protein, which dominated the composition of the organic layer with respect to contaminants initially present, and was not markedly desorbed upon rinsing.

The presence of β-LGB at the quartz particle/substrate interface slightly increased the adherence, which was further increased when the protein was denatured. Comparison with systems investigated before suggests that the influence of protein via droplet spreading and soiling particles aggregation is of minor importance compared to direct effects on the substrate/quartz interface. It is important to realize that stainless steel does not behave as a hydrophilic substrate owing to its surface contamination with organic compounds. A broader study, including the effect of substrate hydrophobicity, is under way to further elucidate the effect of soluble protein and their denaturation on the particulate soils adhesion.

ACKNOWLEDGEMENTS

This study has been supported by the Walloon Region. The support of National Foundation for Scientific Research (FNRS, Belgium) is also gratefully acknowledged. The authors thank Michel J. Genet for the XPS examinations.

REFERENCES

Bansal, B. and Chen X.D. (2009) Fouling of heat exchangers by dairy fluids – a review, *The Berkeley Electronic Press*, **RP2**, 149–57.

Bansal, B. and Chen X.D. (2006) A critical review of milk fouling in heat exchangers, *Science*, **5**(2), 27–33.

Blanpain-Avet, P., Hédoux, A., Guinet, Y., Paccou, L., Petit, J., Six, T. and Delaplace, G. (2012) Analysis by raman spectroscopy of the conformational structure of whey proteins constituting fouling deposits during the processing in a heat exchanger, *J. Food Eng.*, **110**(1), 86–94.

Changani, S.D, Belmar-Beiny, M.T and Fryer, P.J. (1997) Engineering and chemical factors associated with fouling and cleaning in milk processing, *Exp. Them. Fluid Sci.*, **14**(4), 392–406.

Detry, J.G., Sindic, M., Servais M.J., Adriaensen, Y., Derclaye, S., Deroanne, C. and Rouxhet P.G. (2011) Physico-chemical mechanisms governing the adherence of starch granules on materials with different hydrophobicities, *J. Colloid Interface Sci.*, **355**(1), 210–21.

Fickak, A., Al-Raisi, A. and Chen, X.D. (2011) Effect of whey protein concentration on the fouling and cleaning of a heat transfer surface, *J. Food Eng.* **104**(3), 323–31.

Fox, P.F. and Mcsweeney, P.L.H. (1998) Milk proteins, *Dairy Chem. Biochem.*, **1**, 146–264.

Goldstein, A.S. and Dimilla, P.A. (1997) Application of fluid mechanic and kinetic models to characterize mammalian cell detachment in a radial-flow chamber, *Biotechnol. Bioeng.*, **55**(4), 616–29.

Goldstein, A.S. and DiMilla P.A.. (1998) Comparison of converging and diverging radial flow for measuring cell adhesion, *AIChE J.*, **44**(2), 465–73.

Hirayama, K., Akashi S, Furuya, M., Furuya, K. (1990). Rapid confirmation and revision of the primary structure of bovine serum albumin by ESIMS and Frit-FAB LC/MS. *Biochem. Biophys. Res. Commun.*, **173**(2), 639-646.

McClellan, S.J. and Franses E.I. (2003) Effect of concentration and denaturation on adsorption and surface tension of bovine serum albumin, *Colloids Surf. B. Biointerfaces*, **28**(1), 63–75.

Robbins, P.T., Elliott, B.L., Fryer, P.J., Belmar, M.T. and Hasting, A.P.M. (1999) A comparison of milk and whey fouling in a pilot scale plate heat exchanger: implications for modelling and mechanistic studies, *Food Bioprod. Process*, **77** (C2)(2), 97–106.

Rouxhet, P.G., Misselyn-Bauduin, A.M., Ahimou, F., Genet, M.J., Adriaensen, Y., Desille, T., Bodson P. and Deroanne, C. (2008) XPS analysis of food products: toward chemical functions and molecular compounds, *Surf. Interface Anal.*, **40**(3-4), 718–24.

Rouxhet, P.G. and Genet M.J. (2011) XPS analysis of bio-organic systems, *Surf. Interface Anal.*, **43**(12), 1453–70.

Schmitt, C., Bovay, C. Rouvet, M., Shojaei-Rami, S. and Kolodziejczyk E. (2007) Whey protein soluble aggregates from heating with nacl: physicochemical, interfacial, and foaming properties, *Langmuir Acs J. Surfaces Colloids*, **23**(8), 4155–66.

Stephan, O., Weisz, N., Vieths, S., Weiser, T., Rabe, B. and Vatterott, W. (2004) Protein quantification, sandwich elisa, and real-time pcr used to monitor industrial cleaning procedures for contamination with peanut and celery allergens, *J. AOAC Int.*, **87**(6), 1448–57.

Touré, Y., Genet M.J., Dupont-Gillain C.C., Sindic M. and Rouxhet P.G. (2014). Conditioning materials with biomacromolecules: composition of the adlayer and influence on cleanability. *J. Colloid Interface Sci.*, **432**, 158-169.

Touré, Y., Rouxhet, P.G. and Sindic, M. (2013) Influence of soluble proteins on the adherence of particulate soils, *Proc. Int. Conf. Heat Exch. Fouling Clean.*, **X**, 285–290.

Touré, Y., Rouxhet, P.G., Dupont-Gillain, C.C. and Sindic, M. (2011) Influence of soluble polysaccharide on the adherence of particulate soils, *Proc. Int. Conf. Heat Exch. Fouling Clean.*, **IX**, 219–26.

Visser, J. and Jeurnink, T.J.M. (1997) Fouling of heat exchangers in the dairy industry, *Exp. Therm. Fluid Sci.*, **14**(4), 407–24.

Walstra, P. and Jenness, R. (1984) Dairy Chemistry and Physics, *John Wiley Sons, New York*, 467 pp.

SECTION VI

INFLUENCE OF SUBSTRATE NATURE AND β-LACTOGLOBULINE ON CLEANABILITY AFTER SOILING BY SUSPENSION SPRAYING AND DRYING

From:

Yetioman Touré, Christine C. Dupont-Gillain, André Matagne, Erik Goormaghtigh, Marianne Sindic and Paul G. Rouxhet, 2014.

Submitted in Chem. Eng. Sci.

ABSTRACT

Glass and stainless steel (StSteel), previously cleaned with ethanol (-Eth) or with ethanol and UV-Ozone treatment (UVO), were soiled with quartz suspensions in water and in a β-lactoglobulin (β-LGB) solution, and dried. The cleanability in water was evaluated using a radial-flow cell. The soiling suspension containing β-LGB was used as such or after heating for 4 h at 75°C, which provoked coagulation of about 75% of β-LGB. The substrate/solution interfaces were characterized by X-ray photoelectron spectroscopy (XPS) analysis of conditioned substrates and by contact angle measurements.

For three of the substrates tested (Glass-Eth, Glass-UVO, StSteel-UVO) the increase of cleanability when the soiling suspension contained β-LGB may be explained by the influence of capillary forces acting upon drying, which depend primarily on the liquid surface tension. In practice, the substrate contact angle is of less importance.

On the other hand, the order of cleanability observed for the substrates soiled with a suspension of quartz particles in water (Glass-Eth ≅ Glass-UVO < StSteel-UVO < StSteel-Eth) and the influence of β-LGB on the cleanability of StSteel-Eth may not be simply explained by computed capillary forces. Variations of the wetting hysteresis during dynamic contact angle measurements and XPS surface analysis indicated that the presence of organic contaminants, which is often neglected by considering the substrate surface as a model solid surface, may have a significant influence on cleanability. Hypothetical effects are the heterogeneity of the particle–substrate interface and the added complexity of the interactions between protein and contaminants at the interfaces.

Keywords: Fouling; Cleaning; Particulate soiling; Protein denaturation; RFC; XPS; Surface contaminants

1. INTRODUCTION

Cleaning is an important issue in food and pharmaceutical industries. Its efficiency influences the final quality of the products, and is crucial to insure the absence of cross-contaminations and the batch integrity (Stephan et al., 2004). A good control of fouling, accompanied by an effective cleaning process, may contribute to reduce the fouling-related cost such as additional energy, productivity loss, additional equipment, manpower, chemicals and environmental impact.

Particle deposition and drying are a mode of fouling which is of major concern for surfaces exposed to natural environments or surfaces of industrial equipment. Particulate soils may originate from splashing on open surfaces or deposition in storage tanks, ducts or heat exchangers. The issue is of particular concern in food and pharmaceutical processing, where fouling deposits may endanger microbial sterility and product purity.

Compounds present in food and pharmaceutical mixtures may influence interactions with surfaces and adhesion processes (Speranza et al., 2004). A study of starch granules adherence, after suspension spraying onto different substrates and drying, demonstrated that substrate wettability influenced the shape and compactness of the adhering aggregates, the efficiency of shear forces upon cleaning, and finally the adherence of soiling particles (Detry et al., 2011). Moreover, it was reported that the presence of macromolecules, mainly polysaccharides, which were adsorbed from the liquid phase or carried by the retracting water film and deposited at the granule-substrate interface, acted as an adhesive joint, the properties of which seemed to be influenced by the detailed history of drying and subsequent exposure to humidity. The influence of macromolecules (Touré et al., 2014a; 2013; 2011) on the adherence of model particulate soils (quartz particles) was examined using substrates which differed according to hydrophobicity. The effect of dextran was weak, owing to its low adsorption or easy desorption. The presence of BSA had little effect on the adherence to a hydrophobic substrate (polystyrene) but decreased drastically the adherence to a more hydrophilic substrate (glass), bringing its cleanability to the range observed for polystyrene. There was no significant difference in cleanability according to whether the protein was brought by conditioning the substrate before soiling or by its presence in the soiling suspension, or both ways. The influence of BSA was attributed to the lowering of the liquid surface tension, leading to a decrease of capillary forces created during drying.

Whey proteins are often used to improve food product qualities such as texture and appearance. A controversial question concerns their implication in deposit layer formation and removal. Although the connection between the thermal stability and conformational changes of β-lactoblobulin (β-LGB) is well established, the role of its denaturation in the build-up of the fouling deposit is still unclear. Trends reported in the literature are not conclusive and are focused on protein deposits or on the effect of mineral elements concentration on deposit formation (Blanpain-Avet et al., 2012; Bansal and Chen, 2006; 2009). Bansal et al., (2005) reported that aggregated whey proteins and dissolved denatured whey protein took part in deposit formation. Although there is no general consensus in the literature (Bansal and Chen, 2006; Changani et al., 1997), according to Robbins et al., (1999)

β-LGB plays a key role in fouling as it is the most abundant and the most heat-labile whey protein. A matter of interest is the influence of heating and protein denaturation on particle soil adherence. Recently (Touré et al., 2014b), we showed that the presence of β-LGB at the quartz particle/stainless steel interface slightly increased the adherence, which was further slightly increased when the protein was denatured. Comparison with systems investigated before suggested that the influence of protein via droplet spreading and soiling particles aggregation may be of minor importance compared to direct effects occurring at the stainless steel/quartz interface. The study also showed that there was no difference whether the denaturation occurred by drying the soiled substrate at high temperature or by previous heating of the quartz suspension used for soiling.

The surface of stainless steel is made of chromium and iron oxy-hydroxides and is thus expected to be hydrophilic, in contrast with the experimentally measured water contact angle which is frequently above 40°. Actually, inorganic surfaces made of oxides (e.g. stainless steel and glass) or metals (e.g. gold) are characterized by a high surface energy, i.e. an excess of free energy due to broken bonds. This tends to be reduced by retention of organic compounds which originate from material processing or are contaminants adsorbed from the surroundings. As a result, these surfaces are less hydrophilic than expected (Rouxhet, 2013). It thus appears suitable to consider the influence of the initial state of the surface on its behavior regarding soiling and cleaning.

The aim of the present work is to investigate the effect of β-LGB and its denaturation on the adherence of particulate soils, depending on the nature of the substrate and the state of its surface. The particle detachment, i.e. the substrate cleanability, was evaluated after exposure to water in a radial flow chamber (RFC). Glass and stainless steel were taken as models of practically relevant substrates regarding fouling and cleanability. The influence of the initial surface state was examined in relation with hydrophobicity. Therefore the tested substrates were precleaned in two ways before soiling: solvent rinsing, and UV-Ozone treatment (UVO) treatment which insured a more extensive removal of organic contaminants. Quartz particles were kept as a model of hard particulate soil. The protein was involved in the soiling process by its introduction into the quartz suspension. The influence of denaturation was examined by a high temperature pretreatment of the soiling suspension. The soiling suspension was characterized at different stages regarding soluble protein concentration, conformational changes and surface tension. The substrate/solution interfaces were characterized by X-ray photoelectron spectroscopy (XPS) analysis of substrates conditioned with solutions in representative states and by contact angle measurements.

2. MATERIALS AND METHODS

2.1. Materials

Stainless steel (AISI 304-2R, 1mm thick) plates were provided by Arcelor (France). The face used for the study had a mirror finish and was protected with a plastic sheet which was removed before substrate preparation. Glass slides (50 mm x 50 mm x 1 mm, 16 mm x 37 mm x 1 mm) were purchased from Menzel-Gläser (Germany). The substrate coupons were used with dimensions: 50 mm x 50 mm for fouling and cleanability assessment; 16 mm x10 mm for contact angle measurement and for XPS analysis. The coupons were rinsed with ethanol, sonicated (ultrasonic cleaner Branson 3200, USA) in ethanol for 15 min, rinsed thoroughly with ethanol, dried with a gentle flow of nitrogen and wrapped in aluminum until use. These substrates are referred to as Glass-Eth and StSteel-Eth. Certain coupons of glass (named Glass-UVO) and stainless steel (StSteel-UVO) were submitted to an additional UV-Ozone treatment for 20 min (UVO-cleaner, Model 42, Jelight Company, USA) to improve the removal of organic contamination, and used immediately. In order to avoid confusion between substrate preparation and cleanability evaluation, ethanol rinsing followed or not by UVO treatment will be referred to as pre-cleaning.

Ground quartz (M400) was provided by Sibelco Benelux (Belgium). Quartz particles with a size about 10 to 30 µm were isolated from the initial batch (particle size distribution 1 to 60 µm) as described before (Touré et al., 2011). MilliQ water was produced by a MilliQ-50 system from Millipore (France). Absolute ethanol and β-lactoglobulin (β-LGB) from bovine milk (lyophilized powder; ≥85 %,) were purchased from Sigma-Aldrich (Wisconsin, USA).

2.2. Soiling procedure and cleanability assessment

Three kinds of quartz particle suspensions were prepared at a concentration of 150 g/L: (i) in water, (ii) in a native β-LGB solution (3 g/L), (iii) same as (ii) and subsequently heated for 4 h at 75°C and cooled down. Further details on soil preparation and handling can be found in Touré et al. (2013, 2011). The choice of β-LGB concentration in the quartz suspension was based on β-LGB concentration in bovine milk (3 g/L) (Walstra and Jenness, 1984). The soiling procedure, cleanability assessment and data processing are detailed in previous studies (Detry et al., 2011; Touré et al., 2011; 2013; 2014). Briefly, suspension droplets were deposited by aspersion at room temperature. This did not lead to the formation of a continuous film and no drainage occurred. Cleanability assessment was performed at 20°C in RFC. Distilled water was flown during 5 min with a flow rate of 40 ml/min. Pictures taken before and after cleaning, were processed with a specific application of the Matlab software,

which gave the radial position. The radial position at which the residual density was half the initial density was considered as the critical detachment radius (Goldstein and DiMilla, 1998; 1997). At least 10 repetitions of each experiment (soiling/cleaning) were made. The error bars show the standard deviations.

The critical detachment radius, which is the output of the cleaning experiments, is related to a critical wall shear stress and the minimal hydrodynamic drag force required to detach particles in the given experimental conditions (Jensen and Friis, 2004). The conversion of critical detachment radius into critical wall shear stress may be biased when the adhering aggregate height is not negligible with respect to the channel height and when the adherence is such that flow rates above 20 ml/min are required (Detry et al. 2007; 2009). Therefore, the results of the present study are expressed only in terms of critical detachment radius, keeping in mind that, for a defined flow rate, its increase reveals a decrease of the adherence.

2.3. Solution characterization

β-LGB powder was dissolved in MilliQ water at a concentration of 3 g/L providing a clear solution. Some solutions were heated for 4 h at 75°C and rapidly cooled down to room temperature. This resulted in a white turbid liquid, indicating protein aggregation. After centrifugation (Beckman centrifuge; Coulter Inc., USA; 25700 x g for 30 min), the supernatants were collected for different uses described below.

The UV-visible absorption spectra of β-LGB solution and supernatants collected after heating were recorded with a Shimadzu UV 2401PC spectrophotometer, using a quartz cell with a light path length of 10 mm and pure water (MilliQ) as reference.

The intrinsic tryptophan fluorescence intensity of β-LGB solution and supernatants was measured at ambient temperature (spectrometer Jasco V-630, Japan). Fluorescence spectra were acquired with an excitation wavelength of 280 nm and recorded from 290 to 600 nm, using solutions diluted with MilliQ water to reach an absorbance of about 0.12.

The soluble protein content in the β-LGB solution and the supernatants was determined in two ways. One way was the Kjeldahl method, multiplying the nitrogen concentration by 6.34, specific of β-LGB. The other way was based on the absorbance at 278 nm, using the absorption coefficient of 1750 L/mol.cm determined for β-LGB (Stanley and Peter, 1989).

The surface tension of the liquids was measured at increasing dilution, with a Prolabo Tensiometer (Tensimat n°3), using the Wilhelmy plate method with a platinum plate.

Circular dichroism measurements (CD) and attenuated total reflectance-Fourier transform infrared spectroscopy (ATR-FTIR) were used to assess the secondary structure of β-LGB (α-

helix, β-sheet, turn, unordered). Far-UV CD spectra (185-260 nm) were recorded with a Jasco J-810 spectropolarimeter at 20°C in Milli-Q water, using a 1 mm pathlength quartz Suprasil cell (Hellma), with protein concentrations of *ca.* 0.1 mg/ml. Four scans (20 nm/min, 1 nm bandwidth, 0.2 nm data pitch and 2 s DIT) were averaged, base lines were subtracted and no smoothing was applied.

Secondary structure analyses using the CDSSTR (Manavalan et al., 1987; Sreerama and Woody, 2000), CONTINLL (Provencher and Glockner, 1981; Van Stokkum et al., 1990) and SELCON3 (Sreerema et al., 1993, 1999) algorithms were performed on the CD data with the Dichroweb analysis server (Whitmore and Wallace, 2004, 2008), using both reference datasets 3 and 6. The results from the three algorithms were averaged and the standard deviations between the calculated secondary structures are given in Table 2. The accuracy of the analysis was checked through the goodness-of-fit parameter (NRMSD) values. With both CDSSTR and CONTINLL, NRMSD values below 0.1 indicated a good correspondence between the calculated secondary structure and the experimental CD data. In contrast, SELCON3 yielded higher NRMSD values (comprised between 0.1 and 0.23) but, nevertheless, data obtained with this algorithm and with the other two were identical within the error limit.

Attenuated total reflectance Fourier transform infrared (ATR-FTIR) spectra were recorded (4 cm^{-1} resolution, 64 co-added scans) with a Vertex 70 - RAM II Bruker spectrometer (Bruker Analytical, Madison, WI, USA) operating with a Golden Gate diamond ATR accessory (Specac Ltd., Slough, UK). 10 µL of the solution were deposited on the diamond and dried with gentle air flow. More details about the instruments, the mode of measurement, the background used and the acquisition parameters may be found elsewhere (Stefanov et al., 2013; Pierna et al., 2012). After an area normalization with a linear method, mathematical models were applied to evaluate the secondary structure, as described before (Goormaghtigh et al., 2006). Data processing was performed with a homemade software running under the MatLab 7.1 environment (The MathWorks, Natick, MA).

2.4. Substrate characterization

Contact angles of water, β-LGB solution and supernatant collected after heating the β-LGB solution for 4 h at 75°C were measured in static conditions at room temperature, with the sessile drop method, using a goniometer (Krüss, Germany), on the one hand, and image analysis (instrument made by Electronisch Ontwerpbureau de Boer, The Netherlands;

measurement 5 s after drop deposition), on the other hand. The measurements involved at least 10 drops.

Measurements of contact angles were also performed in dynamic conditions with the Wilhelmy plate method, recording 3 successive immersion - emersion (advancing - receding) cycles at a rate of 50 µm/s as a function of the contact line position (Tomasetti et al., 2013).

The surface composition was determined by XPS on substrates either (i) as such without particular treatment, (ii) precleaned with ethanol, (iii) precleaned with ethanol and submitted to UVO treatment, (iv) precleaned as (ii) or (iii) and subsequently conditioned at room temperature by immersion for 1 h in a 3 g/L β-LGB solution, in the supernatant collected after heating a 3 g/L β-LGB solution for 4 h at 75°C, or in a 0.75 g/L β-LGB solution (to get about the same concentration as the supernatant). In order to avoid repeated emersions, two coupons of the same substrate were conditioned together with 10 ml of β-LGB solution and rinsing was performed by dilution with MilliQ water; therefore, 8 ml from 10 ml of conditioning solution were removed and 8 ml of MilliQ water were added. Three dilutions steps were performed with time intervals of 5 min. Finally, the coupon was removed from the solution and the extra liquid film was blown off with a gentle nitrogen flow. Remember that the contribution of elements to the XPS spectrum decreases exponentially as a function of the depth of their location in the analyzed sample (Genet et al., 2008), the photoelectron inelastic mean free path being of the order of 3 nm.

The samples were fixed on a standard stainless steel holder by using a piece of double-sided insulating tape. The XPS analyses were performed with a SSX 100/206 photoelectron spectrometer from Surface Science Instruments (USA) equipped with a monochromatized micro-focused Al X-ray source (powered at 20 mA and 10 kV). A flood gun set at 6 eV and a Ni grid placed 3 mm above the sample surface were used for charge stabilization. The pressure in the analysis chamber was about 10^{-6} Pa. The angle between the perpendicular to the surface and the axis of the analyzer lens was 55°. The analyzed area was approximately 1.4 mm^2 and the pass energy was set at 150 eV for the survey spectrum and 50 eV for high energy resolution spectra. In the latter conditions, the full width at half maximum (FWHM) of the Au $4f_{7/2}$ peak of a gold standard sample was about 1.1 eV. The following sequence of spectra was recorded: survey spectrum, C 1s and K 2p, O 1s, N 1s, Si 2p; Mg 2p, Ca and Na 1s (glass samples only); Fe 2p and Cr 2p (stainless steel only); and C 1s again to check for sample charging stability and absence of sample degradation. The binding energy scale was set by fixing the C 1s component due to carbon bound only to carbon and hydrogen at 284.8 eV. The data treatment was performed with the CasaXPS program (Casa Software,

Teignmouth, UK). Molar concentration ratios were calculated from peak areas (linear background subtraction) normalized on the basis of the acquisition parameters and of sensitivity factors and transmission function provided by the manufacturer. The C 1s peak was decomposed (Genet et al., 2008) by using a least square fitting procedure with a 85:15 Gaussian-Lorentzian product function.

3. RESULTS

3.1. Solution characteristics

Heating the β-LGB solution for 4 h at 75°C resulted in a white turbid liquid, indicating protein coagulation. Figure 1 shows that the absorbance of the maximum near 278 nm decreased from 2.3 for the native solution to 0.7 for the supernatant collected after heating. No significant absorption was observed above 310 nm, in contrast with the non-centrifuged heated solution which showed an absorbance above 3 between 310 and 700 nm. This indicated that centrifugation insured an efficient separation between aggregates, responsible for strong light scattering, and dissolved molecules. Note that preliminary tests showed no significant variation of the supernatant absorbance at 278 nm when heating was performed at 60°C; they showed a progressive variation at 75°C, and a very quick coagulation near 95°C.

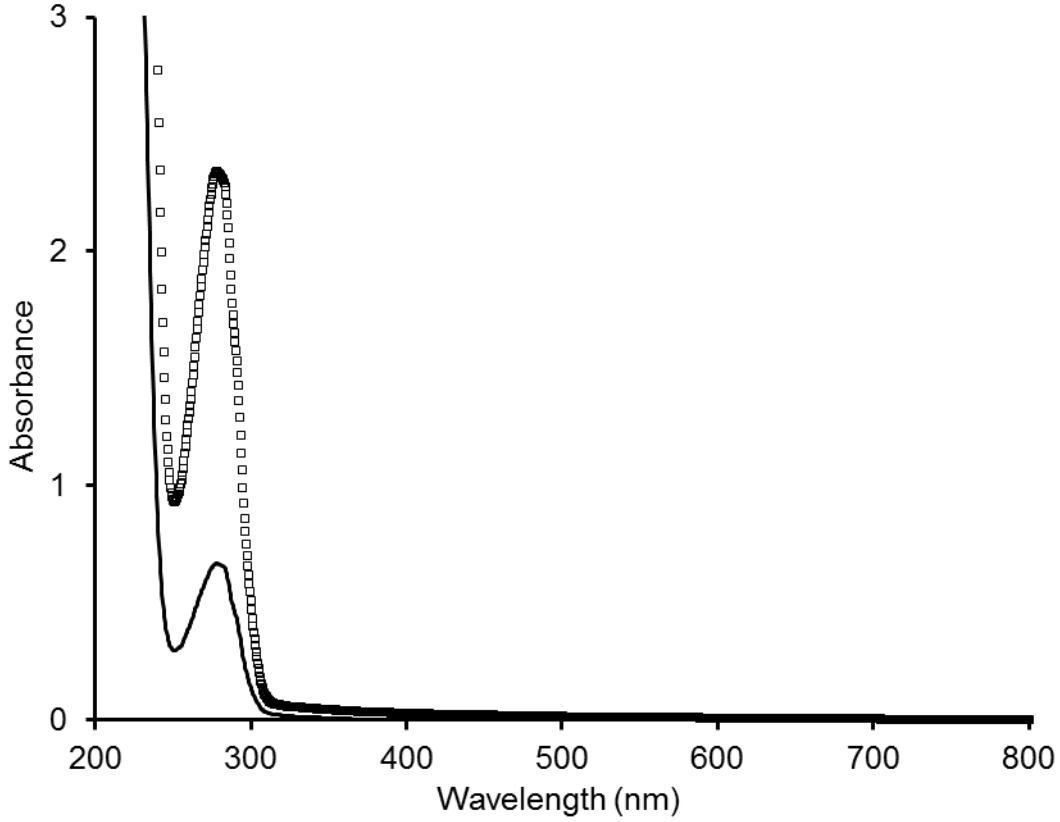

Figure 1. UV-visible absorption spectra of native β-LGB solution (▫▫▫) and supernatant collected after heating a β-LGB solution for 4 h at 75°C (—).

Table 1 presents the protein concentration determined by the Kjeldahl method and from the absorbance at 278 nm. There was no difference between the two methods. The supernatant showed a protein concentration of 0.6 g/L, compared to 2.5 g/L for the native solution.

Table 1. Protein concentration determined from the absorbance at 278 nm and by Kjeldahl method: native β-LGB solution and supernatant collected after heating for 4 h at 75°C (standard deviation, 3 replicates)

Methods	Concentration (g/L)	
	Native	Supernatant
Kjeldahl	2.5 ± 0.1	0.6 ± 0.1
Beer-Lambert	2.5 ± 0.0	0.7 ± 0.0

The intrinsic tryptophan fluorescence emission spectra of native solution and supernatant of heated solution are presented in Figure 2. The native solution showed a maximum intensity at the emission wavelength of 333 nm. The supernatant showed a small increase of intensity and a red shift of 3 nm.

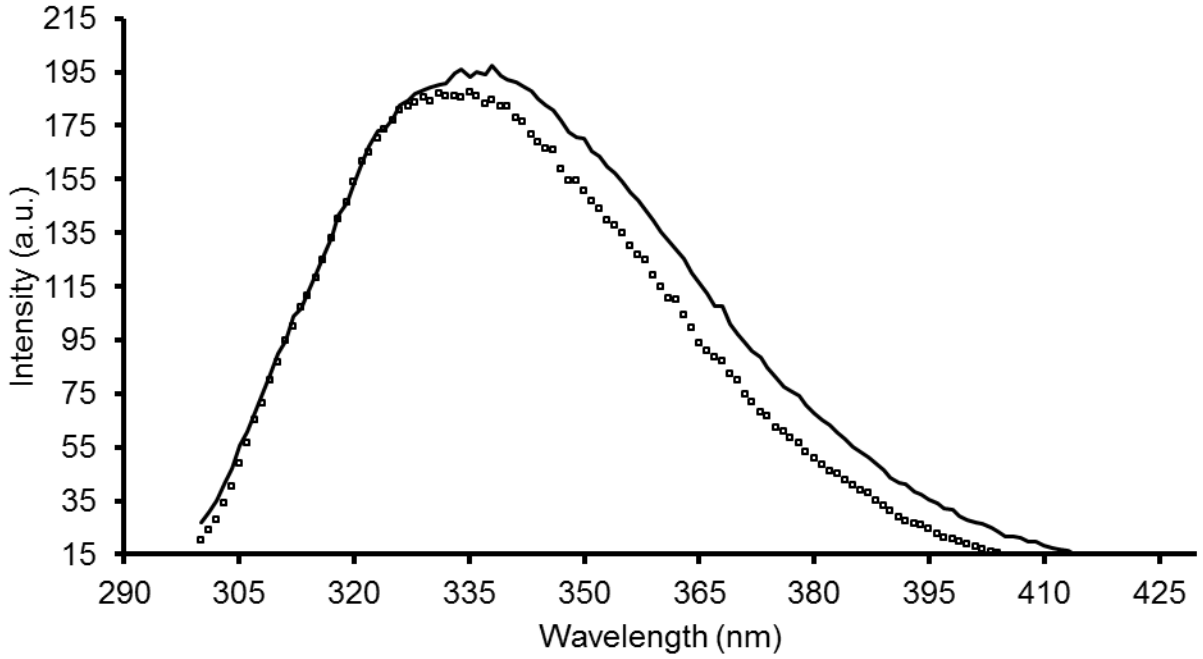

Figure 2. Fluorescence emission spectra (280 nm excitation) of native β-LGB solution (▫▫▫) and supernatant collected after heating a β-LGB solution for 4 h at 75°C (—).

The secondary structure of β-LGB evaluated from CD and ATR-FTIR measurements is presented in Table 2 for native solutions, for the supernatant and for the pellet collected after centrifuging the heated solution (from ATR-FTIR only). Although the α-helical content measured by IR is somewhat overestimated (X-ray and NMR β-LGB structures found in the PDB, e.g. 1CJ5, 1QG5, 2Q2M and 1BEB reveals 10-15 % α-helix and 30-40 % β-sheet), both

techniques showed no significant difference between β-LGB structures in the native solution and the supernatant. According to ATR-FTIR of the pellet, the main effect of denaturation was to reduce the α-helix content and increase the unordered fraction. The spectra did not reveal any significant difference between the native protein and the protein left in the supernatant.

Table 2. Secondary structure composition (% helix, sheet, turn, unordered) of β-LGB in the native solution, and in the supernatant and pellet collected after heating for 4h at 75°C.

Method	Solutions	Secondary structure (%)			
		α-Helix	β-Sheet	Turn	Unordered
Circular dichroism	Native β-LGB (0.11 g/L)	9.5 ± 1.5	40 ± 4	21.5 ± 0.5	28 ± 4
	Supernatant (0.11 g/L)	10.5 ± 1.5	35 ± 3	21.5 ± 1	31 ± 5
Infrared ATR	Native β-LGB (3 g/L)	23 ± 1.2	45 ± 0.7	9 ± 0.1	24 ± 0.1
	Native β-LGB (0.75 g/L)	12 ± 3.1	42 ± 1.1	12 ± 0.7	27 ± 0.5
	Supernatant (0.7 g/L)	20 ± 0.7	37 ± 0.2	11 ± 0.4	28 ± 0.2
	Pellet	-3 ± 2.2	44 ± 0.1	11 ± 0.0	64 ± 1.8

Mean ± standard deviation

Figure 3 presents the evolution of the surface tension as a function of the concentration obtained by increasing dilution of native β-LGB solutions and of supernatants. Remember that the protein concentration in the supernatant was about 4 times lower compared to the native solution. The surface tension of the supernatant was always lower compared to the native solution. The robustness of the observations regarding surface tension was demonstrated by the reproducibility of the two independent sets presented in Figure 3, which were performed at a time interval of 10 months.

3.2. Substrate surface composition

The surface elemental compositions determined by XPS are given in Table 3 for glass samples and Table 4 for stainless steel samples. A distinction is made between substrates conditioned with native β-LGB solutions (3 and 0.75 g/L), conditioned with the supernatant collected after heating for 4 h at 75°C, and not conditioned. On the other hand a distinction is made according to substrate. On the other hand, a distinction is made according to substrate treatment previous to soiling: no pre-cleaning, pre-cleaning with ethanol, pre-cleaning with ethanol and UVO treatment. The letters a and b refer to independent experimental sets; certain data, named a_1 and a_2, were obtained on two distinct areas of the same coupon. Figure 4 shows representative O 1s and C 1s peaks recorded on glass and stainless steel.

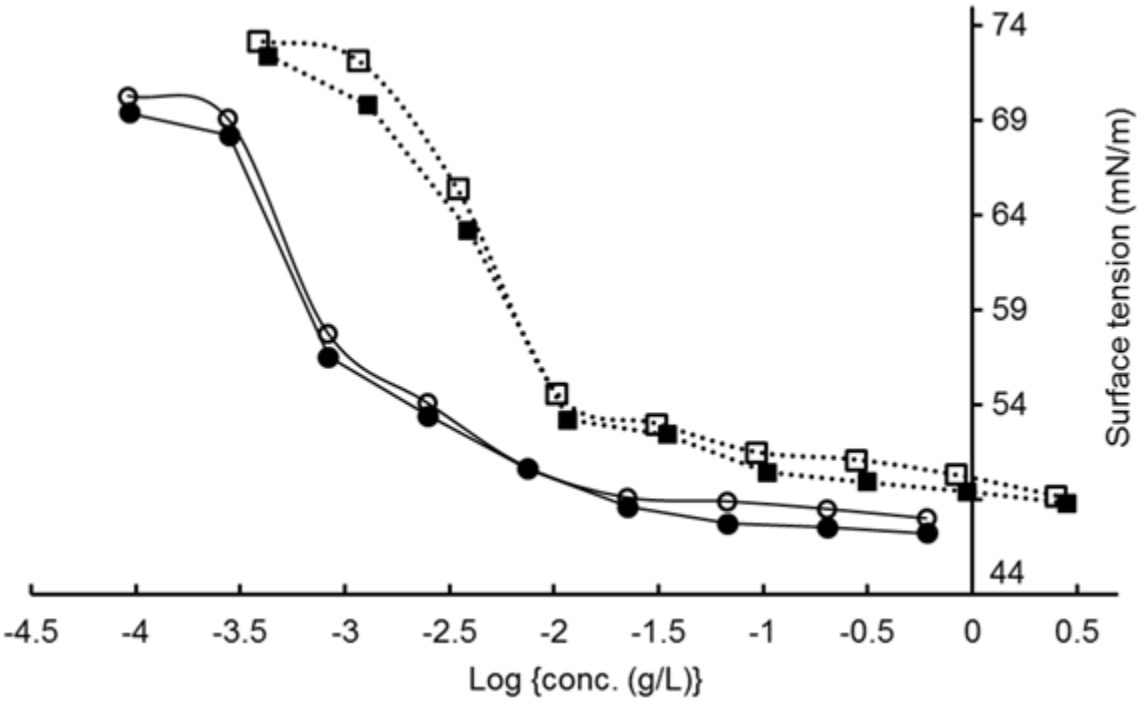

Figure 3. Variation of the surface tension as a function of the protein concentration resulting from increasing dilution of native β-LGB solution (□,■) and supernatant collected after heating a β-LGB solution for 4 h at 75°C (●,○).Open and closed symbols represent two sets of data acquired independently.

Non-conditioned substrates showed the presence of carbon. This was attributed to organic contaminants which were not removed by the pre-cleaning procedure or were adsorbed from the surroundings, either the ambient atmosphere or the spectrometer vacuum chambers (Rouxhet, 2013).

The C 1s peak was decomposed (Rouxhet et al., 2008; Rouxhet and Genet, 2011), allowing the possibility of 4 components. The full width at half maximum (FWHM) was imposed to be the same for the 4 components. No constraint was imposed on the binding energy of the componentsexcept when their intensity was very weak, in which case the binding energy was constrained to be in range observed otherwise. The component attributed to carbon only bound to carbon and hydrogen [**C**-(C,H)] was set at 284.8 eV. For substrates conditioned with β-LGB, other components were found at 286.2 ± 0.1 eV, assigned to carbon making a single bond with oxygen or nitrogen [**C**-(O,N)], and 288.1 ± 0.1 eV, assigned to carbon typical of amide function in proteins [N-**C**=O]. For non-conditioned substrates pre-cleaned with ethanol only, the components due to carbon in oxidized form were less intense and their position was subject to more variation; they may be attributed to carbon making a single bond with oxygen (near 286.2 eV) and carbon making a double bond or two singles bonds with oxygen (near 288.1 eV). These components were still less intense for non-conditioned substrates treated by

UVO. Several samples showed a very weak component near or above 288.8 eV, which may be attributed to ester or carboxyl. The results of the C 1s peak decomposition are presented in Tables 3 and 4.

Table 3. Surface concentration of elements and of carbon in different functions (mole fraction with respect to all elements except hydrogen, in %) measured by XPS on glass: not pre-cleaned, pre-cleaned with ethanol (Glass-Eth) and with additional UVO (Glass-UVO), as such or conditioned with native β-LGB or supernatant.

			Mole fraction of element (%)								**Mole fraction of carbon (%)**			
Element, function			**C**	**O**	**N**	**Si**	**Mg**	**Ca**	**Na**	**K**	**C -(C,H)**	**C-(O,N)**	**C=O O-C-O**	**O-C=O**
Conditioning liquid	Pre-cleaning	set												
None	None	a	43.2	37.8	0.8	8.9	3.6	1.3	3.9	0.6	32.1	5.2	3.0	2.8
		b	47.8	34.5	1.3	9.0	1.6	0.8	4.1	0.9	37.1	6.0	2.1	2.6
	Ethanol	a_1	29.6	50.4	0.9	13.4	3.9	n.m	1.5	0.4	19.6	5.0	2.2	2.7
		a_2	29.7	50.7	0.8	13.1	3.9	n.m	1.5	0.3	20.4	4.7	2.2	2.4
	UVO	a_1	25.0	51.9	b.d.l	17.1	2.6	n.m	2.9	0.6	20.7	1.8	1.0	1.4
		a_2	26.3	50.8	0.1	16.5	2.7	n.m	3.0	0.5	21.7	2.3	1.0	1.4
		b	24.1	53.8	0.1	13.9	5.2	0.6	2.2	0.1	17.8	3.2	1.4	1.7
β-LGB (3 g/L)	Ethanol	a	37.7	40.4	7.8	12.1	1.5	n.m	0.5	b.d.l	19.7	10.7	7.3	0.0
	UVO	a	44.1	35.0	9.2	9.5	1.2	n.m	1.0	b.d.l	23.9	11.7	8.5	0.0
β-LGB (0.75 g/L)	Ethanol	a	39.9	38.5	8.1	11.5	1.4	n.m	0.6	b.d.l	21.1	10.7	8.0	0.1
	UVO	a	36.2	41.3	7.9	13.4	0.3	n.m	0.9	b.d.l	20.4	8.8	6.9	0.0
Supernatant	Ethanol	a	35.9	42.1	6.8	12.7	1.8	n.m	0.7	b.d.l	19.7	9.6	6.7	0.0
	UVO	a	28.5	48.4	5.4	15.9	0.7	n.m	1.2	b.d.l	17.0	6.7	4.8	0.0

a and b refer to independent experimental sets

a_1 and a_2 were obtained on two distinct areas of the same coupon

Table 4. Surface concentration of elements and of carbon in different functions (mole fraction with respect to all elements except hydrogen, in %) measured by XPS on stainless steel (StSteel): not pre-cleaned, pre-cleaned with ethanol (StSteel-Eth) and with additional UVO (StSteel -UVO), as such or conditioned with native β-LGB or supernatant.

			Mole fraction of element (%)							**Mole fraction of carbon (%)**			
Element, function			**C**	**O**	**N**	**Si**	**Fe**	**Cr**	**K**	**C -(C,H)**	**C-(O,N)**	**C=O O-C-O**	**O-C=O**
Conditioning liquid	Pre-cleaning	set											
None	None	a	75.6	19.8	2.4	0.5	1.2	0.5	b.d.l	57.4	11.2	4.6	2.4
	Ethanol	a_1	59.4	31.6	1.1	1.1	4.9	1.2	0.6	38.0	9.1	4.9	7.5
		a_2	48.8	37.7	1.3	1.2	8.8	1.7	0.5	36.3	4.9	3.2	4.4
	UVO	a_1	55.6	33.7	b.d.l	1.5	7.4	1.1	0.8	47.5	4.1	2.0	1.9
		a_2	55.5	33.9	b.d.l	1.6	7.4	1.4	0.3	50.4	2.4	2.3	0.5
β-LGB (3 g/L)	Ethanol	a	50.5	31.4	7.2	1.2	7.7	2.0	b.d.l	31.8	10.1	7.4	1.1
	UVO	a	58.6	28.5	8.5	0.7	2.0	0.4	1.2	32.8	16.1	8.9	0.8
β-LGB (0.75 g/L)	Ethanol	a	52.3	30.2	7.4	1.0	7.1	2.0	b.d.l	33.4	10.6	6.8	1.4
	UVO	a	48.7	33.9	10.0	1.6	5.0	0.8	b.d.l	24.7	13.4	9.7	0.9
Supernatant	Ethanol	a	51.3	30.5	9.1	1.0	6.5	1.7	b.d.l	31.0	11.4	8.8	b.d.l
	UVO	a	47.6	35.0	9.1	1.5	5.9	0.8	b.d.l	25.4	12.3	9.3	0.7

a and b refer to independent experimental sets

a_1 and a_2 were obtained on two distinct areas of the same coupon

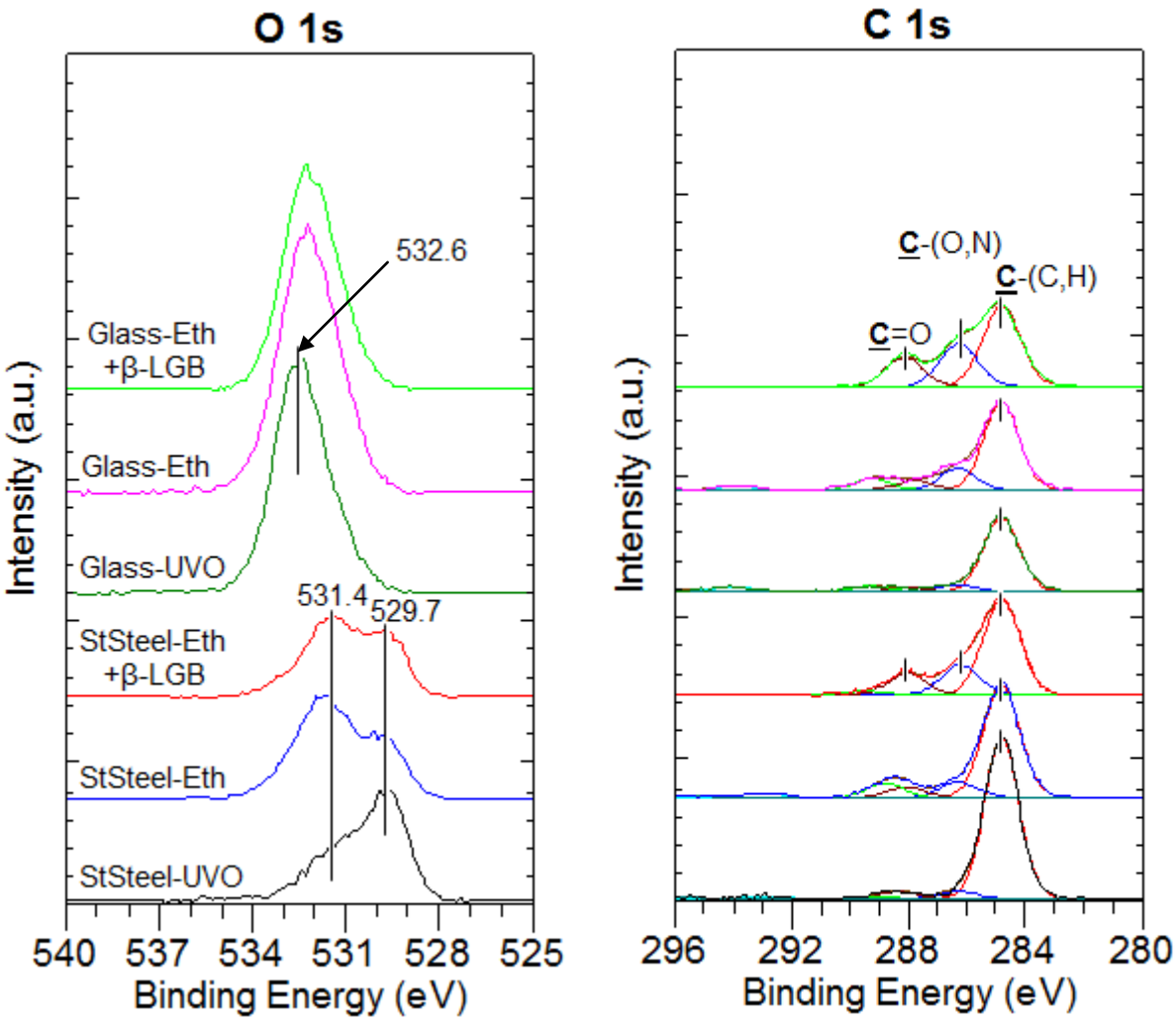

Figure 4. Representative O 1s and C 1s peaks recorded on stainless steel and glass, pre-cleaned with ethanol only (-Eth) or ethanol and additional UV-Ozone (-UVO), and conditioned with native β-LGB solution (+β-LGB). Illustration of C 1s peak decomposition.

The O 1s peak recorded on stainless steel samples showed two major components. The component near 529.7 eV is attributed to metal oxides of stainless steel. The other component found around 531.4 eV may be due to hydroxide of the substrate (Landoulsi et al., 2008) or to oxygen of amide (Rouxhet et al., 2008; Rouxhet and Genet, 2011). The O 1s component at 531.4 eV was relatively less intense on stainless steel treated by UVO. Glass treated by UVO showed an O 1s peak near 532.6 eV. For glass precleaned with only ethanol, the O 1s peak was broader and shifted to lower binding energies. This is attributed to a higher contribution of organic oxygen, in agreement with a higher concentration of carbon in oxidized form.

No decomposition was performed for the O 1s peak, owing to the overlap of contributions of the substrate, of β-LGB and of organic contaminants.

The N 1s peak of conditioned samples (not shown) was found at 400.0 ± 0.1 eV, due to amide, with a minor contribution (less than 10%) near 401.5 – 402.0 eV, due to protonated amine.

Owing to the complexity of the adsorbed layer (presence of organic contaminants in addition to expected adsorbate, overlap of solid and adsorbate contributions), and to uncertainties in modeling the organization of the layer probed by XPS, the adsorbed amount may not be expressed accurately in mass per unit area or in thickness. However comparisons of adsorbed amounts can be made between samples of the same solid, based on the sum of concentrations of elements due to the adsorbed layer, ΣAdlayer, and due to the solid, ΣSubstrate, neglecting hydrogen. The concentrations are given in mole fraction (%); thus, ΣAdlayer + ΣSubstrate = 100. As the O 1s peak could not be decomposed in components specific of different forms of oxygen, the separation between inorganic forms, due to the substrate, and organic forms, due to the adlayer, was made by using other information. In order to cope with uncertainties two independent approaches were followed.

A first approach was based on the evaluation of the organic oxygen concentration from the concentration of carbon in oxidized form $C_{ox} = C_{tot} - C_{284.8}$. Based on the amounts of different amino acids in β-LGB (Walstra and Jenness, 1984; http://www.uniprot.org/uniprot/P02754), the elemental composition and the expected contributions to the C 1s peak components were computed as performed before for BSA and validated by correlations between independent spectral data (Touré et al., 2014a). Details are given in Supporting Information. This provided the stoichiometry formula $C_{3.97}O_{1.20}N_1S_{0.04}H_{6.38}$ (formula mass 88.74 g/mol) for β-LGB, with molar ratios $(O/N)_{\beta\text{-LGB}} = 1.20$ and $(C_{ox}/N)_{\beta\text{-LGB}} = 2.05$. There was no significant difference between variants A and B of β-LGB. Accordingly, the contribution of β-LGB to the oxygen concentration is equal to 1.20*N and the contributions of organic contaminants to the oxygen concentration may be evaluated by $O_{cont} = C_{ox\text{-}cont} = (C_{ox} - 2.05*N)$ if carbon bound to oxygen in surface contaminants is only in the form of alcohol, aldehyde, ketone or ester.

It turns out that

$$\Sigma Adlayer = C + N + O_{\beta LGB} + O_{cont} = C + N + 1.20*N + C_{ox} - 2.05*N$$
$$= C + 0.15 * N + C_{ox} \quad (1)$$

This evaluation does not involve any hypothesis on the nature of the substrate surface but makes an assumption on the chemical nature of the organic contaminants and is based on the separation between oxidized and non-oxidized carbon in the C 1s peak.

An alternative approach was to evaluate the concentration of oxygen due to the substrate from the concentrations of inorganic elements, to compute Σsubstrate and to deduce Σadlayer.

For glass samples,

$$\Sigma Glass = Si*3+Na*1.5+K*1.5+Ca*2+Mg*2 \quad (2)$$

which accounts for inorganic elements and oxygen bound to them, considering the stoichiometries SiO_2, Na_2O, K_2O, CaO and MgO. ΣAdlayer was taken as 100 – ΣGlass

For stainless steel samples, the stoichiometry of the surface oxyhydroxide must lie between M_2O_3, in which case

$$\Sigma StSteel = Fe*1.5 + Cr*1.5 \quad (3)$$

and $M(OH)_3$, in which case

$$\Sigma StSteel = Fe*3 + Cr*3. \quad (4)$$

$$\Sigma Adlayer \text{ was taken as } 100 - \Sigma StSteel - Si - K. \quad (5)$$

Table 5 (left part) gives the values of ΣAdlayer computed according to Eq. (1) for all samples and according to Eq. (2) for glass and Eqs (3) and (4) for stainless steel. For glass samples the difference between the two approaches is only significant when the contribution of the adlayer is low (samples not conditioned with β-LGB). This is due to approximations behind Eqs (1) and (2), including differences of inelastic mean free paths between elements, and will not be discussed here. The two independent ways of evaluating ΣAdlayer were consistent in showing that, for non-conditioned glass samples, the contribution of the organic contaminants to the XPS spectrum follows the order: not pre-cleaned > pre-cleaned with ethanol > pre-cleaned with UVO. Conditioning glass with β-LGB increased the adlayer contribution up to the same range as raw glass. In the case of stainless steel, assuming a hydroxylated passive layer (Eq. 4) provided a better agreement with data from Eq. (1); this will also not be discussed here. The three ways of evaluating the contribution of the organic adlayer to the XPS spectrum were consistent in showing that this was not significantly different between stainless steel conditioned with β-LGB and stainless steel pre-cleaned with ethanol only or treated by UVO. In all cases, the XPS spectrum was dominated by the contribution of the organic adlayer which was strongly screening the substrate.

It appeared thus that conditioning the substrates with β-LGB did not markedly change the amount of organic adlayer, while the Tables 3 and 4 show that it changed its chemical nature. The composition of the organic adlayer may be figured out by the molar ratios O_{org}/C_{tot}, N/C_{tot} and O_{org}/N, where

$$O_{org} = O_{\beta LGB} + O_{cont} = 1.20*N + C_{ox} - 2.05*N = C_{ox} - 0.85*N \quad (6)$$

The results are given by Table 5 (middle part), which gives also the ratios expected for β-LGB (last line). Comparisons between the conditioned substrates, the values expected for pure β-LGB and the values measured on non-conditioned substrates, indicate that the organic adlayer was dominated by the protein for most conditioned samples of stainless steel and glass.

Table 5. Surface composition deduced by XPS for bare substrates and conditioned substrates: contribution of the organic adlayer to the XPS spectrum, composition (mass %) of the organic adlayer present on the solids; and molar ratios in organic adlayer. Values expected for pure β-LGB.

			Proportion (%) of elements due to the adlayer			**Molar ratios in organic adlayer**			**Organic composition (mass %)**	
						O_{org}/C_{tot}	N/C_{tot}	O_{org}/N	Protein	Non protein
Substrate pre-cleaning	set	Conditioning liquid								
Glass			Eq. (1)	Eq.(2)						
None	a	None	54.3	56.8		0.24	0.02	n.r.	8.6	91.4
	b		58.7	60.8		0.20	0.03	n.r.	14.1	85.9
Eth	a_1		39.6	49.1		0.31	0.03	n.r.	13.2	86.8
	a_2		39.1	50.0		0.29	0.03	n.r.	12.4	87.6
UVO	a_1		29.2	38.4		0.17	0.00	n.r.	0.0	100.0
	a_2		31.0	39.7		0.17	0.00	n.r.	2.5	97.5
	b		30.5	43.2		0.26	0.01	n.r.	2.5	97.5
Eth	a	β-LGB (3 g/L)	56.9	59.9		0.30	0.21	1.5	84.4	15.6
UVO	a		65.6	67.5		0.28	0.21	1.3	86.7	13.3
Eth	a	β-LGB (0.75 g/L)	59.9	61.7		0.30	0.20	1.5	83.1	16.9
UVO	a		53.1	57.8		0.25	0.22	1.1	92.6	7.4
Eth	a	Supernatant	53.2	57.4		0.29	0.19	1.5	78.8	21.2
UVO	a		40.7	49.0		0.24	0.19	1.3	81.4	18.6
Stainless Steel			Eq. (1)	Eq.(3)	Eq. (4)					
None	a	None	94.2	97.0	94.5	0.21	0.03	n.r.	15.7	84.3
Eth	a_1		81.0	89.0	79.8	0.34	0.02	n.r.	8.4	91.6
	a_2		61.5	82.6	66.8	0.23	0.03	n.r.	13.0	87.0
UVO	a_1		63.7	85.0	72.2	0.15	0.00	n.r.	0.0	100.0
	a_2		60.6	85.0	71.9	0.09	0.00	n.r.	0.0	100.0
Eth	a	β-LGB (3 g/L)	70.4	84.3	69.7	0.25	0.14	1.8	63.0	37.0
UVO	a		85.6	94.4	90.7	0.32	0.15	2.2	61.2	38.8
Eth	a	β-LGB (0.75 g/L)	72.3	85.4	71.8	0.24	0.14	1.7	62.9	37.1
UVO	a		74.2	89.8	81.1	0.32	0.21	1.5	83.3	16.7
Eth	a	Supernatant	72.9	86.7	74.4	0.25	0.18	1.4	76.8	23.2
UVO	a		71.2	88.4	78.2	0.30	0.19	1.6	78.6	21.4
Expected for β-LBG						0.30	0.25	1.2		

a and b refer to independent experimental sets
a_1 and a_2 were obtained on two distinct areas of the same coupon
n.r. not relevant

In order to get a better quantitative representation of the composition of the organic layer, the relative mass concentration of its constituents was computed from the mole fraction of markers and the related molar mass as shown in previous work for BSA (Touré et al., 2014a). The marker used for β-LGB was nitrogen. The constituents other than β-LGB were considered globally as oxygen, accounted for by the marker $C_{ox} - 2.05*N$, as justified above, and CH_2, in the form of either CH_2 or H-C-OH and accounted for by the marker $C_{tot} - 3.97*N$. The factor 3.97 is the C/N ratio of β-LGB, as shown in Supporting Information. The concentrations of markers, in mole percentage with respect to all elements except hydrogen, may be converted into concentrations of constituents, in mass percentage. The method of

computation used for the conversion is explained in Supporting Information (Table S4 and related text). The results are given in Table 5 (right part). On conditioned samples, the mass concentration of protein in the adlayer varied from 60 to 80% for stainless steel and 79 to 93% for glass.

3.3. Cleanability assessment and contact angle

Figure 5 presents the critical detachment radii measured on Glass-Eth, StSteel-Eth, Glass-UVO and StSteel-UVO, soiled with a quartz suspension in water and in β-LGB solution, either native or previously heated for 4 h at 75°C. Remember that the higher the critical detachment radius the lower the particle adherence (Detry et al., 2011). When the quartz particles were suspended in pure water, no detachment radius could be measured on glass, as observed before (Touré et al., 2013); detachment of a few particles occurred only near the inlet. The critical detachment radius was appreciably higher on StSteel-UVO (about 3 mm) and still higher on StSteel-Eth (about 8 mm). For Glass-Eth, Glass-UVO and StSteel-UVO, the critical detachment radius strongly increased when soiling was made with quartz suspensions in β-LGB solution compared to water, and increased still further when the quartz suspension had been heated for 4 h at 75°C. The critical detachment radii were in the same range for Glass-Eth, Glass-UVO and StSteel-UVO soiled with a suspension containing β-LGB and for StSteel-Eth soiled with a suspension in pure water. In contrast, the critical detachment radius for StSteel-Eth decreased when β-LGB was present in the soiling suspension and decreased still further when β-LGB was previously denatured.

The contact angles measured on the four substrates using water, native β-LGB and the supernatant collected after heating for 4 h at 75°C are given in Table 6. Results noted a are static contact angles measured with the goniometer, while the results b concerns static and dynamic contact angles measured on another set of slides prepared and analyzed together. The static contact angles of water differed slightly between a and b but showed the same trend when substrates were compared with each other. The advancing contact angles of the 3 liquids, measured on stainless steel pre-cleaned with only ethanol, significantly decreased from the beginning to the end of the first immersion. The same feature was noticeable but less marked for glass, submitted or not to the UV-Ozone treatment. Subsequent immersion cycles started close to the value noted at the end of the first cycle. The UVO treatment of glass and stainless steel decreased appreciably the static and advancing contact angles of all liquids. This was more marked for steel. The differences between the contact angles of water, of β-LGB native solution and of the supernatant collected after heating were weaker than the

differences between substrates. Globally the substrate ranged as follows regarding contact angle: Glass-UVO ≅ StSteel-UVO < Glass-Eth < StSteel-Eth. The receding water contact angles were very low. The receding water contact angles were very low. The receding contact angles could not be measured with the solutions of β-LGB owing to the retention of a liquid film upon emersion.

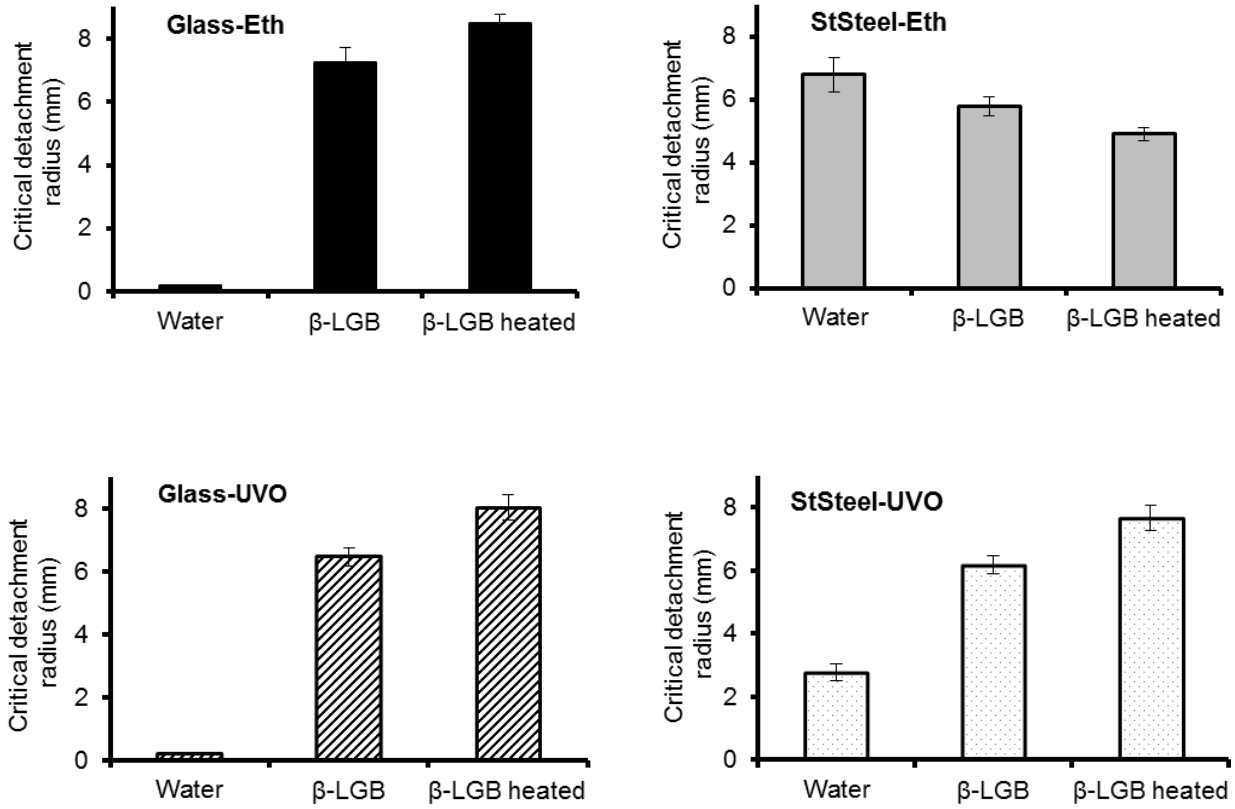

Figure 5. Critical detachment radii measured on glass and stainless steel, just pre-cleaned with ethanol (Eth) or further treated with UV-Ozone (UVO), soiled with quartz particles suspensions in water, with a suspension in β-LGB solution, and with a suspension in β-LGB solution previously heated for 4 h at 75°C.

4. DISCUSSION

4.1. β-LGB denaturation

UV-visible absorption and Kjeldahl analysis (Table 1) showed that heating β-LGB solution for 4 h at 75°C led to coagulation of about one fourth of the dissolved protein. Infrared absorption spectra of the pellet recovered after heating and centrifugation indicated that this was accompanied by a loss of α-helices and an increase of unordered structures. This is in agreement with Ikeda and Li-Chan (2004). Infrared and Raman Spectroscopy have been used to quantify β-LGB secondary structures in aqueous solution after heating for about 0.5 to 1 h at temperatures varying from 50 to 90°C (Allain et al., 1999; Ikeda, 2003; Ikeda and Li-Chan, 2004). Spectra were recorded after cooling down to ambient temperature without

centrifugation. Heating led to a marked loss of α-helical structure accompanied by an increase in disordered structures and formation of intermolecular β-sheets. It was also pointed out that the α-helices in β-LGB are the most heat-labile secondary structures. The optical data presented in Table 2 indicate that changes of the secondary structure are only significant for coagulated β-LGB.

Table 6. Contact angles measured in the indicated conditions on glass and stainless steel, just pre-cleaned with ethanol (Eth) or ethanol and with additional UVO, using water, β-LGB solution and supernatant collected after heating of β-LGB solution for 4 h at 75°C. Standard deviations, when relevant, are given between brackets.

Experimental conditions		Contact angle (°)			
		Glass-Eth	**Glass-UVO**	**StSteel-Eth**	**StSteel-UVO**
Water					
a Static		18 (3)	~9	35 (2)	10 (1)
b Static		34 (2)	~10	47 (7)	< 10
b Advancing	Cycle 1	41 to 36 (1)	12 to 15 (1)	61 to 44 (1)	≤10
	Cycles 2,3	34 to 30 (2)	22 to 17 (2)	42 to 35 (2)	≤12
"Receding"		~0	<10	<10	~0
Native β-LGB					
a Static		14 (2)	11 (2)	35 (3)	14 (3)
b Advancing	Cycle 1	46 to 41 (1)	11	68 to 39 (1)	26 to 0 (1)
"Receding"		~0	~0	~0	~0
Supernatant of heated β-LGB					
a Static		16 (2)	13 (2)	43 (3)	15 (2)
b Advancing	Cycle 1	44 to 37 (1)	<13	74 to 55 (1)	18 to 0 (1)
"Receding"		~0	~0	~0	~0

a and b refer to independent sets of measurements
(1) Variation from the beginning to the end of immersion
(2) Random variation within and between cycles 2 and 3

The secondary structure of β-LGB has also been investigated using CD (Carrotta et al., 2001). The α-helix content given in Table 2 is in agreement with the reported value of 10%. A solution heated at 68°C for different times was fractionated by chromatography; the α-helix content was not altered in the oligomers and in the smaller size fraction but was strongly lowered in the aggregates. The loss of α-helices was also noted for a solution heated at 80°C and not submitted to any separation (Qi et al., 1997). In the present work, no significant difference was observed between the supernatant collected after heating and the native β-LGB solution.

An increase of intrinsic fluorescence intensity and a red shift were reported for several systems involving whey proteins treatment: β-LGB solution treated under high pressure at

50°C during up to 64 min at increasing urea concentrations (Yang et al., 2001); β-LGB solution heated above 70°C for increasing times (Vetri and Militello, 2005; Stănciuc et al., 2012); whey protein isolate submitted to pulsed electric fields (Xiang et al., 2011); whey protein isolate processed under high pressure (20 MPa) of nitrogen or supercritical carbon dioxide up to 60°C for 1 h (Xu et al., 2011). An increase of the intrinsic fluorescence intensity and a red shift of 2 to 4 nm were attributed to a conformational modification leading to the exposure of tryptophan residues to the aqueous, more polar, environment. Accordingly the small change of fluorescence spectra shown in Figure 2 for the supernatant collected after heating may indicate a change of conformation of molecules remaining in the aqueous phase.

Figure 3 is more conclusive by showing that the supernatant has a lower surface tension than a native protein solution at the same concentration. This is in agreement with the observation (Schmitt et al., 2007) of a lowering of the surface tension of a whey protein solution heated at 85°C in presence of NaCl, the decrease being higher as the NaCl concentration and protein aggregation increased. It was also found that heat aggregation of BSA provoked a decrease of the surface tension of the solution (McClellan and Franses, 2003). In the present work, the lower surface tension of the supernatant compared to a native solution of the same β-LGB concentration reveals that molecules which remained dissolved after heating underwent changes of conformation and were more active at the air/water interface.

4.2. Interfaces and cleanability

The organic adlayer found by XPS on substrates which were not conditioned with β-LGB, particularly those pre-cleaned with ethanol only, may be due to contaminants which were not removed by pre-cleaning. The small N 1s peak near 400 eV suggested that certain contaminants were of proteinic nature. The UVO treatment decreased the water contact angle of both substrates (Table 6) but lowered only slightly the amount of adlayer, as measured by XPS (Table 5). It must be kept in mind that inorganic surfaces readily adsorb contaminants from the surroundings, in order to decrease the solid-gas interfacial energy. This may occur in the spectrometer vacuum chambers when the surface of the sample introduced into the spectrometer is clean enough (Rouxhet, 2013) and the adlayer observed after UVO treatment may be partially due to an in situ contamination, limiting the scope of the information provided by XPS.

Conditioning glass with β-LGB, in either native or denatured form, increased the organic adlayer, which was constituted of about 80% of proteins brought by β-LGB. In the case of stainless steel, the amount of organic adlayer was not considerably affected by conditioning

with β-LGB; however, proteins contributed more than 60% to the adlayer present on conditioned samples. This implies that organic contaminants present before conditioning were displaced by β-LGB adsorption or that the presence of β-LGB prevented contamination from the surroundings.

The study of the cleanability of different substrates (glass, stainless steel, polystyrene and polytetrafluoroethylene) soiled with a starch or quartz suspension in water and dried (Detry et al., 2011; Touré et al., 2011; 2014a) indicated that the particle adherence increased as the water contact angle decreased. This was attributed to two effects: increased droplet spreading, giving rise to the formation of flatter aggregates and thus decreasing the efficiency of shear forces upon cleaning; increase of capillary forces generated by drying, insuring a closer contact between their surfaces. The examination of the influence of BSA on the cleanability of glass and polystyrene soiled by suspensions of quartz and dried emphasized the major role of capillary forces and of the liquid surface tension (Touré et al., 2014a).

Assuming spherical particles at a small distance of the substrate surface and considering a bridge of liquid forming a ring around the contact point, the capillary forces created by meniscuses between a quartz particle and the substrate can be evaluated by the following equation (Rabinovich et al., 2002; Pitois et al., 2000):

$$F_{CAP} = 4\pi\gamma_L R\cos\left(\frac{\theta_p + \theta_s}{2}\right)\cos\left(\frac{\theta_s - \theta_p}{2}\right) \qquad (7)$$

where F_{CAP} is the capillary force (N), γ_L is the liquid surface tension (N/m), R is the soil particle radius (m), θ_S and θ_P are the contact angles of the liquid on the substrate and on the particles, respectively. Hypotheses regarding particle size and shape are not critical if the results are only used for comparison with each other. Capillary forces were computed considering quartz particles of 9 µm radius, a particle contact angle θ_p of 10°, and surface tensions of 72.2, 48.8 and 47.2 mN/m for water, β-LGB solution and supernatant of the heated β-LGB solution, respectively. The computations of F_{CAP} were performed with all the measured contact angles and are listed in Table 7.

For glass, F_{CAP} was in the range of 7 to 8 µN when soiling was produced by a quartz suspension in water and below 5.5 µN when soiling was produced by a quartz suspension in β-LGB or denatured β-LGB solution. This was not strongly affected by the value of the contact angle selected for the computation. One may expect that the contact angle governing the capillary forces created during drying is the receding contact angle; however this is not a crucial issue as indicated by the comparison between Table 6 and Table 7. As a matter of fact, for a given liquid surface tension, the capillary forces exerted on hydrophilic particles will not

Table 7. Evaluation of the capillary forces corresponding to contact angles presented in Table 6, considering a contact angle of 10°C of the liquids on quartz particles.

Contact angle measurement		Capillary force (µN)			
		Glass-Eth	**Glass-UVO**	**StSteel-Eth**	**StSteel-UVO**
Water					
a Static		7.9	≥8.0	7.4	≥8.0
b Static		7.4	≥8.0	6.8	≥8.0
b Advancing	Cycle 1	7.2	8	6.0 to 7.0	≥8.0
	Cycles 2,3	7.5	7.9	7.1 to 7.4	≥8.0
"Receding"		~8.0	≥8.0	≥8.0	~8.0
Native β-LGB					
a Static		5.4	5.4	5	5.4
b Advancing	Cycle 1	4.7	5.4	3.8 to 4.9	5.2 to 5.5
"Receding"		~5.5	~5.5	~5.5	~5.5
Supernatant of heated β-LGB					
a Static		5.2	5.2	4.6	5.2
b Advancing	Cycle 1	4.7	5.3	3.4 to 4.2	5.2
"Receding"		~5.3	~5.3	~5.3	~5.3

a and b refer to independent sets of measurements

be reduced by more than 20%, if the contact angle of the substrate increases from 0 to 52°. The influence of β-LGB on the cleanability of glass, whatever the pre-cleaning procedure (Figure 5), may thus be attributed to lower capillary forces due to lower liquid surface tension (Table 7). This same conclusion arised regarding the influence of BSA (Touré et al, 2014) on glass cleanability. The same holds for stainless steel pretreated by UV-Ozone. However the slightly higher cleanability observed when soiling with quartz suspensions in denatured β-LGB solution, compared to native β-LGB solutions, may not be explained by an effect of the liquid surface tension. More numerous and detailed observations would be required to investigate this point.

It is difficult to interpret the behavior of stainless steel initially pre-cleaned with ethanol only. The cleanability of StSteel-Eth observed after soiling with suspensions in water is appreciably higher than the cleanability of other substrates (Figure 5). This may not be explained by differences of F_{CAP} computed using receding contact angles (Table 7), but it is associated with higher static contact angles. It may possibly be related to the particularity of the dynamic contact angle measurements, which decreased significantly from the beginning to the end of the first immersion and suggested that the surface evolved when brought in contact with water. This might be due to a heterogeneity of the layer of contaminants or to its reorganization in contact with water. The complexity may still increase in presence of β-LGB. A clarification of these phenomena and of their influence on cleanability is difficult. Methods

of surface chemical analysis (XPS, Time of Flight - Secondary Ion Mass Spectroscopy) are of little help, as the exposure to vacuum chambers may itself lead to adsorption of contaminants (Rouxhet, 2013). Probing surfaces (pre-cleaned, conditioned in different ways, soiled and cleaned) by Atomic Force Microscopy and mapping interaction forces in air and in water with carefully designed probes seems to be the most promising approach (Alsteens et al., 2007). Such observations may help in understanding the respective role of protein molecules and organic contaminants, particularly regarding the heterogeneity of the interfaces and the accumulation of compounds making bridges at the contact between the adhering particles and the substrate (Detry et al., 2011).

5. CONCLUSIONS

For three of the substrates tested (Glass-Eth, Glass-UVO, StSteel-UVO) the increase of cleanability when the soiling suspension contained β-LGB may be explained by the influence of capillary forces created upon drying, which depend primarily on the liquid surface tension. In practice, the substrate contact angle is of less importance. Indeed, the capillary forces created between hydrophilic particles and different substrates decrease by only 20% as the substrate contact angle increases from 0 to 52°. The denaturation of β-LGB present in the soiling suspension leads to a slightly increased cleanability; this may not be simply explained by the effect of surface tension.

Glass and stainless surfaces are covered by a layer of organic contaminants which are not removed by pre-cleaning or are adsorbed from the surroundings. The presence of β-LGB in the soiling suspension leads to protein adsorption, but a significant amount of contaminants remains however at the surface.

The order of cleanability observed for the substrates soiled with a suspension of quartz particles in water (Glass-Eth ≅ Glass-UVO < StSteel-UVO < StSteel-Eth) and the influence of β-LGB on the cleanability of StSteel-Eth may not be simply explained by capillary forces, whether computed from static, advancing or receding contact angles. Variations of the wetting hysteresis during dynamic contact angle measurements suggest that the organic adlayer evolves when the material is brought in contact with water. It appears that the presence of contaminants, which is often neglected by considering the substrate surface as a model solid surface, may have a significant influence on cleanability. Hypothetical effects are the heterogeneity of the particle-substrate interface and the added complexity of the interactions between protein and organic contaminants at the interfaces.

ACKNOWLEDGEMENTS

This study has been supported by the Walloon Region. The support of National Foundation for Scientific Research (FNRS, Belgium) is also gratefully acknowledged. The authors thank SIBELCO-Benelux for providing quartz particles, Michel J. Genet and Pierre Eloy for the XPS examinations, Ouissam Abbas and Quentin Arnould for ATR-FTIR analysis in Walloon Agricultural Research Centre (CRA-W).

REFERENCES

Allain, A.F., Paquin, P. & Subirade, M. (1999). Relationships between conformation of beta-lactoglobulin in solution and gel states as revealed by attenuated total reflection Fourier transform infrared spectroscopy. *Int. J. Biol. Macromol.*, 26(5), 337-44.

Alsteens, D., Dague, E., Rouxhet, P.G., Baulard, A.R. & Dufrêne, Y.F. (2007). Direct measurement of hydrophobic forces on cell surfaces using AFM. *Langmuir*, 23, 11977-11979.

Andrade, J.D. & Hlady, V. (1987). Plasma protein adsorption : the big twelvea. *Ann. New York Acad. Sci.*, 516, 158-172.

Bansal, B. & Chen, X.D. (2009). Fouling of heat exchangers by dairy fluids – a review. *Berkeley Electron. Press*, RP2, 149-57.

Bansal, B. & Chen, X.D. (2006). A critical review of milk fouling in heat exchangers. *Science*, 5(2), 27-33.

Bansal, B., Chen, X.D. & Lin, S.X.Q. (2005). Skim milk fouling during ohmic heating. *Proc. of 6th Int. Conf. on Heat Exchanger Fouling and Cleaning - Challenges and Opportunities* (Müller-Steinhagen, H., Malayeri, M.R. & Watkinson, P.A., eds.) Eng. Conf. Int., Kloster Irsee, Germany, RP2, 133-140.

Blanpain-Avet, P., Hédoux, A., Guinet, Y., Paccou, L., Petit, J., Six, T. & Delaplace, G. (2012). Analysis by Raman spectroscopy of the conformational structure of whey proteins constituting fouling deposits during the processing in a heat exchanger. *J. Food Eng.*, 110(1), 86-94.

Carrotta, R., Bauer, R., Waninge, R. & Rischel, C. (2001). Conformational characterization of oligomeric intermediates and aggregates in β-lactoglobulin heat aggregation. *Protein Sci.*, 10(7), 1312-1318.

Changani, S.D., Belmar-Beiny, M.T. & Fryer, P.J. (1997). Engineering and chemical factors associated with fouling and cleaning in milk processing. *Exp. Therm. Fluid Sci.*, 14(4), 392-406.

Detry, J.G., Sindic, M., Servais, M.J., Adriaensen, Y., Derclaye, S., Deroanne, C. & Rouxhet, P.G. (2011). Physico-chemical mechanisms governing the adherence of starch granules on materials with different hydrophobicities. *J. Colloid Interface Sci.*, 355(1), 210-21.

Detry, J.G., Deroanne, C., Sindic, M. & Jensen, B.B.B. (2009). Laminar flow in radial flow cell with small aspect ratios: Numerical and experimental study. *Chem. Eng. Sci.*, 64(1), 31-42.

Detry, J.G., Rouxhet, P.G., Boulangé-Petermann, L., Deroanne, C. & Sindic, M. (2007). Cleanability assessment of model solid surfaces with a radial-flow cell. *Colloids Surfaces A. Physicochem. Eng. Asp.*, 302(1-3), 540-548.

Genet, M.J., Dupont-gillain, C.C. & Rouxhet, P.G. (2008). XPS Analysis of Biosystems and Biomaterials. In *Medical applications of colloids* (E. Matijević, ed.) Springer, New York, 177-307.

Goldstein, A.S. & DiMilla, P.A. (1998). Comparison of converging and diverging radial flow for measuring cell adhesion. *AIChE J.*, 44(2), 465-473.

Goldstein, A.S. & Dimilla, P.A. (1997). Application of fluid mechanic and kinetic models to characterize mammalian cell detachment in a radial-flow chamber. *Biotechnol. Bioeng.*, 55(4), 616-29.

Goormaghtigh, E., Ruysschaert, J.-M. & Raussens, V. (2006). Evaluation of the information content in infrared spectra for protein secondary structure determination. *Biophys. J.* 90(8), 2946-57.

Gurdak, E., Rouxhet, P.G. & Dupont-Gillain, C.C. (2006). Factors and mechanisms determining the formation of fibrillar collagen structures in adsorbed phases. *Colloids Surfaces B Biointerfaces*, 52(1), 76-88.

Ikeda, S. & Li-Chan, E.C.Y. (2004). Raman spectroscopy of heat-induced fine-stranded and particulate β-lactoglobulin gels. *Food Hydrocoll.*, 18(3), 489-498.

Ikeda, S. (2003). Heat-induced gelation of whey proteins observed by rheology, atomic force microscopy, and Raman scattering spectroscopy. *Food Hydrocoll.*, 17(4), 399-406.

Jacquemart, I., Pamuła, E., Cupere, V.M. De, Rouxhet, P. G., & Dupont-Gillain, C.C. (2004). Nanostructured collagen layers obtained by adsorption and drying. *J. Colloid Interface Sci.*, 278, 63-70.

Jensen, B.B.B. & Friis, A. (2004). Critical wall shear stress for the EHEDG test method. *Chem. Eng. Process. Process Intensif.*, 43(7), 831-840.

Landoulsi, J., Genet, M.J., Richard, C., Kirat, K.E., Pulvin, S. & Rouxhet, P.G. (2008). Evolution of the passive film and organic constituents at the surface of stainless steel immersed in fresh water. *J. Colloid Interface Sci.*, 318(2), 278-89.

Manavalan, P. & Johnson, W.C.Jr. (1987). Variable selection method improves the prediction of protein secondary structure from circular dichroism spectra. *Anal. Biochem.* 167, 76-85.

McClellan, S.J. & Franses, E.I. (2003). Effect of concentration and denaturation on adsorption and surface tension of bovine serum albumin. *Colloids Surfaces B Biointerfaces*, 28(1), 63-75.

Pierna, F.J.A., Duponchel, L., Ruckebusch, C., Bertrand, D., Baeten, V. & Dardenne, P. (2012). Trappist beer identification by vibrational spectroscopy: A chemometric challenge posed at the "Chimiométrie 2010" congress. *Chemom. Intell. Lab. Syst.*, 113, 2-9.

Pitois, O., Moucheront, P. & Château, X. (2000). Liquid bridge between two moving spheres: an experimental study of viscosity effects. *J. Colloid Interface Sci. 231*(1), 26–31.

Provencher, S.W. & Glockner, J. (1981). Estimation of globular protein secondary structure from circular dichroism. *Biochemistry* 20, 33-37.

Qi, X.L., Holt C., Mcnulty David, D., Clarke D.T., Brownlow S. & Jones G.R. (1997). Effect of temperature on the secondary structure of β-lactoglobulin at pH 6.7, as determined by CD and IR spectroscopy: a test of the molten globule hypothesis. *Biochem. J.*, 346, 341-346.

Rabe, M., Verdes, D. & Seeger, S. (2011). Understanding protein adsorption phenomena at solid surfaces. *Adv. Colloid Interface Sci.*, 162(1-2), 87-106.

Rabinovich, Y.I, Adler, J.J., Esayanur M.S., Ata, A., Singh, R. & Moudgil, B.M. (2002). Capillary forces between surfaces with nanoscale roughness. *Adv. Colloid Interface Sci. 96*(1-3), 213–30.

Robbins, P.T., Elliott, B.L., Fryer, P.J., Belmar, M.T. & Hasting, A.P.M. (1999). A comparison of milk and whey fouling in a pilot scale plate heat exchanger: implications for modelling and mechanistic studies. *Food Bioprod. Process.*, 77 (C2)(2), 97-106.

Rojvoranun, S., Chadavipoo, C., Pengjun, W., Chavadej, S., Scamehorn, J.F. & Sabatini, D.A. (2011). Mechanistic Studies of Particulate Soil Detergency: I. Hydrophobic Soil Removal. *J. Surfactants Deterg.*, 15(3), 277-289.

Rouxhet, P.G. (2013). Contact angles and surface energy of solids: Relevance and limitations, in *Advances in contact angle, wettability and adhesion* (Mittal, K.L., ed.) Vol. 1, Schrivener Publishing LLC, 347-375

Rouxhet, P.G. & Genet, M.J. (2011). XPS analysis of bio-organic systems. *Surf. Interface Anal.*, 43(12), 1453-1470.

Rouxhet, P.G., Misselyn-Bauduin, A.M., Ahimou, F., Genet, M.J., Adriaensen, Y., Desille, T., Bodson, P. & Deroanne, C. (2008). XPS analysis of food products: toward chemical functions and molecular compounds. *Surf. Interface Anal.*, 40(3-4), 718-724.

Schmitt, C., Bovay, C., Rouvet, M., Shojaei-Rami, S. & Kolodziejczyk, E. (2007). Whey protein soluble aggregates from heating with NaCl: physicochemical, interfacial, and foaming properties. *Langmuir Acs J. Surfaces Colloids*, 23(8), 4155-66.

Speranza, G., Gottardi, G., Pederzolli, C., Lunelli, L., Canteri, R., Pasquardini, L., Carli, E., Lui, A., Maniglio, D., Brugnara, M. & Anderle, M. (2004). Role of chemical interactions in bacterial adhesion to polymer surfaces. *Biomaterials*, *25*(11), 2029-2037.

Sreerema, N. & Woody, R.W. (1993). A self-consistent method for the analysis of protein secondary structure from circular dichroism. *Anal. Biochem.*, 209, 32-44.

Sreerema, N., Venyaminov, S.Y. & Woody, R.W. (1999). Estimation of the number of helical and strand segments in proteins using CD spectroscopy. *Protein Sci.*, 8, 370-380.

Sreerama, N. & Woody, R.W. (2000) Estimation of protein secondary structure from CD spectra: Comparison of CONTIN, SELCON and CDSSTR methods with an expanded reference set. *Anal. Biochem.*, 287(2), 252-260.

Stănciuc, N., Aprodu, I., Râpeanu, G. & Bahrim, G. (2012). Fluorescence spectroscopy and molecular modeling investigations on the thermally induced structural changes of bovine β-lactoglobulin. *Innov. Food Sci. Emerg. Technol.*, 15, 50-56.

Stanley, C.G. & Peter H.V.H. (1989). Calculation of protein extinction coefficients from amino acid sequence data. *Anal. Biochem.*, 182, 319-326.

Stefanov, I., Baeten, V., Abbas, O., Vlaeminck, B., De Baets, B. & Fievez, V. (2013). Evaluation of FT-NIR and ATR-FTIR spectroscopy techniques for determination of minor odd- and branched-chain saturated and trans unsaturated milk fatty acids. *J. Agric. Food Chem.*, 61(14), 3403-13.

Stephan, O., Weisz, N., Vieths, S., Weiser, T., Rabe, B. & Vatterott, W. (2004). Protein quantification, sandwich ELISA, and real-time PCR used to monitor industrial cleaning procedures for contamination with peanut and celery allergens. *J. AOAC Int.*, 87(6), 1448-1457.

Touré, Y., Genet M.J., Dupont-Gillain C.C., Sindic M. & Rouxhet P.G. (2014a). Conditioning materials with biomacromolecules: composition of the adlayer and influence on cleanability. *J. Colloid Interface Sci.*, 432, 158-169.

Touré, Y., Rouxhet P.G., Dupont-Gillain, C.C., Sindic M. (2014b). Influence of whey protein denaturation on adherence of soiling particles to stainless steel. *Fouling and Cleaning in Food Processing* (Wilson, D.I & Chew, Y.M.J, eds.), Publishing Depart. Chem. Eng. & Biotech., Cambridge, UK, 30-37

Touré, Y., Rouxhet P.G. & Sindic M.. (2013). Influence of soluble proteins on the adherence of particulate soils. *Proc. Int. Conf. on Heat Exchanger Fouling and Cleaning*, (Malayeri, M.R., Müller-Steinhagen, H. & Watkinson, A.P., eds.), June 09-14, 2013, Budapest, Hungary, http://www.heatexchanger-fouling.com, 285-290.

Touré, Y., Rouxhet P.G., Dupont-Gillain, C.C., Sindic M. (2011). Influence of soluble polysaccharide on the adherence of particulate soils. *Proc. Int. Conf. on Heat Exchanger Fouling and Cleaning*, (Malayeri, M.R., Müller-Steinhagen, H. & Watkinson, A.P., eds.), June 05-10, 2011, Crete Island, Greece, http://www.heatexchanger-fouling.com, 219-226.

Van Stokkum, I.H.M., Spoelder, H.J.W., Bloemendal, M., Van Grondelle, R. & Groen, F.C.A. (1990). Estimation of protein secondary structure and error analysis from CD spectra. *Anal. Biochem.*, 191, 110-118.

Van Tassel, P.R. (2006). Proteins at Solid–Liquid Interfaces . In *Proteins at Liquid – Solid Interfaces* (Dejardin, P., ed.) Springer, Berlin, Germany, 1-22.

Vetri, V. & Militello, V. (2005). Thermal induced conformational changes involved in the aggregation pathways of beta-lactoglobulin. *Biophys. Chem.*, 113(1), 83-91.

Walstra, P. & Jenness, R. (1984). *Dairy chemistry and physics*. John Wiley and Sons, New York, pp. 467.

Whitmore, L. & Wallace, B.A. (2008). Protein secondary structure analyses from circular dichroism spectroscopy: methods and reference databases. *Biopolymers*, 89(5), 392-400.

Whitmore, L. & Wallace, B.A. (2004). DICHROWEB: an online server for protein secondary structure analyses from circular dichroism spectroscopic data. *Nucleic Acids Res.*, 32, W668-W673

Xiang, B.Y., Ngadi, M.O., Ochoa-Martinez, L.A. & Simpson, M.V. (2011). Pulsed Electric Field-Induced Structural Modification of Whey Protein Isolate. *Food Bioprocess Technol.*, 4(8), 1341-1348.

Xu, D., Yuan, F., Jiang, J., Wang, X., Hou, Z. & Gao, Y. (2011). Structural and conformational modification of whey proteins induced by supercritical carbon dioxide. *Innov. Food Sci. Emerg. Technol.*, 12(1), 32-37.

Yang, J., Dunker, A.K., Powers, J.R., Clark, S. & Swanson, B.G. (2001). Beta-lactoglobulin molten globule induced by high pressure. *J. Agric. Food Chem.*, 49(7), 3236-3243.

SUPPORTING MATERIAL

1. Concentrations of elements and chemical functions expected for β-LGB

Table S1 gives the respective amounts of different amino acids in variant B of β-LGB (Walstra and Jenness, 1984; http://www.uniprot.org/uniprot/P02754), the elemental composition of each amino acid, and the elemental composition and molar mass deduced for β-LGB. This provides concentration ratios expressed by the formula $C_{3.97}O_{1.20}N_1S_{0.04}H_{6.38}$ and the molar mass of 18281 g/mol. The variant A (Alexander et al., 1989) has no significant influence on the data computed below.

Tables S2 and S3 give the listing of the chemical functions accounting for C, N and O in each amino acid and the values deduced for β-LGB, respectively. The concentrations of elements in table S3 were pooled according to their expected contribution to components of the C 1s, N 1s and O 1s peaks (Rouxhet and Genet, 2011; Genet et al., 2008). Carbon bound only to carbon and hydrogen [**C**-(C,H)] and carbon bound to sulfur (Dietrich et al., 2011; Singh and Whitten, 2008) are expected to contribute to the component set at 284.8 eV. Carbon making a single bond with oxygen or nitrogen [**C**-(O,N) is expected near 286.3 eV. Carbon of the peptidic link [N-**C**=O] is expected near 288 eV, as well as carbon bound to 2 or 3 nitrogen atoms (arginine, histidine). The component due to carboxylic acid [O=**C**-OH] is expected near 289 eV; it may be noted that carbon of deprotonated carboxyl should contribute to the 288 eV component but this was not considered here. The enumeration of nitrogen atoms makes a distinction between amide [**N**-C=O] expected near 399.8 eV, and other functions. The latter are expected below 400 eV, but some of them may be protonated and be responsible for a component above 401 eV. As the O 1s peak is concerned, above 532 eV are expected contributions of the OH of alcohol (532.6 eV) and carboxyl (533.4 eV) ; below 532 eV are expected contributions of oxygen making a double bond with carbon in carboxylic acid (531.8 eV), amide (531.3 eV) and carboxylate (531.1 eV).

This computation provides the following molar concentration ratios:

$C / N = 3.97$

$O / N = 1.20$

$C_{284.8} / N = 1.92$

$C_{286.3} / N = 1.04$

$C_{288} / N = 0.88$

$C_{289} / N = 0.13$

$C_{ox} / N = (C_{tot} - C_{284.8}) / N = 2.05$

Supporting Material

Table S1. Elemental composition of β-lactoglobulin (β-LGB) variant B, computed from the amount and composition of amino acids.

Amino acid		Number of atoms in amino acid residue					Number of atoms in β-LGB variant B				
Name	**Number**	**C**	**O**	**N**	**S**	**H**	**C**	**O**	**N**	**S**	**H**
alanine (Ala)	15	3	1	1	0	5	45	15	15	0	75
arginine (Arg)	3	6	1	4	0	12	18	3	12	0	36
asparagine (Asn)	5	4	2	2	0	6	20	10	10	0	30
aspartic acid (Asp)	10	4	3	1	0	5	40	30	10	0	50
cysteine (Cys)	5	3	1	1	1	5	15	5	5	5	25
glutamic acid (Glu)	16	5	3	1	0	7	80	48	16	0	112
glutamine (Gln)	9	5	2	2	0	8	45	18	18	0	72
glycine (Gly)	4	2	1	1	0	3	8	4	4	0	12
histidine (His)	2	6	1	3	0	7	12	2	6	0	14
isoleucine (Ile)	10	6	1	1	0	11	60	10	10	0	110
leucine (Leu)	22	6	1	1	0	11	132	22	22	0	242
lysine (Lys)	15	6	1	2	0	12	90	15	30	0	180
methionine (Met)	4	5	1	1	1	9	20	4	4	4	36
phenylalanine (Phe	4	9	1	1	0	9	36	4	4	0	36
proline (Pro)	8	5	1	1	0	7	40	8	8	0	56
serine (Ser)	7	3	2	1	0	5	21	14	7	0	35
tryptophan (Trp)	2	11	1	2	0	10	22	2	4	0	20
threonine (Thr)	8	4	2	1	0	7	32	16	8	0	56
tyrosine (Tyr)	4	9	2	1	0	9	36	8	4	0	36
valine (Val)	9	5	1	1	0	9	45	9	9	0	81
"chain ends"	1	0	1	0	0	2	0	1	0	0	2
Total	162						817	248	206	9	1316
Mass of element per molecule							9813	3968	2885	289	1326
Molar mass of β-LGB variant B							18281				

Supporting Material

Table S2. Listing of chemical functions in amino acids.

	Carbon functions in amino acid residue										Nitrogen fonctions in a.a. residue			Oxygen functions in a.a. residue		
Amino acid	**CH3**	**CH2**	**CH**	**C-C_3**	**C-S**	**C-O**	**C-N**	**N-C=O**	**O=C-OH**	**Sum C**	**N-C=O**	**C-N**	**Sum N**	**O=COH**	**OH**	**Sum O**
								N-C-N				**N=C**				
alanine (Ala)	1	0	0	0	0	0	1	1	0	3	1	0	1	0	0	1
arginine (Arg)	0	2	0	0	0	0	2	2	0	6	1	3	4	0	0	1
asparagine (Asn)	0	1	0	0	0	0	1	2	0	4	2	0	2	0	0	2
aspartic acid (Asp)	0	1	0	0	0	0	1	1	1	4	1	0	1	2	0	3
cysteine (Cys)	0	0	0	0	1	0	1	1	0	3	1	0	1	0	0	1
glutamic acid (Glu)	0	2	0	0	0	0	1	1	1	5	1	0	1	2	0	3
glutamine (Gln)	0	2	0	0	0	0	1	2	0	5	2	0	2	0	0	2
glycine (Gly)	0	0	0	0	0	0	1	1	0	2	1	0	1	0	0	1
histidine (His)	0	1	0	0	0	0	3	2	0	6	1	2	3	0	0	1
isoleucine (Ile)	2	1	1	0	0	0	1	1	0	6	1	0	1	0	0	1
leucine (Leu)	2	1	1	0	0	0	1	1	0	6	1	0	1	0	0	1
lysine (Lys)	0	3	0	0	0	0	2	1	0	6	1	1	2	0	0	1
methionine (Met)	0	1	0	0	2	0	1	1	0	5	1	0	1	0	0	1
phenylalanine (Phe)	0	1	5	1	0	0	1	1	0	9	1	0	1	0	0	1
proline (Pro)	0	2	0	0	0	0	2	1	0	5	1	0	1	0	0	1
serine (Ser)	0	0	0	0	0	1	1	1	0	3	1	0	1	0	1	2
tryptophan (Trp)	0	1	4	2	0	0	3	1	0	11	1	1	2	0	0	1
threonine (Thr)	1	0	0	0	0	1	1	1	0	4	1	0	1	0	1	2
tyrosine (Tyr)	0	1	4	1	0	1	1	1	0	9	1	0	1	0	1	2
valine (Val)	2	0	1	0	0	0	1	1	0	5	1	0	1	0	0	1

Supporting Material

Table S3. Listing of chemical functions in β-lactoglobulin (β-LGB) variant B, computed from the amount (Table S1) and composition (Table S2) of amino acids, pooled according to the expected contribution in the XPS spectrum.

	Carbon in β-LGB variant B										Nitrogen in β-LGB variant B			Oxygen in β-LGB variant B				
amino	**CH3**	**CH2**	**CH**	**$\underline{C}C_3$**	**C-S**	**C-O**	**C-N**	**N-C=O**	**O=COH**	**Sum C**	**N-C=O**	**C-N**	**Sum N**	**OH**	**O=C$\underline{O}$H**	**O=C$\underline{O}$H**	**N-C=O**	**Sum O**
acid								**N-C-N**				**N=C**						
Ala	15	0	0	0	0	0	15	15	0	45	15	0	15	0	0	0	15	15
Arg	0	6	0	0	0	0	6	6	0	18	3	9	12	0	0	0	3	3
Asn	0	5	0	0	0	0	5	10	0	20	10	0	10	0	0	0	10	10
Asp	0	10	0	0	0	0	10	10	10	40	10	0	10	0	10	10	10	30
Cys	0	0	0	0	5	0	5	5	0	15	5	0	5	0	0	0	5	5
Glu	0	32	0	0	0	0	16	16	16	80	16	0	16	0	16	16	16	48
Gln	0	18	0	0	0	0	9	18	0	45	18	0	18	0	0	0	18	18
Gly	0	0	0	0	0	0	4	4	0	8	4	0	4	0	0	0	4	4
His	0	2	0	0	0	0	6	4	0	12	2	4	6	0	0	0	2	2
Ile	20	10	10	0	0	0	10	10	0	60	10	0	10	0	0	0	10	10
Leu	44	22	22	0	0	0	22	22	0	132	22	0	22	0	0	0	22	22
Lys	0	45	0	0	0	0	30	15	0	90	15	15	30	0	0	0	15	15
Met	0	4	0	0	8	0	4	4	0	20	4	0	4	0	0	0	4	4
Phe	0	4	20	4	0	0	4	4	0	36	4	0	4	0	0	0	4	4
Pro	0	16	0	0	0	0	16	8	0	40	8	0	8	0	0	0	8	8
Ser	0	0	0	0	0	7	7	7	0	21	7	0	7	7	0	0	7	14
Trp	0	2	8	4	0	0	6	2	0	22	2	2	4	0	0	0	2	2
Thr	8	0	0	0	0	8	8	8	0	32	8	0	8	8	0	0	8	16
Tyr	0	4	16	4	0	4	4	4	0	36	4	0	4	4	0	0	4	8
Val	18	0	9	0	0	0	9	9	0	45	9	0	9	0	0	0	9	9
Ch. Ends								-1	1		-1	1			1	1	-1	1
Total	105	180	85	12	13	19	196							19	27	27	175	
			395			215		180	27	817	175	31	206	46		202		248

Supporting Material

2. Conversion of elemental concentration ratios into weight % of compounds

The composition of the organic layer present at the surface of conditioned substrates may be quantified by using appropriate markers (Touré et al., 2014). The concentrations of markers (mole %) may be converted into concentrations of constituents (mass %), which provide a more practical presentation of the surface composition. Multiplying the molar concentration of markers (X, mole/100 moles) by the molar mass (MM) of the relevant constituent provides the concentration of each constituent (W, in g/100 mol of elements detected by XPS). Dividing W of each constituent by the sum of W for all constituent (T) and multiplying by 100 finally gives the mass concentration in % of the constituent in the volume probed by XPS. Table S4 presents the scheme of the procedure used for the conversion and recalls the markers used in the model.

Table S4. Table used for converting marker concentrations (molar percentage of relevant element) into mass concentration (%) of model compounds.

Constituent		Marker		W= X∗MM (b)	Concentration W∗100 / T (mass %)
Nature	MM	Nature	X (a) (mol %)		
Model: β-LGB + contaminants					
β-LGB $C_{3.97}O_{1.20}N_1S_{0.04}H_{6.38}$	88.7	N	●●●	●●●	●●●
Contaminants					
Oxygen	16	C_{ox} – 2.05*N	●●●	●●●	●●●
CH_2	14	C_{tot} – 3.97*N	●●●	●●●	●●●
Total				T = ●●●	100

(a) measured marker concentration X (mole/100 moles excluding hydrogen).
(a) in g of compounds / 100 moles of elements, excluding hydrogen.

REFERENCES

Alexander, L. J., Hayes, G., Pearse, M. J., Beattie, C. W., Stewart, A. F., Willis, I. M., & Mackinlay, A. G. (1989). Complete sequence of the bovine beta-lactoglobulin cDNA. *Nucleic Acids Res., 17*(16), 6739.

Genet, M. J., Dupont-gillain, C. C., Rouxhet, P. G. (2008). XPS analysis of biosystems and biomaterials. In *Medical applications of colloids* (E. Matijević, ed.) Springer, New York. 177–307.

Supporting Material

Dietrich P. M., Horlacher, T., Girard-Lauriault, P.-L., Gross, T., Lippitz, A., Min, H., Wirth, T., Castelli R., Seeberger P. H., & Unger W. E. S. (2011). Adlayers of dimannoside thiols on gold: surface chemical analysis. *Langmuir 27*(8), 4808–15.

Rouxhet, P. G., & Genet, M. J. (2011). XPS analysis of bio-organic systems. *Surf. Interface Anal. 43*(12), 1453–1470.

Singh, J., & Whitten, J. E. (2008). Adsorption of 3-Mercaptopropyltrimethoxysilane on Silicon Oxide Surfaces and Adsorbate Interaction with Thermally Deposited Gold. *J. Phys. Chem. C 112*(48), 19088–19096.

Touré Y., Genet M.J., Dupont-Gillain C.C., Sindic M. & Rouxhet P.G. (2014). Conditioning materials with biomacromolecules: composition of the adlayer and influence on cleanability. *J. Colloid Interface Sci.*, 432, 158-169.

Walstra, P., & Jenness, R. (1984). Dairy chemistry and physics. *New York : Wiley,* 467.